Sclerotinia sclerotiorum necrosis-inducing effectors

A Thesis Submitted to the College of Graduate and Postdoctoral Studies

In Partial Fulfillment of the Requirements

For the Degree of Doctor of Philosophy

In the Department of Biology

University of Saskatchewan

By

Shirin Seifbarghi

PERMISSION TO USE

In presenting this thesis in partial fulfillment of the requirements for a Postgraduate degree from the University of Saskatchewan, I agree that the Libraries of this University may make it freely available for inspection. I further agree that permission for copying this thesis in any manner, in whole or in part, for scholarly purposes may be granted by the professor or professors who supervised my thesis work, or in their absence, by the Head of the Department or the Dean of the College in which my thesis was done. It is understood that any copying or publication or use of this thesis, in whole or in part, for financial gain shall not be allowed without my written permission. It is also understood that due recognition shall be given to me and to the University of Saskatchewan in any scholarly use which may be made of any material in my thesis.

Requests for permission to copy or to make other use of material in this thesis in whole or in part should be addressed to:

Head of the Department of Biology
University of Saskatchewan
Saskatoon, Saskatchewan,
S7N 5E2, Canada

OR

Dean
College of Graduate and Postdoctoral Studies
University of Saskatchewan
116 Thorvaldson Building, 110 Science Place
Saskatoon, Saskatchewan
S7N 5C9, Canada

ABSTRACT

Stem rot disease in canola caused by *Sclerotinia sclerotiorum* leads to lodging and severe yield losses in Canada. *Sclerotinia sclerotiorum* is equipped with small, secreted proteins (effectors) to induce plant cell death to facilitate nutrient uptake. Characterizing cell death/necrosis-inducing effectors might enable devising strategies to identify disease tolerant germplasm that is impervious to select necrosis-inducing effectors. In this study, RNA-Seq analysis was performed with a focus on the events occurring through the early (1 hour) to the middle (48 hours) stages of infection to reveal the gene expression patterns during the course of *S. sclerotiorum* infection on *B. napus*. The differentially expressed genes including those encoding hydrolytic enzymes, secreted effectors, enzymes involved in the synthesis of secondary metabolites or their detoxification, signaling, development, as well as oxalic acid and reactive oxygen species production. This investigation provides a broad overview of the sequential expression of virulence/pathogenicity-associated genes during infection of *B. napus*. To identify candidate necrosis-inducing effectors, the genome of *S. sclerotiorum* was searched for genes encoding small, secreted, cysteine-rich proteins. These effectors were tested for their ability to induce necrosis in *Nicotiana benthamiana* via *Agrobacterium tumefaciens*-mediated transient expression and for their host cellular localization. Six novel necrosis-inducing effectors were discovered, of which all but one required a signal peptide and secretion to the extracellular space for necrotic activity. These five effectors were localized to the endoplasmic reticulum and nucleus, while one that did not require signal peptide for necrotizing activity was localized in cytoplasm and nucleus. Virus-induced gene silencing (VIGS) experiments were conducted to reveal the participation of plant receptor-like kinases (RLK) in the induction of cell death. VIGS revealed that these five effectors required the RLKs, BAK1 and SOBIR1, for the induction of necrosis. These results illustrated the importance of necrosis-inducing effectors for *S. sclerotiorum* virulence and the potential role of host extra-cellular receptor(s) in the perception of *S. sclerotiorum* effectors. Substitution of cysteine residues with alanine and examination of truncated peptides for one of these effectors suggested that the native protein is necessary for necrotizing activity. These effectors could be applied for effector-assisted breeding of resistance to stem rot disease in canola.

ACKNOWLEDGEMENTS

The first and foremost person I would like to thank and express my gratitude and appreciation is my supervisor, Dr. Dwayne Hegedus for his scientific advices, kindness, encouragement and continuous support throughout my PhD program. Your extreme patience at every stage of my degree program, made the entire experience positively memorable and I will always be grateful.

My special thanks go to my co-supervisor Dr. Yangdou Wei for his insightful guidance, valuable suggestions and encouragement. I would like to thank Dr. Stephen Robinson for his assistance in RNA-Seq data analysis and Drs. Mohammad Hossein Borhan and Lisong Ma for providing advisory supports. I wish to express my appreciation to my research committee members Drs. Randy Kutcher, Christopher Todd and Chris Ambrose, who returned me thoughtful feedback and valuable comments. I would also like to thank Dr. Dilantha Fernando for agreeing to be my external examiner.

Special thanks also goes to Diney Bekkaoui, Cathy Coutu and Myrtle Harrington for their technical and analytical assistance. Your continuous support in the lab was invaluable in completion of my thesis research. I am also grateful to Drs. May Hijazi, Parham Haddadi and anyone who helped me in this project.

I thank the Saskatchewan Canola Development Commission and Canola Council of Canada, Agriculture and Agri-Food Canada and University of Saskatchewan for providing the financial support.

In the end, I am particularly indebted to my husband Ehsan whose love, endurance, continued support and encouragement enabled me to complete this degree. I also wish to express my heartfelt appreciation and gratitude to my parents, brother, sisters and their family. I will always be thankful to them for their strong support.

DEDICATION

To my husband who supported me with unconditioned love.

TABLE OF CONTENTS

LIST OF TABLES

CHAPTER 2

CHAPTER 3

LIST OF FIGURES

CHAPTER 2

CHAPTER 3

CHAPTER 4

LIST OF APPENDICES

LIST OF ABBREVIATIONS

ABC	ATP-binding cassette
Agro-infiltration	*Agrobacterium tumefaciens*-mediated transient expression
AtEV	*Agrobacterium tumefaciens* harboring the empty vector
Avr	Avirulence
CAZymes	Carbohydrate-active enzymes
CE	Carbohydrate esterase
CFEM	Common fungal extracellular membrane
CHS	Chalcone synthase
CRN	Crinkler
CWDE	Cell wall degrading enzymes
ddPCR	Droplet digital PCR
DMI	Demethylation inhibitor
ECS	*Escherichia coli* culture supernatants
ECSEV	*Escherichia coli* culture supernatants from empty vector control strains
ER	Endoplasmic reticulum
EST	Expressed sequence tag
ETI	Effector-triggered immunity
ETS	Effector-triggered susceptibility
FDR	False discovery rate
GFP	Green fluorescent protein
GH	Glycoside hydrolase
GO	Gene ontology
GPI	Glycosylphosphatidylinositol
GST	Glutathione S-transferase
hpi	Hours post-inoculation
hpif	Hours post-infiltration
HR	Hypersensitive reaction
IPTG	Isopropyl β-D-1-thiogalactopyranoside
LB	Luria-Bertani
LysM	Lysine motif

MAMP	Microbe-associated molecular pattern
MFS	Major facilitator superfamily
NADPH	Nicotinamide adenine dinucleotide phosphate
Nep	Necrosis and ethylene-inducing proteins
NES	Nuclear export signal
NGS	Next generation sequencing
NLP	Nep-like proteins
NLS	Nuclear localization signal
NRPS	Non-ribosomal peptide synthase
OA	Oxalic acid
OAH	Oxaloacetate acetyl hydrolase
PAMP	Pathogen-associated molecular pattern
PCA	Principal component analysis
PCD	Programmed cell death
PCS	*Pichia pastoris* culture supernatants
PCSEV	*Pichia pastoris* culture supernatants from empty vector control strains
PG	Polygalacturonase
PKS	Polyketide synthase
PM	Plasma membrane
PRR	Pattern recognition receptor
PTI	PAMP-triggered immunity
PVX	Potato Virus X
R	Resistance
RLK	Receptor-like kinases
RLP	Receptor-like proteins
ROS	Reactive oxygen species
RT	Reverse transcriptase
SP	Signal peptide
TF	Transcription factor
TM	Transmembrane
TMM	Trimmed means of means

TRV	Tobacco rattle virus
UPR	Unfolded protein response
VIGS	Virus-induced gene silencing

CHAPTER 1. INTRODUCTION AND LITERATURE REVIEW

1.1. General introduction

Oilseed rape or canola (*Brassica napus* L.) is one of the most economically important oil crops in Canada with an annual economic contribution of more than six billion dollars (https://www.canolacouncil.org/). *Sclerotinia sclerotiorum* causes stem rot, one of the most destructive diseases of canola in Canada, leading to yield losses of up to 50 % in epidemic years (https://www.canolacouncil.org/canola-encyclopedia/diseases/sclerotinia-stem-rot/).

The management of this disease relies mostly on the application of fungicides. Disease management has been a great challenge due to the wide host range of the pathogen and the relatively long survival time of the pathogen's sclerotia in the soil, rendering crop rotation insufficient for the control of this disease (Derbyshire and Denton-Giles, 2016). To date, only partial resistance to stem rot has been reported in *B. napus* and levels of resistance are not adequate in commercially available varieties (Derbyshire and Denton-Giles, 2016; Denton-Giles et al., 2018). Given these challenges, a more efficient control strategy for *S. sclerotiorum* based on developing new types of resistance is required.

To date, much effort has been directed toward understanding the interaction of hosts with *S. sclerotiorum* that could enable partial deciphering of the pathogenicity/virulence mechanisms (pathogenicity is the ability to cause disease, virulence is the degree of disease severity). However, understanding of these factors could lead to the identification of novel virulence mechanisms and strategies for improved resistance in the host plants. As cell death is the main consequence of *S. sclerotiorum* infection, characterizing the factors involved in the induction of cell death might unveil the potential for cell death inhibition as a mechanism for tolerance. Although, some cell death-inducing factors in *S. sclerotiorum* have been identified, many likely remain to be discovered.

This research was conducted within three main interconnected studies that addressed the main objective of this project, which was the identification and characterization of necrosis-inducing effectors of *S. sclerotiorum.* The first study focused on investigating how the *S. sclerotiorum* transcriptome is deployed in the *S. sclerotiorum-B. napus* interaction. In addition to providing a comprehensive overview of the factors contributing to the virulence of this pathogen, RNA-Seq analyses provided resources for characterizing gene expression patterns of the candidate

effectors. The second study focused on identifying candidate effectors of *S. sclerotiorum* through a combination of bioinformatics and RNA-Seq analyses. The candidate effectors were then expressed *in planta* to investigate their ability to induce cell death, subcellular localization, and finally their predicted host targets. The third study focused on characterizing a novel necrosis-inducing protein using a recombinant protein infiltration assay *in planta* and examination of domain(s) involved in necrotizing activity.

These studies provided insight into the molecular mechanisms, important genes and pathways involved in *S. sclerotiorum* infection and provided the knowledge required to devise effector-assisted breeding and genetic engineering of stem rot resistance in canola that could be utilized for cost-effective and environmentally safe methods of control.

1.2. Literature review

1.2.1. *Brassica napus*

Canola (*Brassica napus* L., genome AACC, 2n = 38) is one of the most important oil crops in the world and is grown extensively in Canada, Europe, Asia, Australia, and United states. In Canada, Saskatchewan has the largest seeded area among all the provinces. The estimated total production of canola in Canada was 19.2 million tonnes in 2018 of which 10.1 million tonnes was produced in Saskatchewan (https://www150.statcan.gc.ca/n1/daily-quotidien/180831/dq180831b-eng.htm). *B. napus* originated from natural interspecies hybridization between two phylogenetically close species, *B. rapa* (AA, 2n = 20) and *B. oleracea* (CC, 2n = 18) (Nagaharu, 1935; Rana et al., 2004). Some scholars believe that *B. napus* originated in the Mediterranean region, the same place where both wild *B. rapa* and *B. oleracea* originated (Song and Osborn, 1992). Canola is not only an important source of vegetable oil for human consumption, but is also utilized in other forms, for example for producing bio-fuels (Raman et al., 2012). Furthermore, the meal cake remaining after oil extraction from seeds is a source of feed for animals. Canola has been commercially grown in the western provinces of Canada since the early 20th century, as a supply of lubricant for steam engines its cultivation dramatically increased during World War II in order to secure the supply of industrial lubricants (https://www.canolacouncil.org/).

1.2.2. Canola diseases in Canada

Fungal, viral and bacterial diseases that attack at different growth stages threaten canola production in Canada. Stem rot or white mold caused by *S. sclerotiorum*, blackleg by *Leptosphaeria maculans*, black spot by *Alternaria* spp., clubroot by *Plasmodiophora brassicae*, seedling disease complex and root rot complex by *Rhizoctonia* spp., *Fusarium* spp. and *Pythium* spp. are the main fungal diseases of canola in Canada (https://www.canolacouncil.org/). Among these, stem rot is a significantly more damaging disease in Saskatchewan (http://www.agriculture.gov.sk.ca). Yield losses reported for *S. sclerotiorum* exceed 50% in some canola growing regions under epidemic conditions. The annual economic losses have been estimated $347 million on the Canadian prairies and the annual cost of fungicide application for stem rot control exceeds $220 million (https://www.canolacouncil.org/canola-encyclopedia/diseases/sclerotinia-stem-rot/).

1.2.3. *Sclerotinia sclerotiorum*

Sclerotinia sclerotiorum (Lib.) de Bary, a wide host-range necrotrophic fungus, is one of the most deleterious diseases of canola and causes lodging and severe yield losses. It belongs to the phylum Ascomycota and family Sclerotiniaceae (Willetts and Wong, 1980). Libert first described this pathogen as *Peziza sclerotiorum* in 1837, but Fuckel later changed the name to *Sclerotinia libertiana* when the genus Sclerotinia was described (Purdy, 1979). Wakefield then showed the inconsistency of this name with the international rules of Botanical Nomenclature and the fungus subsequently was renamed as *S. sclerotiorum* (Lib) and because de Bary was the first one to use this name in 1884, the proper name became *S. sclerotiorum* (Lib.) de Bary (Purdy, 1979).

Sclerotinia sclerotiorum is a host non-specific, widespread, necrotrophic pathogen that is known to cause disease in more than 400 plant species with the majority being dicotyledonous plant species (Boland and Hall, 1994). Although this pathogen is reported worldwide, it is more common in regions with a cool and wet growing season (Purdy, 1979). *Sclerotinia sclerotiorum* induces various types of disease symptoms in different host plants. Typically, stems close to where senescent petals collect exhibit watery lesions that quickly extend to the leaves. These lesions develop into necrotic zones and subsequently a layer of dense white mycelium appears on top, which is the most obvious symptom of diseases caused by *S. sclerotiorum* (Bolton et al., 2006).

The pathogen over-winters as hard and melanized sclerotia that germinate to release ascospores, the primary source of inoculum in the disease cycle for most hosts (Willetts and Wong A.,L., 1980). Depending on environmental conditions, sclerotia may produce either apothecia or mycelia, referred to as carpogenic and myceliogenic germination, respectively (Bolton et al., 2006).

After apothecia formation on the soil surface, ascospores are released into the air. Prior to direct infection of healthy and intact plant tissue, ascospores need a nutrient source to initiate infection, such as senescent or necrotic tissue, on which they germinate and colonize (Lumsden, 1979). The mycelia then penetrate the host cuticle by way of compound appresorium formation (Lumsden, 1979). As a necrotrophic pathogen, it then releases acids, enzymes and toxins to induce necrosis for tissue colonization and to destroy host tissue before it can mount a defense.

1.2.4. Infection mechanisms of *Sclerotinia sclerotiorum*

Based on their modes of nutrition and infection strategies, plant pathogens have been classified as biotrophs, necrotrophs and hemibiotrophs. Biotrophs obtain nutrients from living host plant cells and tissues and maintain their hosts alive, while necrotrophs kill the host as they feed and derive energy from dead or dying cells (Stergiopoulos and de Wit, 2009; Horbach et al., 2011). Hemibiotrophs have an early biotrophic phase followed by a necrotrophic phase in their life cycle (Horbach et al., 2011). As biotrophs need living host cells, they do not produce large amounts of hydrolytic enzymes; hence, they cause little damage to the host plant. For successful infection, biotrophs secrete small proteins (effectors) to suppress the host's immune system (Horbach et al., 2011). In contrast, necrotrophs secrete a variety of toxic molecules and hydrolytic enzymes to dissolve the plant tissues ahead of pathogen invasion or during colonization and use the disrupted plant tissues for growth. Infection by necrotrophs often triggers an oxidative burst in plants as a result of an accumulation of reactive oxygen species (ROS) in the challenged host cells. They also secrete various types of effectors to manipulate the host defense response and induce cell death. Research on the molecular mechanisms of virulence in *S. sclerotiorum* has focused on the inducers of cell death, which are a necessary and common mechanism of virulence in all necrotrophs. The main general factors contributing to cell death and necrosis in necrotrophs are oxalic acid (OA), hydrolytic enzymes (Collmer and Keen, 1986) and necrosis-inducing proteins.

1.2.4.1. Oxalic acid

OA is a key pathogenicity factor produced by necrotrophic fungi, such as *Botrytis cinerea* and *S. sclerotiorum* (Germeier et al., 1994). OA lowers host cell pH and sequesters calcium in the middle lamellae resulting in perturbed host cell wall integrity (Godoy et al., 1990). Williams et al., (2011) demonstrated that *S. sclerotiorum* produces a reducing environment in the host via OA that suppresses the oxidative burst and callose deposition during the early stages of the infection to overcome host defenses. At the late stage of infection, OA induces ROS production leading to host cell death (Williams et al., 2011). OA also enhances the activity of cell wall degrading enzymes (CWDE), such as polygalacturonase (PG), by creating an acidic environment favorable for PG attack on pectin in the middle lamella. Therefore, OA plays important and complex roles in infection processes. *Sclerotinia sclerotiorum* strains with UV mutations affecting OA biosynthesis lost their ability to induce disease, suggesting that OA is required for the development of disease symptoms (Godoy et al., 1990). However, recent studies showed that genetically mutated *S. sclerotiorum* is capable of causing disease on some plants in the absence of OA, suggesting that an unknown pH regulator could provide acidic pH, which is necessary condition for disease development (Liang et al., 2015a; Xu et al., 2015; Xu et al., 2018).

1.2.4.2. Hydrolytic enzymes

Host colonization by plant pathogenic fungi is facilitated by the production of a wide array of CWDEs, including pectinases, beta-1,3-glucanases, glycosidases, cellulases, xylanases and cutinases (Annis and Goodwin, 1997). During the interaction with its host, *S. sclerotiorum* secretes CWDEs that facilitate penetration, macerate tissues and degrade plant cell-wall components (Riou et al., 1991). Pectin is a major constituent of the plant cell wall and pectinases produced by *S. sclerotiorum* play a vital role in pectin degradation. The PGs are important pectinases that degrade un-esterified pectate polymers, the structural polysaccharides found in the middle lamella and the primary cell wall of higher plants. PG activity in *S. sclerotiorum* is induced by pectin or pectin monomers, such as galacturonic acid, but is repressed by the presence of simple sugars (Riou et al., 1992; Fraissinet-Tachet and Fevre, 1996; Li et al., 2004).

The regulation of *S. sclerotiorum* genes encoding PG1 (*SsPG1*) and cutinase (*SsCutA*) was studied by Bashi et al. (2012). They suggested that contact of mycelia with hard surfaces is an important factor for the expression of *SsPG1* during the earliest stages of the infection.

Carbohydrate starvation also triggered the transcription of *SsPG1*, while expression was inhibited by galacturonic acid (Bashi et al., 2012). *B. cinerea* is also dependent on pectinolytic enzymes for infection, but only *BcPG1* is necessary for full virulence (ten Have et al., 2002; ten Have et al., 1998). The expression of PG genes varies by host plant species, the type of tissues infected and the environment surrounding the infected tissues, suggesting that pectinolytic activities can be adapted to maximize virulence (ten Have et al., 2001).

In addition to pectinolytic CWDEs, non-pectinolytic enzymes like proteases, cellulases and glucoamylases are involved in *S. sclerotiorum* virulence (Riou et al., 1991; Poussereau et al., 2001b). Proteases are important for the virulence of *S. sclerotiorum* because protein forms about 10 % of host cell protoplasm (Carpita and Gibeaut, 1993). Aspartic protease is a cell death-inducing factor secreted by *S. sclerotiorum* and *B. cinerea* (Movahedi and Heale, 1990) and Poussereau et al. (2001) identified *aspS*, a gene encoding aspartyl protease in *S. sclerotiorum*.

1.2.4.3. Necrosis-inducing proteins

During the last decade it became clear that the molecular mechanisms underlying necrotrophic pathogen-plant interaction are more complex in nature than earlier thought and involve complicated recognition and signaling networks. Necrotrophic fungal pathogens and hemibiotrophs in their necrotrophic stage are known for their ability to induce cell death by deploying an armory of proteinaceous effectors, such as necrosis and ethylene-inducing (NEP)-like proteins (NLP). NLPs are secreted by various pathogens and were initially identified as toxic and cell death-inducing effectors in dicotyledonous plants (Pemberton and Salmond, 2004). *Sclerotinia sclerotiorum* secretes two NLPs, SsNep1 and SsNep2, that cause significant necrosis when infiltrated into plant tissues (Bashi et al., 2010). In addition, BcNep1 and BcNep2 have been identified in *B. cinerea* and exhibit necrosis-inducing activity (Staats et al., 2007). Not all NLPs have cell death-inducing activity, but both cytotoxic and non-cytotoxic NLPs activate the plant defense system following the recognition of a conserved 20 amino acid peptide by the host receptor-like kinase RLP23 (Cabral et al., 2012; Böhm et al., 2014; Albert et al., 2015).

Of the other *S. sclerotiorum* proteinaceous effectors, the cerato-plantanin effector (SsCP1) (Yang et al., 2018a), the small secreted virulence-related protein 1 (SsSSVP1) (Lyu et al., 2016) and the compound appressorium formation-related protein 1 (Ss-Caf1) (Xiao et al., 2014), have also been shown to induce cell death in host plants.

1.2.5. Effector proteins and functions

1.2.5.1. Effectors of plant pathogens

Most pathogens deliver an array of effectors into the host plant, the composition of which is dependent upon their particular virulence strategy and the plant defense response that they encounter at different stages of the infection in order to suppress these defenses. Effectors have numerous functions based on their targets location and their biological and molecular function in plant cells (Khan et al., 2018). Effectors contributing to host infection are known as virulence factors, while those triggering plant defense systems are known as avirulence (Avr) effectors. Pathogens deliver effectors either to the extracellular or inside the plant cell (cytoplasm) where they function to disarm host defense responses employed to restrict pathogen growth, unless they are recognized and trigger host plant defense.

Effectors can target multiple locations in plant cells. Bacterial effectors are mostly localized in the plasma membrane (PM), nucleus and/or cytoplasm, but a large number of oomycete effectors localize to the peroxisome and endoplasmic reticulum (ER), and most fungal effectors localize to the cytoplasm (Khan et al., 2018). Effectors can target single or multiple host proteins, for example the majority of bacterial effectors target multiple proteins and have multiple functions in the plant cell (Khan et al., 2018). The contribution of each effector to virulence may be different. Some are individually required for full virulence, such as Avr3 (Six1) of *Fusarium oxysporum* f. sp. *lycopersici* (Rep et al., 2004), while others work collectively to contribute to virulence, hence, their individual contribution to virulence is not easily detectable. For example, Avr1 (Six4) of *F. oxysporum* f. sp. *lycopersici* is not a virulence factor, but suppresses I-3-mediated resistance triggered by Avr3 (Six1) (Houterman et al., 2008).

1.2.5.2. Effector discovery

Characterization of pathogen effectors has been challenging due to the lack of genome sequences and tools for high-throughput functional analysis. Recently, various genetic, biochemical, and computational approaches have been used to predict effector repertoires. Map-based cloning is one of the strategies that have been used for cloning of effector genes, for example, AvrLm4-7 effector of *Leptosphaeria maculans* was cloned using this approach (Parlange et al., 2009). Low cost and high-throughput next generation sequencing (NGS)

methods has allowed whole genome sequencing of several hundred fungal pathogens enabling computational analysis of the secretomes, transcriptomes and proteomes (Stergiopoulos and de Wit, 2009). Transcriptomics analysis based on NGS, such as RNA-Seq of fungal pathogens during host infection by various pathogenic isolates or mutants and at multiple stages of infection, is a useful strategy to predict candidate effectors (Jones et al., 2018). Analysis of expressed sequence tag (EST) libraries to identify up-regulated genes during infection was used for identification of the *Melampsora lini* AvrL567 effector (Dodds et al., 2004). Sequence homology searches can also be used for the identification of potential effectors, for example, this approach led to the identification of homologues of the *Cladosporium fulvum* effector genes *Avr4*, *Ecp2*, and *Ecp6* in the genome of the banana pathogen *Mycosphaerella fijiensis* (Stergiopoulos and de Wit, 2009). In addition, *in silico* effector prediction pipelines have been developed that combine different bioinformatics tools to identify candidate effectors (Raffaele et al., 2010; Laurie et al., 2012). Using *in silico* pipelines, 200 putative effectors of *M. lini* (Nemri et al., 2014) and 78 *S. sclerotiorum* effectors (Guyon et al., 2014) were identified. Due to the large number of candidate effectors identified through *in silico* pipelines, they are usually prioritized and filtered to exclude false positive candidates, which might not have an actual function in plant-pathogen interactions. Hierarchical clustering can be applied to exclude groups containing known non-effectors or members with non-effector-like properties (Saunders et al., 2012). Alternatively, machine-learning approaches are used to decrease the number of false positive effectors (de Guillen et al., 2015). Taken together, combinational approaches involving transcriptomics, comparative genomics, and bioinformatics are the best to identify reliable effector candidates (Jones et al., 2018). Given the availability of a large number of pathogen genomes, bioinfomatics tools serve as a valuable strategy for identification of candidate effectors; however, the function of these putative effectors still need to be confirmed by experimental approaches, such as *Agrobacterium tumefaciens*/Potato Virus X (PVX)-mediated expression in host plants, overexpression, and gene disruption or silencing in fungal isolates followed by subsequent virulence assays on host plants.

1.2.5.3. Translocation of effectors into plant cells

Effectors from different groups of phytopathogens, such as bacteria, oomycetes, and fungi, can enter plant cells by various mechanisms. For example, bacteria have six secretory systems of

which the type II, III and IV secretion systems deliver effectors into plant cells (Lindeberg et al., 2006; Cunnac et al., 2009). Oomycete effector translocation to the plant cell mostly relies on a host targeting signal domain with a conserved motif, such as RXLR, CRN or CHxC amino acid sequences. The genome of the potato pathogen *Phytophthora infestans* encodes 425 secreted RXLR proteins (Jiang et al., 2008; Khan et al., 2018). Similar to oomycetes, fungal effectors have an N-terminal secretion signal peptide that is essential for secretion outside of the pathogen cell (von Heijne, 1998); however, they lack a conserved signature for translocation into host cells. Based upon distinct infection lifestyles, fungi have different effector delivery systems; biotrophic and hemibiotrophic fungal pathogens use specialized infection structures, such as appressoria or haustoria, for effector delivery (Selin et al., 2016). For example, rust or powdery mildew fungi use haustorium that develop within the mesophyll cells (Selin et al., 2016), whereas, necrotrophs lack such specialized infection structures.

1.2.5.4. Recognition of effectors by plants

All pathogens, regardless of their different lifestyles, may be recognized by plants and activate plant defense system. Plants are able to sense invading pathogens, due to a combination of localized PM and intracellular receptors (Jones and Dangl, 2006). The initial defense response is triggered within the plant apoplast by recognition of pathogen-associated molecular patterns (PAMP), such as bacterial proteins, Tu elongation factors, flagellin, and fungal cell wall components, such as polysaccharides and chitin (Selin et al., 2016). PAMPs are recognized by membrane-localized pattern recognition receptors (PRRs) and induce the first layer of defense responses called PAMP-triggered immunity (PTI) (Jones and Dangl, 2006). To facilitate infection, pathogens needs to suppress PTI through secreting effectors; however, PTI-suppressing effectors can also be recognized by the plant surveillance system and trigger a second wave of defense response known as effector triggered immunity (ETI). Resistance (R) proteins, which are often from the intracellular nucleotide-binding leucine rich repeat receptor (NB-LRR) family, are involved in direct or indirect recognition of effectors and subsequently ETI activation (Cui et al., 2015). ETI activation usually ends in a hypersensitive reaction (HR) that plays a contrasting role in the plant defense response against pathogens with different lifestyles and infection strategies (Jones and Dangl, 2006; Mukhtar et al., 2016). HR-associated cell death leads to resistance against biotrophs by eliminating nutrient supply, while necrotrophs use HR as their infection

strategy and this type of recognition is known as effector-triggered susceptibility (ETS) (Mukhtar et al., 2016). *Cochliobolus victoriae*, the causal agent of Victoria blight of oats, secretes victorin, which is recognized by the R-protein Vb in oat and the Locus Orchestrating Victorin effects 1 (LOV1) in *Arabidopsis thaliana*, and leads to susceptibility (Navarre and Wolpert, 1999; Lorang et al., 2004; Lorang et al., 2007).

1.2.5.5. Roles of effector proteins in plant-pathogen interactions

Effectors secreted by pathogens play different roles in penetration and colonization of host plants. They may facilitate pathogen penetration into the host by breaking the physical barriers of plant, for example, *Pseudomonas syringae* secretes the phytotoxin coronatine that interferes with plant hormone signaling to open the stomata and allow the pathogen to enter (Melotto et al., 2006). Some effectors disarm host anti-microbial hydrolytic enzymes in the apoplastic compartment, like the glucanase inhibitors GIP1 and GIP2 that are secreted by *P. sojae* to escape the enzymatic activity of the soybean endo-beta-1,3 glucanase EGaseA (Rose et al., 2002). Effectors containing the lysine motif (LysM) interfere with host detection of the pathogen by binding to and masking fungal cell wall–derived chitin fragments that would normally induce host defense responses (Mentlak et al., 2012). Avr4 and Ecp6 secreted by *C. fulvum* have overlapping functions in protecting the pathogen cell wall from plant chitinases or keeping chitin fragments from inducing plant immune responses (Libault et al., 2007; Bolton et al., 2008). A number of effectors are involved in suppression of PTI by suppressing the defense signaling cascade. For example, the AvrPto and AvrPtoB type III effectors of *P. syringae* suppress multiple PAMP-mediated signaling pathways upstream of MAPKKK at the PM linked to the receptor (He et al., 2006). Other effectors are involved in suppression of R gene-triggered resistance, for example, AVR2 and AVR3 secreted by *F. oxysporum* f.sp. *lycopersici* are recognized by resistance proteins I-2 or I-3, respectively, in resistant genotypes. The virulent strain of *F. oxysporum* f. sp. *lycopersici* secretes AVR1, a small cysteine-rich protein that suppresses the resistance triggered by I-2 and I-3 (Rep, 2005; Houterman et al., 2008). A number of effectors interfere with hormone signaling networks in plants in order to disturb plant growth, development or defense responses, for example, *P. sojae* and *Verticillium dahliae* secrete Pslsc1 and Vdlscl that disrupt salicylic acid biosynthesis to suppress salicylate-mediated innate immunity (Liu et al., 2014; Toruno et al., 2016). Plant gene expression is another important target of some

effectors. The RxLR effector Pi03192 secreted by *P. infestans* targets host NAC transcription factors and interferes with their functions in the host by preventing their relocalization from the ER to the nucleus (McLellan et al., 2013). *Xanthomonas oryzae* pv. *oryzae* secretes the transcriptional activator-like (TAL) effector, PthXo1, that binds to the promoter of *OsSWEET11* in rice, a sucrose transporter gene. Higher expression of *OsSWEET11* facilitates sugar export for bacterial consumption and pathogenicity (Yang et al., 2006; Chen et al., 2010).

Several CWDEs may act as necrosis-inducing effectors independent of their enzymatic activity, such as BcXyl1 (Yang et al., 2018b), BcXyn11A (Brito et al., 2006; Noda et al., 2010) and BcXYG1 (Zhu et al., 2017), secreted xylanases and xyloglucanase, respectively, from *B. cinerea* that induces cell death in the plant. Crinkler (CRN) effectors are also necrosis-inducing effectors that are mostly secreted by oomycetes (Schornack et al., 2010; Toruno et al., 2016). These effectors carry an N-terminal LxFLAK translocation domain and cause leaf crinkling (Schornack et al., 2010; Toruno et al., 2016). The *P. infestans* CRN8 effector has kinase activity and localizes to the nucleus, and interferes with host signaling pathways during infection leading to cell death induction (Schornack et al., 2010; van Damme et al., 2012).

Necrotrophs also secrete effectors that can be recognized by corresponding host receptors, encoded by susceptibility genes, which function in opposite of ETI and result in disease susceptibility rather than resistance (Wolpert et al., 2002). *Stagonospora nodorum* and *Pyrenopora tritici-repentis* secrete the effectors TOXA, SnTOX1, SnTOX2, SnTOX3 and SnTOX4 that interact specifically with host susceptibility receptors in wheat, namely Tsn1, Snn1, Snn2, Snn3 and Snn4, respectively, to induce necrosis and promote disease (Oliver et al., 2012; Wang et al., 2014).

1.3. Research objectives

i) To understand the sequential expression of *S. sclerotiorum* virulence factors during infection of *B. napus* using RNA-Seq analyses.

ii) To evaluate *S. sclerotiorum* candidate effectors identified through transcriptomic and bioinformatic analyses using *in planta* expression to identify novel necrosis-inducing effectors.

iii) To determine the subcellular localization of candidate effectors in the host plant and to conduct functional analyses of novel necrosis-inducing effectors.

CHAPTER 2. CHANGES IN THE *SCLEROTINIA SCLEROTIORUM* TRANSCRIPTOME DURING INFECTION OF *BRASSICA NAPUS*

This chapter has been published as a refereed journal article in BMC Genomics.
Seifbarghi S., Borhan M.H., Wei Y., Coutu C., Robinson S.J., Hegedus D.D. 2017. Changes in the *Sclerotinia sclerotiorum* transcriptome during infection of *Brassica napus*. BMC Genomics 18: 266.

Authors' contributions:

SS, DH, YW and HB designed the study. SS performed the experiments. SS, CC and SR analyzed the RNA-Seq data. SS and DH wrote the manuscript. DH, YW and HB revised the manuscript. All authors read and approved the final manuscript. All authors agreed upon presenting this as a chapter of SS Ph.D. thesis.

2.1. Abstract

Sclerotinia sclerotiorum causes stem rot in *B. napus*, which leads to lodging and severe yield losses. Although recent studies have made significant progress in the characterization of individual *S. sclerotiorum* pathogenicity/virulence factors, a gap exists in profiling gene expression throughout the course of *S. sclerotiorum* infection on a host plant. In this study, RNA-Seq analysis was performed with a focus on the events occurring through the early (1 hour) to the middle (48 hours) stages of infection. Transcript analysis revealed the temporal pattern and amplitude of the deployment of genes associated with aspects of pathogenicity or virulence during the course of *S. sclerotiorum* infection on *B. napus*. These genes were categorized into eight functional groups: hydrolytic enzymes, secondary metabolites, detoxification, signaling, development, secreted effectors, oxalic acid and reactive oxygen species production. The induction patterns of nearly all of these genes agreed with their predicted functions. Principal component analysis delineated gene expression patterns that signified transitions between pathogenic phases, namely host penetration, ramification and necrotic stages, and provided

evidence for the occurrence of a brief biotrophic phase soon after host penetration. The current observations support the notion that *S. sclerotiorum* deploys an array of factors and complex strategies to facilitate host colonization and mitigate host defenses. This investigation provides a broad overview of the sequential expression of virulence/pathogenicity-associated genes during infection of *B. napus* by *S. sclerotiorum* and provides information for further characterization of genes involved in the *S. sclerotiorum*-host plant interactions.

2.2. Introduction

Sclerotinia sclerotiorum causes one of the most devastating diseases of canola, stem rot. This pathogen has a wide host-range and can infect more than 400 plant species, including many other important crop plants (Boland and Hall, 1994). This fungus was long considered to be a prototypical necrotrophic pathogen whereby immediately upon host cuticle penetration a highly aggressive pathogenic phase ensues where acids and hydrolytic enzymes are liberated in advance of the invading mycelia with a trailing saprophytic phase that supports sclerotia formation (Hegedus and Rimmer, 2005). Recent studies, however, have provided evidence for a brief biotrophic phase occurring within the apoplastic space immediately after cuticle penetration and the pathogen may, therefore, be more accurately classified as a hemi-biotroph (Kabbage et al., 2015). Transition between these various developmental and pathogenic phases is governed by physical and metabolic cues including detection of contact with hard surfaces (Bashi et al., 2012), glucose levels (Vautard-Mey et al., 1999), cAMP levels (Jurick II and Rollins, 2007), pH (Rollins, 2003) and oxidative stress (Kim et al., 2011). Communication between the associated signaling pathways is critical and involves numerous protein kinases (Chen and Dickman, 2005; Duan et al., 2013; Hegedus et al., 2016) and phosphatases (Harel et al., 2006; Erental et al., 2007).

Much of the research on the molecular mechanisms of virulence in *S. sclerotiorum* has focused on OA, which plays various roles during several stages of the infection (Godoy et al., 1990). OA suppresses the oxidative burst and callose deposition during the early stages of the infection (Williams et al., 2011). Suppression of host defenses by OA during the biotrophic phase is thought to allow sufficient time for the pathogen to establish itself in the host as a prelude to mycelial ramification (Kabbage et al., 2015). Subsequently, OA induces the production of host ROS, which in turn leads to host cell death (Kim et al., 2008). As a central player in *S. sclerotiorum* pathogenesis, it is not surprising that plants expressing oxalate-degrading enzymes

exhibit increased resistance to this pathogen (Calla et al., 2014). Pathogen-derived ROS generated through NADPH oxidase activity are associated with appressoria formation and sclerotial development, as well as oxalic acid synthesis (Kim et al., 2011). Catalase (SCat1) (Yarden et al., 2014) and superoxide dismutase (SsSodI) (Xu and Chen, 2013) appear to modulate the deleterious effects of these compounds internally. The apoptosis inhibitor, BAX inhibitor-1 (SsBI1), is also required for full virulence and was postulated to prevent hyphal apoptosis resulting from exposure to host-derived ROS (Yu et al., 2015).

The production of numerous types of hydrolytic and CWDEs facilitates host cuticle penetration, lesion expansion and tissue maceration (Poussereau et al., 2001a; Poussereau et al., 2001b; Bashi et al., 2012). Although pectinolytic CWDEs, such as SsPG1, SsPG3, SsPG5 and SsPG6, have captured more attention as the main group of hydrolytic enzymes involved in *S. sclerotiorum* virulence (Li et al., 2004), non-pectinolytic enzymes like proteases, cellulases and glucoamylases also contribute to the infection process in this fungus (Poussereau et al., 2001a).

Several other factors are known to contribute to *S. sclerotiorum* pathogenicity and host interactions. Both γ-glutamyl transpeptidase (SsGgt1) and Ss-Caf1 influence the production of compound appressoria and subsequent host penetration, but also development of sclerotia (Li et al., 2012; Xiao et al., 2014). A secreted integrin-like protein (SSITL) inhibits the deployment of plant defenses through the jasmonic/ethylene signaling pathways (Zhu et al., 2013) and a chorismate mutase (SsCm1) may function similarly to suppress plant defense responses during the biotrophic phase (Kabbage et al., 2013). Host chemical defenses may be inactivated by inducible detoxification systems (Pedras et al., 2004), while other proteins, such as SsPemG1 (protein elicitor from *Magnaporthe grisea*), are recognized by the host and induce defenses (Pan et al., 2015). SsNep1 and SsNep2 encode NLP proteins, which induce necrosis in host tissues (Bashi et al., 2010), as does cutinase (Zhang et al., 2014a). SsCP1 (Yang et al., 2018a) and SsSSVP1 (Lyu et al., 2016) also induce cell death in host plant. A gene (SS1G_00263, ssv263) encoding a hypothetical protein with unknown mode of action is a virulence factor in *S. sclerotiorum* (Liang et al., 2013).

Transcriptomics and proteomics approaches have been used to gain insight into molecular interaction of *S. sclerotiorum* with its various hosts. EST analysis was used to identify genes associated with pathogenesis by comparing the transcriptome of *S. sclerotiorum* grown on artificial medium to that during infection of *B. napus* (Li et al., 2004). A similar approach was

used to identify genes expressed during different stages of *S. sclerotiorum* development on this host (Sexton et al., 2006), which was later supported by proteomics analysis (Liang et al., 2010). Subsequently, microarray (Zhao et al., 2009) and RNA-Seq analysis (Joshi et al., 2016) were used to explore the *B. napus* responses to *S. sclerotiorum*. The release of the *S. sclerotiorum* genome sequence (Amselem et al., 2011) in combination with next generation sequencing has allowed for in-depth analysis of the *S. sclerotiorum*-pea (Zhuang et al., 2012), *S. sclerotiorum*-*Phaseolus vulgaris* (Oliveira et al., 2015) and *S. homoeocarpa*-creeping bentgrass (Orshinsky et al., 2012) pathosystems. Proteomic analysis of exudates from liquid cultures has identified several secreted proteins that may be involved in aspects of pathogenesis (Yajima and Kav, 2006). Bioinformatics studies revealed that *S. sclerotiorum* has the potential to secrete a large number of proteins, many of which have the potential to influence host-pathogen interactions (Guyon et al., 2014; Heard et al., 2015).

While significant progress has been made in the characterization of individual *S. sclerotiorum* virulence and pathogenicity factors, a gap exists in our understanding of how the transcriptome is deployed throughout the course of *S. sclerotiorum* infection on a host plant. In this study, I used RNA-Seq analysis to comprehensively catalogue genes that were expressed and up-regulated during infection of *B. napus*, with a particular focus on the events occurring early in the infection. This work provided new insight into *S. sclerotiorum* pathogenesis through examination of the sequential expression of virulence and pathogenicity genes during infection establishment.

2.3. Methods

2.3.1. Biological materials and disease assay

Sclerotinia sclerotiorum isolate 1980 was used in this study as the genome sequence of this strain is available (Amselem et al., 2011). The doubled haploid *B. napus* cultivar DH12075 for which a genome sequence is available (Parkin, unpublished) was used as the host plant. *Sclerotinia sclerotiorum* was grown on minimal salts-glucose (MS–Glu: 2 g/L NH_4NO_3, 1 g/L KH_2PO_4, 0.1 g/L $MgSO_4 \cdot 7H_2O$, 0.5 g/L yeast extract, 3 g/L DL-malic acid, 1 g/L NaOH, supplemented with 1% glucose) medium and mycelia were used for inoculation as described earlier (Li et al., 2004). One gram of mycelia (wet weight) was spread over a 5-cm diameter circle on a detached leaf of a four-week-old plant and incubated in a sealed and humidified tray at room temperature. The experiment was conducted with three biological replicates. Samples collected from the fungal isolate grown in culture and on plants at 1, 3, 6, 12, 24 and 48 hours

post-inoculation (hpi) were subjected to RNA-Seq analysis.

2.3.2. RNA extraction, library preparation and Illumina sequencing

Fungal mats and the infected plant tissues beneath it were flash-frozen in liquid nitrogen and stored at -80 °C. The samples were ground to a fine powder with an RNAse-free mortar and pestle precooled with liquid nitrogen. Total RNA was extracted using an Illustra RNAspin mini RNA isolation kit (Illumina, San Diego, USA). RNA quantity and quality was assessed using a Qubit fluorometry assay (Invitrogen, Carlsbad, USA) and an Agilent 2100 Bioanalyzer (Agilent Technologies, Palo Alto, CA, USA), respectively. Libraries were prepared using a Truseq stranded mRNA kit (Illumina, San Diego, USA) following the manufacturer's instructions. Sequencing was conducted on an Illumina MiSeq sequencing system using the Illumina MiSeq reagent kit V3 (Illumina, San Diego, USA) following the manufacturer's instructions.

2.3.3. Data analysis

Sclerotinia sclerotiorum transcripts available in the database (http://www.broadinstitute.org/annotation/genome/sclerotinia_sclerotiorum/MultiHome.html) were used as a reference for mapping the short reads using CLC Genomics Workbench 7.0.4 (http://www.clcbio.com). Gene expression was estimated by extracting read counts as integers from the CLC Genomics alignments. The count data were normalized to generate effective library sizes using the scaling method Trimmed Means of Means values (TMM) (Robinson and Oshlack, 2010). Statistical analysis was performed with these data using a generalized linear model linked to the negative binomial distribution performed using the EdgeR package (Robinson and Oshlack, 2010). Pair-wise analyses were performed to assess differential gene expression using the control library as a common reference standard. Genes were considered differentially expressed when the probability after adjustment for multiple hypothesis testing [false discovery rate (FDR)] was less than 0.05. The extent of the observed differential expression was considered meaningful if the fold change exceeded a factor of two. Finally, all significantly up-regulated genes at different sampling times were assigned a functional classification using the BLAST2GO plugin (v1.4.4) in the CLC Genomics Workbench 8.0.1 for functional annotation using Interpro and the NCBI refseq protein database. Gene ontology (GO) terms for each gene were extracted. The results were filtered to remove top-level

annotations and apply the GO-slim categorization from Aspergillus in order to summarize the results. ANNEX in Blast2GO (Myhre et al., 2006) was used to add implicit GO terms for a more complete annotation. Finally, Blast2GO was used to calculate the abundance of GO classifications for the significantly up-regulated genes for each time point. Candidate genes were categorized into different groups based on known functions of orthologous genes in other fungi.

2.3.4. Validation of RNA-Seq analysis using droplet digital PCR (ddPCR)

cDNA was synthesized from 1µg of total RNA using the iScript Reverse Transcription Supermix for RT-qPCR kit (Bio-Rad, CA, USA) following the manufacturer's instructions. The ddPCR was conducted with three biological replicates using a droplet digital PCR QX200 system (Bio-Rad, CA, USA). No-reverse transcriptase (no-RT) controls were also used to detect genomic DNA contamination. Primers and probe for each gene were designed using the PrimerQuest tool (IDT) and all probes were labeled with fluorescein amidite (FAM), except for the reference gene (β-tubulin), which was labeled with hexachloro-fluorescein (HEX). Sequences and details of the primers and probes have been provided in Table A.1. The ddPCR reaction mixtures (20 µl) contained 1X ddPCR supermix (Bio-Rad, CA, USA), 900 nM of each primer, 250 nM of probe and 4 µl of 1:100 diluted cDNA. The PCR was performed in a C1000 Touch Thermal Cycler (Bio-Rad, CA, USA) with the following cycling conditions: 95°C for 10 min; 50 cycles of 94°C for 30 s, 53°C for 75 s, Ramp 2°C/s; 98°C for 10 min. The droplet generation and reading for ddPCR were conducted using a Droplet Generator and Reader (Bio-Rad QX200 system), respectively, according to the manufacturer's instructions. The gene expression ratio was calculated using the QuantaSoft droplet reader software (Bio-Rad, CA, USA). The expression of the β-tubulin gene (SS1G_ 04652) is constant during the infection, confirming its validity as a reference gene. The fold change in the expression of each gene was calculated by dividing the ratio of the target to the reference (β-tubulin) gene for each time point by the ratio from the sample collected from fungi grown in culture (i.e. time zero).

2.4. Results and discussion

2.4.1. RNA sequencing

Illumina sequencing (RNA-Seq) was used to conduct sequential transcriptional profiling in order to identify differentially expressed genes involved in *S. sclerotiorum* establishment on and subsequent infection of *B. napus*. Mycelia were collected from liquid media immediately prior to

inoculation (time 0) and at 1, 3, 6, 12, 24 and 48 hpi. The number of reads per each biological replicate per each time point is shown in Table A.2. A total of 40,210,134 paired-end reads were generated. Reads mapped to 14,503 of the 14,522 predicted genes (99% of total reference transcripts), indicating sufficient sequencing depth. Genes with expression ratios greater than two relative to the inoculum grown on MS-Glu medium and a false discovery rate (FDR) p-value correction of < 0.05 were considered to be up-regulated. The numbers of up-regulated genes were 584, 582, 526, 371, 822 and 1283 at 1, 3, 6, 12, 24 and 48 hpi, respectively, ranging from 2.6% to 8.8% of total expressed genes. The RNA-Seq data was submitted to NCBI (accession # GSE83935).

To confirm the relatedness of the three biological replicates and the accuracy of the RNA-Seq analysis, principal component analysis (PCA) was conducted (Fig. 2.1). Individual replicates of each time point clustered together, indicating a high degree of similarity in the expression profiles and low biological variability among the experimental replicates. Of the early infection time points sampled (1-12 hpi), the 1 hpi sample was most different from the zero time point with successive early time points becoming increasingly more similar to the inoculum. PCA also showed a clear distinction between the *S. sclerotiorum* transcriptomes at 24 and 48 hpi compared to the other time points, which was due to a significant increase in both the number and types of genes expressed at these time points.

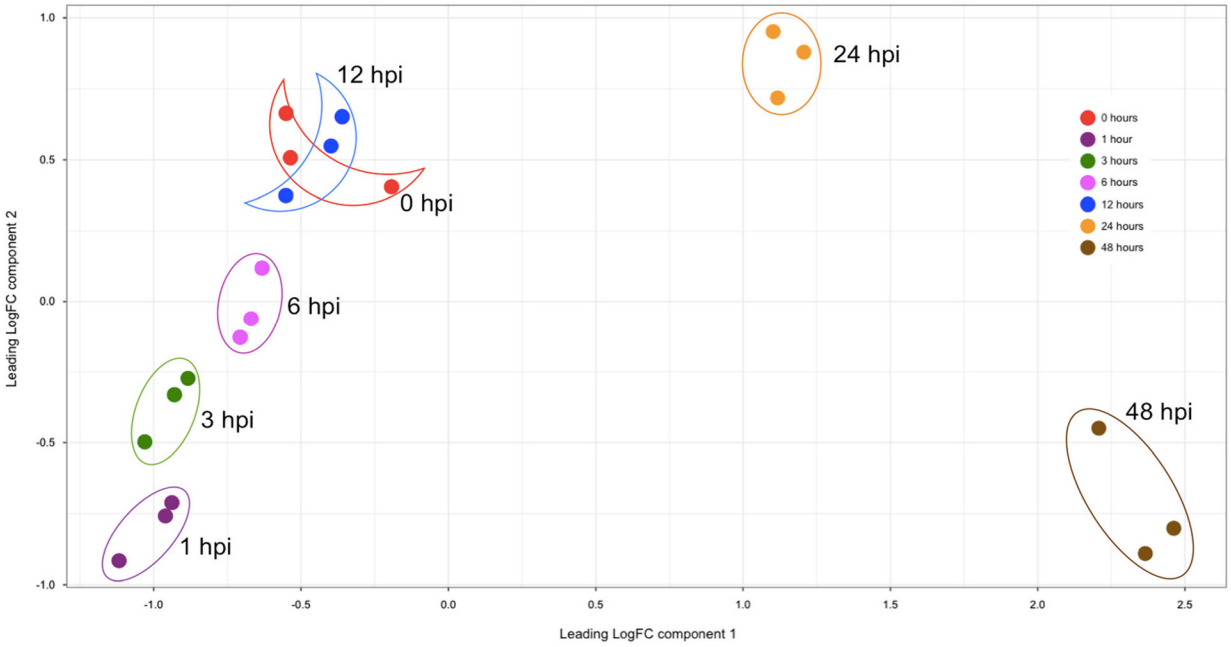

Fig. 2.1 Principal component analysis showing the relatedness among the gene expression patterns of samples used for RNA-Seq analysis. Samples were collected from the inoculum (0 time) and at 1, 3, 6, 12, 24 and 48 h post *Sclerotinia sclerotiorum* inoculation on *Brassica napus* leaves in three biological replicates.

2.4.2. Gene ontology analysis of up-regulated genes

To obtain an overall view of the genes involved in *S. sclerotiorum* infection, gene ontology (GO) analysis of the up-regulated genes was performed. Blast2GO using different forms of annotations, including Interpro, GOslim, enzyme code and Annex, was used to calculate the abundance of GO classifications in each of these ontology categories, molecular function (Fig. 2.2) and biological processes (Fig. 2.3) for each time point. In total, 25%, 25%, 26%, 22%, 15% and 18% of the up-regulated genes at the 1, 3, 6, 12, 24 and 48 hpi sampling times, respectively, were annotated as encoding proteins with unknown functions and, therefore, could not be assigned to a GO category. The majority of up-regulated genes in the molecular function group fell into the subcategories of oxidoreductase and hydrolase activity at all sampling times. The highest proportion of up-regulated genes belonging to oxidoreductase and hydrolase activity subcategories was at 24 hpi, and declined at 48 hpi coincident with the appearance of visible necrotic lesions. For the other molecular function subcategories, genes classified as encoding proteins with transferase, transporter, protein binding, DNA binding, protein kinase and signal

transducer activity, the lowest proportion of up-regulated genes was at 48 hpi, suggesting a decrease in the expression of these genes after the start of necrotic stage.

The majority of up-regulated genes within the biological processes category belonged to carbohydrate metabolic process subcategory. The highest proportion of genes within this subcategory was found at 24 hpi, with a notable increase compared with 12 hpi, and a decline by 48 hpi, similar to the hydrolytic activity subcategory. This supports the connection between carbohydrate metabolic activity and hydrolytic enzyme activity as these processes work in concert to supply nutrients and energy for mycelial proliferation and to facilitate the transition to the necrotrophic phase occurring beyond 24 hpi in this experimental system.

The highest proportion of up-regulated genes related to transcription and signal transduction was observed at 1 and 3 hpi, respectively. This was expected, as the pathogen needs to modulate the expression of a wide variety of developmental and metabolic genes during the early stages of the infection as it penetrates the host cuticle and then establishes within the host. Beyond this, the 6 hpi time point had the highest percentage of up-regulated genes involved in response to stress. This is likely a response to the exposure of the pathogen to host plant defense mechanisms. Kabbage et al. (2015) proposed that a brief biotrophic phase occurs soon after cuticle penetration where the pathogen either remains undetected or compromises/tolerates host defenses. The induction of stress-related genes soon after cuticle penetration would alleviate some of the effects of these stress conditions and allow host colonization. Interestingly, after events leading to cuticle penetration (1 hpi), dramatic changes in gene expression appear to subside as the overall gene expression profiles at 3, 6 and 12 hpi become increasingly similar to that of the inoculum at time 0 (Fig. 2.1). This period may constitute the biotrophic phase, which is followed by a mycelial ramification phase (24 hpi) and finally a necrotic phase (48 hpi), each of which has unique expression profiles. This is in accordance with the gene expression profiles of *B. cinerea* on *Arabidopsis thaliana* leaves where three distinct groups of genes were identified, these being early, onset of colonization and complete colonization, based on expression patterns (Gioti et al., 2006).

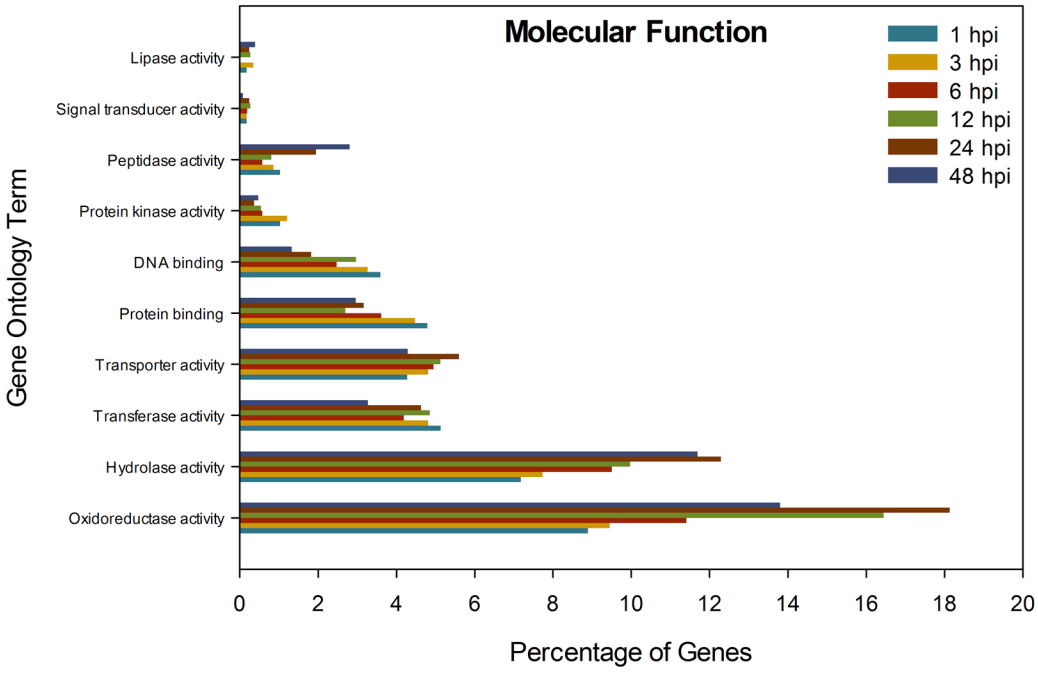

Fig. 2.2 Percentage of *Sclerotinia sclerotiorum* genes encoding enzymes assigned to Molecular Function subcategories that were up-regulated during *Brassica napus* infection. Gene ontology analysis was conducted using Blast2Go software. hpi, hours post-inoculation.

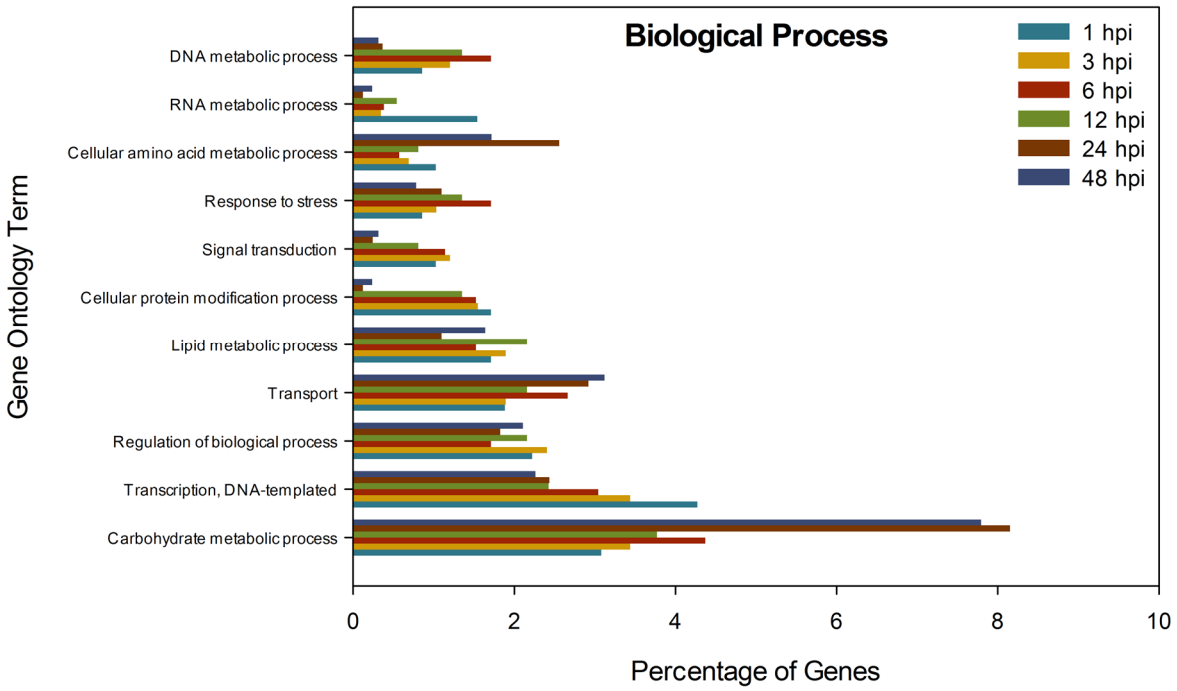

Fig. 2.3 Percentage of *Sclerotinia sclerotiorum* genes encoding enzymes assigned to Biological Process subcategories that were up-regulated during *Brassica napus* infection. Gene ontology analysis was conducted using Blast2Go software. hpi, hours post-inoculation.

2.4.3. Validation of RNA-Seq analysis using droplet digital PCR (ddPCR)

Three different types of genes from the RNA-Seq data list were selected for validation, including three highly expressed genes that were induced in most of the sampling times (SS1G_07027, SS1G_07661 and SS1G_08104, genes encoding a hypothetical protein cutinase and acetylxylan esterase, respectively), three that were not induced during the sampling time points (SS1G_14133, SS1G_02486 and SS1G_05839, genes encoding SSITL, SsCaf1 and SsBi1, respectively) and four well-characterized *S. sclerotiorum* genes (SS1G_08218, SS1G_10796, SS1G_10167 and SS1G_07355, encoding oxaloacetate acetyl hydrolase (OAH), oxalate decarboxylase, SsPG1 and the Pac1 transcription factor, respectively). The ddPCR analysis generated patterns of expression for the induced genes that were very similar to that predicted from the RNA-Seq data (Fig. 2.4). Only one out of the seven genes (SS1G_08104) tested showed a slightly different trend between ddPCR and RNA-Seq. Previous work showed about 90% correlation between qPCR and RNA-Seq (De Cremer et al., 2013) suggesting that slight variation between the two methods is expected, but is generally negligible. Furthermore, for the three genes that were not induced in the RNA-Seq analysis, the fold-change in expression did not

exceed a factor of 2 when examined by ddPCR, providing additional evidence that they were not induced in the current study (data not shown).

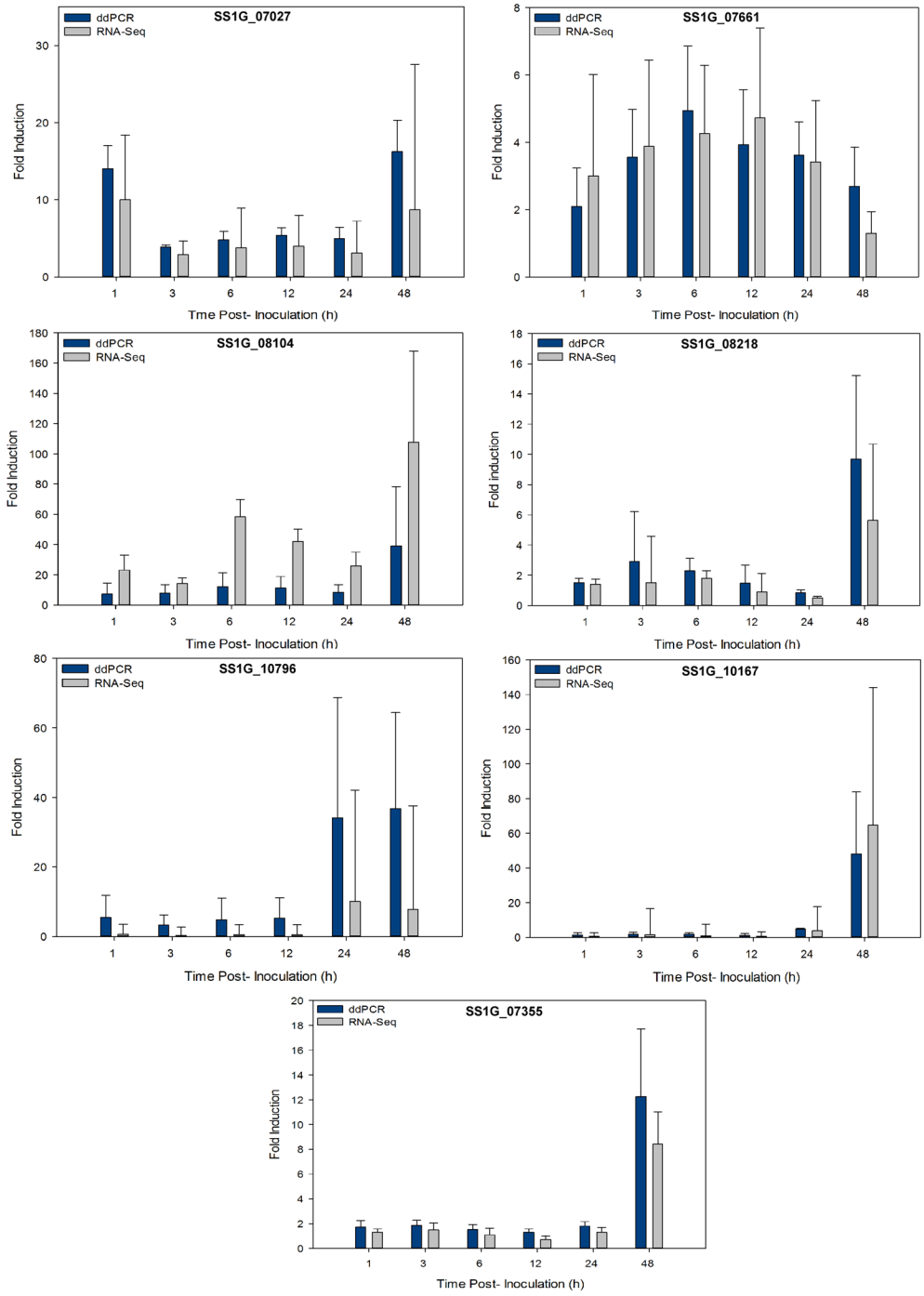

Figure 2.4 Expression of various *Sclerotinia sclerotiorum* genes during infection of *Brassica napus* as determined by RNA-Seq and ddPCR analysis. Histograms show the relative expression level (fold change) and are reported as means and standard errors of three biological replicates for hour post-inoculation (hpi).

2.4.4. Functional classification of the genes

To simplify the exploration of genes expressed during the course of *S. sclerotiorum* infection, genes were clustered based on expression patterns and categorized based on their functional annotation and predicted roles in pathogenicity or virulence; these are discussed below.

2.4.4.1. Hydrolytic enzymes

The current study revealed that a large number of the genes induced during infection encoded enzymes with hydrolytic activity (Table 2.1). The largest group of these genes encoded carbohydrate-active enzymes (CAZymes). Most of the CAZyme genes predicted in the *S. sclerotiorum* genome by Amselem et al. (2011) were up-regulated during infection in this study and in the study by Lyu et al. (2015), which examined different *S. sclerotiorum* developmental stages. These results consistently support the important role of these enzymes during infection. The majority of the genes encoding CAZymes reported in the current study were from the glycoside hydrolase (GH) and carbohydrate esterase (CE) families. The expression of numerous genes encoding GH and CE enzymes in the current study and in a similar study of *Sclerotinia homoeocarpa* reflects the ability of these pathogens to infect a wide range of plant hosts (Orshinsky et al., 2012). These are discussed in more detail below.

2.4.4.1.1.Cutinases/lipases

The first barrier to pathogen invasion is the plant cuticle, a composite layer of C:16 and C:18 fatty acids and their derivatives that form cutin and surface waxes (Yeats and Rose, 2013). Among the genes from the CE family, the gene encoding the cutinase, SsCuta (SS1G_07661), was up-regulated during the early stages of infection (from 1-24 hpi). The induction of *SsCuta* soon after contact with the leaf surface in the current study agrees with the previous report showing that it was induced upon contact of mycelia with hard surfaces (Bashi et al., 2012) and supports the predicted role of this enzyme in degrading plant cuticle. Additionally, it is not surprising that expression of this gene declined after 24 hpi since host penetration has already been achieved by this time. In addition to *SsCuta*, three other genes from the lipid degradation group (Table 2.1), SS1G_09557, SS1G_01953 and SS1G_11930, were also induced during the early stages of infection. The similarity between the expression patterns of these genes and that of *SsCuta*, as well as their potential lipolytic enzymatic activity, suggest that these enzymes may also be involved in host penetration. Evidence that lipase acts as virulence factor in fungal

phytopathogens derives from a study with *B. cinerea* (Lip1) (Reis et al., 2005). The secreted lipase in *Fusarium graminearum* encoded by FgL1 is also a virulence factor contributing to the infection of cereals (Voigt et al., 2005). Genes encoding other lipases and members of the CE family, such as the cutinases (SS1G_13386 and SS1G_12907) and an extracellular lipase (SS1G_14146), were significantly up-regulated at 24 and 48 hpi (Table 2.1).

2.4.4.1.2. Plant cell wall degrading enzymes

Once the cuticle has been breached, the pathogen must establish within the host and then proceed to ramify through host tissues. The production of enzymes that degrade plant cell wall components physically allows this to occur, while providing nutrients to drive the infection process (Zhao et al., 2013). The primary plant cell wall is composed mainly of cellulose, hemicellulose and pectin, along with structural glycoproteins (e.g. hydroxyproline-rich extensins) and phenolic esters (e.g. ferulic and coumaric acid). The secondary cell wall consists mostly of lignin, a highly cross-linked phenolic macromolecule.

The GH28 subfamily contains the PGs, enzymes that degrade cell wall pectin. Previously, four genes encoding endo-PGs (SsPG1, SsPG3, SsPG5, and SsPG6) and two genes encoding exo-PGs (SsXPG1 and SsXPG2) were found to be expressed during *S. sclerotiorum* infection of *B. napus* (Li et al., 2004). In the current study, the genes encoding SsPG1 (SS1G_10167) and SsPG3 (SS1G_10698) were up-regulated at 24-48 hpi and 48 hpi with expression levels 3.7- 64.6 and 5.5-fold greater than the inoculum, respectively. The two exo-PG genes, *SsXPG1* (SS1G_04207) and *SsXPG2* (SS1G_02553), were up-regulated at 24-48 hpi and 48 hpi with expression levels 14.6-168.3 and 22.6- fold greater than the inoculum, respectively. While the main pectin backbone is a homopolymer of alpha-(1→4)-linked D-galacturonic acid residues, branched and unbranched side chains are appended to it that contain several different types of sugars. Most of the genes encoding these ancillary pectin-degrading enzymes were highly expressed at 24 and 48 hpi in concert with the endo-PG genes *SsPG1* and *SsPG3*, except for SS1G_05832 (exo-PG), SS1G_04095 (rhamnogalacturanan acetylhydrolase) and SS1G_08229 (rhamnogalacturonase) which were up-regulated at 1-3 hpi, 1-24 hpi and 1-12 hpi, respectively.

Li et al. (2004) reported that *SsPG1* expression could be induced by contact with hard surfaces, while Bashi et al. (2012) reported that *SsPG1*, but not *SsPG2*, was moderately induced by contact with *B. napus* leaves and that *SsPG1* expression was restricted to the expanding margin of the lesion. They suggested that since *SsPG1* expression was also induced by carbon

starvation and repressed by galacturonic acid that it may be involved in both early penetration events and lesion expansion. During *P. vulgaris* infection, *SsPG1* is induced during the later stages of the interaction (48-72 hpi), *SsPG3* is up-regulated earlier at 12 hpi, while *SsPG6* exhibits a bimodal pattern with peaks of expression at 6 and 48 hpi (Oliveira et al., 2015). SsPG3 and SsPG6 are also potent inducers of light-dependent necrotic reactions (Bashi et al., 2013). Similarly, *B. cinerea* BcPG1 and BcPG2 exhibit strong necrosis-inducing activity (Kars et al., 2005) and deletion of either of the gene encoding them reduces *B. cinerea* virulence (ten Have et al., 1998; Kars et al., 2005). The induction of SsPG or orthologous genes well after host penetration and their ability to cause tissue necrosis suggests that the primary role of these enzymes is in lesion expansion and movement of the pathogen through the host tissues.

Many of the up-regulated GH and CE family members reported in this study also have a putative role in the degradation of hemicellulose and cellulose. This was similar to the previous results obtained for up-regulated GH genes in *S. homoeocarpa* (Orshinsky et al., 2012). Cellulose is a homopolymer of beta-(1, 4)-linked D-glucose and is sequentially hydrolyzed into its component glucose by enzymes including cellulases (endo-1,4-glucanases), cellobiosidases (exo-glucanases) and beta-glucosidases. Numerous genes encoding putative cellulases were up-regulated at some point during the infection, mostly at the later stages, with SS1G_09821 and SS1G_03041 up-regulated 144 and 292 fold at 48 hpi (Table 2.1). Genes encoding putative exoglucanases and beta-glucosidases followed a similar pattern of expression with most being up-regulated at the later stages and only a few during the earlier stages of the infection. In higher plants, hemicellulose comprises approximately 20% of the total biomass. Unlike the more homogenous cellulose, hemicellulose is composed not only of glucose, but also of other sugars such as xylose, mannose, galactose, rhamnose, and arabinose. As such, its deconstruction requires a more complicated bevy of enzymatic reactions. Similar to the genes encoding cellulose-degrading enzymes, genes encoding putative hemicellulose degrading enzymes were also up-regulated later in the infection. The exceptions were genes encoding enzymes involved in the release of xylose from xylan (beta-1,4-linked xylose), namely SS1G_12191, SS1G_05140 and SS1G_08104, which were first induced at the earlier stages. Two other genes encoding xylanases (SS1G_10092 and SS1G_03618) were among the most highly induced genes found in this study with levels of expression 155 and 451 fold higher than that of the inoculum at 48 hpi. These patterns may attest to the abundance of this sugar in the plant cell wall and/or its

significance to *S. sclerotiorum* nutrition. Interestingly, SS1G_10092 is likely orthologous to the gene encoding *B. cinerea* xylanase11A (90% amino acid identity), which induces a strong necrotic reaction and is required for virulence (Noda et al., 2010). Both proteins share a 30 amino acid region associated with necrotizing activity (Noda et al., 2010). In the *S. sclerotiorum–P. vulgaris* interaction, SS1G_01493 (beta-xylosidase) was up-regulated during the early stages before the emergence of visible necrotic symptoms on the stem, whereas genes encoding cellulose-degrading enzymes, SS1G_13255 (beta-1,4-glucanase) and SS1G_07146 (cellobiohydrolase), were induced during the later stages of infection coinciding with the formation of visible stem lesions (Oliveira et al., 2015). In *B. cinerea*, the expression pattern of genes encoding xyloglucan-degrading enzymes was found to be vastly different dependent upon the host plant (Blanco-Ulate et al., 2014).

Two genes encoding other hemicellulose-degrading enzymes with alpha-L-arabinofuranosidase activity, SS1G_02462 and SS1G_03602, were also up-regulated at 24-48 hpi. These enzymes target the L-arabinofuranose residues of hemicellulose with pectin side chains (Kleman-Leyer et al., 1996). Alpha-L-arabinofuranosidase was first reported in *S. sclerotiorum* by Yajima and Kav (2006). An earlier study on *Sclerotinia fructigena* suggested that there was significant correlation between the quantity of alpha-L-arabinofuranosidase and virulence of this fungus through its contribution to disease initiation or fungal proliferation (Howell, 1975).

Arabinogalactans are structurally complicated branched galactans with arabinose side chains and can be found as either beta-1,4-galactans linked to rhamnogalacturonan I in pectin, or as beta-1,4-galactans associated with proteins (Sakamoto and Ishimaru, 2013). As with the other cell wall degrading enzymes, the majority of the genes encoding putative arabinogalactan-degrading enzymes were induced later in the infection (24-48 hpi) (Table 2.1). However, a gene encoding an arabinogalactan endo-beta-galactosidase (SS1G_01216) and another encoding a beta-galactosidase (SS1G_10842) were already induced at 1 hpi.

Mannans are polymers of mannose. Those with beta-(1–4)-linkages are typical of plant storage polysaccharides, while mannans with alpha-(1–6)-linked backbone and alpha-(1–2)- and alpha-(1–3)-linked branches are often associated with glycoproteins. As noted above, glycoproteins are a significant cell wall component and several genes encoding mannosidases capable of hydrolyzing these chemical bonds were up-regulated during the later stages of the infection

(Table 2.1).

Lignin provides additional structure and rigidity to the plant cell wall and increased lignification is often a consequence of imposed biotic and abiotic stresses (Barros et al., 2015). Three genes encoding extracellular dihydrogeodin oxidases were up-regulated at the mid to later stages of the infection (Table 2.1). All contain three multicopper oxidase domains, which are often associated with enzymes, such as laccases, that oxidize phenolic compounds. Laccases are involved in the disassembly of lignin (Janusz et al., 2013), though some may detoxify phenolic secondary metabolites as discussed below.

Collectively, the plethora of CAZymes expressed by *Sclerotinia* species allows this group of pathogens to break down most host polysaccharides to efficiently access nutrients from a wide variety of hosts. The expression patterns of the CAZyme genes in the current study, which were mostly expressed at later stages of infection (24-48 hpi), support the hypothesis that they are primarily involved in tissue maceration. Factors such as host plant species, the type of tissues being colonized and the environment also influence the expression of different CAZyme genes. In *B. cinerea*, the expression of PG genes, in particular *BcPG1* and *BcPG2*, was markedly different on different hosts or on the same host at different temperatures (Blanco-Ulate et al., 2014). This same phenomenon was observed with genes encoding various pectin lyases, pectate lyases and pectin methylesterases (Blanco-Ulate et al., 2014). The large number of genes encoding CAZymes and their different patterns of expression strongly indicate that they make an important contribution to pathogenesis and host range through adaptation to various environmental and host factors.

2.4.4.1.3. Proteases

Although CAZymes have captured most of the attention as the main group of hydrolytic enzymes involved in pathogenesis, there are other groups of hydrolytic enzymes, which also play crucial roles. Many genes encoding endo-proteases, as well as mono-, di and tri-peptidyl peptidases were up-regulated during infection (Table 2.1). The *in planta* expression of *acp1* (non-aspartyl acid protease, SS1G_07836) was recorded during *S. sclerotiorum* infection of sunflower cotyledons with the peak expression level at 24-56 hpi (Poussereau et al., 2001a). *Acp1* was also up-regulated in the current study with 40-fold greater expression than the inoculum at 48 hpi. The expression of this gene only at the necrotic stage is in support of the previous study. During infection of *P. vulgaris*, *acp1* is first induced during the very early stages of the infection and

then again at the later stages (Oliveira et al., 2015). The expression of *acp1* is regulated by several environmental factors including glucose and nitrogen starvation and acidification. The PacC transcription factor is involved in the regulation of *acp1* expression under acidic conditions (Poussereau et al., 2001a).

A gene encoding an aspartyl protease (aspS, SS1G_03629) from *S. sclerotiorum* was previously reported as being induced at the very early stages of the infection and was involved in decomposition of host defense proteins (Poussereau et al., 2001b). An aspartyl protease was also reported as a cell death-inducing factor secreted by *S. sclerotiorum* and *B. cinerea* (Movahedi and Heale, 1990). Although the *aspS* gene was not up-regulated in the current study, genes encoding proteases similar to aspS (SS1G_05329 and SS1G_02870), were up-regulated at the very early stages of the infection in support of the previous studies. However, a gene encoding another aspartyl protease, SS1G_03181, was also detected in the *S. sclerotiorum–P. vulgaris* interaction with increased expression at the spreading necrosis stage (Oliveira et al., 2015). SS1G_03181 was up-regulated at 24-48 hpi in the current study which is in agreement with these earlier findings.

Most of the genes encoding subtilisin-like serine proteases (SS1G_07655, SS1G_02423, SS1G_03282, SS1G_12210 and SS1G_07168) were up-regulated at the later stages of the infection (24-48 hpi) (Table 2.1). Subtilisins were proposed to play a role in penetration and colonization because of their ability to degrade plant cell wall glycoproteins or pathogenesis-related proteins (Olivieri et al., 2002); however, the expression profiles of genes encoding these enzymes in the current study suggest that they are also involved in events occurring at the necrotic stage. Genes encoding enzymes with metalloprotease activities (SS1G_05348 and SS1G_05349) were also up-regulated at 48 hpi. These proteases play a role in degrading plant materials for nitrogen utilization (Zuccaro et al., 2011). In accordance with this notion, the majority of the genes encoding exo-peptidases, which complete the hydrolysis of peptides generated by endo-proteases into their component amino acids, were expressed at the later stages of the infection similar to the genes encoding serine and metalloproteases (Table 2.1).

The current study revealed one calpain family cysteine protease gene (SS1G_00862) that was induced at 1 hpi and continued to be expressed during the middle stages of the infection out to 24 hpi. A gene encoding a caspase domain-containing cysteine protease (SS1G_10992) was also up-regulated at 1 hpi and was detected again at 48 hpi at a higher expression level (7.1-fold greater

than the inoculum). According to previous studies, these types of endo-peptidases contribute to programmed cell death (PCD) processes (Vardar and Ünal, 2008). Among these, cysteine proteases, specifically the caspases, have a key role in PCD, more commonly apoptosis (Vardar and Ünal, 2008). In addition, cysteine proteases along with other proteolytic systems, such as calpain, 26S proteasome, granzyme B, cathepsin D and matrix metalloproteinases, also have a role during PCD processes (Beers et al., 2000). There is a report suggesting that victorin, a toxin produced by *Cochliobolus victoriae*, induces proteolytic cleavage of the Rubisco large subunit (LSU) through activation of a host cysteine protease (Navarre and Wolpert, 1999). Considering these previous studies, understanding the precise role of these genes in the pathogenesis of *S. sclerotiorum* warrants further investigation, as they may be involved in processes linked to phase transitions during the infection (Hegedus et al., 2016).

Proteases are important for *S. sclerotiorum* nutrition as protein forms about 10% of host cell protoplasm (Carpita and Gibeaut, 1993). Numerous proteases were also captured in the *S. homoeocarpa* transcriptome, but these were mostly serine endo-proteases (Orshinsky et al., 2012). In the current study, the up-regulated endo-protease genes encoded enzymes with a much broader range of catalytic mechanisms. Several genes encoding putative aspartyl (active at acidic pH) and cysteine (active at acidic to neutral pH) proteases were up-regulated very early in the infection, while most of the serine protease genes (active at high pH) and two genes encoding metalloproteases were up-regulated at the later stages. It is possible that the coordinated and systematic deployment of proteolytic enzymes with different catalytic mechanisms reflects the lesion environment, the pathogen's nutritional requirements and interactions with host defense systems at different stages of the infection.

Table 2.1 Description and expression of up-regulated genes encoding hydrolytic enzymes.

Gene ID	Description[1]	Expression Level (hpi)[2]					
		1	3	6	12	24	48
1. Lipid Degradation							
SS1G_07661	cutinase (SsCuta)	3	3.9	4.3	4.7	3.4	-
SS1G_13386	cutinase	-	-	-	-	14.9	29.6
SS1G_12907	cutinase	-	-	-	-	29.7	236
SS1G_09557	lipase/esterase	3.4	5.5	6.5	6.1	2.6	-
SS1G_11473	lipase/esterase	2.2	-	-	-	-	3.2
SS1G_05990	lipase/esterase	-	-	-	-	2.2	-
SS1G_00767	lipase/esterase	-	-	-	-	-	34.4
SS1G_03597	lipase/esterase	-	-	-	-	-	5.1
SS1G_01849	lipase/esterase	-	-	-	-	-	2.7
SS1G_08869	lipase class 3	-	-	-	-	-	2.8
SS1G_14146	extracellular lipase	-	-	-	-	31.5	38.7
SS1G_04490	extracellular lipase	-	-	-	-	2.5	3
SS1G_00877	extracellular lipase	-	-	-	-	-	4.3
SS1G_14441	triacylglycerol lipase	-	-	-	-	5	6.9
SS1G_13982	triacylglycerol lipase	-	-	-	-	4.8	27.5
SS1G_01472	triacylglycerol lipase	-	-	-	-	3.6	13.1
SS1G_03007	alpha beta-hydrolase (esterase)	-	2.6	2.6	-	-	-
SS1G_09718	alpha beta-hydrolase (esterase/lipase)	-	2.1	2.9	-	-	-
SS1G_01703	alpha beta-hydrolase (esterase/lipase)	-	3.9	3.5	2.2	3.8	6.5
SS1G_13361	alpha beta-hydrolase (esterase/lipase)	-	-	-	2.3	3.2	2.2
SS1G_11402	alpha beta hydrolase (esterase/lipase)	-	-	-	3.6	4.8	3.7
SS1G_13263	alpha beta hydrolase (esterase/lipase)	-	-	-	-	3.8	3.8
SS1G_08133	alpha beta-hydrolase (esterase/lipase)	-	-	-	-	-	2.5
SS1G_02163	alpha beta-hydrolase (esterase/lipase)	-	-	-	-	-	12.5
SS1G_01953	GDSL lipase acylhydrolase family protein	3.6	4	5	4.9	4.8	5.6
SS1G_13560	GDSL lipase acylhydrolase family protein	-	-	-	-	2.7	2.7
SS1G_06389	GDSL lipase acylhydrolase family protein	-	-	-	-	-	2.7
SS1G_02708	cellulose-binding GDSL lipase	-	-	-	-	3.3	7.8
SS1G_14289	cellulose-binding GDSL lipase	-	-	-	-	5.3	6.6
SS1G_03610	cellulose-binding GDSL lipase	-	-	-	-	5.1	22.4
SS1G_04592	cellulose-binding GDSL lipase	-	-	-	-	11.8	9.4
SS1G_11930	carboxylesterase/lipase (cholinesterase)	4	3.9	8.9	5.2	-	-
SS1G_00376	carboxylesterase/lipase (cholinesterase)	-	-	-	-	4.4	9.2
SS1G_09613	carboxylesterase/lipase (cholinesterase)	-	-	-	-	-	4.7
SS1G_04422	carboxylesterase/lipase (cholinesterase)	-	-	-	-	-	3.2

SS1G_11853	carboxylesterase/lipase (cholinesterase)	-	-	-	-	-	3
SS1G_04030	lysophospholipase	-	-	3.6	-	2.3	-
SS1G_10482	lysophospholipase	-	-	-	-	-	4.1
2. Polysaccharide Degradation							
2.1 Cellulose							
SS1G_08493	beta-1,4-endo-glucanase	2.6	-	-	-	-	-
SS1G_00891	beta-1,4-endo-glucanase (cellulase)	-	4.5	5.8	3.5	-	3.8
SS1G_01485	beta-glucanase	-	-	-	-	-	2.1
SS1G_09365	endo-glucanase	-	-	-	-	2.7	-
SS1G_03387	endo-glucanase	-	-	-	-	5.3	41.4
SS1G_08837	endo-glucanase	-	-	-	-	10.3	36.4
SS1G_04945	endo-glucanase	-	-	-	-	-	2.3
SS1G_01828	endo-glucanase	-	-	-	-	-	2.6
SS1G_09821	endo-glucanase	-	-	-	-	-	144
SS1G_03041	endo-glucanase	-	-	-	-	-	292
SS1G_00321	endo-glucanase	-	-	-	-	-	4.2
SS1G_00471	endo-glucanase	-	-	-	-	-	2.1
SS1G_06037	exo-glucanase	-	3	3.2	-	9.9	12.3
SS1G_02334	exo-glucanase (cellobiohydrolyase)	-	-	-	-	3.8	-
SS1G_09020	exo-glucanase	-	-	-	-	15.1	79
SS1G_00892	exo-glucanase	-	-	-	-	5.4	22.2
SS1G_09118	exo-glucanase	-	-	-	-	-	2.5
SS1G_02245	exo-glucanase	-	-	-	-	-	3.3
SS1G_13872	exo-glucanase	-	-	-	-	-	7.6
SS1G_02501	Concanavalin A-like lectin/glucanase	5.1	8.7	6.1	3.1	-	-
SS1G_08907	glycoside hydrolase (beta-glucanase)	2.6	-	-	-	-	-
SS1G_07863	cellobiose dehydrogenase	3.7	-	-	-	-	22.1
SS1G_05151	cellobiose dehydrogenase	-	-	-	-	5.9	6.6
SS1G_05118	beta-glucosidase	2.4	-	-	-	-	-
SS1G_01662	beta-glucosidase	-	-	-	-	2.8	9.5
SS1G_09366	beta-glucosidase	-	-	-	-	2.8	8
SS1G_06304	beta-glucosidase	-	-	-	-	2.6	6.8
SS1G_07847	beta-glucosidase	-	-	-	-	3.1	4.7
SS1G_07146	beta-glucosidase	-	-	-	-	7.4	18.7
SS1G_13255	beta-glucosidase	-	-	-	-	40.4	54.8
SS1G_05368	beta-glucosidase	-	-	-	-	3.2	4.6
SS1G_12622	beta-glucosidase	-	-	-	-	-	2.1
SS1G_07162	beta-1,4-glucosidase	-	-	-	-	-	2.3
SS1G_09129	beta-glucosidase	-	-	-	-	-	13.1
SS1G_04264	beta-glucosidase	-	-	-	-	-	2.2

SS1G_01021	beta-glucosidase	-	-	-	-	-	5.2
2.2 Pectin							
SS1G_10167	endo-polygalacturonase (SSPG1)	-	-	-	-	3.7	64.6
SS1G_10698	endo-polygalacturonase (SSPG3)	-	-	-	-	-	5.5
SS1G_05832	exo-polygalacturonase	4.1	6.5	-	-	4.2	32.4
SS1G_02553	exo-polygalacturonase (exoPG2)	-	-	-	-	-	22.6
SS1G_04207	exo-polygalacturonase (exoPG1)	-	-	-	-	14.6	168
SS1G_12057	exo-polygalacturonase	-	-	-	-	-	4.2
SS1G_03540	pectin lyase	-	-	-	-	4.5	3.3
SS1G_10071	pectin lyase	-	-	-	-	-	6.2
SS1G_14449	pectin lyase	-	-	-	-	-	2.4
SS1G_04551	pectin methylesterase	-	-	-	-	11.6	35.8
SS1G_00332	pectin methylesterase	-	-	-	-	33.9	178
SS1G_03286	pectin methylesterase	-	-	-	-	4.8	16.5
SS1G_00468	pectin methylesterase	-	-	-	-	-	21.4
SS1G_04095	rhamnogalacturanan acetylhydrolase	2.8	6.2	7.7	5.3	2.7	-
SS1G_12048	rhamnogalacturanan acetylhydrolase	-	-	-	-	-	33.5
SS1G_11992	rhamnogalacturonan acetylesterase	-	-	-	-	-	37.5
SS1G_09857	rhamnogalacturonyl hydrolase	-	-	-	-	-	8.6
SS1G_12964	alpha-l-rhamnosidase	-	-	17.5	-	-	-
SS1G_13501	alpha-l-rhamnosidase	-	-	-	-	3.1	21.2
SS1G_04541	alpha-l-rhamnosidase	-	-	-	-	2	8.3
SS1G_08229	rhamnogalacturonase	2.1	4.5	4.5	2.6	-	-
SS1G_07039	rhamnogalacturonase	-	-	-	-	-	6
SS1G_04552	endo-xylogalacturonan hydrolase	-	-	-	-	7.1	15.9
2.3 Hemicellulose							
SS1G_12191	endo-1,4-beta-xylanase	-	5.3	7.9	4.6	6.4	25
SS1G_10092	endo-beta-xylanase	-	-	-	-	-	155
SS1G_03618	endo-beta-xylanase	-	-	-	-	-	451
SS1G_07749	endo-beta-xylanase	-	-	-	-	-	56.7
SS1G_05140	xylanase	3.6	3.5	4.2	4.3	3.4	8.1
SS1G_08104	acetylxylan esterase	23	14.2	58.3	42.1	26	107
SS1G_05434	acetylxylan esterase	-	-	-	-	4	11.8
SS1G_00746	beta-mannosidase	-	-	-	-	6.6	42.3
SS1G_05977	beta-mannosidase	-	-	-	-	3.6	6.4
SS1G_08208	endo-1,4-beta-mannosidase	-	-	-	-	3.6	8.9
SS1G_08118	alpha-xylosidase	-	-	-	-	4.5	3.8
SS1G_09367	alpha-xylosidase	-	-	-	-	2.2	-
SS1G_11535	alpha-fucosidase	-	-	-	-	-	2.5

SS1G_04662	alpha-galactosidase	-	-	-	-	4.5	3.9
SS1G_03386	alpha-galactosidase	-	-	-	-	-	3.7
SS1G_07904	feruloyl esterase	-	-	-	-	3.6	12
SS1G_02462	alpha-l-arabinofuranosidase	-	-	-	-	5.3	21
SS1G_03602	alpha-l-arabinofuranosidase	-	-	-	-	6.3	17.6
2.4 Arabinogalactans							
SS1G_01216	arabinogalactan endo-beta-galactosidase	4.1	9.6	11.9	7.2	4.1	-
SS1G_11585	arabinogalactan endo-beta-galactosidase	-	-	-	-	-	19.3
SS1G_02618	galactan 1,3-beta-galactosidase	-	-	-	-	5.7	11
SS1G_10842	beta-galactosidase	4.1	2.5	2.4	-	2.2	5.8
SS1G_11763	beta-galactosidase	-	-	-	-	4.7	-
SS1G_01572	beta-galactosidase	-	-	-	-	6.8	18.3
SS1G_03647	beta-galactosidase	-	-	-	-	3.5	6.9
SS1G_02781	beta-galactosidase	-	-	-	-	-	2.7
SS1G_09866	1,6-beta-galactanase	-	4.8	4.5	3.1	3	12.4
SS1G_11922	arabinan endo-1,5-alpha-L-arabinosidase	-	-	-	-	144.3	245
SS1G_01238	beta-D-glucuronidase	7.6	-	4.7	-	-	-
SS1G_02620	beta-glucuronidase	-	-	-	-	3.5	8.2
2.5 Lignin							
SS1G_04196	dihydrogeodin oxidase/laccase	-	3.1	2.6	4.6	-	-
SS1G_06365	dihydrogeodin oxidase/laccase	-	3.1	5.7	4.1	-	3.4
SS1G_05112	dihydrogeodin oxidase/laccase	-	-	-	-	-	6
2.6 Starch							
SS1G_01776	alpha-amylase	-	-	2.1	-	-	-
SS1G_11100	alpha-amylase	-	-	-	-	6.6	5.2
SS1G_01083	alpha-glucosidase	2.4	4.7	3	-	4.6	5.3
SS1G_01005	alpha-glucosidase	-	-	-	-	9.2	7.2
2.7 Mannans							
SS1G_10867	endo-1,6-alpha-mannosidase	-	-	-	-	6.4	-
SS1G_04468	endo-1,6-alpha-mannosidase	-	-	-	-	7.5	25.3
SS1G_12937	endo-1,6-alpha-mannosidase	-	-	-	-	-	10.4
SS1G_05110	endo-1,6-alpha-mannosidase	-	-	-	-	-	3.5
SS1G_11579	endo-1,6-alpha-mannosidase	-	-	-	-	-	3.5
SS1G_09229	alpha 1,2 mannosidase	-	-	-	-	55	40.2
SS1G_00505	alpha-1,2-mannosidase	-	-	-	-	9.8	4.7
SS1G_04148	alpha-mannosidase	-	-	-	-	4.1	4
SS1G_02022	alpha-mannosidase	-	-	-	-	12.5	10.9

SS1G_04200	alpha-mannosidase	-	-	-	-	6	56.3
SS1G_01334	alpha-mannosidase	-	-	-	-	-	11.5
2.8 Callose							
SS1G_01422	1,3 (4)-beta-D-glucanase	2.2	-	-	-	-	-
SS1G_10048	1,3 (4)-beta-D-glucanase	-	2.1	-	-	2.1	-
3. Protein Degradation							
3.1 Proteases							
SS1G_10992	caspase domain-containing protease	2.1	-	-	-	-	7.1
SS1G_00862	cysteine protease (calpain family)	6.1	5.1	6.3	3.4	3.2	-
SS1G_09978	peptidase (family 41 protein)	3.2	-	3.2	2.9	-	6.4
SS1G_07836	(acid) non-aspartyl protease (ACP1)	-	-	-	-	-	40.4
SS1G_05329	aspartyl protease	12.2	-	-	-	-	4.6
SS1G_02870	aspartyl protease	2	2.6	3	3	2.7	3.3
SS1G_03181	aspartyl protease	-	-	-	-	3.9	16.6
SS1G_06534	serine protease (trypsin-like)	2.8	3	-	-	-	3.9
SS1G_12419	serine protease (subtilisin-like)	-	-	3	-	-	-
SS1G_07655	serine protease (subtilisin-like)	-	-	-	-	8.5	19.8
SS1G_02423	serine protease (subtilisin-like)	-	-	-	-	-	2.2
SS1G_03282	serine protease (subtilisin-like)	-	-	-	-	-	2.2
SS1G_07168	serine protease (subtilisin-like)	-	-	-	-	-	2.5
SS1G_12210	serine protease (subtilisin-like)	-	-	-	-	-	7.3
SS1G_05348	metalloprotease	-	-	-	-	-	2.6
SS1G_05349	metalloprotease	-	-	-	-	-	3.1
3.2 Peptidases							
SS1G_04565	cytosolic no-pecific dipeptidase	-	-	-	-	26	9.2
SS1G_10529	cytosolic no-pecific dipeptidase	-	-	-	-	-	2.2
SS1G_04140	dipeptidyl-peptidase	-	2.5	-	-	-	-
SS1G_03087	membrane dipeptidase	-	-	-	-	-	2.6
SS1G_03392	proline dipeptidase	-	-	-	-	4.5	-
SS1G_08920	proline dipeptidase	-	-	-	-	2.4	2
SS1G_04958	tripeptidyl-peptidase	-	-	-	-	5	22.9
SS1G_07268	tripeptidyl-peptidase	-	-	-	-	3.5	2.1
SS1G_13922	tripeptidyl peptidase	-	-	-	-	8.9	50.4
SS1G_09225	tripeptidyl peptidase	-	-	-	-	6.9	16.9
SS1G_09268	tripeptidyl-peptidase	-	-	-	-	5.9	3.4
SS1G_02857	tripeptidyl peptidase	-	-	-	-	6.4	2.5
SS1G_03518	tripeptidyl peptidase	-	-	-	-	-	6.1
SS1G_01236	tripeptidyl peptidase	-	-	-	-	-	9.7

SS1G_08558	prolyl aminopeptidase	2.5	4.3	4.4	3.4	2.4	2.2
SS1G_00617	prolyl aminopeptidase	-	-	-	9.5	4.9	5.2
SS1G_12775	prolyl aminopeptidase	-	-	-	-	-	3
SS1G_05449	carboxypeptidase	-	2.5	-	-	3.3	13.3
SS1G_12413	carboxypeptidase	-	-	-	-	3.5	4.2
SS1G_08855	carboxypeptidase	-	-	-	-	3.7	4.1
SS1G_03361	carboxypeptidase	-	-	-	-	4.2	21.1
SS1G_09475	carboxypeptidase	-	-	-	-	-	13.1
SS1G_13633	carboxypeptidase	-	-	-	-	-	7.6
SS1G_12499	carboxypeptidase	-	-	-	-	-	11.5
SS1G_04819	carboxypeptidase	-	-	-	-	-	5.5
4. Other Hydrolytic Enzymes							
SS1G_01113	metallo-dependent amidohydrolase	-	-	-	-	3.2	-
SS1G_09143	metallo-dependent amidohydrolase	-	-	-	-	-	6.1
SS1G_02141	alpha beta-hydrolase	4.6	-	-	-	-	-
SS1G_11096	alpha beta-hydrolase	-	-	-	2.1	5.7	2.6
SS1G_08093	alpha beta-hydrolase (epoxide hydrolase)	-	-	-	-	4.4	9.2
SS1G_04475	endo-alpha-1,4-polygalactosaminidase	3	-	-	-	-	3.8
SS1G_11842	sialidase	3.1	-	3.6	-	-	9.8
SS1G_01389	polysaccharide lyase family 7 protein	-	4.9	4.9	5.2	-	-
SS1G_01493	glycoside hydrolase family 3 protein	-	-	-	-	4.2	17
SS1G_09000	glycoside hydrolase family 5 protein	2.7	-	-	-	2.7	-
SS1G_02369	glycoside hydrolase family 12 protein	-	-	-	-	-	3.4
SS1G_04497	glycoside hydrolase family 16 protein	-	-	-	-	-	2
SS1G_09789	glycoside hydrolase family 16 protein	-	-	-	-	-	2.8
SS1G_06426	glycoside hydrolase family 43 protein	-	-	-	-	2.4	5.9
SS1G_07515	glycoside hydrolase family 43 protein	-	-	-	-	138	518
SS1G_07656	glycoside hydrolase family 61 protein	-	-	-	-	-	93.6
SS1G_09251	glycoside hydrolase family 61 protein	-	-	-	-	-	9.1
SS1G_12106	glycoside hydrolase family 76 protein	-	-	-	-	3	13
SS1G_12083	glycoside hydrolase family 115 protein	-	-	-	-	7.8	17
SS1G_04152	glycoside hydrolase family 125 protein	-	2.2	-	-	6	12.5
SS1G_12917	glycoside hydrolase family 128 protein	-	-	-	-	2.3	17.3

[1]Annotation based on the presence of conserved PFAM domains and BLAST reports.
[2]Fold change relative to 0 hours post-inoculation (hpi). (-) No significant change in expression.

2.4.4.2. Secondary metabolite biosynthesis

Several genes encoding enzymes involved in the biosynthesis of secondary metabolites were up-regulated in the current study (Table 2.2). These included key enzymes associated with pathways for production of toxic compounds, including polyketide synthase (PKS), nonribosomal peptide synthase (NRPS), hybrid PKS/NRPS, and chalcone synthase (CHS). These fungal toxins interfere with host cell functions to suppress plant defense and/or enhance development of disease symptoms (Choquer et al., 2007). Of the various types of phytotoxic metabolites produced by *B. cinerea*, botrydial has been most intensively studied (Colmenares et al., 2002). BcBOT1 is part of the botrydial biosynthesis pathway and is a cytochrome P450 monooxygenase (Siewers et al., 2005). Cytochrome P450 enzymes are also involved in the aflatoxin biosynthetic pathways (Kelkar et al., 1997). SS1G_09638 and SS1G_11247 encode enzymes with some similarity to StcL, which is involved in aflatoxin biosynthesis in *Aspergillus nidulans*. These genes were expressed, but not up-regulated compared to the inoculum in the current study, while SS1G_13923 was up-regulated at 1 to 6 hpi (Table 2.3). It should be noted that while cytochrome P450 enzymes are involved in the production of secondary metabolites and mycotoxins, some members are also involved in the detoxification of host metabolites in different fungi (Cresnar and Petric, 2011).

Polyketides are a structurally diverse group of secondary metabolites derived from the decarboxylative condensation of malonyl-CoA and include many mycotoxins. In *B. cinerea*, two genes encoding PKS, *BcPKS6* and *BcPKS9*, that act in concert to synthesize the phytotoxin botcinic acid, are up-regulated during infection of tomato leaves (Dalmais et al., 2011). Transcripts from the *S. sclerotiorum* orthologue of *PKS6* (SS1G_09237) were detected at 48 hpi, while *PKS9* (SS1G_09240) was expressed, but not up-regulated in this study. This agrees with the findings of Pedras and Ahiahonu (2004) regarding the absence of botcinic acid in *S. sclerotiorum* as both enzymes are required for its synthesis. Both botrydial and botcinic acid toxins contribute to the virulence of *B. cinerea* (Dalmais et al., 2011). SS1G_02592 encodes a protein similar to ToxD, which is involved in the synthesis of the polyketide lovastatin in *Aspergillus terreus* (Kennedy et al., 1999). It was initially up-regulated within 1 hpi with expression peaking at 48 hpi.

Among the genes similarly induced during the infection by *B. cinerea* and *S. sclerotiorum* are those conserved in ascomycetes and encode proteins/enzymes involved in the biosynthesis of

melanin (PKS13), coprogen (NRPS6) and intracellular siderophores (NRPS2, NRPS3) (Amselem et al., 2011). *PKS13* (SS1G_13322) and *NRPS6* (SS1G_04250) were expressed, but not up-regulated in the current study, while homologues of the genes encoding enzymes responsible for siderophore biosynthesis, NRPS2 and NRPS3, (SS1G_03693T0 and SS1G_06185T0) were up-regulated at 3-48 and 1-24 hpi, respectively. Siderophores scavenge iron and are important virulence factors for many pathogens, including phytopathogenic fungi such as *Cochliobolus heterostrophus* (Oide et al., 2006) and *Aspergillus fumigatus* (Schrettl et al., 2004). Iron-containing cofactors, such as heme and siroheme are required for the catalytic activity of enzymes associated with nitrogen and sulfur assimilation, as well as xenobiotic detoxification (Tripathy et al., 2010). In the current study, a gene encoding siroheme synthase (SS1G_09177), also known as S-adenosyl-L-methionine: uroporphyrinogen III methyltransferase, was sharply induced during the earliest stages of the infection (1-12 hpi) attesting to the importance of iron sequestration and metabolism.

In addition to key enzymes involved in secondary metabolite biosynthesis, transporters are also required to deploy or secrete secondary metabolites (Table 2.4). For example, HC-toxin is a virulence factor of *Cochliobolus carbonum* on maize and is synthesized by a NRPS named HTS1 (Walton, 2006). It is exported from the cell by two major facilitator superfamily (MFS) transporters, TOXA and TOXB (Pitkin et al., 1996). Three genes encoding transporters with similarity to TOXA proteins were up-regulated in the current study. The proteins encoded by SS1G_09759, SS1G_00919 and SS1G_06662 exhibited 51% similarity to putative HC-toxin efflux carrier TOXA from *Aspergillus lentulus*, 61% to the HC-toxin efflux carrier TOXA from *Glarea lozoyensis* and 84% to the MFS toxin efflux pump protein of *B. cinerea*, respectively. It might therefore be inferred that these transporters are involved in the efflux of toxins into the host plant during *S. sclerotiorum* infection, but characterization of their precise substrate specificities requires further study.

To date, sclerin is the only selective phytotoxin reported from *S. sclerotiorum*. It has phytotoxic effects and causes necrotic and chlorotic tissue formation in *B. napus*, *B. juncea*, and *Sinapis alba* which are susceptible to sclerotinia stem rot disease, but not on a resistant species *Erucastrum gallicum* (Pedras and Ahiahonu, 2004). The genes involved in the sclerin synthesis pathway have not been reported; however, the presence of various genes encoding enzymes involved in the synthesis of known secondary metabolites in *S. sclerotiorum* and the comparably

high levels of expression of these genes during infection suggests that, similar to *B. cinerea*, *S. sclerotiorum* has the capacity to secrete several different types of secondary metabolites. The transcriptome information reported in the current study will be useful in characterizing these secondary metabolite biosynthetic pathways.

Table 2.2 Description and expression of up-regulated genes involved in secondary metabolite synthesis.

Gene ID	Description[1]	Expression Level (hpi)[2]					
		1	3	6	12	24	48
1. Polyketides							
SS1G_02356	polyketide synthase (PKS1)[3]	-	-	-	5.1	7.5	5
SS1G_05681	polyketide synthase (PKS4)[3]	-	-	3.4	2.5	-	-
SS1G_09237	polyketide synthase (PKS6)[3]	-	-	-	-	-	34.3
SS1G_01997	polyketide synthase (PKS8)[3]	3.1	4.9	6.4	4.5	-	-
SS1G_11789	polyketide synthase (PKS12)[3]	-	2.3	-	-	-	2.4
SS1G_11404	polyketide synthase (PKS14)[3]	2.8	2.1	2.9	4.7	4.7	9.2
SS1G_04125	polyketide synthase (PKS16)[3]	2.7	3	-	-	3.5	-
SS1G_05787	polyketide synthase (PKS18)[3]	-	-	-	-	3.5	3
SS1G_03591	polyketide synthase (PKS21)[3]	-	-	2.5	-	2.2	-
SS1G_04127	polyketide synthase	2.1	-	-	-	2.9	-
SS1G_10474	polyketide synthase	4	-	-	-	5.2	-
SS1G_05788	polyketide synthase	-	-	-	2.5	4.9	3.5
SS1G_11352	DBSA oxidoreductase (FmE)	4.4	2.8	3.3	-	-	-
SS1G_09239	FAD-dependent monooxygenase (similar to BcBOA8)	-	-	-	-	10.9	17.6
SS1G_02592	zinc-binding oxidoreductase (ToxD)	4	-	-	4.2	5.8	17.8
SS1G_02338	chalcone and stilbene synthase (CHS1)	-	-	-	-	2.1	-
2. Non-ribosomal Peptides							
SS1G_08561	non-ribosomal peptide synthase (NRPS1)[3]	-	-	-	4.7	8.9	32.5
SS1G_03693	siderophore peptide synthase (NRPS2)[3]	-	2.2	2.3	-	4	3.1
SS1G_06185	siderophore peptide synthase (NRPS3)[3]	3.6	8.2	8.8	9.3	4.7	-
SS1G_10563	non-ribosomal peptide synthase (NRPS5)[3]	-	-	-	-	2.3	-
SS1G_12986	NRPS-like enzyme	-	6.3	5.2	4.3	5.8	7
SS1G_09846	NRPS-like enzyme	2.9	2.2	2.6	-	2.1	-
SS1G_03440	NRPS-like enzyme	-	-	-	3.5	4	-
SS1G_00726	NRPS-like enzyme	-	-	-	18.8	-	-
SS1G_01217	NRPS-like enzyme	-	-	-	5.4	10.5	7.7
3. Other							
SS1G_09177	siroheme synthase	10.9	8.7	8.3	5.7	-	-

[1]Annotation based on the presence of conserved PFAM domains and BLAST reports.
[2]Fold change relative to 0 hours post-inoculation (hpi). (-) No significant change in expression.
[3]Gene abbreviations used by Amselem et al., (2011).

Table 2.3 Description and expression of up-regulated genes encoding cytochrome P450 enzymes.

Gene ID	Description[1]	Expression Level (hpi)[2]					
		1	3	6	12	24	48
SS1G_02340	cytochrome p450 (pistatin demethylase)	3.0	5.4	6.7	5.1	-	-
SS1G_04805	CYP51 (eburicol 14 alpha-demethylase)	3.4	3.6	2.4	2.2	-	-
SS1G_00406	CYP55a3 (nitric oxide reductase)	2.1	2.5	2.1	-	-	-
SS1G_00623	cytochrome p450	2.3	-	-	-	-	2.5
SS1G_13470	cytochrome P450 (alkane hydroxylase)	2.2	-	-	-	-	-
SS1G_05491	cytochrome p450	-	86	271	495	1067	5372
SS1G_13909	cytochrome P450	-	2.1	2.2	-	-	-
SS1G_05384	cytochrome p450	-	2.6	-	2.4	-	-
SS1G_02363	cytochrome p450 (trichodiene oxygenase)	-	-	-	4.2	3.3	3.9
SS1G_04088	cytochrome p450 (oxidoreductase)	-	-	-	3.5	7.5	18.7
SS1G_11553	cytochrome p450	-	-	-	2.0	2.3	2.9
SS1G_03436	cytochrome p450 (benzoate 4-monooxygenase)	-	-	-	4.0	2.6	-
SS1G_05490	cytochrome p450 (benzoate 4-monooxygenase)	-	-	-	-	4.6	8.6
SS1G_01843	cytochrome p450 (benzoate 4-hydroxylase)	-	-	-	-	5.5	3.0
SS1G_13957	cytochrome p450	-	-	-	-	14.9	20.4
SS1G_02157	cytochrome p450	-	-	-	-	3.6	9.9
SS1G_04780	cytochrome p450	-	-	-	-	2.2	2.8
SS1G_06101	cytochrome p450	-	-	-	-	4.9	12.7
SS1G_10037	cytochrome p450	-	-	-	-	8.6	9.0
SS1G_11430	cytochrome p450 (alkane hydroxylase)	-	-	-	-	2.1	4.7
SS1G_11697	cytochrome p450	-	-	-	-	2.4	2.5
SS1G_14168	cytochrome p450	-	-	-	-	2.1	6.0
SS1G_11768	cytochrome p450	-	-	-	-	5.3	-
SS1G_01006	cytochrome p450	-	-	-	-	-	3.5
SS1G_08136	cytochrome p450	-	-	-	-	-	7.0
SS1G_14163	cytochrome p450	-	-	-	-	-	3.1
SS1G_08677	cytochrome P450 (monooxygenase)	-	-	-	-	-	2.8

[1]Annotation based on the presence of conserved PFAM domains and BLAST reports.
[2]Fold change relative to 0 hours post-inoculation (hpi). (-) No significant change in expression.

2.4.4.3. Detoxification

Plant pathogens must contend with various host biochemical defense mechanisms during the infection process. This can be achieved through avoidance (e.g. intracellular growth of pathogens to avoid extracellular phytoalexins), resistance (e.g. mutations that alter sensitivity to antimicrobial compounds) or detoxification (e.g. modification or degradation of host phytoalexins). The energy-dependent efflux of toxic phytochemicals by membrane-associated

transporters is a general detoxification mechanism that is common in pathogens with broad host ranges (VanEtten et al., 2001). A total of 33 genes encoding ATP-binding cassette (ABC) transporters and 218 major facilitator superfamily (MFS) transporters have been identified in the *S. sclerotiorum* genome (Amselem et al., 2011). As a group, the ABC and MFS transporters exhibit a wide range of specificities (polysaccharides, drugs, sugars, heavy metals, peptides, amino acids and inorganic ions); however, some have been implicated in the secretion of fungal toxins or the efflux of host phytoalexins (Perlin et al., 2014).

In total, genes encoding 91 MFS transporters and 14 ABC transporters were up-regulated in the current study (Table 2.4). The contribution of ABC transporters to the ability of pathogens to tolerate phytoalexins is well known. In *B. cinerea*, the gene encoding the ABC transporter BcAtrB was induced during the early stages of infection and in the presence of camalexin. Inactivation of the *BcAtrB* gene lead to increased sensitivity to camalexin and reduced virulence (Stefanato et al., 2009). BcAtrB has also been implicated in the transport of the phytoalexin resveratrol, certain antibiotics and fungicides, as well as the plant phenylpropanoid eugenol (Schoonbeek et al., 2001; Schoonbeek et al., 2003). The *S. sclerotiorum* orthologue of *BcAtrB* (SS1G_13659) was also up-regulated at 24-48 hpi in the current study and is likely to play a similar role in phytoalexin avoidance. While BcAtrA was not associated with *B. cinerea* virulence on bean, it is believed to be a multidrug transporter based on its ability to reduce the sensitivity of yeast to cycloheximide and catechol (Del Sorbo et al., 2008). The *S. sclerotiorum* orthologue of *BcAtrA* (SS1G_06715) was slightly induced at 1 hpi. The ABC transporter AtrD has been implicated in resistance to demethylation inhibitor fungicides in *B. cinerea* (Hayashi et al., 2002a) and *S. homeocarpa* (Hulvey et al., 2012), but the *S. sclerotiorum* orthologue (SS1G_02407) was not up-regulated during *B. napus* infection in the current study. The *S. sclerotiorum* orthologue of *BMR1* (SS1G_04483), which is involved in resistance to polyoxin and iprobenfos toxicants in *B. cinerea* (Makizumi et al., 2002), was up-regulated at 48 hpi in the current study.

BcMFS1 encodes a MFS transporter in *B. cinerea*, which is involved in detoxification of natural toxic compounds, such as camptothecin and cercosporin, and provides resistance to some fungicides, such as demethylation inhibitors (DMI) (Hayashi et al., 2002b). SS1G_12842 is orthologous to *BcMFS1* and was expressed, but not up-regulated, in the current study. Some of the MFS transporters up-regulated in the current study may be involved in detoxification, but this

needs further investigation.

While transport of phytoalexins from the pathogen provides a mechanism to avoid the effects of host phytoalexins, enzymes may also be employed to permanently inactivate these compounds or transform them to a less toxic state. The gene encoding brassinin glucosyltransferase 1 (SsBGT1) (SS1G_09997) was up-regulated during infection of *B. napus* cultivar Surpass 400 leaves by *S. sclerotiorum* isolate UQ1280 (Sexton et al., 2009). *SsBGT1* was induced by plant phytoalexins, such as brassinin, and involved in detoxification of plant defense compounds via glucosylation (Sexton et al., 2009). This gene was also up-regulated at 24 and 48 hpi with expression levels 28 and 223-fold greater than the inoculum, respectively, in *S. sclerotiorum* 1980 in the current study.

The plant pathogen *Nectria haematococca* demethylates and detoxifies the pea phytoalexin, pisatin, by means of pisatin demethylase (PDA), a cytochrome P450 enzyme (George and VanEtten, 2001). As such, PDA contributes to virulence of this fungus on pea (Han et al., 2001). SS1G_02340 encodes a cytochrome P450 enzyme (Table 2.3) with similarity to PDA from other plant pathogens, such as *Penicillium chrysogenum* and *Verticillium dahliae*, and was up-regulated at 1 to 12 hpi in the current study. It may be involved in the detoxification of structurally similar phytoalexins from *B. napus*.

Plant pathogens degrade aromatic compounds produced by plant defense systems, such as benzoic acid derivatives arising from the β-ketoadipate pathway (Harwood and Parales, 1996). The CYP53 family of cytochrome P450 enzymes play an essential role in this pathway through the hydroxylation of benzoic acid to 4-hydroxybenzoate. The first report of CYP53A1 enzyme function was from *Aspergillus niger* (Faber et al., 2001). The enzyme encoded by the *Cochliobolus lunatus* orthologue of this gene, CYP53A15, was capable of para hydroxylation of benzoate (Podobnik et al., 2008). The SS1G_01843 gene encodes a benzoate 4-hydroxylase and was up-regulated at 24 and 48 hpi in the current study and it may have a role in detoxification.

Propiconazole is a type of sterol DMI fungicide that inhibits the biosynthesis of ergosterol by targeting CYP51 (eburicol 14 alpha-demethylase) (Yoshida, 1993). CYP51 is involved in the biosynthesis of fungal sterols that are required for membrane stability (Parks and Casey, 1995). It has been speculated that over-expression of *CYP51* or its paralogues in *S. homoeocarpa* and *Monilinia fructicola* is one of the mechanisms that decrease sensitivity to DMI (Luo and Schnabel, 2008; Hulvey et al., 2012). SS1G_04805 is the orthologue of *S. homoeocarpa CYP51*

and was up-regulated at 1 to 12 hpi in the current study. It may play a similar role in detoxifying phytoalexins.

Glucosinolates, found mainly in the Brassicaceae, and the more ubiquitous hydroxynitrile glycosides, are important plant defense compounds. These compounds undergo enzymatic transformation to release a wide variety of toxic metabolites upon tissue damage, including hydrogen cyanide, a potent inhibitor of cell respiration (Frisch et al., 2015). Cyanide hydratases were reported to have a role in detoxifying hydrogen cyanide in *B. cinerea* (Gonzalez-Fernandez et al., 2014) and *L. maculans* (Sexton and Howlett, 2000). In the current study, four genes encoding cyanide hydratases or cyanate hydrolases, SS1G_13754, SS1G_10174, SS1G_01652 and SS1G_11485 (Table 2.5), were significantly up-regulated during different infection stages from 1 to 48 hpi. These may be important for the detoxification of metabolites generated from glucosinolates during infection of *B. napus*.

Glutathione S-transferases (GST) are best known for their ability to conjoin the reduced form of glutathione to xenobiotic chemicals leading to their detoxification. Several genes encoding GSTs were significantly induced during different infection from 1 to 48 hpi with the majority being induced at 24 hpi (Table 2.5). SS1G_01918 was highly induced from 1 to 48 hpi with a peak expression level 189-fold greater than the inoculum. GSTs were first reported in plants because of their ability to detoxify herbicides (Riechers et al., 1997). Xenobiotic detoxification by this group of enzymes has also been reported in other fungi, such as *Phanerochaete chrysosporium* (Dowd et al., 1997). Bcgst1 from *B. cinerea* was the first GST reported in filamentous fungi; however, disruption of the *Bcgst1* gene indicated that the enzyme did not play a role in virulence (Prins et al., 2000). Bcgst1 has been suggested to be a potential virulence factor as it is involved in tolerance against plant defense compounds, but the exact mechanism remains to be investigated. The orthologue of *Bcgst1* in *S. sclerotiorum* (SS1G_07195) was up-regulated at 24 and 48 hpi in the current study.

2-nitropropane dioxygenase is an enzyme that catalyzes the oxidation of nitroalkanes, such as 2-nitropropane, into carbonyl compounds and nitrite. Nitroalkanes are toxic compounds (Mijatovic, 2008) and 2-nitropropane dioxygenase is involved in detoxification of nitroalkanes in the *Trichoderma harzianum*-tomato interaction (Samolski et al., 2009). 2-nitropropane dioxygenase is also involved in xenobiotic degradation by *Pseudomonas jeseenii* (Garrido-Sanz et al., 2016). In the current study, four genes encoding 2-nitropropane dioxygenases,

SS1G_10881, SS1G_14466, SS1G_00355 and SS1G_11235 (Table 2.5), were significantly up-regulated at different infection times from 1 to 48 hpi. These may be important for the detoxification of toxic nitroalkanes during infection of *B. napus*.

Table 2.4 Description and expression of up-regulated genes encoding transporters.

Gene ID	Description[1]	Expression Level (hpi)[2]					
		1	3	6	12	24	48
1. ABC transporter superfamily							
1.1 Pleiotropic Drug Resistance							
SS1G_06715	Pleiotropic Drug Resistance (PDR)	2.0	-	-	-	-	-
SS1G_13659	pleiotropic drug resistance-like (PDR)	-	-	-	-	3.1	13.5
SS1G_04483	pleiotropic drug resistance-like (PDR)	-	-	-	-	-	4.6
1.2 Multi Drug Resistance							
SS1G_04756	ABC multidrug transporter	3.4	7.9	6.5	3.7	2.4	-
SS1G_07287	ABC multidrug transporter	3.5	3.2	2.6	-	-	2.2
SS1G_03324	ABC multidrug transporter	3.5	4.8	4.4	-	-	-
SS1G_13112	ABC multidrug transporter	-	4.1	6.2	3.9	-	-
SS1G_02000	ABC multidrug transporter	-	-	3.9	3.2	-	-
SS1G_06062	ABC multidrug transporter	-	-	-	-	2.4	2.8
1.3 Other families							
SS1G_04757	mitochondrial ATP-binding cassette protein involved in iron homeostasis	-	6.5	5.1	3.4	-	-
SS1G_07963	ABC transporter with iron-containing redox enzyme with death domains	-	-	-	-	4.0	8.5
SS1G_12070	ABC lipid transporter	-	-	-	-	-	2.6
SS1G_10747	ABC peroxysomal fatty Acyl CoA transporter	-	-	-	-	-	3.2
SS1G_05904	ABC peroxysomal fatty Acyl CoA transporter	-	-	-	-	-	2.0
2. MFS transporter superfamily							
2.1 Efflux pumps and drug resistance							
SS1G_10155	MFS drug efflux and drug resistance	10.1	5.5	3.7	-	-	-
SS1G_11948	MFS drug efflux and drug resistance	2.8	6.7	5.5	-	-	-
SS1G_00919	MFS gliotoxin efflux transporter	-	2.7	3.0	-	-	-
SS1G_09759	MFS aflatoxin efflux transporter	-	8.0	-	-	-	-
SS1G_05556	MFS drug efflux and drug resistance	-	-	2.4	-	-	-
SS1G_06662	MFS toxin efflux pump	-	-	3.0	-	-	-
SS1G_05572	MFS drug resistance transporter	11.4	2.9	-	-	-	-
SS1G_02358	MFS drug resistance transporter	-	-	-	4.1	3.7	4.3
SS1G_12101	MFS drug resistance transporter	-	-	-	-	2.4	-
SS1G_02394	MFS drug resistance transporter	-	-	-	-	-	4.6
SS1G_05756	MFS drug resistance transporter	-	-	-	-	-	15.2
SS1G_10566	MFS drug resistance transporter	-	-	-	-	-	5.5
SS1G_05556	MFS drug resistance transporter	-	-	-	-	-	2.0
SS1G_05095	MFS fungal trichothecene efflux pump (TRI12)	-	-	-	-	-	7.1
SS1G_05145	MFS fungal trichothecene efflux pump	-	-	-	-	5.0	-

	(TRI12)						
SS1G_13024	MFS drug resistance transporter	-	-	-	-	-	3.6
SS1G_11919	MFS multidrug transporter	-	2.7	2.3	-	-	-
SS1G_02623	MFS multidrug transporter	-	-	-	-	-	4.7
SS1G_08554	MFS multidrug transporter	-	-	-	-	-	2.9
SS1G_10279	MFS multidrug transporter	-	-	-	-	-	2.1
SS1G_09892	MFS multidrug transporter	-	-	-	-	-	10.2
SS1G_02931	MFS multidrug transporter	-	-	-	-	-	2.8
SS1G_02048	spermidine drug resistance transporter	2.1	-	-	-	-	3.2
2.2 Sugar transporters							
SS1G_04841	hexose transporter	4.1	2.9	-	-	-	-
SS1G_13734	hexose transporter HXT13	-	2.1	-	-	-	-
SS1G_04273	hexose transporter	-	-	-	-	6.1	15.8
SS1G_12412	hexose transporter	-	-	2.1	-	2.5	2.4
SS1G_09710	MFS sugar transporter	-	-	2.7	2.6	4.8	6.5
SS1G_06023	MFS monosaccharide transporter	6.9	6.7	7.0	4.9	-	-
SS1G_10125	MFS monosaccharide transporter	2.1	2.4	-	-	-	-
SS1G_06620	MFS monosaccharide transporter	-	-	-	-	2.4	-
SS1G_07618	MFS monosaccharide transporter	-	-	-	-	-	2.1
SS1G_08794	MFS sucrose transporter	-	-	2.6	-	-	-
SS1G_04208	MFS sugar transporter	-	-	-	4.0	36.7	49.2
SS1G_10413	MFS sugar transporter	-	-	-	2.3	4.6	4.8
SS1G_06751	MFS sugar transporter	-	-	-	-	2.0	-
SS1G_08117	MFS sugar transporter	-	-	-	-	2.8	-
SS1G_11591	MFS sugar transporter	-	-	-	-	10.7	9.4
SS1G_01523	MFS sugar transporter	-	-	-	-	13.1	12.5
SS1G_00928	MFS sugar transporter	-	-	-	-	7.2	10.6
SS1G_08467	MFS sugar transporter	-	-	-	-	2.9	2.5
SS1G_07132	MFS sugar transporter	-	-	-	-	8.3	6.3
SS1G_01759	MFS sugar transporter	-	-	-	-	-	2.8
SS1G_14316	MFS sugar transporter	-	-	-	-	-	6.1
SS1G_06402	MFS sugar transporter	-	-	-	-	-	16.2
SS1G_01302	MFS sugar transporter	-	-	-	-	-	47.6
SS1G_03579	MFS sugar transporter	-	-	-	-	-	4.1
SS1G_05006	MFS sugar transporter	-	-	-	-	-	11.8
SS1G_08982	MFS quinate transporter	-	-	-	-	18.9	26.1
SS1G_09293	MFS quinate transporter	-	-	-	-	3.5	2.9
SS1G_08981	MFS quinate transporter	-	-	-	-	49.3	38.4
SS1G_00139	MFS carbohydrate transporter	-	3.1	2.2	2.0	-	-
SS1G_04149	MFS carbohydrate transporter	-	3.2	2.5	-	-	8.2
SS1G_07210	MFS carbohydrate transporter	-	-	-	-	2.5	2.3
SS1G_08328	MFS carbohydrate transporter	-	-	-	-	5.8	4.1
SS1G_13671	MFS carbohydrate transporter	-	-	-	-	2.4	-
SS1G_11142	MFS monocarboxylate transporter	-	-	-	-	3.6	-
SS1G_14028	MFS carbohydrate transporter	-	-	-	-	2.1	2.0

SS1G_13819	MFS carbohydrate transporter	-	-	-	-	-	8.1
SS1G_01656	MFS monocarboxylate transporter	-	-	-	-	-	2.2
SS1G_07861	MFS galactonate transporter	2.8	-	-	-	-	-
SS1G_09368	MFS galactonate transporter	-	-	3.6	5.8	8.3	9.0
SS1G_09803	MFS galactonate transporter	-	-	-	4.2	14.9	13.1
SS1G_01055	MFS galactonate transporter	-	-	-	-	3.8	-
SS1G_10065	MFS galactonate transporter	-	-	-	-	73.2	487.6
SS1G_11224	MFS galactonate transporter	-	-	-	-	3.3	2.2
SS1G_11609	MFS galactonate transporter	-	-	-	-	3.0	13.0
SS1G_12649	MFS galactonate transporter	-	-	-	-	6.9	2.9
SS1G_12698	MFS galactonate transporter	-	-	-	-	4.0	5.7
SS1G_05090	MFS galactonate transporter	-	-	-	-	7.2	5.7
SS1G_10896	MFS alpha glucoside:h+ symporter	-	-	-	-	4.4	2.3
SS1G_13094	MFS alpha glucoside:h+ symporter	-	-	-	-	5.0	18.6
SS1G_03673	4-hydroxyphenylacetate permease and sugar transporter	-	-	-	-	-	5.3
SS1G_04849	MFS-fucose permease	-	-	-	-	-	3.1
SS1G_02117	lactose permease	-	-	-	2.8	23	31.3
SS1G_08398	maltose permease	-	4.2	-	-	-	3.8
SS1G_07922	maltose permease	-	-	-	-	2.2	-
SS1G_12954	maltose permease	-	-	-	-	-	8.2
2.3 Oligopeptides							
SS1G_02676	oligopeptide transporter	2.0	-	-	-	4.0	5.2
SS1G_09296	oligopeptide transporter	-	-	-	-	3.3	3.1
SS1G_09297	oligopeptide transporter	-	-	-	-	-	2.8
SS1G_10121	MFS peptide transporter	5.9	7.4	5.7	3.0	-	-
SS1G_07522	MFS peptide transporter	-	-	2.1	-	-	4.1
2.4 others							
SS1G_08628	MFS transporter	5.9	6.6	5.6	3.0	2.4	-
SS1G_04769	MFS transporter	-	-	-	-	-	7.3
SS1G_13941	MFS general substrate transporter	-	3.0	-	-	-	-
SS1G_13194	MFS general substrate transporter	-	-	-	-	2.2	-
SS1G_07517	MFS vacuole effluxer Atg22 transporter	-	3.5	3.5	-	2.7	2.4
SS1G_04978	MFS sulfate transporter	-	-	-	-	2.2	-
SS1G_12690	MFS nitrite transporter	-	7.0	12.2	10.7	-	-
SS1G_02906	MFS nicotinic acid transporter	-	-	-	-	3.8	2.1
3. Amino acid transporters							
SS1G_08387	amino acid transporter	-	-	-	3.0	10.4	9.5
SS1G_11233	amino acid transporter	-	-	-	-	2.7	-
SS1G_01802	amino acid transporter	-	-	-	-	-	3.9
SS1G_09839	amino acid transporter	-	-	-	-	-	13.3
SS1G_14102	choline, amino acid permease transport	-	-	-	2.3	-	-
SS1G_05293	choline, amino acid permease transport	-	-	-	-	-	5.0
SS1G_06535	choline, amino acid permease transport	-	-	-	-	-	5.1

SS1G_06536	choline, amino acid permease transport	-	-	-	-	-	3.1
SS1G_04884	ammonium transporter	-	-	-	-	6.8	-
SS1G_11781	arginine permease	2.2	-	-	-	-	-
SS1G_11563	amino acid permease	3.2	4.7	4.9	5.5	-	-
SS1G_02549	amino acid permease	3.1	4.2	3.9	2.2	-	-
SS1G_14381	amino acid permease	2.6	4.6	3.8	3.3	-	-
SS1G_13916	amino acid permease	9.1	11.5	8.6	6.9	2.3	-
SS1G_10633	amino acid permease	-	2.1	2.7	2.1	2.4	4.9
SS1G_03403	amino acid permease	-	-	-	-	3	-
SS1G_11780	amino acid permease	-	-	-	-	-	2.9
SS1G_06841	amino acid permease	-	-	-	-	-	2.7
4. Others							
SS1G_03654	formate nitrate transporter	3.0	3.2	3.1	3.4	4.0	3.9
SS1G_09621	mitochondrial phosphate carrier protein	3.8	5.0	4.4	3.3	-	3.0
SS1G_01720	C4-dicarboxylate transporter	20.2	19.0	18.8	8.5	-	-
SS1G_02619	C4-dicarboxylate transporter	2.2	2.7	2.6	-	-	-
SS1G_12337	calcium proton exchanger	2.5	3	2.2	-	-	2.6
SS1G_02802	Putative Mg2+ transporter	2.6	2.8	2.4	-	-	3.8
SS1G_02548	UDP-N-acetylglucosamine transporter	2.4	2.8	2.8	-	-	-
SS1G_11564	lysosomal cystine transporter	2.1	3.0	2.5	-	-	-
SS1G_06298	cation efflux family transporter	3.1	4.0	3.5	-	-	-
SS1G_09822	monocarboxylate permease-like protein	2.1	2.5	-	-	-	2.7
SS1G_06910	vacuolar iron transporter	2.7	-	2.3	-	3.1	4.0
SS1G_03019	carnitine mitochondrial carrier protein	2.4	-	2.6	-	-	3.4
SS1G_08146	AGZA family xanthine/uracil permease	3	-	-	-	-	-
SS1G_10280	polyamine transport protein	-	2.7	2.1	-	-	-
SS1G_04686	Phosphate/sulfate permease	-	4.2	-	-	3.3	-
SS1G_12991	cation, potassium transporter	-	-	2.4	-	-	-
SS1G_08795	succinate fumarate, mitochondrial transporter	-	-	5.4	-	-	8.0
SS1G_06006	purine-cytosine permease	-	-	-	6.4	3.7	-
SS1G_03305	solute carrier protein	-	-	-	3.0	-	-
SS1G_11712	cation, magnesium transporter	-	-	-	-	2.4	-
SS1G_07645	cation, potassium transporter	-	-	-	-	2.2	2.5
SS1G_02434	mitochondrial 2-oxoglutarate malate carrier protein	-	-	-	-	45.3	44.7
SS1G_06806	3-oxoacyl-[acyl-carrier protein] reductase	-	-	-	-	3.7	5.3
SS1G_10890	acetyl-CoA acetyltransferases	-	-	-	-	3.0	3.4
SS1G_04606	arsenite efflux transporter	-	-	-	-	-	2.8
SS1G_01231	sulfate permease	-	-	-	-	-	5.7
SS1G_01111	cytosine permease	-	-	-	-	-	3.6
SS1G_10204	mitochondrial carrier protein	-	-	-	-	-	2.2
SS1G_06998	peroxisomal, mitochondrial carrier protein	-	-	-	-	-	2.0

SS1G_04019	mitochondrial carrier protein	-	-	-	-	-	2.5
SS1G_08663	solute carrier protein	-	-	-	-	-	2.5
SS1G_05281	fatty acid transporter involves in acyl-CoA synthetase)	-	-	-	-	-	4.3
SS1G_06664	nucleoside transporter	3.7	5.7	5.7	4.3	2.8	-
SS1G_06212	nucleoside transporter	3.2	-	-	-	-	-
SS1G_04537	nucleoside transporter	-	-	-	-	2.6	-
SS1G_09667	nucleoside transporter	-	-	-	-	-	2.3

[1]Annotation based on the presence of conserved PFAM domains and BLAST reports.
[2]Fold change relative to 0 hours post-inoculation (hpi). (-) No significant change in expression.

Table 2.5 Description and expression of up-regulated genes involved in detoxification

Gene ID	Description[1]	Expression Level (hpi)[2]					
		1	3	6	12	24	48
SS1G_01918	glutathione S-transferase	19.1	24.8	34.6	45.0	189.0	19.1
SS1G_10108	glutathione S-transferase	-	-	-	3.5	4.1	2.3
SS1G_08210	glutathione S-transferase	-	-	-	-	2.6	-
SS1G_04914	glutathione S-transferase	-	-	-	-	2.1	-
SS1G_07195	glutathione S-transferase	-	-	-	-	2.7	2.8
SS1G_14440	glutathione S-transferase	-	-	-	-	4.5	3.7
SS1G_09479	glutathione S-transferase	-	-	-	-	-	40.1
SS1G_08258	glutathione S-transferase with glutathionyl-hydroquinone reductase, ECM4 domain	-	-	-	-	3.1	2.4
SS1G_09997	UDP-glucuronosyl and udp-glucosyltransferase (brassinin)	-	-	-	-	28.0	223.2
SS1G_03517	UDP-glucoronosyl and udp-glucosyltransferase family protein	4.5	3.7	-	5.0	8.2	10.8
SS1G_13524	glucosyltransferase family	6.3	4.9	4.2	2.5	-	2.9
SS1G_13754	nitrilase-cyanide hydratase	3.2	3.5	3.1	2.2	4.6	4.4
SS1G_10174	nitrilase-cyanide hydratase	-	11.6	16.3	19.7	29.8	58.6
SS1G_01652	nitrilase-cyanide hydratase	-	-	-	-	3.4	2.3
SS1G_11485	cyanate lyase, cyanase superfamily	-	-	-	-	2.4	-
SS1G_10881	2-nitropropane dioxygenase	2.8	-	-	-	-	-
SS1G_14466	2-nitropropane dioxygenase	2.8	4.0	2.5	-	-	3.0
SS1G_00355	2-nitropropane dioxygenase	-	-	-	-	3.4	5.4
SS1G_11235	2-nitropropane dioxygenase	-	-	-	-	2.7	3.5

[1]Annotation based on the presence of conserved PFAM domains and BLAST reports.
[2]Fold change relative to 0 hours post-inoculation (hpi). (-) No significant change in expression.

2.4.4.4. Oxalic acid production

OA is crucial for *S. sclerotiorum* infection and is required for suppression of host defenses (Williams et al., 2011), regulation of hydrolytic enzyme synthesis and activity (Favaron et al., 2004), and the induction of processes leading to host colonization (Davidson et al., 2016) and tissue necrosis (Kim et al., 2008; Kabbage et al., 2013). OA can be synthesized from a variety of precursors, but in fungi the most common mechanism is through the hydrolysis of oxaloacetate to form OA and carbon dioxide. An oxaloacetate acetyl hydrolase (OAH) has been characterized in *S. sclerotiorum* (Maxwell, 1973) and disruption of the *OAH* gene in *Aspergillus niger*, *B. cinerea* (Han et al., 2007) and *S. sclerotiorum* leads to loss of oxalic acid production and reduced virulence (Liang et al., 2015a). In the current study, the *S. sclerotiorum OAH* gene (SS1G_08218) was expressed from 1 hpi, but only up-regulated at 48 hpi with 5- fold greater levels than the inoculum. *OAH* expression was also detected in the *S. sclerotiorum–P. vulgaris* system, but at 6 and 72 hpi, with relatively higher expression levels at the later time (Oliveira et al., 2015). Interestingly, the gene encoding oxalate decarboxylase (SS1G_10796), an enzyme that degrades OA (Magro et al., 1988), was also induced at 24 and 48 hpi at 10 and 7-fold greater than the inoculum, respectively. Simultaneous expression of these genes with contrasting roles fits well with the biological functions of OA, which are dependent on a balance between the biosynthesis and decomposition of OA to tightly regulate OA levels through the course of infection (Kabbage et al., 2013). The results of the current study showing concurrent expression of *OAH* and the gene encoding oxalate decarboxylase are in agreement with Amselem et al. (2011). The acidic environment produced by OA has a significant role in virulence/ pathogenesis of *S. sclerotiorum*. Release of OA causes a reduction in ambient pH, which stimulates hydrolytic enzyme production throughout the course of the infection (Cotton et al., 2003; Favaron et al., 2004), as well as sclerotogenesis during its final stages (Rollins and Dickman, 2001; Rollins, 2003), though OA may not be the sole determinant affecting tissue acidification (Xu et al., 2015). Interestingly, fine-tuning of OA levels through the activity of OA biogenic (Liang et al., 2015b) and degradative (Liang et al., 2015a) enzymes appears to be critical for early host-pathogen interactions as well, including compound appressorium formation and lesion expansion.

2.4.4.5. Generation of reactive oxygen species

ROS including superoxide, hydrogen peroxide (H_2O_2) and hydroxyl radicals, are produced by

all aerobic organisms (Apel and Hirt, 2004). Plants generate ROS as part of the defense response against pathogen attack (Baker and Orlandi, 1995), but they may also be involved in cell proliferation and differentiation, signal transduction and ion transport (Foreman et al., 2003). Nicotinamide adenine dinucleotide phosphate (NADPH) oxidases (NOX) are key enzymes in oxidative burst activation resulting in ROS production (Segmüller et al., 2008; Kim et al., 2011). NOXs produce superoxide, an important precursor of several ROS, which is then converted to H_2O_2 by superoxide dismutase (Segmüller et al., 2008).

In filamentous fungi, NOX enzymes are involved in various aspects of differentiation, such as sexual reproduction and the formation of penetration structures (Malagnac et al., 2004). In *B. cinerea* both BcNOXA and BcNOXB enzymes are involved in the formation of sclerotia and pathogenicity, while BcNOXB has been specifically implicated in events leading to penetration and BcNOXA in the spreading of lesions (Segmüller et al., 2008). Importantly, NOX enzymes in *B. cinerea* do not play a role in ROS production (Segmüller et al., 2008). Two genes encoding *S. sclerotiorum* NADPH oxidases, *SsNOX1* (SS1G_05661) and *SsNOX2* (SS1G_11172), have been reported (Kim et al., 2011). SsNOX1 is important for both virulence and fungal development and is also connected to oxalate production (Kim et al., 2011). *SsNOX1* and *SsNOX2* were expressed, but not up-regulated in the current study. Interestingly, Kim et al. (2011) proposed that the bicupin domain enzyme encoded by SS1G_10796 may be an oxalate oxidase. Oxalate oxidase catalyzes the generation of hydrogen peroxide (H_2O_2) from oxalate (Kim et al., 2011) suggesting that ROS generated by *S. sclerotiorum* during pathogenesis may be oxalate-mediated. SS1G_10796 was up-regulated at 24 and 48 hpi in the current study which coincided with the beginning of necrotic stage. This is in agreement with the previous study showing that oxalate-induced H_2O_2 in the host has a role in programmed cell death (Kim et al., 2008).

2.4.4.6. Signaling

2.4.4.6.1. Transcription factors

Transcription factors (TFs) are essential players in the regulatory networks that govern developmental processes and the deployment of pathogenicity factors during infection. In the current study, many genes encoding diverse putative TFs were up-regulated at different stages of the infection from 1 to 48 hpi (Table 2.6). Several of these encoded zinc-binding TFs from the major families prevalent in fungi, namely, Cys2 His2, Cys4, and Zn2 Cys6 families (MacPherson

et al., 2006).

The gene encoding the Pac1 zinc finger domain transcription factor (SS1G_07355) was up-regulated 8-fold at 48 hpi in the current study. Pac1 is an orthologue of *A. nidulans* PacC and controls pH-sensitive gene expression. Its activity was required for the control of a variety of physiological and pathogenesis-related processes in *S. sclerotiorum* (Rollins, 2003). In response to increasing ambient pH, Pac1 triggers OA biosynthesis leading a reduction in pH; this in turn causes an increase in *SsPG1* expression and promotes sclerotial development (Rollins and Dickman, 2001). By affecting ambient pH, Pac1 is thought to play a role in OA and PG accumulation and, therefore, its activity is critical for *S. sclerotiorum* pathogenesis.

Biosynthesis of the *B. cinerea* phytotoxin, botrydial, is regulated by the Cys2 His2 zinc finger TF BcCRZ1 (Schumacher et al., 2008a), as well as upstream signaling components phospholipase C (BcPLC1) and calcineurin (Schumacher et al., 2008b). Four genes encoding phospholipase C-like enzymes (SS1G_03548, SS1G_05073, SS1G_08747 and SS1G_13589) were up-regulated at 48 hpi in the current study, suggesting they might be involved in secondary metabolite biosynthesis signaling pathways or events related to the later stages of the infection.

The *Penicillium roqueforti Pcz1* gene encodes a Zn2 Cys6 TF that contributes to the regulation of growth, conidiation, and conidial germination (Gil-Durán et al., 2015). *BcYOH1* from *B. cinerea* encodes a Cys2 His2 TF that is involved in the regulation of secondary metabolite synthesis (Simon et al., 2013). A number of genes encoding zinc cluster TFs similar to BcYOH1 and Pcz1 were differentially expressed at various stages of infection in the current study, including SS1G_10532, SS1G_01109 and SS1G_02054 (Table 2.6). Several genes encoding other types of TFs involved in fungal development were also up-regulated and are discussed below.

Table 2.6 Description and expression of up-regulated genes encoding transcription factors.

Gene ID	Description[1]	Expression Level (hpi)[2]					
		1	3	6	12	24	48
1. Zn2Cys6 (C6)							
SS1G_06255	Zn2 Cys6 transcription factor	7.0	4.6	3.9	2.4	-	-
SS1G_14383	Zn2 Cys6 transcription factor	3.5	4.4	3.5	2.1	-	-
SS1G_08819	Zn2 Cys6 transcription factor	3.6	2.5	2.1	3.0	-	-
SS1G_06907	Zn2 Cys6 transcription factor	4.1	4.1	3.3	-	-	-
SS1G_02793	Zn2 Cys6 transcription factor	6.0	3.0	-	-	-	-
SS1G_10324	Zn2 Cys6 transcription factor	2.0	-	-	-	2.0	-
SS1G_02851	Zn2 Cys6 transcription factor	2.2	-	-	-	-	-
SS1G_12532	Zn2 Cys6 transcription factor	2.2	-	-	-	-	-
SS1G_12799	Zn2 Cys6 transcription factor	-	2.5	2.5	-	-	-
SS1G_11949	Zn2 Cys6 transcription factor	-	2.7	2.5	-	-	-
SS1G_00732	Zn2 Cys6 transcription factor	-	2.4	-	5.0	-	-
SS1G_00398	Zn2 Cys6 transcription factor	-	4.1	-	-	-	4.8
SS1G_01905	Zn2 Cys6 transcription factor	-	-	-	-	2.7	-
SS1G_06876	Zn2 Cys6 transcription factor	-	-	-	-	2.3	-
SS1G_00170	Zn2 Cys6 transcription factor	-	-	-	-	2.3	-
SS1G_02339	Zn2 Cys6 transcription factor	-	-	-	-	2.0	-
SS1G_07143	Zn2 Cys6 transcription factor	-	-	-	-	2.7	-
SS1G_02791	Zn2 Cys6 transcription factor	-	-	-	-	2.9	3.0
SS1G_00392	Zn2 Cys6 transcription factor	-	-	-	-	2.2	2.2
SS1G_13144	Zn2 Cys6 transcription factor	-	-	-	-	2.1	3.0
SS1G_02054	Zn2 Cys6 transcription factor	-	-	-	-	6.6	36.9
SS1G_05109	Zn2 Cys6 transcription factor	-	-	-	-	6.7	7.2
SS1G_05755	Zn2 Cys6 transcription factor	-	-	-	-	2.6	3.8
SS1G_07003	Zn2 Cys6 transcription factor	-	-	-	-	-	4.6
SS1G_10447	Zn2 Cys6 transcription factor	-	-	-	-	-	2.5
SS1G_01353	Zn2 Cys6 transcription factor	-	-	-	-	-	4.1
SS1G_11367	Zn2 Cys6 transcription factor	-	-	-	-	-	3.3
SS1G_08351	Zn2 Cys6 transcription factor	-	-	-	-	-	2.1
SS1G_03775	Zn2 Cys6 transcription factor	-	-	-	-	-	6.8
SS1G_00787	Zn2 Cys6 transcription factor	-	-	-	-	-	2.8
SS1G_01733	Zn2 Cys6 transcription factor	-	-	-	-	-	2.6
SS1G_04056	Zn2 Cys6 transcription factor	-	-	-	-	-	2.7
SS1G_11081	Zn2 Cys6 transcription factor	-	-	-	-	-	2.8
SS1G_09741	fungal specific transcription factor	2.2	3.7	3.9	2.7	-	-
SS1G_04333	fungal specific transcription factor	2.0	2.3	2.0	-	-	-
SS1G_12561	fungal specific transcription factor	2.3	2.1	-	-	-	-
SS1G_09823	fungal specific transcription factor	-	-	2.1	-	2.2	2.4
SS1G_04846	fungal specific transcription factor	-	-	-	-	2.6	4.0
SS1G_13882	fungal specific transcription factor	-	-	-	-	2.0	-
SS1G_13729	fungal specific transcription factor	-	-	-	-	2.4	-
SS1G_02758	fungal specific transcription factor	-	-	-	-	2.5	-
SS1G_08406	fungal specific transcription factor	-	-	-	-	2.3	-

SS1G_05809	fungal specific transcription factor	-	-	-	-	3.9	-
SS1G_04057	fungal specific transcription factor	-	-	-	-	-	2.4
SS1G_11395	fungal specific transcription factor	-	-	-	-	-	2.3
SS1G_06361	fungal specific transcription factor	-	-	-	-	-	2.1
2. Cys2His2							
SS1G_01109	C2H2 transcription factor	19.8	26.1	26.6	15.6	-	-
SS1G_01684	C2H2 transcription factor	2.6	3.1	2.7	2.0	-	-
SS1G_04676	C2H2 transcription factor	2.0	-	-	-	-	7.3
SS1G_07355	C2H2 transcription factor (Pac1)	-	-	-	-	-	8.4
SS1G_10532	C2H2 transcription factor	-	-	-	-	-	20.5
SS1G_00104	C2H2 binding site	-	-	2.5	3.1	-	5.4
SS1G_09588	C2H2 binding site	-	-	-	-	2.9	4.4
SS1G_06370	C2H2 binding site	-	-	-	-	-	2.1
SS1G_09499	C2H2 binding site	-	-	-	-	-	3.1
SS1G_07425	C2H2 binding site	-	-	-	-	-	4.3
SS1G_06044	C2H2 binding site	-	-	-	-	-	2.3
3. basic leucine zipper (bZIP)							
SS1G_10244	bZIP transciption factor	4.4	5.2	-	5.6	-	-
SS1G_01411	bZIP transciption factor	-	-	-	-	2.0	-
SS1G_00816	bZIP transciption factor	-	-	-	-	-	5.4
SS1G_06075	bZIP transciption factor	-	-	-	-	-	7.7
4. Others							
SS1G_14328	transcription regulator BDF1	2.7	6.5	5.5	3.6	-	-
SS1G_11030	CP2 transcription factor	4.9	3.2	2.5	-	-	-
SS1G_04107	MYB family transcription factor	2.5	2.9	-	-	-	-
SS1G_06257	pex2/pex12 superfamily, zinc finger of C3HC4-type	3.0	2.4	-	-	-	-
SS1G_07430	zinc finger domain	3.0	-	-	-	-	2.8
SS1G_03881	regulator of G protein signaling domain protein (RGS) (GTPase activating proteins (GAPs)	2.0	-	-	-	-	-
SS1G_14385	CBF/Mak21 transcription factor	2.4	-	-	-	-	-
SS1G_03280	helix-loop-helix dna-binding protein (HlH)	2.4	-	-	-	-	-
SS1G_10206	CHY and ring, zinc finger protein	-	2.1	-	-	-	-
SS1G_04050	NF-X1 zinc finger transcription factor	-	3.0	-	-	-	-
SS1G_11663	large tegument protein UL36 and similar to TFIIIC transcription initiation factor complex subunits Tfc3	-	-	2.1	2.0	-	-
SS1G_03992	transcription mediator subunit Med12	-	-	2.2	-	-	-
SS1G_13930	Bro1-Alix- like domain and pH-response regulator protein	-	-	-	-	2.3	-
SS1G_07542	RING-H2 zinc finger protein	-	-	-	-	2.3	-

SS1G_06124	mads-box mef2 type transcription factor (SRF type)	-	-	-	-	-	3.5
SS1G_03098	homeobox transcription factor	-	-	-	-	-	2.2
SS1G_03835	homeobox C2H2 transcription factor	-	-	-	-	-	3.1
SS1G_06987	yippee zinc-binding protein	-	-	-	-	-	2.4
SS1G_01859	MYB dna-binding containing domain protein	-	-	-	-	-	6.2
SS1G_08831	(vWA) transcription factor (Von Willebrand factor type A)	-	-	-	-	-	2.3
SS1G_09890	RAP transcription factor	-	-	-	-	-	2.6
SS1G_02756	transcription factor protein	-	-	-	-	-	8.5
SS1G_10304	tetratricopeptide (TPR) repeat transcriptional corepressor	-	-	-	-	-	2.3
SS1G_13511	lipopolysaccharide (LPS)-induced transcription factor and LITAF-like zinc ribbon domain	-	-	-	-	-	2.7

[1]Annotation based on the presence of conserved PFAM domains and BLAST reports.
[2]Fold change relative to 0 hours post-inoculation (hpi). (-) No significant change in expression.

2.4.4.6.2. Phosphorylation-dependent signaling

The *S. sclerotiorum* genome contains many different types of kinases that are involved in signaling pathways, including the G protein-coupled receptor, MAP kinase, heterotrimeric G protein, cAMP, and Ca2+-related signaling pathways (Amselem et al., 2011). A number of genes associated with these pathways were up-regulated during infection in the current study (Table 2.7) and are discussed below. While the induction of genes encoding signaling pathway components is not always necessary for activation of their associated pathways, it does imply that they may be involved in more critical aspects or regulatory checkpoints during the infection process.

Two-component histidine kinases are known to be involved in regulating responses to environmental stimuli in fungi and bacteria (Tanaka and Izumitsu, 2010). The gene encoding the two-component sensor histidine protein kinase Shk1 (SS1G_10091) was up-regulated only at the beginning of the infection (1 hpi) in the current study. Shk1 was previously shown to have a role in hyphal growth and sclerotial formation in *S. sclerotiorum*, but was not required for pathogenicity on plant leaves (Duan et al., 2013).

The suite of genes encoding eukaryotic protein kinases in *S. sclerotiorum* has been catalogued (Hegedus et al., 2016). Genes encoding two MAPKKK genes (SS1G_00606 and SS1G_10983) were up-regulated at 48 and 1-6 hpi, respectively. SS1G_00606 encodes an orthologue of STE11

in *S. cerevisiae* and belongs to the *S. sclerotiorum* STE11-like MAPKKK family, while SS1G_10983 encodes an orthologue of BCK1 in the yeast cell wall integrity pathway. Mutation of the *STE7* and *STE11* orthologues in *B. cinerea* (Schamber et al., 2010) or *MST7* and *MST11* in *M. grisea* (Zhao et al., 2005) disrupted the formation of infection structures leading to loss of pathogenicity. The protein encoded by SS1G_10021 belongs to the CAMK1 family in *S. sclerotiorum* and is orthologous to the *S. cerevisiae* CMK1/ CMK2 kinases. SS1G_10021 was up-regulated at 48 hpi in the current study. CAMKs were reported to have a role in the regulation of cell wall integrity and the response to oxidative stress (Ding et al., 2014). A gene (SS1G_03455) orthologous to *S. cerevisiae SAT4*/*HAL4* was induced at 24-48 hpi in this study. HAL family kinases play a role in the regulation of membrane permeases that are responsible for amino acid and glucose transport (Pérez-Valle et al., 2010). Genes encoding two other protein kinases, SS1G_09511 and SS1G_06542, were both significantly up-regulated at 48 hpi in the current study. The kinase encoded by SS1G_09511 has some similarity to PHO85 (SS1G_07226), a cyclin-dependent kinase involved in the regulation of cell division in response to environmental stresses (Nishizawa, 2015). SS1G_06542 encodes an ortholog of SHA3/SKS1 that is involved in integration of the response to glucose with hyphal development (Johnson et al., 2014). The FunK1 protein kinases are similar to eukaryotic protein kinases, but are only found in multi-cellular fungi (Stajich et al., 2010). The *S. sclerotiorum* genome contains three genes encoding members of the FunK1 family (SS1G_09355, SS1G_12423 and SS1G_14212), all of which were up-regulated at the earliest stages of the infection.

SS1G_06571, SS1G_03234 and SS1G_10333 encode proteins annotated as having GTPase or GTP-binding activity and were first up-regulated at 1, 1 and 48 hpi, respectively. In *S. sclerotiorum*, the small GTPase Rap-1 is involved in mediating the inhibitory actions of cAMP on the SMK1 MAPK signaling cascade and events leading to sclerotial development (Chen and Dickman, 2005). GTP-binding proteins belonging to the Ras superfamily also play a role in MAPK inhibition as effectors acting downstream of cAMP (Chen and Dickman, 2005). Other studies have shown that in addition to Ras, other small GTPases, such as Rap-1 and Rho/Rac/ Cdc42, also have important roles in transmitting signals via activation of MAPK cascades (Zimmermann and Moelling, 1999).

Protein dephosphorylation is also employed to both activate and attenuate kinase-dependent signaling pathways. Calcineurin, a Type 2B serine/threonine phosphatase, is required for proper

sclerotial formation and hyphal cell wall formation (Harel et al., 2006). The Type 2A serine/threonine phosphatase (PP2A) encoded by SS1G_08489 (PPH1) was shown to play a role in several aspects of *S. sclerotiorum* pathogenesis including hyphal growth, infection cushion formation, sclerotia development and synthesis of secondary metabolites such as melanin (Erental et al., 2007). The genes encoding calcineurin and PPH1 were not up-regulated in the current study; however, a possible PPH1 paralogue (SS1G_08513), which encodes a serine/threonine phosphatase with a PP2A catalytic subunit, was up-regulated at 48 hpi. It is possible that the protein encoded by SS1G_08513 complements the function of PPH1in the *S. sclerotiorum* infection process, but characterization of its precise roles awaits further study. The SMK1 MAPK also positively regulates PPH1 activity through a nitrous oxide-dependent mechanism (Erental et al., 2007).

Table 2.7 Description and expression of up-regulated genes involved in signaling or gene regulation.

Gene ID	Description[1]	Expression Level (hpi)[2]					
		1	3	6	12	24	48
1. Protein Kinases							
SS1G_10983	MAPKK kinase (SsBCK1)	4.7	5.4	4.4	2.4	-	-
SS1G_11525	protein kinase-like protein	2.5	3.6	6.9	6.1	-	-
SS1G_00606	MAPKK kinase (SsSTE11)	2.1	2.2	-	-	-	2.1
SS1G_08085	AGC protein kinase (SsRIM15)	-	2.1	2	-	-	-
SS1G_03455	HAL family protein kinase	-	-	-	-	3.3	3.7
SS1G_06203	CAMK protein kinase (SsRCK2)	-	-	-	-	-	2.3
SS1G_10021	CAMK protein kinase (SsCMK2)	-	-	-	-	-	4.1
SS1G_06542	ran1-like protein kinase (SsSKS1)	-	-	-	-	-	2.3
SS1G_09511	protein kinase (Ss-Other-03)	-	-	-	-	-	5.8
SS1G_14212	Funk1 serine threonine-protein kinase	2.1	-	-	-	-	-
SS1G_12423	Funk1 serine threonine-protein kinase	2.3	2.4	-	-	-	-
SS1G_09355	Funk1 serine threonine-protein kinase	2.1	2.3	-	-	-	-
SS1G_10091	two-component histidine protein kinase (SHK1)	2.6	-	-	-	-	-
2. Phosphatases							
SS1G_11340	tyrosine phosphatase	2.6	2.1	2.2	-	-	2
SS1G_01711	protein phosphatase type 1 complex subunit hex2 reg1	3.3	3.2	2.2	-	-	-
SS1G_04320	tyrosine-protein phosphatase non-receptor type partial	2.1	3.5	2.5	-	-	-
SS1G_06382	protein phosphatase regulator	2.1	-	-	-	-	-
SS1G_12383	histidine acid phosphatase	-	2.8	-	-	-	-
SS1G_08513	serine threonine-protein phosphatase PP2A	-	-	-	-	-	2.8
SS1G_10466	diketo-5-methylthio-1-phosphopentane phosphatase	-	-	-	-	-	2.5
3. GTPase/GTP-binding							
SS1G_03234	rho GTPase activator	3.1	5	4.6	4.8	-	-
SS1G_06571	GTP-binding protein rho2	3.2	3	2.1	-	-	-
SS1G_01564	nuclear GTP-binding protein NUG1	2.9	-	-	-	-	-
SS1G_04075	ARF GTPase activator	-	-	-	-	-	2.5
SS1G_10333	GTP-binding protein	-	-	-	-	-	2.3
SS1G_08371	CLP1 GTPase	-	-	-	-	-	2.9
SS1G_13589	phosphatidyl inositol phospholipase C	-	-	-	-	-	2.1

	(PL-PLC)						
SS1G_03548	phosphatidyl inositol phospholipase C (PL-PLC)	-	-	-	-	-	2.1
SS1G_05073	phosphatidyl inositol phospholipase C (PL-PLC)	-	-	-	-	-	5
SS1G_08747	phosphatidyl inositol phospholipase C (PL-PLC)	-	-	-	-	-	9
4. Other							
SS1G_06667	sir2 chromatin regulatory protein	2.1	3	2.6	2.1	-	-
SS1G_06180	Pal1 morphogenesis-related protein	9.5	8.7	7.9	4.5	-	-
SS1G_04402	Arrestin (chitin synthesis regulation)	-	-	-	-	2.1	-
SS1G_03525	ankaryin repeat protein	-	-	-	-	2.7	-
SS1G_04325	SUR7/Pal1 family (pH-response regulator)	-	-	-	-	-	2.2
SS1G_10456	SUR7/Pal1 family (pH-response regulator)	-	-	-	-	-	12.6
SS1G_09665	inositol-pentakisphosphate 2-kinase	-	-	-	-	-	2.8
SS1G_00378	SRP19 signal recognition particle protein	-	-	-	-	-	3
SS1G_08048	Sok1 cAMP-mediated signaling protein	-	-	-	-	-	2.7

[1]Annotation based on the presence of conserved PFAM domains and BLAST reports.
[2]Fold change relative to 0 hours post-inoculation (hpi). (-) No significant change in expression.

2.4.4.7. Development

As is the case in most multi-cellular pathogens, *S. sclerotiorum* undergoes dramatic morphological and biochemical changes as it passes through the various stages of the infection process. The *S. sclerotiorum* genome contains orthologues of *M. oryzae* genes encoding proteins that are involved in infection structure production and penetration (Amselem et al., 2011). Among them, SS1G_13339, SS1G_10311 and SS1G_11468 were up-regulated in the current study (Table 2.8). SS1G_10311 and SS1G_11468 are orthologous to mas2 and mas3 in *M. oryzae*, respectively, where they play a role in appressoria formation during the very early stages of infection (Xue et al., 2002). However, in the current study SS1G_10311 was up-regulated at 3 and 12 hpi and SS1G_11468 was up-regulated at 6-48 hpi, while SS1G_13339 was induced only at 48 hpi, suggesting that they may have alternate roles in this necrotrophic pathogen.

Morphological changes can also be triggered by environmental cues. The enzyme γ-glutamyl transpeptidase regulates glutathione levels and in turn cellular redox potential. In *S. sclerotiorum*, the γ-glutamyl transpeptidase encoded by SS1G_14127 (SsGgt1) plays a role in the production of compound appressoria during host penetration as well as in the development of sclerotia, but is

not necessary for host colonization and symptom development (Li et al., 2012). In the current study, SS1G_14127 was up-regulated from 6-48 hpi, while genes encoding two other γ-glutamyl transpeptidases (SS1G_05530 and SS1G_10940) were up-regulated during the later stages at 24 and 48 hpi, respectively.

The *SSP1* gene (SS1G_14065) was up-regulated 47- fold at 48 hpi in the current study. The *SSP2* gene (SS1G_12133), a paralogue of *SSP1*, was also up-regulated in the later stages of the infection. SSP1 is a sclerotium-specific protein that is associated with sclerotial and apothecial development and is only detected during sclerotial formation (Li and Rollins, 2009). The up-regulation of SSP1 and SSP2 at 24-48 hpi is an indication of the onset of sclerotia development at these time points in the current study. SOP1 is similar to microbial opsins, a component of the photosensory system, and is also required for sclerotial development, as well as growth and virulence in *S. sclerotiorum*. SOP1 was first induced at early stages of infection in *A. thaliana* and then more so at the sclerotial development stage (3 days post inoculation) (Lyu et al., 2015b). In the current study, the gene encoding SOP1 (SS1G_01614) was highly up-regulated (17-fold) at 24 and 48 hpi suggesting that this protein also contributes to the sclerotial development program in the *S. sclerotiorum-B. napus* pathosystem. Members of the velvet protein family coordinate fungal differentiation processes, including the formation of spores, sclerotia and fruiting bodies (Bayram and Braus, 2012). SS1G_07626 encodes a velvet protein and was induced only at 48 hpi indicating that it may also be involved in sclerotogenesis in *S. sclerotiorum*. Another gene (SS1G_07404) encoding Ss-Rhs1, *S. sclerotiorum* rearrangement hotspot repeat 1, was up-regulated at 24 and 48 hpi in the current study and has been reported to be involved in sclerotial development and important for virulence in *S. sclerotiorum* (Yu et al., 2016).

MADS-box proteins are a conserved family of TFs and are involved in the regulation of a wide variety of functions including primary metabolism, cell cycle and cell identity (Qu et al., 2014). A gene encoding a MADS-box TF (SS1G_06124) was reported as being a component of the mating process in *S. sclerotiorum* (Amselem et al., 2011) and was up-regulated 3-fold at 48 hpi in the current study. The MADS-box TF SsMADS (SS1G_05588) is required for growth and virulence (Qu et al., 2014). Homeobox genes regulate aspects of anatomical development and in fungi are involved in hyphal growth, appressorium formation or conidia production (Kim et al., 2009). In the current study, a gene (SS1G_03835) encoding a homeobox C2H2 TF was expressed at 48 hpi, but the precise function of this gene in *S. sclerotiorum* needs to be characterized. A

homeobox TF (BcHOX8) that plays a role in the vegetative growth and conidiogenesis has been reported in *B. cinerea* (Antal et al., 2012).

In fungi, programmed cell death associated with vegetative incompatibility is determined by the interactions of proteins containing heterokaryon incompatibility (HET) domains (Paoletti and Clavé, 2007). In the current study, 11 genes encoding heterokaryon incompatibility proteins were up-regulated at some point during the infection with one group induced during the early stages (SS1G_02742, SS1G_02602, SS1G_03889, SS1G_11165 and SS1G_06855) and a second group induced during the later stages (SS1G_08974, SS1G_06855, SS1G_12973, SS1G_09167 and SS1G_11315) (Table 2.8). Some genes encoding HET domain-containing proteins in *S. sclerotiorum* are orthologues of HET-E-1 family genes of *Podospora anserina* (Paoletti and Saupe, 2009; Amselem et al., 2011), but these were not up-regulated in the current study. The role of HET domain-containing proteins in *S. sclerotiorum* and *B. cinerea* speciation has also been suggested (Amselem et al., 2011). Some *S. sclerotiorum* orthologues of *A. nidulans* genes involved in mating and fruiting body development, such as SS1G_09861 and SS1G_07526 (Amselem et al., 2011), were also up-regulated in the current study. Additionally, SS1G_06124 (transcription factor) and SS1G_00606 (STE 11 kinase), which are also orthologues of *A. nidulans* genes involved in mating process signaling pathways (Amselem et al., 2011), were significantly induced in the current study.

Mobilization of storage reserves, including those derived from cell wall turnover and reconstruction, accompanies major morphological phase transitions, such as sclerotial formation. Trehalose is a common storage carbohydrate in fungi and a gene encoding an acid trehalase (SS1G_05192) was induced at the later stages of the infection. Alpha-1,3-glucan (mutan) is a component of the fungal cell wall, but is also considered to be a major energy reserve (Wei et al., 2001). Two genes encoding 1,3-alpha-glucanase/mutanase (SS1G_01494 and SS1G_09861) were sharply induced (15 and 30 fold) at 48 hpi. The expression of these genes closely coincided with the expression of a wide variety of genes encoding enzymes capable of degrading fungal cell walls, including chitinases, chitin deacetylases, N-acetylglucosaminidases and various endo-glucanases. In another study, 19 % of all *S. sclerotiorum* genes encoding fungal cell wall degrading enzymes were up-regulated during infection (Lyu et al., 2015a). They hypothesized that these enzymes were involved in cell wall reorganization or rearrangement as the pathogen progressed through different developmental stages.

Table 2.8 Description and expression of up-regulated genes involved in fungal development.

Gene ID	Description[1]	Expression Level (hpi)[2]					
		1	3	6	12	24	48
1. Reserve Mobilization							
SS1G_05192	acid trehalase	-	-	-	-	6.7	5.8
SS1G_01494	1,3-alpha-glucanase/mutanase	-	-	-	-	-	30.7
SS1G_09861	1,3-alpha-glucanase/mutanase	-	-	-	-	-	15
2. Cell Wall							
2.1 Turnover							
SS1G_05454	chitinase	-	-	2.4	-	3.5	2.7
SS1G_11700	chitinase	-	-	-	-	3.7	69.1
SS1G_05897	chitinase	-	-	-	-	3	2.6
SS1G_11304	chitinase	-	-	-	-	-	4.8
SS1G_08695	class III chitinase	-	-	-	5.8	8.2	11.7
SS1G_11212	class III chitinase	-	-	-	-	-	9.3
SS1G_12510	class V chitinase	-	-	-	-	11.2	66.9
SS1G_09403	alpha-N-acetylglucosaminidase	-	-	-	-	2.9	-
SS1G_12837	beta-N-acetylglucosaminidase	-	-	-	-	2.3	-
SS1G_10038	beta-N-acetylglucosaminidase	-	-	-	-	-	3
SS1G_04898	polysaccharide (chitin) deacetylase	-	-	15.2	-	-	12.7
SS1G_01131	polysaccharide (chitin) deacetylase	-	-	-	-	3	3.6
SS1G_00642	polysaccharide (chitin) deacetylase	-	-	-	-	-	8.3
SS1G_12836	N-acetylglucosamine-6-phosphate deacetylase	-	-	-	-	-	6.7
SS1G_01229	exo-beta 1,3 glucanase	-	-	-	-	3.4	22.8
SS1G_09858	exo-beta 1,3 glucanase	-	-	-	-	-	2.8
SS1G_12930	GPI-anchored cell wall beta-1,3-endoglucanase	8.5	6.4	3.9	-	-	2.2
SS1G_04852	GPI-anchored cell wall beta-endoglucanase	2.1	-	-	-	-	-
2.2 Biosynthesis							
SS1G_04969	glycosyl transferase (cell wall synthesis)	2.2	-	-	-	-	-
SS1G_04062	glycosyl transferase (cell wall synthesis)	-	3.6	3.8	-	-	-
SS1G_07313	lipopolysaccharide biosynthesis protein	-	-	-	-	-	2.4
3. Other							
SS1G_02742	heterokaryon incompatibility protein	3.8	3.6	3.1	2.8	-	-
SS1G_02744	heterokaryon incompatibility protein (SEC1)	3.7	5.5	-	5	3	3
SS1G_02602	heterokaryon incompatibility protein	2.3	-	-	-	-	-
SS1G_03889	heterokaryon incompatibility protein	-	3.2	-	-	-	-

SS1G_11165	heterokaryon incompatibility protein	-	3.3	2.2	-	-	-
SS1G_06800	heterokaryon incompatibility protein	-	3.6	-	-	-	-
SS1G_08974	heterokaryon incompatibility protein (WD40 repeat)	-	-	-	-	2.7	-
SS1G_06855	heterokaryon incompatibility protein	-	-	-	-	5.2	2.4
SS1G_12973	heterokaryon incompatibility protein	-	-	-	-	-	2
SS1G_09167	heterokaryon incompatibility protein	-	-	-	-	-	2.5
SS1G_11315	heterokaryon incompatibility protein	-	-	-	-	-	4
SS1G_07526	ferritin-like sexual development protein	3	2.5	2.5	-	-	23.9
SS1G_04316	acyltransferase (hard surface induced)	2.5	-	-	-	-	-
SS1G_10311	DUF cell surface protein (MAS2 orthologue)	-	2.1	-	2.5	-	-
SS1G_11468	CAS1 appressorium specific protein (MAS3 orthologue)	-	-	2.9	7.3	12.9	10.5
SS1G_14127	gamma-glutamyltranspeptidase (SsGGT1)	-	-	3.4	6.5	4.8	2.7
SS1G_05330	gamma-glutamyltranspeptidase	-	-	-	-	2.1	-
SS1G_12877	conidiation-specific expression protein	-	-	-	-	2.3	2.3
SS1G_12133	predicted protein (SSP2)	-	-	-	-	4.7	9.6
SS1G_07404	predicted protein (Ss-Rh1)	-	-	-	-	4.9	3.8
SS1G_01614	G protein-coupled receptor (SOP1)	-	-	-	-	17.7	17.1
SS1G_07626	Velvet family	-	-	-	-	-	5.2
SS1G_13339	choline carnitine O-acyltransferase	-	-	-	-	-	3.4
SS1G_02422	UDP-galactopyranose mutase (GLF)	-	-	-	-	-	3.9
SS1G_10940	gamma-glutamyltranspeptidase	-	-	-	-	-	4
SS1G_14065	predicted protein (SSP1)	-	-	-	-	-	47

[1]Annotation based on the presence of conserved PFAM domains and BLAST reports.
[2]Fold change relative to 0 hours post-inoculation (hpi). (-) No significant change in expression.

2.4.4.8. Secreted effectors

Sclerotinia sclerotiorum secretes a large repertoire of various effector proteins that may be involved in aspects of pathogenesis or virulence (Guyon et al., 2014). Several of these, and others, were found to be up-regulated during infection of *B. napus* in the current study (Table 2.9) and are discussed below.

One of the hallmarks associated with *S. sclertoriorum* infection is the rapid onset of necrosis. Two *S. sclerotiorum* Nep proteins (SsNep1 and SsNep2) were characterized by Bashi et al. (2010) and their necrosis-inducing activity demonstrated. In that study, both genes were induced at the mid to later times in the infection with *SsNep2* being expressed at much higher levels than *SsNep1*. This is in agreement with the current study where the *SsNep2* gene (SS1G_11912) was

induced at 24 and 48 hpi. Orthologues of these genes are also present in *B. cinerea* (*BcNep1* and *BcNep2*) and both proteins are capable of inducing necrosis in the host plants (Schouten et al., 2008). Cerato-plantanins are small, hydrophobic, secreted proteins found in many fungal phyto-pathogens and have been shown to induce plant defenses leading to systemic acquired resistance (Frías et al., 2013). In *B. cinerea*, cerato-platanin is one of the most abundant secreted proteins and elicits a strong hypersensitive response in the host plant leading to localized necrotic lesions (Frías et al., 2011). An *S. sclerotiorum* gene encoding cerato-platanin (SS1G_10096) was up-regulated at both the early and later stages of the infection in the current study and was recently reported as SsCP1 that targets plant PR1 and triggers cell death induction (Yang et al., 2018a). *SsSSVP1* (SS1G_02068) encodes a small secreted, cysteine-rich protein that induces plant cell death by interfering with host energy metabolism and, as such, plays an important role in virulence in *S. sclerotiorum* (Lyu et al., 2016). In the current study, SS1G_02068 was up-regulated 21-fold at 48 hpi. In the *S. sclerotiorum-A. thaliana* interaction, *SsSSVP1* showed significant up-regulation starting from 3 hpi and slowly increased from 6 to 12 hpi (Lyu et al., 2016), suggesting that the expression pattern of this gene could be host-dependent. As noted above, several hydrolytic enzymes, including certain PGs (Kars et al., 2005; Bashi et al., 2013) and xylanases (Noda et al., 2010), are also potent inducers of host necrosis.

A gene encoding a cysteine-rich protein with a CFEM (common fungal extracellular membrane) domain (SS1G_07295) did not show significant induction in a previous study conducted on a number of host plants (Guyon et al., 2014), whereas in the current study it was induced between 2 and 4.8 fold throughout the course of the infection supporting the notion that expression of effector genes in *S. sclerotiorum* may be host dependent. In *M. grisea*, the CFEM protein Pth11 is involved in appressorium development (DeZwaan et al., 1999), while in *Candida* species CFEM proteins were involved in biofilm formation and iron acquisition (Ding et al., 2011). *SsCVNH* (SS1G_02904), which encodes a small, cysteine-rich, secreted protein with a CyanoVirin-N Homology (CVNH) domain, was previously predicted to be a candidate effector of *S. sclerotiorum* (Guyon et al., 2014), and was shown to be important for infection, sclerotial development and growth of *S. sclerotiorum* (Lyu et al., 2015a). *SsCVNH* was up-regulated at 48 hpi in the current study. Similarly, Lyu et al. (2015a) showed that *SsCVNH* was significantly up-regulated during the initial stages of sclerotial development occurring at 3 days post-inoculation. The induction of *SsCVNH* coincided with that of *Pac1*, which is also involved in sclerotial

development through OA-mediated pH reduction, suggesting that the expression of *SsCVNH* might also be pH dependent. A gene encoding another cysteine-rich protein (SS1G_03611) was one of the most highly up-regulated genes detected in the current study and exhibited a 247- fold increase in expression at 48 hpi, while a gene encoding a protein unique to *S. sclerotiorum* and *B. cinerea* (SS1G_00263) was induced 49-fold at this time. The protein encoded by SS1G_00849 had none of the domains associated with fungal effectors; however, it is an orthologue of *Colletotrichum hingginsianum* effector candidate 91 (CHEC91) (Kleemann et al., 2012) and analogous to the *Alternaria alternate* AltA-1 allergen (Guyon et al., 2014). SS1G_00849 was significantly induced at 1–3 and 48 hpi in the current study supporting the view that it may also be a *S. sclerotiorum* effector.

Some effectors facilitate infection by abrogating the ability of the host to deploy appropriate defense responses. LysM effectors interfere with host detection of the pathogen by binding to and masking fungal cell wall–derived chitin fragments that would normally induce host defense responses (Mentlak et al., 2012). A gene encoding a LysM protein (SS1G_12509) was up-regulated during the mid to later stages of the infection, while a gene encoding another chitin-binding protein (SS1G_12336) was up-regulated at 3 hpi. Salicylic acid is a signaling molecule required for the induction of plant defenses in response to many biotic and abiotic stresses. Enzymes that degrade salicylic acid are released by some fungal endophytes to suppress the deployment of such defenses (Ambrose et al., 2015). In the current study, a gene encoding salicylate hydroxylase (SS1G_08557) was induced very early in the infection and remained up-regulated throughout, although this gene does not have signal peptide and might be secreted through an alternative endoplasmic reticulum/Golgi-independent protein secretion mechanism.

Table 2.9 Description and expression of up-regulated genes encoding putative effector proteins.

Gene ID	Description[1]	Expression Level (hpi)[2]					
		1	3	6	12	24	48
SS1G_08557	salicylate hydroxylase	4.1	5.4	5.1	3.6	5.1	10.8
SS1G_00849	22kda glycoprotein (AltA-1 allergen)	7.4	3.2	-	-	-	7.1
SS1G_10096	cerato-platanin (SsCP1)	3.8	3.7	-	-	-	3.3
SS1G_07295	cfem domain-containing protein	2	-	-	-	3.9	4.8
SS1G_12336	chitin binding protein	-	3.3	-	-	-	-
SS1G_12509	LysM domain protein	-	-	-	3.8	11.8	35.4
SS1G_03611	cysteine-rich protein	-	-	-	-	85.1	247
SS1G_11912	npp1 domain protein (NEP2)	-	-	-	-	5.8	8.2
SS1G_03282	serine protease inhibitor	-	-	-	-	-	2.2
SS1G_02904	cyanoVirin-N homology (SsCVNH)	-	-	-	-	-	3.9
SS1G_00263	protein unique to *S. sclerotiorum* and *B. cinerea* (Ssv263)	-	-	-	-	-	49.2
SS1G_02068	predicted protein (SsSSVP1)	-	-	-	-	-	21.5

[1]Annotation based on the presence of conserved PFAM domains and BLAST reports.
[2]Fold change relative to 0 hours post-inoculation (hpi). (-) No significant change in expression.

2.5. Conclusions

Sclerotinia sclerotiorum deploys a wide variety of factors and complex strategies to establish disease and complete the infection of the host plant. Soon after encountering the surface of a suitable host plant, the pathogen releases enzymes that begin to digest the cuticle. The induction of *SsCuta* and genes encoding related cutinases/lipases at the earliest stages of the infection supports their role in cuticle penetration. The enzymatic degradation of other plant surface polymers and polysaccharides is also required for successful penetration and is carried out by an armory of hydrolytic enzymes, which were induced from 1 to 12 hpi in this study. These enzymes are released from the base of infection cushions, which apply pressure to assist cuticle penetration. Induction of orthologous genes encoding proteins involved in appressorium formation in other fungi, such as mas2 and mas3 (Xue et al., 2002; Amselem et al., 2011) and SsGgt1 (Li et al., 2012) during the early stages of infection in the current study supports their role in the production of penetration-associated structures.

During penetration and subsequent proliferation through the host, the fungus must sequentially breach various layers of plant barriers. To do so, it releases a cocktail of hydrolytic enzymes, detoxification systems and effector proteins. A plethora of genes encoding hydrolytic enzymes

were induced concurrent with cell wall and host plant tissue disruption and are required to release nutrients to facilitate spread of the pathogen. Noxious compounds liberated as a form of plant defense or through the activities of the pathogen itself must also be detoxified. This study revealed that *S. sclerotiorum* induces the expression of genes encoding a wide variety of ABC and MFS transporters, cytochrome 450 enzymes, GSTs., etc, during the infection that may allow it to contend with various host plant defense mechanisms and toxins.

Recent studies have identified a brief biotrophic phase within the apoplastic space immediately after cuticle penetration (Kabbage et al., 2015). During infection of *B. napus* in the current study, this biotrophic stage might occur between 12 and 24 hpi since biotrophy-related effector genes, such as those encoding the LysM domain protein and salicylate hydroxylase, were up-regulated during this period. These proteins may assist with suppression of host-pathogen recognition and defense systems. However, the genes encoding SSITL (Zhu et al., 2013) and chorismate mutase (SsCM1) (Kabbage et al., 2013), which also help to suppress plant defense responses during the biotrophic phase, were not induced in the current study. This discrepancy might indicate that *S. sclerotiorum* is armed with alternate, unelucidated, strategies to suppress host defenses to establish a biotrophic phase in different host plants.

The appearance of necrotic lesions at 24 hpi indicated that initial penetration and the biotrophic phase had ended by this time. The onset of the necrotrophic stage requires that a different set of genes be expressed, including those encoding hydrolytic enzymes, enzymes involved in secondary metabolite synthesis or toxins to trigger host programmed cell death. Numerous genes encoding enzymes involved in the synthesis of polyketides and non-ribosomal peptides were up-regulated throughout the infection, but more so during the later stages. Previous studies also suggested that the induction of genes encoding Nep proteins coincides with the beginning of the necrotrophic phase (Qutob et al., 2002). The expression of *SsNep2* in the current study was induced beginning at 24 hpi, confirming that *S. sclerotiorum* had switched to the necrotrophic stage around this time.

The acidic environment resulting from OA accumulation is a critical step during the necrotrophic phase of *S. sclerotiorum*. In the present study, the genes encoding Pac1 and subsequently OAH which are indirectly and directly involved in OA biosynthesis, respectively, were up-regulated at 48 hpi, supporting the notion that OA accumulates during the necrotrophic phase of infection. The acidic environment produced by OA stimulates hydrolytic enzyme

production, specifically SsPG1 (Rollins and Dickman, 2001; Cotton et al., 2003; Rollins, 2003; Favaron et al., 2004). Induction of *acp1*, whose expression is sensitive to pH, is also regulated by Pac1 (Poussereau et al., 2001a). Interestingly, the concurrent expression of *OAH* and the gene encoding oxalate decarboxylase suggests that a balance between biosynthesis and decomposition of OA is required for tight regulation of OA levels through the course of infection (Amselem et al., 2011). In addition to its role in regulating the transition to the necrotrophic phase, OA also plays a role in suppression of the oxidative burst in the host plant during the early stages of the infection (Williams et al., 2011) and may therefore contribute to the establishment of a biotrophic phase. However, *OAH* expression was not induced during the early stages of infection in the current study suggesting that an alternative pathway for OA biosynthesis independent of OAH exists or more likely that a basal amount of OA is sufficient for suppression of oxidative burst.

In addition to the well-known effectors that have been mentioned above, a number of genes encoding other *S. sclerotiorum* effectors, including SsBi1 (Yu et al., 2015), SsCaf1 (Xiao et al., 2014), SCat1 (Yarden et al., 2014), SsSodI (Xu and Chen, 2013) and SsPemG1 (Pan et al., 2015) were expressed, but not significantly induced in the current study. The discrepancy might be due to host and isolate dependent differences in the expression of these genes or differences in experimental design.

In summary, the current study revealed a vast set of genes encoding various hydrolytic enzymes, enzymes involved in secondary methobolite biosynthesis, proteins associated with detoxification systems and effector proteins that collectively facilitate the infection of *B. napus* by *S. sclerotiorum*. The present investigation gives a global view of the gene expression of *S. sclerotiorum* as it infects *B. napus* and provides a baseline for further characterization of important genes involved in the *S. sclerotiorum-B. napus* and other host molecular interactions.

CHAPTER 3. IDENTIFICATION OF NECROSIS-INDUCING EFFECTORS

3.1. Abstract

Sclerotinia sclerotiorum is the causative agent of stem rot, the most important disease of canola worldwide. *Sclerotinia sclerotiorum* is dependent on necrosis-inducing effectors to induce cell death for nutrient uptake, a characteristic of all necrotrophic plant pathogens. To identify necrosis-inducing effectors, the genome of *S. sclerotiorum* was searched for genes encoding small, secreted, cysteine-rich proteins. These effectors were tested for the ability to induce necrosis in *Nicotiana benthamiana* via Agrobacterium-mediated infiltration and to determine their host cellular localization. Six novel necrosis-inducing proteins were discovered, of which all but one required a signal peptide and secretion to the extracellular space for necrotic activity. Virus-induced gene silencing (VIGS) experiments were conducted to reveal the role of plant receptor-like kinases (RLK) in the induction of cell death. VIGS revealed that the five effectors that required secretion for activity also required the RLKs, BAK1 and SOBIR1, for the induction of necrosis. These results illustrate the importance of necrosis-inducing effectors for *S. sclerotiorum* virulence and the potential role of host extra-cellular receptor(s) in the perception of *S. sclerotiorum* and as targets in effector-assisted breeding for resistance of *B. napus* against stem rot disease.

3.2. Introduction

The infection of a host plant by a fungal pathogen most often begins with an attempt to penetrate the cuticle. Beyond this barrier, pathogens face a multi-faceted defense system triggered by perception of the pathogen, which restricts further growth and dissemination. To overcome plant defenses, pathogens secrete an array of effector proteins to suppress the host immune system and to reprogram the expression of host genes involved in signaling, cell structure and metabolism (Dalio et al., 2018). Characterizing these effectors, determining their targets and understanding their interaction with host defenses is key to uncovering pathogenicity/virulence mechanisms and devising strategies to control diseases in economically important crops.

In addition to mechanical and cellular defense barriers conferring passive resistance, fungal

pathogens encounter a series of active defense mechanisms induced by the perception of conserved PAMPs, termed PTI. Multiple plasma membrane-localized PRRs, such as membrane-associated receptor-like kinases (RLK) or receptor-like proteins (RLP), can be simultaneously engaged in pathogen recognition (Saijo et al., 2018). RLKs have an extracellular domain, a transmembrane (TM) domain and an intracellular kinase domain, while RLPs lack the intracellular kinase domain. These, together with the brassinosteroid receptor insensitive 1-associated kinase 1 (BAK1)/somatic embryogenesis receptor kinase 3 (SERK3), mediate PAMP recognition and induction of defenses (Cook et al., 2015; Ben Khaled et al., 2015). Pathogens secrete an array of effector proteins to suppress PTI immunity that either mask the PAMPs, prevent PAMP recognition or interfere with defense responses (de Jonge et al., 2010; Dou and Zhou, 2012; Liebrand et al., 2014). These effectors can be recognized in the cytoplasm or apoplast by R proteins and plasma membrane-localized PRRs, respectively, as a second layer of plant defense known as ETI (Rivas and Thomas, 2005; Jones and Dangl, 2006). This recognition often ends in a HR that can restrict infection by biotrophic pathogens, but may lead to enhanced host susceptibility to hemibiotrophic and necrotrophic pathogens through a cellular process called ETS (Jones and Dangl, 2006). Perception of effectors by host plant cells can occur directly (ETI or ETS) or through indirect sensing of alterations caused by effectors on non-receptor host cell targets (Cui et al., 2015). Overlap between the recognition of effectors and PAMPs by PRRs and R proteins in the plant may also occur (Ma and Borhan, 2015). For example, upon *Avr4* recognition, resistance protein *Cf4* along with BAK1 and suppressor of BAK1- interacting receptor-like kinase1 (SOBIR1) were required for ETI and HR initiation in tobacco (Liebrand et al., 2013; Postma et al., 2015). Similarly, RLP30 along with SOBIR1 and BAK1 were required for recognition of a novel elicitor from *S. sclerotiorum*, called Sclerotinia culture filtrate elicitor 1 (SCFE1) (Zhang et al., 2013).

Sequencing the genomes of plant pathogens has enabled *in silico* approaches for predicting their effector repertoires (Sperschneider et al., 2015a; Dalio et al., 2018). The general primary criteria for *in silico* identification of effectors includes being relatively small, the presence of a signal peptide (SP), elevated cysteine content, and the absence of TM domains or membrane anchors (Kamoun, 2006; Liu et al., 2012; Lyu et al., 2015a). The SP is essential as it mediates the secretion of the effectors outside of the pathogen so they may interact with the host (von Heijne, 1998). The disulfide bonds between cysteine residues in effector proteins are suggested to

enhance stability in this environment and are, hence, important for biological function. For example, cysteine residues are necessary for the biological activity of ToxA, a necrosis-inducing effector secreted from *P. tritici-repentis* (Tuori et al., 2000). Effectors target diverse cellular functions (Toruno et al., 2016) and are generally classified as apoplastic (function in the host extracellular space) or cytoplasmic (function inside host cells) (Stotz et al., 2014). Previous studies showed that fungal and oomycete effector targets are located in a wide variety of subcellular compartments, including the plasma membrane, tonoplast, vacuole, ER, nucleus and cytosol (Bozkurt et al., 2012; Caillaud et al., 2012; McLellan et al., 2013). Therefore, expression profile during host invasion, prediction of subcellular localization, and structural properties can also contribute to the identification of candidate effectors (Dalio et al., 2018). Ultimately, functional validation with approaches such as *in planta* expression using *Agrobacterium tumefaciens*-mediated infiltration (agro-infiltration) and silencing of effectors or their host targets provide further evidence for their function (Sparkes *et al.*, 2006; Mesarich *et al.*, 2014).

Sclerotinia sclerotiorum causes stem rot, one of the most devastating diseases of canola. *Sclerotinia sclerotiorum* is a necrotrophic pathogen that switches to a highly aggressive pathogenic phase soon after host cuticle penetration aided by the secretion of acids and hydrolytic enzymes (Hegedus and Rimmer, 2005). Recent studies, however, have provided evidence for a two-phase infection model for this pathogen with a brief biotrophic phase (Kabbage et al., 2015; Liang and Rollins, 2018). According to these studies, *S. sclerotiorum* first suppresses the plant defense systems in the biotrophic phase followed by rapid induction of host cell death at the onset of the necrotrophic phase (Liang and Rollins, 2018). Seifbarghi *et al.*, (2017) suggested that the biotrophic stage might occur within the first 24 hours post-infection since biotrophy-related candidate effector genes, such as those encoding the LysM domain protein and salicylate hydroxylase, are up-regulated during this period. This study also provided an overview on how the *S. sclerotiorum* transcriptome is deployed in a compatible *S. sclerotiorum-B. napus* interaction. To date, much effort has been directed toward understanding the interaction of *S. sclerotiorum* with its various hosts, which has cast light on the complexity of *S. sclerotiorum*-host interactions. For example, 78 candidate effectors were identified in the genome of *S. sclerotiorum* using various computational tools (Guyon et al., 2014). Some of these play crucial roles during different stages of *S. sclerotiorum* infection, but the exact functions of most of these effectors remain unknown. Several effectors involved in pathogenesis or virulence, including two *S.*

sclerotiorum Nep proteins (SsNep1 and SsNep2) (Bashi et al., 2010), SsCVNH (Lyu *et al*., 2015), SSITL (Zhu et al., 2013), SsCM1 (Kabbage et al., 2013), SsSSVP1 (Lyu et al., 2016), SsBI1 (Yu et al., 2015), SsCaf1 (Xiao et al., 2014), SCat1 (Yarden et al., 2014), SsSodI (Xu and Chen, 2013), SsCP1 (Yang et al., 2018a) and SsPemG1 (Pan et al., 2015) have been characterized.

Sclerotinia sclerotiorum is dependent on necrosis-inducing effectors to induce cell death and to initiate the switch to the necrotrophic stage of infection. In this study, I used bioinformatics and transcriptomic approaches to identify and characterize *S. sclerotiorum* candidate effector proteins. The necrotizing activities of these candidate effectors were examined by *in planta* transient expression and subcellular localization studies conducted to facilitate identification of host targets. This study revealed that the receptor-like kinases BAK1 and SOBIR1 were required for necrotizing activity of most *S. sclerotiorum* necrosis-inducing effectors. This study highlights the potential of novel necrosis-inducing effectors for use in targeted effector-guided breeding to identify germplasm with improved resistance to this pathogen.

3.3. Methods

3.3.1. Bioinformatics analyses

Sclerotinia sclerotiorum isolate 1980 was used in this study, as the genome sequence of this strain is available. The sequence as described by Amselem *et al*., (2011) was used, although this was revised by Derbyshire *et al.*, (2017) after initiation of this work. The genome-wide search for candidate effectors was conducted using a general pipeline for *in silico* prediction of pathogen effectors (Sperschneider et al., 2015b). The bioinformatic tools used to identify candidate effectors were SignalP 4.1 (Petersen et al., 2011) for predicting the presence of a SP, TMHMM v2.0 (Chen et al., 2003) for TM helixes, Big-PI predictor (Eisenhaber et al., 1998) for glycosylphosphatidylinositol (GPI)-anchored proteins and TargetP 1.1 (Emanuelsson et al., 2007) for subcellular location of proteins. The number of cysteine residues in a given protein was computed using an in-house Perl script and those with more than 2% cysteine residues were retained. Predicted effector proteins smaller than 55 amino acids were excluded from the analysis because the GPI prediction algorithm does not work with smaller proteins. The remaining candidate genes were scanned for the presence of an N-terminal [N/L]-[P/I/L]-[I/P]-[R/N/S] (the core canonical NPIR) vacuole localization motif using the CLC Genomics Workbench 7.0.3

(http://www.clcbio.com) motif search tool and genes encoding proteins without this motif were retained.

The final list of candidate effectors produced from a combination of the bioinformatic and transcriptomic methods were subjected to functional annotation using the BLAST2GO plugin (v1.4.4) in CLC Genomics Workbench 8.0.1 (http://www.clcbio.com). The candidate protein sequences were used for searches with BLASTP (https://blast.ncbi.nlm.nih.gov/Blast.cgi) to identify conserved protein domains. WoLF PSORT (Horton et al., 2007) was used to predict the subcellular localization of these proteins.

3.3.2. RNA-Seq analysis: RNA extraction, library preparation and Illumina sequencing

The data from the RNA-Seq study conducted by Seifbarghi *et al*., (2017) (Chapter 2) was used to evaluate the *in planta* expression patterns of candidate effectors during the course of infection. Briefly, fungal mats and infected *B. napus* cv. DH12075 plant tissues beneath were collected at 1, 3, 6, 12, 24 and 48 hours post-inoculation, flash-frozen in liquid nitrogen and stored at -80 °C. Total RNA was extracted using an Illustra RNAspin mini RNA isolation kit (Illumina, San Diego, USA). Libraries were prepared using a Truseq stranded mRNA kit (Illumina, San Diego, USA) following the manufacturer's instructions. Sequencing was conducted on an Illumina MiSeq sequencing system using the Illumina MiSeq reagent kit V3 (Illumina, San Diego, USA) following the manufacturer's instructions. Data analysis was conducted using CLC Genomics Workbench 7.0.4 (http://www.clcbio.com). The expression profile of candidate effector genes identified by *in silico* analysis was extracted from the RNA-Seq analysis output. Only candidate effector genes expressed during infection were considered for further analysis.

3.3.3. Cloning of candidate effectors

cDNA was synthesized using the iScript reverse transcription supermix available in the RT-qPCR kit (Bio-Rad, CA, USA) following the manufacturer's instructions. The cDNA was used as a template for PCR amplification of candidate genes to generate amplicons encoding proteins with and without the native SP. Two different constructs were made to test the necrotizing activity of each protein, one with the SP using primer pairs F1 and R1, and the other without the SP using primer pairs F2 and R1 (Table A.3). Two additional constructs were made to test the subcellular localization of each protein, one with the SP using primer pairs F1 and R2, and the

other without the SP using primer pairs F2 and R2 (Table A.3). The DNA amplicons were then cloned into the Gateway® entry vector pDONRzeo© (Invitrogen, Carlsbad, USA) following the manufacturer's protocol. To convert the entry vector into a Gateway® expression vector, candidate genes were transferred from pDONRzeo to pEarlyGate100 (pEG100) and pEarlyGate103 (pEG103) (Earley et al., 2006) using the Gateway protocol (Invitrogen, Carlsbad, USA) and used for phenotypic and microscopic experiments, respectively. pEG103 provides a C-terminal fusion to Green Fluorescent Protein (GFP).

3.3.4. Agrobacterium-mediated transient expression of candidate effectors in *Nicotiana benthamiana*

All constructs were transformed into *Agrobacterium tumefaciens* strain GV3101. The transformed *A. tumefaciens* colonies were selected on Luria-Bertani (LB) agar containing 10 mg/mL rifampicin and 100 mg/mL kanamycin. Four to five-week-old plants were transformed using an agro-infiltration technique for both phenotypic and microscopic experiments following the method described by Ma et al., (2012). *A. tumefaciens* was grown in LB-mannitol medium supplemented with 20 µM acetosyringone and 10 mM MES (pH 5.6). Cells were harvested by centrifugation at 2800 *g* for 15 min and then re-suspended in infiltration buffer containing 10 mM MES, 2 % w/v sucrose, 0.05 % w/v MS salts and 200 µM acetosyringone. After 1 or 2 hours, the leaves were pressure-infiltrated with a 1-ml needleless syringe. *A. tumefaciens* harboring the empty vector (AtEV) was used as a negative control, while a strain carrying a construct designed to express the *P. infestans* Nep1-like protein (PiNPP1.1) was used as a positive control (Kanneganti et al., 2006). The appearance of cell death in infiltrated areas was visually evaluated 3-7 days post-infiltration. Each experiment was conducted three times. To assess localization in the ER, *A. tumefaciens* strains harboring pEG103 constructs were co-infiltrated with a second *A. tumefaciens* strain expressing an mCherry fluorescent protein marker containing an ER retention signal (KDEL) (http://www.bio.utk.edu/cellbiol/markers/) at a 1:1 ratio.

3.3.5. Subcellular location of candidate effectors *in planta* using confocal laser-scanning microscopy (CLSM)

The *N. benthamiana*-infected leaf cells expressing the GFP fusion proteins were examined using a Zeiss LSM 710 CLSM at 36-48 hours post-infiltration (hpif). Images were obtained using a 63 X objective lens. An argon laser was used to excite GFP at 488 nm and emission was

collected at 493–540 nm. mCherry was excited at 561 nm and emission was collected at 589–754 nm.

3.3.6. Evaluation of host plant ER stress-related gene expression using droplet digital PCR (ddPCR)

To assess the association of host plant ER stress with the necrotizing activity of the necrosis-inducing effectors, the expression of genes induced under ER stress or involved in the unfolded protein response (UPR) was examined in *N. benthamiana* leaf tissues infiltrated with *A. tumefaciens* strains carrying effector constructs or AtEV as a negative control at 24, 48 and 72 hpif. The expression of genes encoding the ER luminal binding protein (BiP)-like protein 4 (BLP4, GenBank accession FJ463755.1), protein disulfide isomerase (PDI, GenBank accession Y11209.1) and basic-leucine zipper 60 (bZIP60, GenBank accession AB281271.1) were examined. Primers and probes for each gene were designed using PrimerQuest software (IDT) and all probes were labeled with fluorescein amidite (FAM), except for the reference gene probe (*α-tubulin*), which was labeled with hexachloro-fluorescein (HEX). Sequences and details of primers and probes are provided in Table A.4. Leaf samples infiltrated with tunicamycin, a known inducer of ER stress, were used as a positive control and leaves of untreated plants were used for constructing an expression baseline for non-infiltrated plants. The experiment was conducted with three biological replicates. Total RNA extraction, cDNA synthesis and ddPCR were conducted as outlined in Chapter 2.

3.3.7. Virus-induced gene silencing in *Nicotiana benthamiana*

To examine the involvement of BAK1 and SOBIR1 in the necrotizing activity of the necrosis-inducing effectors, VIGS was conducted using a tobacco rattle virus (TRV) based vector system. *A. tumefaciens* GV3101 strains harboring pTRV1 (Ratcliff et al., 2001) and pTRV2 constructs including *pTRV2:GFP* (Burch-Smith et al., 2006), *pTRV2:PDS* (PDS: phytoene desaturase) (Liu et al., 2002), *pTRV2:NbSOBIR1* (Liebrand et al., 2013) and *pTRV2:NbBAK1* (Chaparro-Garcia et al., 2011) were grown to an OD600 = 1. Each *A. tumefaciens* strain carrying pTRV2 construct was mixed at a 1:1 ratio with the *A. tumefaciens* strain carrying pTRV1 and infiltrated into leaves of 2-week-old *N. benthamiana* seedlings similar to agro-infiltration (Ma et al., 2012).

Three weeks after agro-infiltration, *N. benthamiana* leaf samples from three biological

replicates infiltrated with VIGS constructs, including *pTRV2:GFP, pTRV2:NbSOBIR1, pTRV2:NbBAK1* and untreated *N. benthamiana* leaves as an un-infected negative control, were collected and ground to a fine powder with an RNAse-free mortar and pestle precooled with liquid nitrogen. Total RNA extraction and cDNA synthesis were conducted as described above. Quantitative PCR (qPCR) was performed using a CFX96 real-time machine (Bio-Rad, CA, USA) and SsoAdvanced™ Universal SYBR® Green Supermix (Bio-Rad, CA, USA). The amplification conditions were 30 s at 95° C followed by 40 cycles of 10 s at 95° C, 30 s at 60° C, and a melt curve of 5 s at 65° to 95° C. The primer pairs used for qPCR were previously described by Liebrand *et al*., (2013), and Ma and Borhan (2015). qPCR data were normalized using expression of the endogenous *actin* gene as a reference. The expression (fold change) was reported using the $2^{-\Delta\Delta Ct}$ method (Livak and Schmittgen, 2001) and compared to the control (*pTRV2:GFP*).

Three weeks after agro-infiltration with the VIGS constructs, leaves of *N. benthamiana* were infiltrated with *A. tumefaciens* carrying the effector constructs, a Bcl2-Associated protein X construct (BAX; Lacomme and Santa Cruz, 1999) as a BAK1/SOBIR1-independent necrosis-inducing protein positive control or AtEV as a negative control. The development of necrosis symptoms was evaluated visually 3-7 days post-infiltration. The experiment was conducted three times.

3.4. Results

3.4.1. Defining a catalogue of *Sclerotinia sclerotiorum* effectors

As a first step towards the identification of *S. sclerotiorum* necrosis-inducing effectors, bioinformatic approaches were applied to predict effector proteins from the *S. sclerotiorum* genome. First, a search for the presence of a SP using SignalP 4.1 (Petersen et al., 2011) resulted in approximately 912 genes encoding potential secreted proteins. Subsequently, proteins with an N-terminal SP were screened for their subcellular localization signals to exlude membrane-bound and membrane-anchored proteins using TargetP (Emanuelsson et al., 2007), TMHMM (Chen et al., 2003), and Big-PI software (Eisenhaber et al., 1998), respectively. Proteins harbouring an NPIR motif immediately adjacent to the predicted SP cleavage site that are targeted to the vacuole (Vitale and Raikhel, 1999; Carter et al., 2004) were also excluded from the list of candidate effectors. NPIR motifs direct proteins to the lytic vacoules where hydrolysis of macromolecules and cellular structures occurs (Vitale and Raikhel, 1999). To enrich for potential

effectors, only small proteins (55- 250 amino acids) with more than 2% cysteine content (105 proteins) were considered as most likely candidate effectors.

3.4.2. The expression pattern of candidate effectors

RNA-Seq time course data (Seifbarghi *et al*., 2017) were analysed to determine the expression profiles of the genes encoding the 105 *S. sclerotiorum* candidate effectors during different infection stages on *B. napus* leaves. Of these, the expression of 27 genes was up-regulated during infection compared to *S. sclerotiorum* grown *in vitro*. These effectors were considered as the best candidates and exhibited a wide range of expression patterns (Table 3.1). Eight genes were up-regulated at the very early stages of the infection (1 hpi), while eight genes were up-regulated at the later stages (48 hpi). Further annotation of the proteins using BLASTP revealed that many did not possess known structural domains (Table 3.1). Two proteins, namely cutinase (SS1G_07661) (Bashi et al., 2012) and SsSSVP1 (SS1G_02068) (Lyu et al., 2016), had been investigated previously and were excluded from the analysis. An additional gene, SS1G_03611, was also excluded due to difficulties in cloning that was likely caused by mis-annotation arising from incorect assembly of the genome.

Table 3.1 List of *Sclerotinia sclerotiorum* candidate effector genes, putative functions and expression patterns inferred from RNA-Seq analysis

Gene ID Version one model	Gene ID Version two model[1]	Genbank accession number	Description[2]	Expression Level (hpi)[3]					
				1	3	6	12	24	48
Necrosis-inducing effectors									
SS1G_07027*	Sscle06g052360	XP_001591581	Hypothetical protein	10.1	2.9	3.8	4.0	3.1	8.8
SS1G_00872*	Sscle03g023810	XP_001598783	Hypothetical protein	2.1	2.9	2.6	-	-	-
SS1G_00849*	Sscle03g024000	XP_001598760	22kda glycoprotein	7.4	3.2	-	-	-	7.1
SS1G_10096	Sscle16g107670	XP_001588549	SsCP1	3.8	3.7	-	-	-	3.3
SS1G_09232*	Sscle15g106560	XP_001589511	Hypothetical protein	2.3	-	-	-	-	2.7
SS1G_08706*	Sscle14g098920	XP_001589942	Plant expansin	-	-	-	3.1	4.6	4.8
SS1G_09150*	Sscle15g107190	XP_001589429	Hypothetical protein	-	-	-	-	28.8	92.3
SS1G_11912	Sscle12g090490	XP_001586883	SsNEP2	-	-	-	-	5.8	8.2
SS1G_02068	Sscle01g003850	XP_001597872	SsSSVP1	-	-	-	-	-	21.6
Non necrosis-inducing effectors									
SS1G_07661	Sscle11g084380	XP_001591036	Cutinase	3.0	3.9	4.3	4.7	3.4	-
SS1G_00263	Sscle03g028510	XP_001598177	SsV263	4.8	-	-	-	-	49.2
SS1G_04519	Sscle02g016170	XP_001594711	Hypothetical protein	2.1	-	-	-	-	3.7
SS1G_09844	Sscle01g001890	XP_001589211	Hypothetical protein	-	6.7	9.1	6.0	-	-
SS1G_13668	Sscle14g097630	XP_001585429	GAS2 domain-containing	-	7.4	6.8	5.3	-	-
SS1G_07669	Sscle11g084330	XP_001591044	DNase1 protein	-	6.9	3.6	3.4	-	-
SS1G_01867	Sscle01g005390	XP_001597671	Long chronological lifespan	-	2.5	-	-	-	-
SS1G_13126	Sscle02g020840	XP_001586033	Hypothetical protein	-	-	25.9	13.6	10.3	12.5
SS1G_04382	Sscle02g017190	XP_001594575	Thaumatin-like protein	-	-	-	-	4.8	8.2
SS1G_05939	Sscle05g046060	XP_001593017	Hypothetical protein	-	-	-	-	31.8	-
SS1G_03611	Sscle07g055350	XP_001595522	Cysteine-rich protein	-	-	-	-	85.1	247.0
SS1G_09420	Sscle15g105160	XP_001589698	Hypothetical protein	-	-	-	-	-	6.0
SS1G_13696	Sscle14g097380	XP_001585457	Hypothetical protein	-	-	-	-	-	8.3
SS1G_10534	Sscle09g071930	XP_001588088	Hypothetical protein	-	-	-	-	-	31.8
SS1G_09248	Sscle15g106410	XP_001589527	Hydrophobin precursor	-	-	-	-	-	6.1
SS1G_00744	Sscle03g024730	XP_001598655	Hypothetical protein	-	-	-	-	-	2.1
SS1G_01235	Sscle01g010360	XP_001597041	Hypothetical protein	-	-	-	-	-	34.6
SS1G_02904	Sscle04g038020	XP_001596682	SsCVNH	-	-	-	-	-	3.9

[1]Results of reciprocal best hits BLAST analysis between version one and version two gene models (Derbyshire et al., 2017).
[2]Annotation based on BLAST reports and gene symbols that have already reported.
[3]Fold change relative to 0 hours post-inoculation (hpi). (-) No significant change in expression.
*Necrosis-inducing proteins identified in the current study.

3.4.3. Identification of cell death inducing effectors by transient expression in *Nicotiana benthamiana*

In planta transient expression was conducted to examine the necrotizing activity of the 24 candidate effectors. *A. tumefaciens* strains carrying constructs to express each protein with and without their SP along with positive and negative controls, were infiltrated into *N. benthamiana* leaves. Six of the candidate proteins (SS1G_07027, SS1G_00872, SS1G_00849, SS1G_08706, SS1G_09150 and SS1G_09232) induced cell death (Fig. 3.1). Only one of these (SS1G_09232) displayed a necrosis phenotype both in the presence and absence of the native SP, while the rest were able to induce cell death only when the SP was included (Fig. 3.1). The necrotizing activity was highly consistent over three biological replicates.

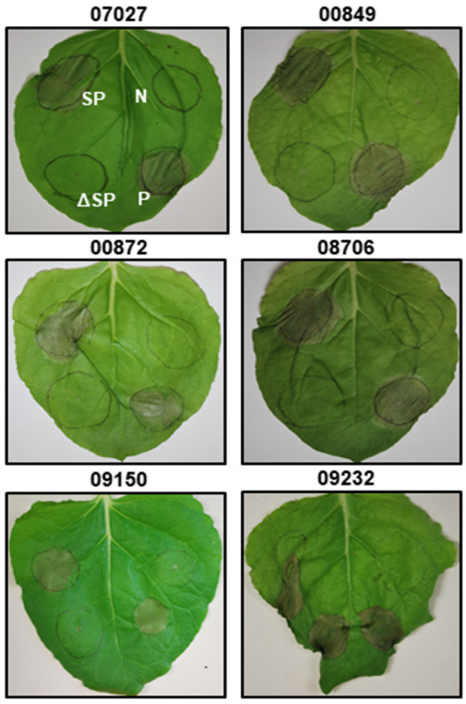

Fig. 3.1 *Agrobacterium tumefaciens*-mediated transient expression of *Sclerotinia sclerotiorum* necrosis-inducing effectors in *Nicotiana benthamiana*. Zones on each leaf show effector with signal peptide (SP), effector without signal peptide (ΔSP), *A. tumefaciens* harboring the empty vector negative control (N), and *P. infestans* Nep1-like protein (PiNPP1.1) positive control (P). Leaves were infiltrated with the four constructs at the same locations as shown for SS1G_07027.

3.4.4. Subcellular localization of candidate effectors

The subcellular localization of the 24 candidate effectors were determined by agro-infiltration in *N. benthamiana* using constructs with and without SP and with a GFP tag fused to the C-

terminus. CLSM was used to image samples at 36–48 hpif. The proteins were mainly localized either to both the plant cell nucleus (but not the nucleolus) and ER, or only the ER and/or different compartments of the endomembrane system. Co-localization of the GFP with an ER-mCherry marker confirmed the localization of the effectors in the ER. In some cases, the localization of the GFP fusion proteins with the native SP was different from those lacking SP. Of the 24 proteins tested, seven (SS1G_01867, SS1G_05939, SS1G_13126, SS1G_00744, SS1G_02904, SS1G_09844, and SS1G_01235) with the SP localized to the ER and/or different ER subcompartments, while these mostly localized to the cytoplasm and nucleus, but still associated with ER subcompartments in the absence of a SP (Fig. 3.2). For four proteins (SS1G_09248, SS1G_10534, SS1G_07669, and SS1G_11912), GFP signals were detected mostly in the cytoplasm and nucleus both in the presence and absence of SP, but also associated with ER subcompartments (Fig. 3.3). Two proteins (SS1G_04519, and SS1G_13696) were localized to the ER and/or different ER subcompartments and nucleus both in the presence and absence of a SP (Fig. 3.4). The other five proteins (SS1G_09420, SS1G_13668, SS1G_10096, SS1G_04382, and SS1G_00263) were detected only in the ER and/or different ER subcompartments both in the presence and absence of SP (Fig. 3.5).

Of the proteins that caused necrosis, SS1G_07027, SS1G_00849, SS1G_09150, SS1G_08706 and SS1G_00872 full-length proteins localized to the ER and/or different ER subcompartments and nucleus, while proteins without a SP localized mostly to the cytoplasm and nucleus, but still associated with ER subcompartments (Fig. 3.6). SS1G_09232 was the only necrosis-inducing protein that localized to the cytoplasm and nucleus both in the presence and absence of SP (Fig. 3.6). The subcellular localizations of 24 effectors with and without SP are summarized in Table 3.2.

Table 3.2 Subcellular localization of *Sclerotinia sclerotiorum* effectors with and without SP.

Subcellular localization with SP	← Gene ID →	Subcellular localization without SP
ER	SS1G_09420	ER
	SS1G_13668	
	SS1G_10096	
	SS1G_04382	
	SS1G_00263	
	SS1G_01867	Cytoplasm + Nucleus
	SS1G_05939	
	SS1G_13126	
	SS1G_00744	
	SS1G_02904	
	SS1G_09844	
	SS1G_01235	
Cytoplasm + Nucleus	SS1G_09248	
	SS1G_10534	
	SS1G_07669	
	SS1G_11912	
	SS1G_09232*	
ER + Nucleus	SS1G_00872*	
	SS1G_07027*	
	SS1G_00849*	
	SS1G_04519	ER + Nucleus
	SS1G_13696	
	SS1G_08706*	
	SS1G_09150*	Nucleus

*Necrosis-inducing proteins identified in the current study.

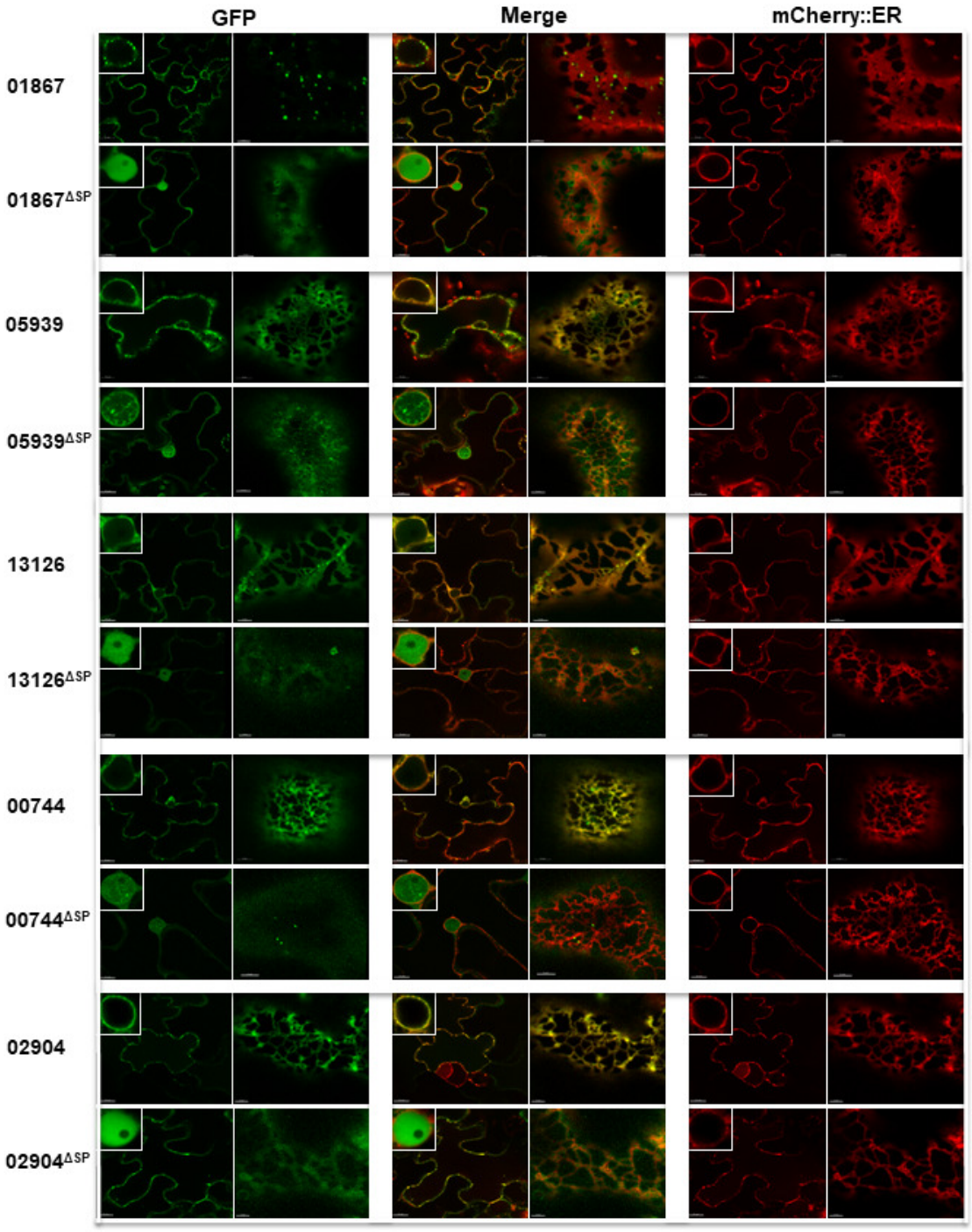
GFP
Merge
mCherry::ER
01867
01867ΔSP
05939
05939ΔSP
13126
13126ΔSP
00744
00744ΔSP
02904
02904ΔSP

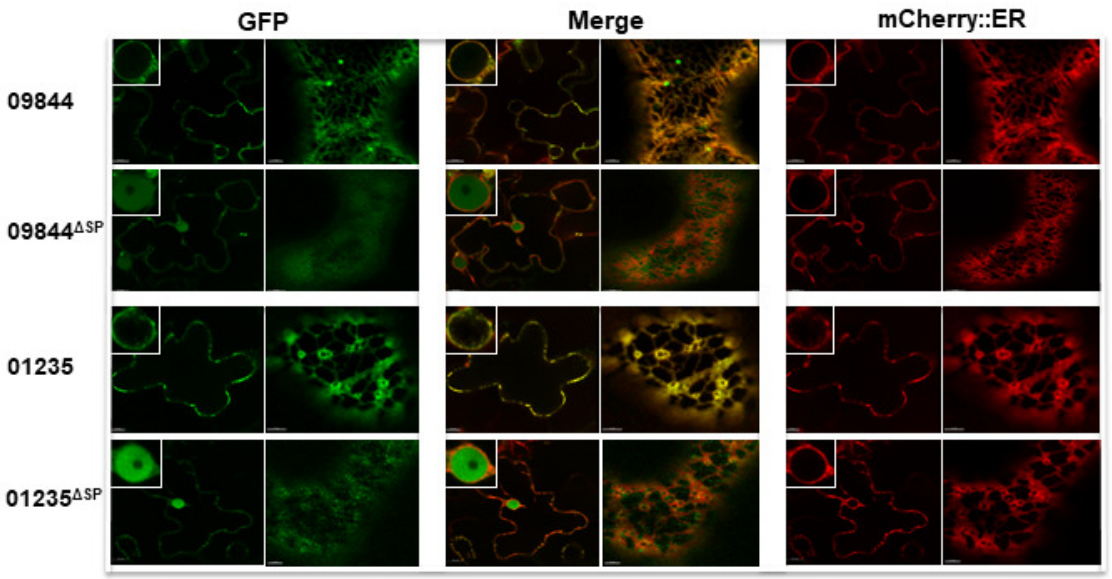

Fig. 3.2. Subcellular localization of *Sclerotinia sclerotiorum* non necrosis-inducing effectors that show **different patterns in the presence and absence of the signal peptide (SP).** Each protein was tested with and without a SP ($^{\Delta SP}$) with GFP fused to the C-terminus. To determine the ER localization, GFP-fused candidate proteins were co-expressed with an mCherry::ER marker.

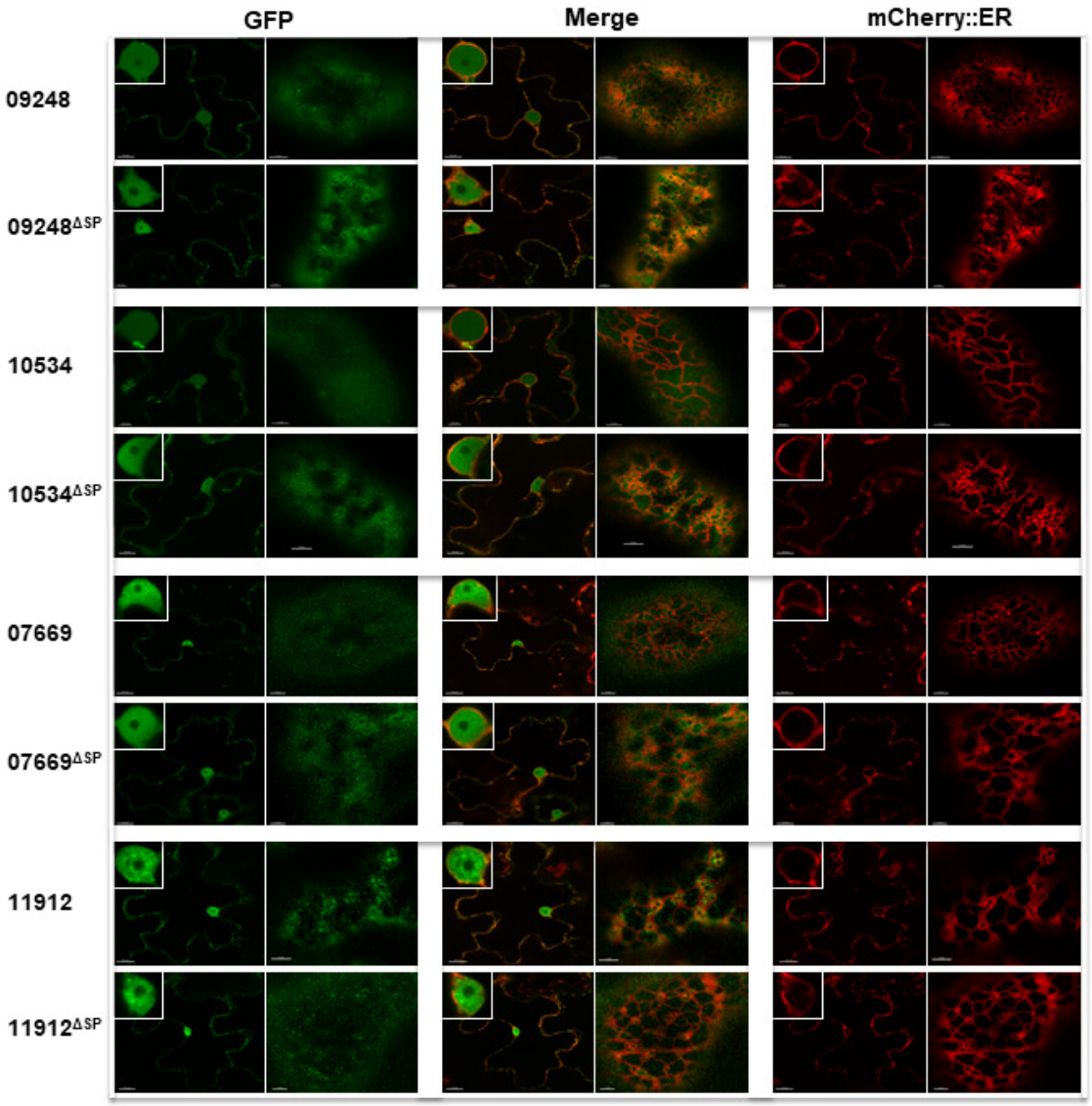

Fig. 3.3 Subcellular localization of *Sclerotinia sclerotiorum* non necrosis-inducing effectors that were present **in the cytoplasm and nucleus both in the presence and absence of the signal peptide (SP)**. Each protein was tested with and without SP ($^{\Delta SP}$) with GFP fused to the C-terminus. To determine the ER localization, GFP-fused candidate proteins were co-expressed with an mCherry::ER marker.

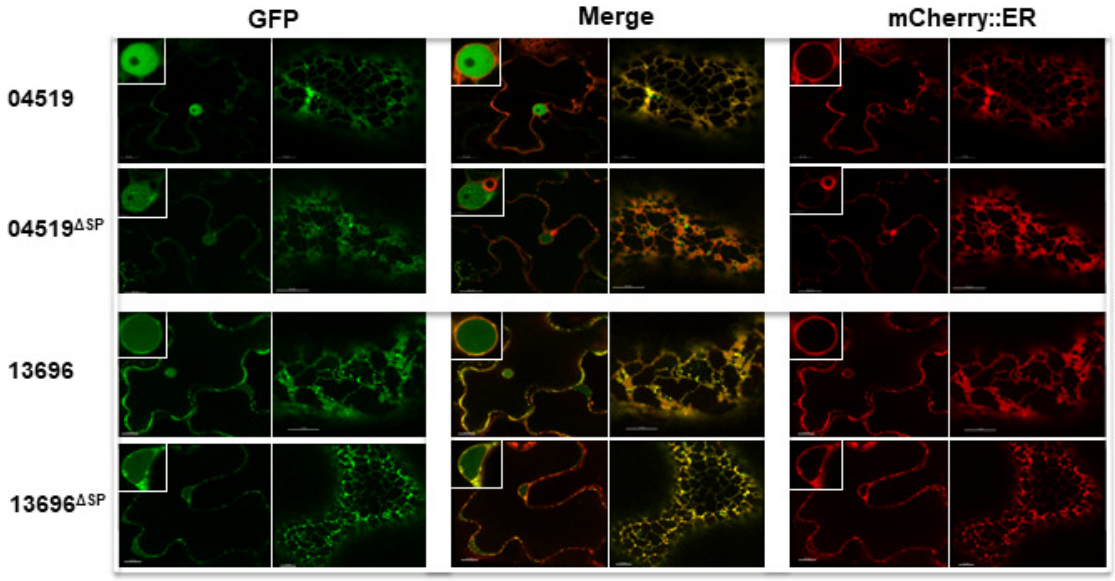

Fig. 3.4 Subcellular localization of *Sclerotinia sclerotiorum* non necrosis-inducing effectors that were present **in the ER and nucleus both in the presence and absence of the signal peptide (SP).** Each protein was tested with and without SP ($^{\Delta SP}$) with GFP fused to the C-terminus. To determine the endoplasmic reticulum (ER) localization, GFP-fused candidate proteins were co-expressed with an mCherry::ER marker.

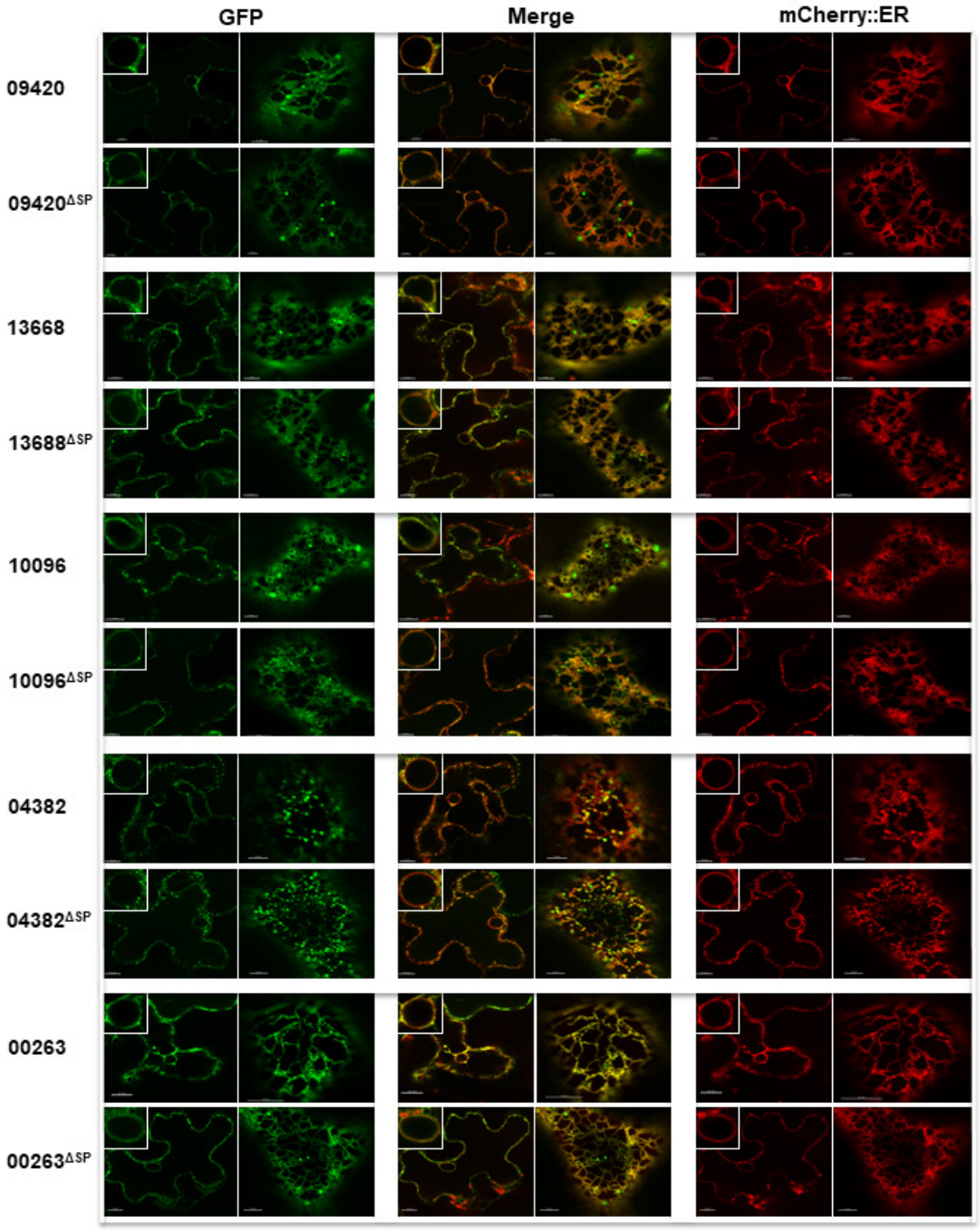

Fig. 3.5 Subcellular localization of *Sclerotinia sclerotiorum* non necrosis-inducing effectors that were present only **in the ER and/or different compartments of the endomembrane system both in the presence and absence of the signal peptide (SP)**. Each protein was tested with and without SP ($^{\Delta SP}$) with GFP fused to the C-terminus. To determine the ER localization, GFP-fused candidate proteins were co-expressed with an mCherry::ER marker.

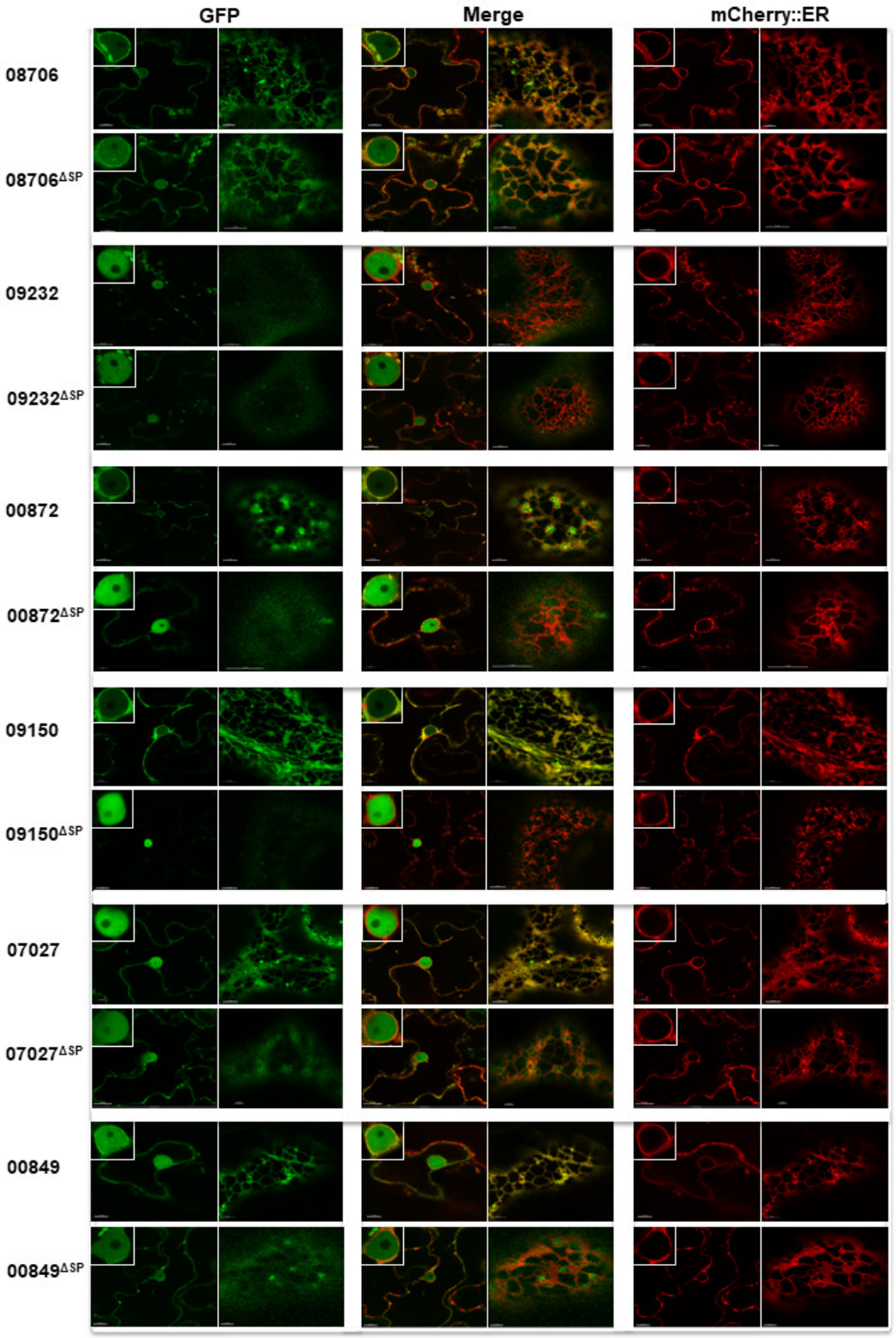

Fig. 3.6 Subcellular localization of *Sclerotinia sclerotiorum* necrosis-inducing effectors in *Nicotiana benthamiana.* Each protein was tested with and without signal peptide ($^{\Delta SP}$) with GFP fused to the C-terminus. To determine ER localization, GFP-fused candidate proteins were co-expressed with an mCherry::ER marker.

3.4.5. Expression of ER stress-related genes in *Nicotiana benthamiana*

Based on the subcellular localization results, five of the six necrosis-inducing effectors were localized to the ER. When ER stress is sustained, the UPR is induced and activates the cell death-signaling pathway (Ron and Walter, 2007). To assess whether the necrosis phenotype involved in induction of the UPR, the expression of ER stress-related genes encoding BLP4, PDI and bZIP60 was measured in *N. benthamiana* leaves infiltrated with *A. tumefaciens* strains containing constructs for the six necrosis-inducing effectors. A candidate effector (SS1G_04519) that was located in the ER, but did not induce necrosis symptoms, and an *A. tumefaciens* line carrying the empty vector (AtEV) were used as a negative controls, while tunicamycin (Iwata and Koizumi, 2005) was used as a positive control. The expression of all three genes was induced in tunicamycin-infiltrated plants by 72 hpif compared to untreated plants, indicating that this system reliably measures ER stress responses.

Interestingly, the expression of these genes was elevated in plants treated with AtEV compared to untreated plants indicating that infiltration with the bacterium alone causes some degree of ER stress (Fig. 3.7). A similar pattern of expression was observed with the ER-localized, but non necrosis-inducing protein (SS1G_04519) and with the necrosis-inducing protein SS1G_07027 indicating that they do not perturb the ER any more than infiltration with *A. tumefaciens* alone. Infiltration with SS1G_09150 or SS1G_09232 caused a dramatic increase in the expression of ER stress-related genes within 24 hpif. This began to subside by 48 hours, and in the case of *BLP4*, returned to near basal levels by 72 hpif. Infiltration with SS1G_00849, SS1G_00872 or SS1G_08706 resulted in an attenuated ER stress response compared to AtEV control.

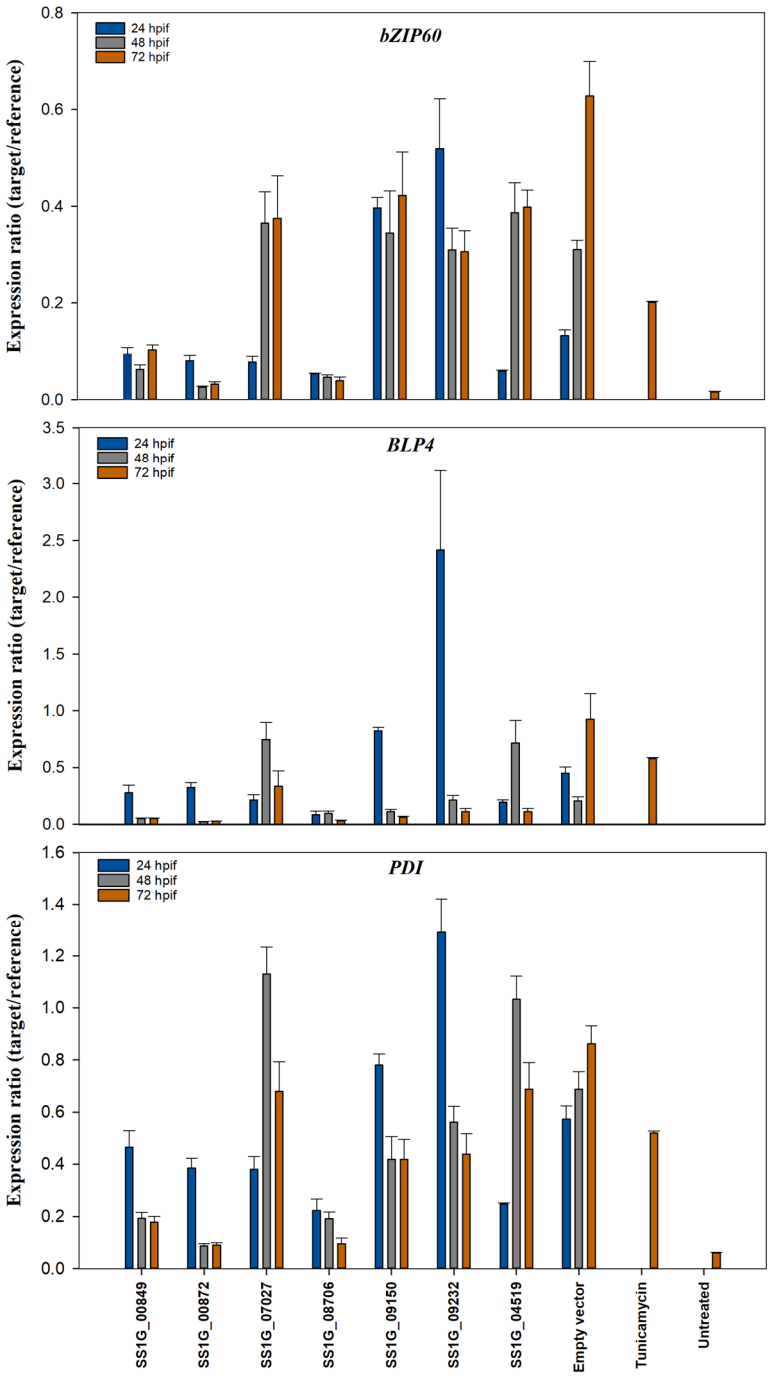

Fig. 3.7 Expression of ER stress-related genes (*bZIP60, BLP4 and PDI*) at 24, 48 and 72 hours post-infiltration (hpif) with *Agrobacterium tumefaciens* strains expressing *Sclerotinia sclerotiorum* effectors as determined using droplet digital PCR. Graphs show the relative expression ratio (target/*α-tubulin* reference gene) and are reported as means and standard errors of three biological replicates. *Nicotiana benthamiana* leaves were infiltrated with *A. tumefaciens* carrying effector constructs. Tunicamycin, a known inducer of ER stress pathway, was used as a positive control. *A. tumefaciens* carrying empty vector (empty vector) was used as a negative control. Untreated plants were used to assess the expression baseline for non-infiltrated plants.

3.4.6. Dependence of SOBIR1 and BAK1 for necrotizing activity of candidate effectors

The dependency of necrotizing activity of five necrosis-inducing proteins on the presence of a SP lends supports to the notion that they must be directed by the plant's secretory pathway to the extracellular space where they interact directly with their natural target(s), possibly receptors. To test this hypothesis, the impact of silencing the genes encoding the BAK1 and SOBIR1 co-receptors was tested on the necrotizing activity of the six necrosis-inducing proteins. Two to three weeks after infiltration with the VIGS constructs, photo-bleaching was observed in all of the *PDS*-silenced *N. benthamiana* plants (data not shown) confirming the systemic spread of virus throughout the plants. *NbSOBIR1*- and *NbBAK1*-silenced plants had 80% lower *SOBIR1* and *BAK1* expression compared to the control *GFP*-silenced plants (Fig. 3.8). In *NbSOBIR1*- and *NbBAK1*-silenced plants, the five necrosis-inducing proteins with a requirement for secretion (SS1G_07027, SS1G_00872, SS1G_00849, SS1G_08706 and SS1G_09150) exhibited reduced incidence and/or reduced necrosis symptoms compared with the control plants (Fig. 3.8). For SS1G_00849, necrosis was observed in 55% and 43% of *NbSOBIR1*- or *NbBAK1*- silenced plants, respectively, compared with 89% in the control plants. SS1G_07027 generated necrosis symptoms in 50% and 42% of *NbSOBIR1*- or *NbBAK1*- silenced plants, respectively, compared with 91% in the control plants. Necrosis was observed in 40% and 35% for SS1G_08706, in 35% and 30% for SS1G_09150, and in 42% and 50% for SS1G_00872 of *NbSOBIR1*- or *NbBAK1*- silenced plants, respectively, compared with more than 90% in the control plants. The lesions that did form were also much smaller in the silenced plants compared to the control plants (arrows shows the small lesions in Fig. 3.8). As well, the necrosis symptoms induced by necrosis-inducing proteins were delayed by 2 to 3 days in the silenced plants compared with the control plants.

The necrotizing activity of SS1G_09232, which does not require secretion, was independent of BAK1 and SOBIR1 (Fig. 3.8) as silencing did not change the incidence or severity of necrosis compared to control plants, as was also seen for BAX (positive control) which is a BAK1/SOBIR1-independent necrosis-inducing protein.

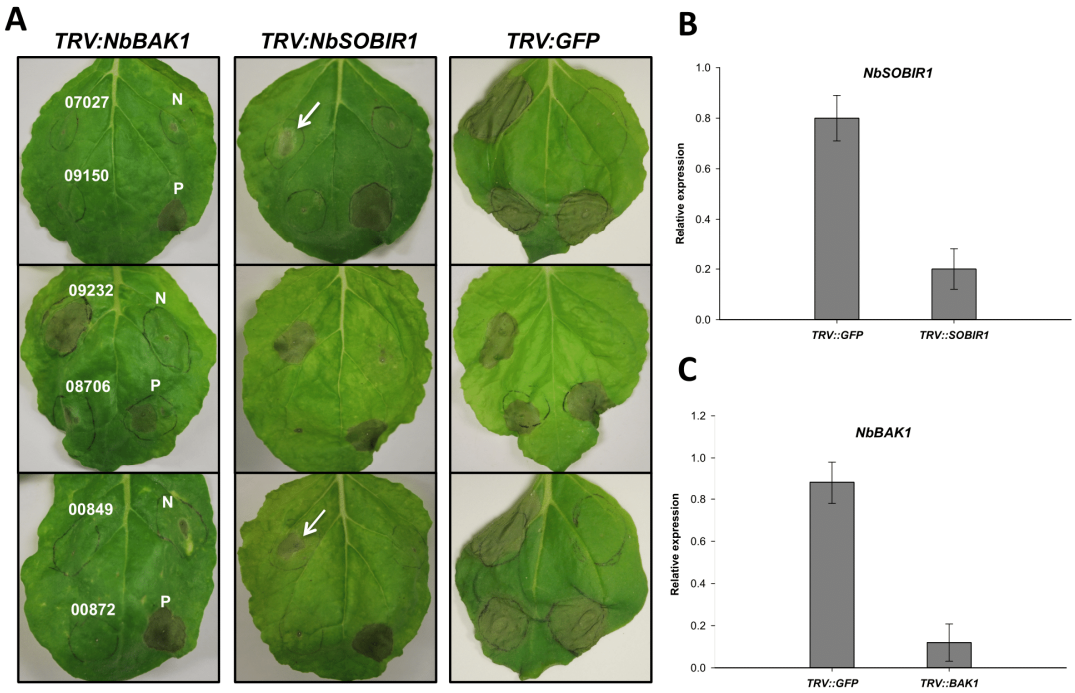

Fig. 3.8 The effect of virus-induced gene silencing of *NbSOBIR1* and *NbBAK1* on the necrotizing activity of *Sclerotinia sclerotiorum* necrosis-inducing effectors. (A) *Nicotiana benthamiana* plants were subjected to VIGS using the TRV-based vectors (*TRV:NbBAK1* and *TRV:NbSOBIR1*). *TRV:GFP* was used as a control. Leaves were infiltrated with *Agrobacterium tumefaciens* strains carrying effector constructs three weeks after TRV infiltration. Zone P: Bcl2-associated protein X (BAX) positive control, N: *A. tumefaciens* carrying empty vector negative control. Leaves in each row were infiltrated with the four constructs at the same locations as shown for the first leaf. Arrows show lesions that were smaller than the control plants. (B, C) *N. benthamiana SOBIR1* and *BAK1* expression level after VIGS treatment as determined by qRT-PCR analysis. *Actin* was used as an endogenous control. Means and standard errors of three biological replicates are shown.

3.5. Discussion

In the current study, bioinformatics and transcriptome approaches were combined to predict genes encoding putative effectors within the *S. sclerotiorum* genome. Of the 24 predicted effectors, 6 were found to exhibit necrotizing activity in *N. benthamiana*. Five of the necrosis-inducing proteins were dependent on the presence of a SP for activity; however, most were localized to the ER/endomembrane system and/or the nucleus. These observations suggested that, once secreted, these necrosis-inducing effectors either interact with targets in the extracellular space or that their intracellular targets can be accessed only upon entry into the host cell via a specific route beginning in the apoplast.

Localization of the necrosis-inducing proteins to the ER/endomembrane system might simply have been due to their transport to the extracellular space through this apparatus; however, since 5 of the 6 necrosis-inducing proteins were dependent upon a signal peptide for activity, this raised the possibility that the necrosis was due to the induction of an ER stress response during their synthesis and secretion. The necrosis-inducing effectors identified in the present study were selected based on elevated cysteine content (more than 2% cysteine). Cysteine residues form disulfide bonds that are essential for protein maturation, stability, and/or function (Walker et al., 1996). Occasionally, they form disulfide bonds with cysteine residues in ER resident proteins leading to unfolded or misfolded proteins (Malhotra and Kaufman, 2007). A surveillance system monitors the quality of mature proteins processed within the ER; ER resident sensors activate the UPR when unfolded or misfolded proteins accumulate. Should the UPR fail to restore ER homeostasis, the apoptotic cell death pathway is initiated (Ron and Walter, 2007). BLP4, bZIP60 and PDI are key indicators of ER stress and expression of the genes encoding them is induced in response to ER stress, such as that caused by cadmium (Xu et al., 2013), as well as infection by rice black-streaked dwarf virus (Sun et al., 2013) and Potato virus X (Ye et al., 2013). BLP4 is a BiP-like binding protein that interacts with ER stress sensors and plays an important role in UPR regulation (Korner et al., 2015). bZIP60 is a transcription factor that is activated downstream of the IRE1-mediated ER stress pathway and plays a key role in the induction of ER stress genes (Iwata and Koizumi, 2005; Korner et al., 2015). PDI catalyzes the formation of disulfide bonds between cysteine residues and is induced in response to ER stress to shuffle incorrect disulfide bonds into their correct pairings (Walker et al., 1996). Interestingly, infiltration with AtEV or a construct expressing an effector that does not induce necrosis induced the expression of these ER stress indicator genes to a significant degree. Two necrosis proteins (SS1G_09150 or SS1G_09232) rapidly induced the expression of ER stress-related genes, even though SS1G_09232 is localized primarily in the nucleus and cytoplasm. Conversely, SS1G_00849, SS1G_00872 and SS1G_08706 attenuated the basal ER stress response caused by infiltration with *A. tumefaciens* alone. Taken together, the results indicate that ER stress and/or induction of the UPR response are not the primary triggers for cell death caused by the necrosis-inducing proteins and may be a consequence of the onset of cell death processes, with the possible exception of SS1G_09150 or SS1G_09232.

The dependency on secretion for activity may also indicate that the necrosis-inducing proteins

interact with a target receptor(s) in the apoplast leading to the induction of ETS-mediated cell death. These proteins could then be imported into the plant cell via the endosomal system to access secondary intracellular targets. The dependency on secretion for necrosis-inducing activity has also been noted for effectors from other fungal pathogens. For example, in the wheat-pathogen *Zymoseptoria tritici*, most necrosis-inducing effectors need to be secreted to the extracellular space to function (Kettles *et al*., 2017). Necrosis-inducing effectors from the rice false smut pathogen, *Ustilaginoidea virens*, also require a SP for full activity (Fang et al., 2016). Plant cells are equipped with cell surface PRRs that sense pathogen-derived components and subsequently activate downstream signal transduction pathways leading to induction of defense responses. PRRs participate in multi-protein complexes at the PM (Monaghan and Zipfel, 2012). RLPs are PRRs that lack a kinase domain and, therefore, are dependent on other PRRs with a kinase domain to activate the downstream defense signal transduction pathway (Rivas and Thomas, 2005). SOBIR1 is one of the key regulatory proteins interacting with RLPs involved in triggering immunity (Liebrand et al., 2013; Zhang et al., 2013). BAK1 acts as either a co-receptor or a general regulator of downstream signaling pathways of the RLP complex (Monaghan and Zipfel, 2012; Liebrand et al., 2014). For example, the RLP23-BAK1-SOBIR1 complex is involved in the activation of plant immunity upon perception of *S. sclerotiorum* nlp20 (a conserved 20 amino acid peptide present in NLP proteins (Albert et al., 2015). The RLP30-BAK1-SOBIR1 complex is required for induction of PTI in *A. thaliana* against *S. sclerotiorum* upon perception of SCFE1, an elicitor secreted by *S. sclerotiorum* (Zhang et al., 2013). In the current study, VIGS of *BAK1* and *SOBIR1* lowered the incidence and severity of the necrosis phenotype for all of the necrosis-inducing proteins that were dependent upon secretion (SS1G_07027, SS1G_00872, SS1G_00849, SS1G_08706 and SS1G_09150) lending support to the notion that the necrotizing activity was dependent on SOBIR1 and BAK1. Similarly, BcXYG1, a xyloglucanase with necrosis-inducing activity from *B. cinerea*, lost its necrosis-inducing activity when it was expressed in *BAK1* or *SOBIR1* mutant plants (Zhu et al., 2017). Additionally, necrotizing activity of *Z. tritici* effectors was dependent on the SOBIR1/BAK1-dependent pathway induced in non-host plants (Kettles et al., 2017). The necrotizing activity of SS1G_09232 was not dependent on BAK1 and SOBIR1. This was not surprising because, in contrast to other five necrosis-inducing effectors, SS1G_09232 does not require a SP for its necrotizing activity and was located in the cytosol. It is possible that this protein targets a

cytoplasmic protein leading to induction of cell death and, therefore, does not require export to the apoplast and BAK1/SOBIR1 for necrosis. *S. sclerotiorum* is known for its broad host range, suggesting that its effectors might be host non-specific and interact with RLPs that are widely distributed amongst dicotyledonous plants, reflecting the widespread susceptibility in dicots. A previous study with NLP and RLP23 revealed that dicot and monocot plants carry different forms of RLP23 and that NLP is only recognized by the dicot isoform (Lenarcic et al., 2017). The similarity between the necrosis-inducing effectors characterized here and NLP in their dependency on BAK1 and SOBIR1 support the involvement of receptors, similar to RLP23 in dicots, mediating susceptibility to *S. sclerotiorum* effectors. Alternatively, the availability of numerous necrosis-inducing effectors in *S. sclerotiorum* that are specifically recognized by their targets in different hosts might lead to susceptibility of a large number of dicot plant species.

Effectors that function in the extracellular space are often small cysteine-rich proteins and the disulfide bonds formed between the cysteine residues are important for their stability in the apoplast (Rep, 2005; Kamoun, 2006). The necrosis-inducing effectors identified in the current study are also small, secreted cysteine-rich proteins with four cysteine residues in SS1G_09150, SS1G_09232, SS1G_00849, SS1G_08706 and six in SS1G_07027 and SS1G_00872. Disulfide bonds are important for the activity of the apoplastic effector PtrToxB (Figueroa et al., 2015). However, since most of the necrosis-inducing effectors reported in this study were localized to the ER and/or nucleus, some secondary functions could also be postulated for these proteins. Some plant pathogen effectors have been reported to target ER-associated proteins, for example, *P. infestans* RXLR effector Pi03192 interferes with the function of specific NAC proteins (NAC Targeted by Phytophthora: NTP1 and NTP2) by preventing their translocation from the ER to the nucleus (McLellan et al., 2013). NAC proteins are ER membrane-bound transcription factors that relocate to the nucleus in response to various stresses to trigger defense responses (McLellan et al., 2013). Alternatively, necrosis-inducing effectors might interact directly with ER-resident proteins, such as BiP and lectin-type calreticulin (CRT3) that are involved in folding of Cf4 and along with SOBIR1 and BAK1 mediate recognition of Avr4 (Liebrand et al., 2012; Postma et al., 2015). Mis-regulation or over-expression of PRRs can also impose stresses that lead to cell death (Park et al., 2008). The localization of the necrosis-inducing proteins in the endomembrane might also result from re-entry into the cell via the endosomal system to access intracellular targets. SsSSVP1 (SS1G_02068), another candidate effector identified in this study, was excluded from

further analysis since its function was characterized previously (Lyu et al., 2016). However, similar to the effectors characterized in the current study, SsSSVP1 was localized to the ER with its native SP, but localized in the cytoplasm, the periphery of the cell membrane and in the nucleus without its SP (Lyu et al., 2016). The similar localization of SsSSVP1 and most of the proteins in this study suggests this common pattern for localization of cysteine-rich effectors from *S. sclerotiorum*.

Several of the candidate effectors identified in this study were reported previously by Guyon *et al*., (2014), including SS1G_00849, SS1G_10096, SS1G_02904, and SS1G_11912. In addition to the general pipeline used in this study, they also examined other criteria such as gene duplication, protein domains and motifs to identify 78 candidate effectors of *S. sclerotiorum* (Guyon et al., 2014). Among these, SS1G_11912 (*SsNep2*) and SS1G_10096 (*SsCP1*) were reported to be inducers of cell death (Bashi et al., 2010; Yang et al., 2018a). However, these proteins did not exhibit necrosis-inducing activity using the protocol in the current study. In the current study, transient expression was conducted using *A. tumefaciens* strains harboring vectors with the CaMV 35S promoter to deliver the effector proteins, whereas, the two previous studies (Bashi et al., 2010; Yang et al., 2018a) used virus-based transient expression systems. Kettles et al. (2017) also reported variation between experiments using *A. tumefaciens* versus a virus-based system in testing *Z. tritici* effectors for necrotizing activity in *N. benthamiana*. The necrosis was usually weak or sometimes absent with the *A. tumefaciens* system and was attributed to lower levels of expression in plants relative to the virus-based systems (Kettles et al., 2017). The necrotizing activity of the six *S. sclerotiorum* effectors was comparable to *PiNPP1.1*, except that the necrotic lesions appeared one or two days later. This suggests that the protocol used in the current study was reliable for identifying potent *S. sclerotiorum* necrosis-inducing effectors, while a virus-based system might identify these as well as other less potent effectors.

The genes encoding four (SS1G_07027, SS1G_00849, SS1G_00872 and SS1G_09232) of the six necrosis-inducing proteins were expressed at early stages of *S. sclerotiorum* infection (1 hour post-inoculation) when the pathogen is present in the apoplast (Liang and Rollins, 2018). This suggests that *S. sclerotiorum* is secreting effectors at the very earliest stages of the infection to promote cell death. This may provide patches of dead tissue allowing the pathogen to establish a foothold and resembles the ETS induced by *P. tritici-repentis* through secretion of the PtrToxB effector into the apoplast where it interacts with the corresponding wheat susceptibility protein to

induce necrosis (Figueroa et al., 2015).

In conclusion, the discoveries made through this study have led to the identification of six novel necrosis-inducing effectors from *S. sclerotiorum.* The dependency of necrotizing activity on the presence of a SP and BAK1/SOBIR1 indicated that an apoplastic receptor might be involved in the recognition of these effectors. The involvement of ER stress responses in necrosis was generally ruled out, lending further support to involvement of apoplastic receptors in necrosis. Subcellular localization of these effectors in the ER suggested that a secondary target of unknown function might also exist. The identification of host targets of these effectors may identify factors conferring susceptibility to this pathogen and enable the development of strategies for enhancing *S. sclerotiorum* resistance. These effectors could be used for developing effector-guided breeding protocols for rapid phenotyping of *B. napus* germplasm.

CHAPTER 4. FUNCTIONAL ANALYSES OF NECROSIS-INDUCING PROTEINS

4.1. Abstract

Small, cysteine-rich proteins are a group of effectors secreted by phytopathogens to trigger resistance or susceptibility in plants. A number of these proteins from necrotrophic plant pathogens are known for their necrosis-inducing activity. Here, I studied two *S. sclerotiorum* Necrosis-inducing Effectors (SsNE1 and SsNE2); of these, SsNE2 was subjected to further functional and structural studies. SsNE2 is a small, secreted protein with 152 amino acids and four cysteine residues. Conversion of the cysteine residues to alanine reduced the incidence and severity of necrosis symptoms in *N. benthamiana*, indicating the involvement of these residues in the function of this protein. Investigating the biological function of orthologous proteins from four other fungal pathogens, namely *B. cinerea*, *F. oxysporum*, *C. higginsianum* and *Monilinia fructigena*, showed similar ability to induce necrosis. VIGS confirmed that the necrosis-inducing ability of a recombinant form of this protein was dependent on the presence of plant receptor-like kinases BAK1 and SOBIR1, suggesting the involvement of cell surface receptors in recognition of the protein. This study enabled the discovery of a novel necrosis-inducing effector in *S. sclerotiorum* that may contribute to the virulence of this pathogen.

4.2. Introduction

Phytopathogens employ an arsenal of effectors with various functions to facilitate penetration, colonization and dissemination of and within host plants. The contribution of effectors to cell death and, subsequently to resistance or susceptibility of host plants varies between different host–pathogen interactions. In a susceptible host-biotrophic pathogen interaction, effectors allow the pathogen to evade or to not trigger the specific defense response leading to cell death, whereas in resistant hosts, effectors induce responses resulting in cell death to arrest the pathogen (Nimchuk et al., 2003). With hemibiotrophic and necrotrophic pathogens, cell death is a consequence of successful infection, hence, these pathogens are equipped with cell death-promoting effectors to accelerate the infection process (Greenberg and Yao, 2004). Evidence suggests that cell death in both resistant and susceptible plants might share similar regulatory features, and that the timing of cell death induction might be more important in presenting a

barrier for establishment of biotrophic pathogen or as a mechanism used by necrotrophic pathogens to facilitate infection (Greenberg and Yao, 2004; Gijzen and Nurnberger, 2006).

The most well-known form of cell death response in plants is the HR, which is a consequence of recognition of pathogen Avr proteins by their corresponding host R receptors leading to ETI. This is most often observed in biotrophic pathogens that can infect only if they have mechanisms to escape or suppress this recognition, otherwise host resistance occurs (Greenberg and Yao, 2004). The PTI response pathway may also cause cell death by direct or indirect recognition of PAMPs by PRRs. For example, xylanases from *B. cinerea* and *Trichoderma viride*, BcXyl1 and EIX, respectively, interact with cell surface receptors, activate PTI and cause cell death independent of their enzymatic activity (Ron and Avni, 2004; Yang et al., 2018b). It has been suggested that necrotrophs might use effectors as a weapon to regulate host cell death to their benefit and cell death can serve as a mechanism for virulence in these pathogens (Dickman et al., 2001; Qutob et al., 2002).

Sclerotinia sclerotiorum is known for its rapid onset of necrosis upon infection of a suitable host. The pathogen hijacks cell death processes to promote infection, therefore, factors that enhance cell death are vital for infection. Of the repertoire of effector proteins secreted by this pathogen, several are known to contribute to cell death induction, such as SsNep1 and SsNep2 (Bashi et al., 2010). *SsSSVP1* encodes a small secreted, cysteine-rich protein that induces plant cell death by interfering with host energy metabolism (Lyu et al., 2016), while SsCP1 targets plant PR1 and triggers cell death (Yang et al., 2018a). SsCaf1 is a secreted effector with the ability to induce cell death and is required for host penetration and sclerotial development (Xiao et al., 2014).

The previous study (Chapter 3) demonstrated the necrotizing-activity of six effectors that induced strong cell death in *N. benthamiana*. The necrotizing activity for five of them required a SP for secretion to the extracellular space. VIGS revealed that necrosis-inducing ability of these five proteins was dependent on the presence of the plant receptor-like kinases BAK1 and SOBIR1, implying that cell surface receptors are involved in the recognition of these proteins. In this study, I conducted additional experiments on one of these necrosis-inducing effectors (SsNE2) for a more detailed functional characterization. This protein was expressed in a heterologous system and induced necrosis in *N. benthamiana*. This protein shares sequence similarity with proteins from other fungal plant pathogens and the necrotizing activity in *N.*

bethamiana of the orthologous proteins proved their functional similarity. The conversion of cysteine residues to alanine indicated that cysteine residues are important for the necrotizing function. Truncated peptides were also examined to identify the biologically active domain conferring the necrotizing activity. Overall, the results suggested that this protein is a potent member of *S. sclerotiorum* necrosis-inducing protein repertoire with a role in cell death induction and promoting infection.

4.3. Methods

4.3.1. Bioinformatics analyses

The protein sequences were subjected to analysis with BLASTP (https://blast.ncbi.nlm.nih.gov/Blast.cgi) to identify conserved protein domains. SignalP 4.1 (Petersen et al., 2011) was used to identify SPs. Protein structure prediction was conducted using SWISS-MODEL workspace (http://swissmodel.expasy.org/interactive), I-TASSER (https://zhanglab.ccmb.med.umich.edu/I-TASSER/) and Predict Protein (https://www.predictprotein.org/). The amino acid sequences were aligned using Clustal omega (https://www.ebi.ac.uk/Tools/msa/clustalo/).

4.3.2. Constructs for recombinant protein expression

For expression of the six necrosis-inducing proteins in *E. coli*, the open reading frames without the region encoding the SP were amplified from cDNA using primers provided in Table A.5. The resultant PCR products were purified, digested with *XbaI* and *XhoI* restriction enzymes and ligated to pET 28a^{+} linearized with the same enzymes. The constructs were verified by sequencing and transformed into either *E. coli* Rosetta DE3 (SsNE1 only) or *E. coli* SHuffle® T7 (New England Biolabs, Massachusetts, USA).

For ectopic expression of protein in yeast, the open reading frame of *SsNE1* without the region encoding the SP was amplified from cDNA using primers F.XhoI-pPICZαA (5' CCGCTCGAGAAAAGACAACAATTCATGGTTCCTGCC 3') and R.XbaI-pPICZαA (5' GCTCTAGAGCACAGAACTCGCACTTCTCGCTGG 3'). The resultant PCR products were purified, digested with *XhoI* and *XbaI* enzymes and ligated to pPICZαA linearized with the same enzymes. The constructs were verified by sequencing and transformed into *Pichia pastoris* KM71 and GS115.

4.3.3. Expression of recombinant protein in *E. coli* and *P. pastoris*

To express the proteins in *E.coli*, transformed cells were grown in 10 ml LB medium containing 50 mg/ml kanamycin at 37°C (Rosetta) and 30°C (SHuffle® T7) on a rotary shaker at 220 rpm. After reaching an OD600 of 0.4-0.8, isopropyl β-D-1-thiogalactopyranoside (IPTG) was added to a final concentration of 1 mM to induce expression of the inserted gene. After 3-4 hours of incubation at 30°C, cells were harvested by centrifugation at 4800 × *g* at 4º C for 30 min and then re-suspended in 0.1 M phosphate buffer (pH 7.2) containing 1 mg/ml lysosome and cOmplete™, an EDTA-free protease inhibitor cocktail (Sigma-Aldrich, Ontario, Canada). The suspension was sonicated on ice (3 × 10 second bursts at high intensity with a 10 second cooling period) to lyse the cells and cellular debris removed by centrifugation at 20,000 × *g* at 4º C for 30 min and the supernatant used for further experiments.

To express the SsNE1 protein using the yeast system, the EasySelect Pichia Expression kit (Invitrogen, Carlsbad, USA) was used according to the manufacturer's instructions. Briefly, the transformed cells were grown in BMGY (buffered glycerol complex medium) at 30°C on a rotary shaker at 250 rpm. After reaching an OD600 of 2-6, cells were harvested by centrifugation at 3000 × *g* for 5 min and then re-suspended to an OD600 of 1.0 in BMMY (buffered methanol complex medium) to induce expression. 100% methanol was then added to a final concentration of 0.5% every 24 hours to maintain induction. Finally, the supernatant was collected by centrifugation at 3000 × *g* for 10 min at 4º C and used for further experiments. Different *P. pastoris* strains (KM71 and GS115) were screened for protein expression. A KM71 transformant was selected for subsequent experiments based on high yields of the expressed protein.

The presence of recombinant protein was analyzed by SDS-polyacrylamide gel electrophoresis (PAGE) using 12% mini-protein® precast stain-free gels (Bio-Rad, CA, USA), and then visualized and detected by western blotting using anti-His (C-term)-HRP and anti-Myc-HRP antibodies (Invitrogen, Carlsbad, USA) for proteins expressed in *E. coli* and *P. pastoris*, respectively. Precision Plus protein standard (Bio-Rad, CA, USA) was used as a reference for molecular weight.

4.3.4. Protein infiltration assays

To test the necrotizing activity of recombinant proteins, *E. coli* culture supernatants (ECS) and *P. pastoris* culture supernatants (PCS) containing the protein of interest were infiltrated into

leaves of *N. benthamiana* using a syringe. *E. coli* culture supernatants from empty vector control strains (ECSEV) and *P. pastoris* culture supernatants from empty vector control strains (PCSEV) were used as a negative controls. The cell-death response was monitored and recorded daily for seven days after infiltration.

4.3.5. Constructs for agro-infiltration assays

The cysteine residues in SsNE2 were converted to alanine to test the impact of cysteine residues on necrotizing activity. DNA fragments with C^{38}, C^{45}, C^{64}, and C^{86} replaced with alanine individually or simultaneously were synthesized and cloned into pEG100 by Thermo Fisher Scientific (Massachusetts, USA).

To transiently express the orthologous genes of *SsNE2* from *B. cinerea* (BCIN_14g01200, GenBank accession XP_001552872.1), *C. higginsianum* (CHEC91, GenBank accession XP_018152473.1), *M. fructigena* (DID88_010138, GenBank accession RAL61042.1), and *F. oxysporum* f.sp. *lycopersici* (FOXG_04016, GenBank accession XP_018238493.1), the open reading frames were synthesized and cloned into pEG100 by Thermo Fisher Scientific (Massachusetts, USA).

Constructs of SsNE1 and SsNE2 tagged with different targeting signals including nuclear localization signal (NLS), nuclear export signal (NES), myristoylation signal (CBL1) and PR1 signal peptide were synthesized and cloned into pEG103 (with a C-terminal fusion to GFP) by Thermo Fisher Scientific, Massachusetts, USA. Constructs of SsNE1 and SsNE2 tagged with GFP along with C-terminal ER retention signal (KDEL) were synthesized and cloned into pEG100 by Thermo Fisher Scientific (Massachusetts, USA). Synthetic DNA sequences are provided in Table A.6.

4.3.6. Agro-infiltration assay

To test the necrotizing activity of the SsNE2 cysteine mutants, SsNE2 orthologues, and SsNE1 and SsNE2 tagged with different cell compartment targeting signals, all constructs were transformed into *A. tumefaciens* strain GV3101. Agro-infiltration was performed as described by Ma et al., (2012) and outlined in Chapter 3.

4.3.7. Plasmolysis

To detect localization of proteins in the apoplast, small infiltrated leaf pieces were treated with KCL (0.85M) for 5 min to induce plasmolysis and then examined using CLSM.

4.3.8. Evaluation of host plant ER stress-related gene expression using ddPCR

To assess the association of host plant ER stress with the necrotizing activity of the SsNE2, the expression of *N. benthamiana* genes induced under ER stress or involved in the UPR was examined in leaf tissues infiltrated with ECS containing SsNE2 or ECSEV as a negative control at 24, 48 and 72 hpif. The expression of genes encoding BLP4 (GenBank accession FJ463755.1), PDI (GenBank accession Y11209.1) and bZIP60 (GenBank accession AB281271.1) was examined as outlined in Chapter 3. Leaf samples infiltrated with tunicamycin, a known inducer of ER stress, were used as a positive control and leaves of untreated plants were used for establishing an expression baseline for non-infiltrated plants. The experiment was conducted with three biological replicates.

4.3.9. Virus-induced gene silencing (VIGS) of *BAK1* and *SOBIR1* in *Nicotiana benthamiana*

To examine the involvement of BAK1 and SOBIR1 in the necrotizing activity of SsNE2, VIGS was conducted using *A. tumefaciens* GV3101 strain harboring pTRV1 and pTRV2 constructs including *pTRV2:GFP*, *pTRV2:PDS, pTRV2:NbSOBIR1* and *pTRV2:NbBAK1* as outlined in Chapter 3. Three weeks after agro-infiltration with the VIGS constructs, leaves of *N. benthamiana* were infiltrated with ECS containing SsNE2 protein and ECSEV as a negative control. *A. tumefaciens* carrying BAX (Lacomme and Santa Cruz, 1999) was used as a positive control. The development of necrosis symptoms was visually evaluated daily for seven days after infiltration.

4.3.10. Synthesis of SsNE2 truncated peptides and infiltration assay

To assess the involvement of specific peptides derived from SsNE2 in necrotizing activity, truncated peptides were synthesized by Bio Basic (Toronto, Canada) and dissolved in sterile distilled water. Different concentrations of each peptide were tested by infiltrating 25 µg/ml to 1 mg/ml into the leaves of *N. benthamiana* plants using a syringe. Five different peptides were designed and named M1, M2, M3, M1+M2, and M2+M3 (Table A.7). The development of

necrosis symptoms was visually evaluated daily for seven days after infiltration.

4.4. Results

4.4.1. *Sclerotinia sclerotiorum* necrosis-inducing effector 1 (SsNE1); SS1G_07027

The necrosis-inducing effector encoded by SS1G_07027 gene was selected for further study based on its expression at the early to late stage of infection with the peak expression level at 1 hpi (Table 3.1). This effector was named *S. sclerotiorum* necrosis-inducing effector 1 (SsNE1).

4.4.1.1. Bioinformatic analyses of SsNE1

SsNE1 is a 710 bp gene harboring three introns and a 525 bp coding region. It encodes a predicted protein with 174 amino acids, including the N-terminal SP (1–19 amino acids) and six cysteine residues. Annotation of SsNE1 using BLASTP revealed that this protein did not possess known structural domains. Protein structure prediction using homology modeling of SWISS-MODEL workspace (http://swissmodel.expasy.org/interactive) did not reveal any similarity to known protein structures.

4.4.1.2. Transient expression of SsNE1 with various targeting signals in *Nicotiana benthamiana*

In Chapter 3, I showed that SsNE1 was localized to the ER/endomembrane system and nucleus. To determine if the ER/endomembrane system and/or the nucleus are involved in necrotizing activity, I constructed *A. tumefaciens* strains expressing SsNE1 with various subcellular targeting signals. As expected, the SsNE1 without SP and fused to the NLS (SsNE1$^{\Delta SP}$-NLS-GFP) was detected in the nucleus, but necrosis was abolished (Fig 4.1). SsNE1 tagged with a NES and without a SP (SsNE1$^{\Delta SP}$-NES-GFP) was detected both in the cytosol and nucleus; however, with much lower concentration in the nucleus; this construct did not trigger necrosis. Since the protein fused to NES was only partially translocated from the nucleus to the cytoplasm, another construct with a CBL1 plus an NES motif (CBL-SsNE1$^{\Delta SP}$-NES-GFP) was tested. As expected, CBL-SsNE1$^{\Delta SP}$-NES-GFP was found exclusively in the plasma membrane, but this construct did not induce necrosis. Another construct was made where the N-terminal native SP of SsNE1 was replaced with the plant PR1 SP (SP^{PR1}-SsNE1$^{\Delta SP}$-GFP). This construct

induced cell death, although the response was delayed slightly in comparison with the construct with native SsNE1 SP. CLSM showed that SP^{PR1}-$SsNE1^{\Delta SP}$-GFP was localized only to the ER and not to the nucleus. This specimen was treated with KCL (0.85M) to induce the plasmolysis to allow detection of localization in the apoplast, which ruled out the localization of this protein in the apoplast, in contrast to PR1 linked only to GFP (data not shown). The C-terminal KDEL sequence, which retains proteins in the ER, was fused to the SsNE1 with SP (SsNE1-GFP-KDEL). This construct localized to the ER and was able to induce cell death (Fig 4.1).

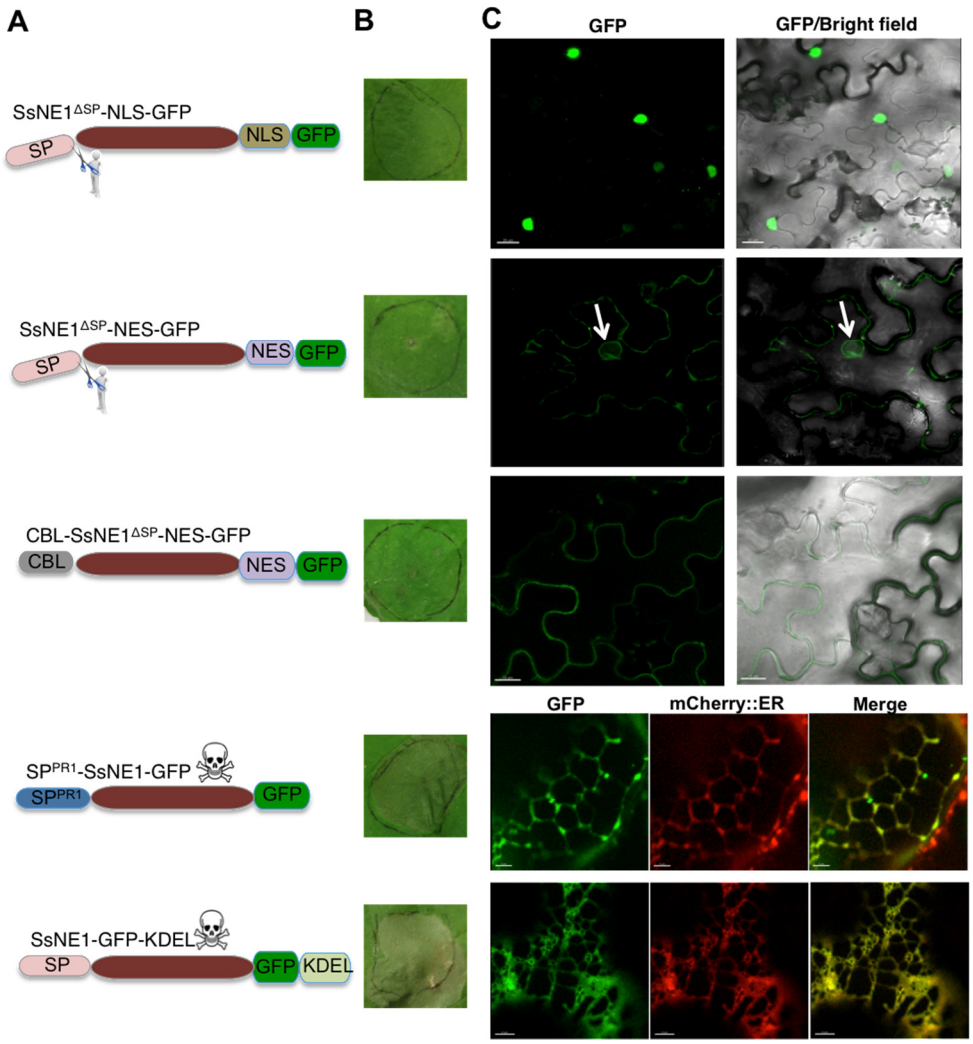

Fig. 4.1 Transient expression of SsNE1 with various targeting signals in *Nicotiana benthamiana.* (A) Schematic presentation of the designed constucts. (B) Analysis of cell death produced by each construct in *N. benthamiana* leaves. (C) Microscopic localization of SsNE1 tagged with various targeting signals. To confirm ER localization, GFP-fused candidate proteins were co-expressed with an mCherry::ER marker.

4.4.1.3. Necrotizing activity of recombinant SsNE1 protein

To test the necrotizing activity of SsNE1, recombinant protein expression was performed in *E. coli* Rosetta (DE3). The results demonstrated that the recombinant protein formed insoluble aggregates or inclusion bodies (Fig. 4.2). Efforts to enhance the solubility of the expressed protein by lowering the growth temperature (between 25º and 28º C) and adjusting the inducer concentration (between 0.5 to 1 mM) were unsuccessful.

In an attempt to alleviate this issue, recombinant protein expression was performed in a yeast system using *P. pastoris* KM71 and GS115 strains. The screening results of different colonies of each strain for protein expression showed that KM71 produced more protein (Fig. 4.2) and, therefore, this strain was selected for testing of necrotizing activity in plants. PCS containing SsNE1 protein was infiltrated into *N. benthamiana* leaves. The recombinant SsNE1 protein did not induce cell death in *N. benthamiana* (data not shown), suggesting that heterologous expression in yeast is also inadequate for generating active SsNE1 protein.

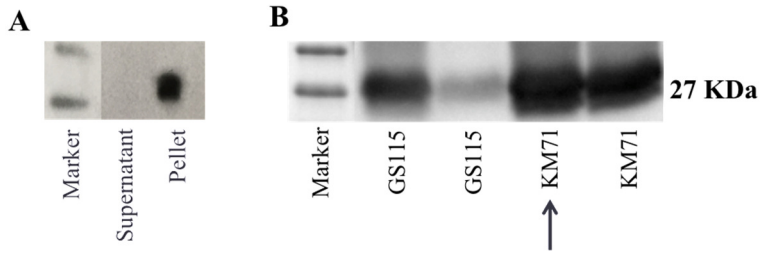

Fig 4.2 Analysis of recombinant SsNE1 protein by western blotting. (A) SsNE1 expressed in *E.coli*; supernatant and pellet of bacterial lysate. (B) SsNE1 expressed in *P. pastoris* strains of GS115 and KM71. Arrow showes the protein expressed in a selected colony of KM71 used for further experiments.

4.4.2. *Sclerotinia sclerotiorum* necrosis-inducing effector 2 (SsNE2); SS1G_00849

4.4.2.1. Necrotizing activity of recombinant SsNE2 protein

Since active SsNE1 could not be generated using either the *E. coli* or *P. pastoris* systems, the expression of all necrosis-inducing effectors identified in Chapter 3 was evaluated in the *E. coli* SHuffle strain. The possibility of disulfide bond formation in these effectors with two or more cysteine residues is likely. SHuffle is a strain of *E. coli* with a more oxidizing cytoplasmic environment that helps to avoid abnormal disulfide bond formation (Lobstein et al., 2012).

Infiltration of *N. benthamiana* leaves with ECS containing these necrosis-inducing proteins showed that only one was able to induce cell death in *N. benthamiana*. This protein induced cell death after 3 days post infiltration and is encoded by SS1G_00849; this was designated as *S. sclerotiorum* necrosis-inducing effector 2 (SsNE2) and selected for further functional analyses.

4.4.2.2. Bioinformatics analysis of SsNE2

The open reading frame of *SsNE2* is 459 bp and encodes a 152 amino acid protein, with the first 18 aa predicted as a SP and with four cysteine residues (C^{38}, C^{45}, C^{64} and C^{86}). SsNE2 had none of the known domains associated with fungal effectors. A BLASTP search with SsNE2 identified orthologues in other necrotrophic and hemibiotrophic ascomycete plant pathogens with sequence identity of 66 % to *B. cinerea* BCIN_14g01200, 65.77 % to *M. fructigena* DID88_010138, 59.38 % to *C. higginsianum* CHEC91 and 42.55 % to *F. oxysporum* f.sp. *lycopersici* FOXG_04016. A multiple sequence alignment using Clustal omega between SsNE2 and its putative orthologues revealed four conserved cysteine residues (Fig. 4.3).

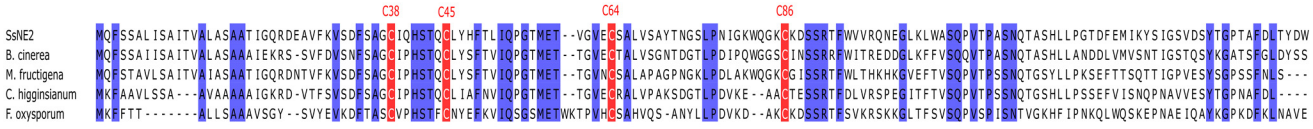

Fig. 4.3 Multiple sequence alignment of *Sclerotinia sclerotiorum* SsNE2 and its putative orthologues from other ascomycete fungal pathogens. The cysteine residues are marked with red boxes. Blue regions show high sequence identity.

The 3D structure prediction of SsNE2 using I-TASSER (https://zhanglab.ccmb.med.umich.edu/I-TASSER/) showed that it had structural similarity with AltA-1 from *Alternaria alternate* and PevD1 from *Verticillium dahlia* (Zhou et al., 2017; Zhang et al., 2019). Sequence alignment of SsNE2 and its structural homologues (AltA-1 and PevD1) also exhibited a conserved cysteine at position 64 (C^{64}) (Fig. 4.4).

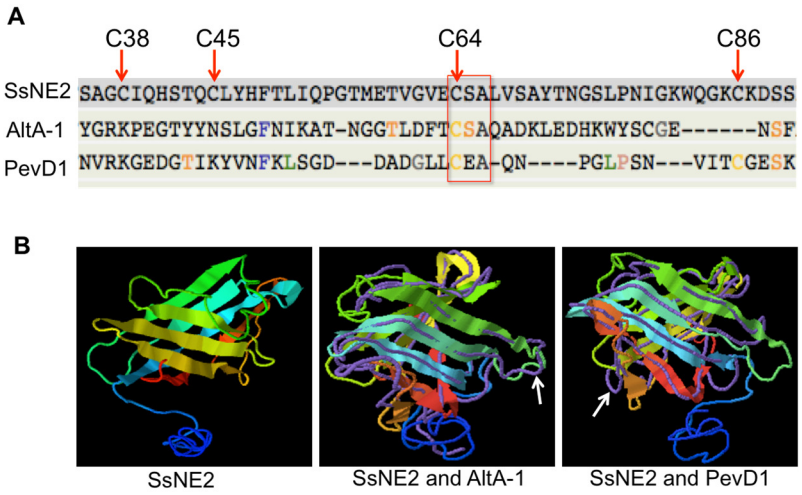

Fig. 4.4 Sequence and structural alignments of *Sclerotinia sclerotiorum* SsNE2 and its structural homologues (AltA-1 and PevD1). (A) Aligned regions of SsNE2, AltA-1 and PevD1. The conserved cysteine residue is marked with red boxes. Arrows show cysteine residues. (B) Structural alignment of SsNE2, AltA-1 and PevD1. Arrows show purple lines, which are proteins structurally similar to the target protein, SsNE2.

4.4.2.3. Functional evaluation of SsNE2 orthologues

To determine if SsNE2 putative orthologues had a similar function, the *B. cinerea* BCIN_14g01200, *C. higginsianum* CHEC91, *M. fructigena* DID88_010138 and *F. oxysporum* f.sp. *lycopersici* FOXG_04016 proteins were transiently expressed in *N. bethamiana* using the agro-infiltration system. AtEV was used as a negative control, while a strain carrying a construct expressing SsNE2 protein was used as a positive control. All proteins induced necrosis. The necrosis symptoms from *M. fructigena* DID88_010138 were visible within 24-48 hpif and prior to the observation of necrosis for SsNE2. Taken together, the results revealed that the orthologous proteins share a similar function.

4.4.2.4. The effects of cysteine residues on the necrotizing activity of SsNE2

Structural analysis of SsNE2 using Predict Protein (https://www.predictprotein.org/) predicted the formation of disulfide bonds between the cysteine residues (Fig. 4.5 A). To determine whether the necrotizing activity of SsNE2 depends on disulfide bonds between the cysteine residues, and thus its intact tertiary structure, SsNE2 C^{38}, C^{45}, C^{64}, and C^{86} were replaced with alanine, either individually or simultaneously.

All of the mutant constructs were transiently expressed using agro-infiltration in *N. benthamiana* along with the wild type SsNE2 as a positive control and AtEV as a negative control. The incidence of disease symptoms were reduced by 40% in $SsNE2^{C38}$ and $SsNE2^{C45}$, 50% in $SsNE2^{C64}$, 60% in $SsNE2^{C86}$, and 50% in $SsNE2^{C38,45,64,86}$ which lacked all four cysteine residues (Fig. 4.5 B). The lesions that did form were also much smaller compared to the lesions caused by the wild type SsNE2. This suggests that cysteine residues might be important, but not absolutely critical, for necrotizing activity of this protein.

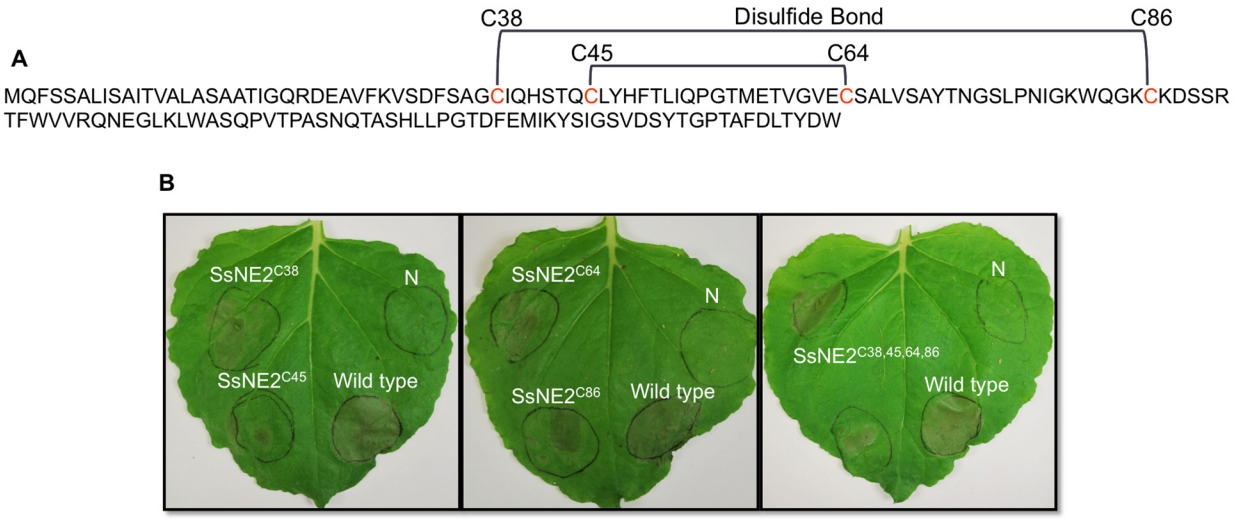

Fig. 4.5 The role of cysteine residues on the necrotizing activity of SsNE2 in *Nicotiana benthamiana*. (A) Prediction of disulfide bond formation between the cysteine residues based on Predict Protein software. (B) The cysteine residues at four positions of C^{38}, C^{45}, C^{64}, and C^{86} were replaced either individually or simultaneously by alanine. Wild type SsNE2 was used as a positive control and *Agrobacterium tumefaciens* strains carrying an empty vector as a negative control (N). The representative of 20 replicates is shown.

4.4.2.5. Transient expression of SsNE2 with various targeting signals in *Nicotiana benthamiana*

To determine if the potential secondary targets of SsNE2, which are the ER/endomembrane system and nucleus, are involved in necrotizing activity, *A. tumefaciens* strains were constructed to express SsNE2 with various subcellular localization and targeting signals. In this experiment, constructs were developed to express SsNE2 with and without its native SP and fused to the same targeting signals used for SsNE1, including NLS (SsNE2-NLS-GFP), NES (SsNE2-NES-GFP), CBL1 (CBL-SsNE2$^{\Delta SP}$-NES-GFP and CBL-SsNE2-NES-GFP), KDEL (SsNE2-GFP-KDEL) and a construct in which the native SP was replaced with the PR1 SP (SP^{PR1}-SsNE2$^{\Delta SP}$-GFP). All constructs, except for CBL-SsNE2$^{\Delta SP}$-NES-GFP and CBL-SsNE2-NES-GFP, induced cell death when expressed using agro-infiltration in the *N. benthamaina* leaves (Fig 4.6). The subcellular localization of all the constructs were as expected; SsNE2-NLS-GFP localized to the nucleus, SsNE2-NES-GFP to the cytosol with lower concentration in the nucleus, CBL-SsNE2$^{\Delta SP}$-NES-GFP and CBL-SsNE2-NES-GFP to the plasma membrane, SsNE2-GFP-KDEL and SP^{PR1}-SsNE2$^{\Delta SP}$-GFP localized to the ER (Fig 4.6). Leaves expressing SP^{PR1}-SsNE2$^{\Delta SP}$-GFP was also treated with KCL (0.85M) to induce the plasmolysis, which ruled out the localization of this protein in the apoplast (data not shown).

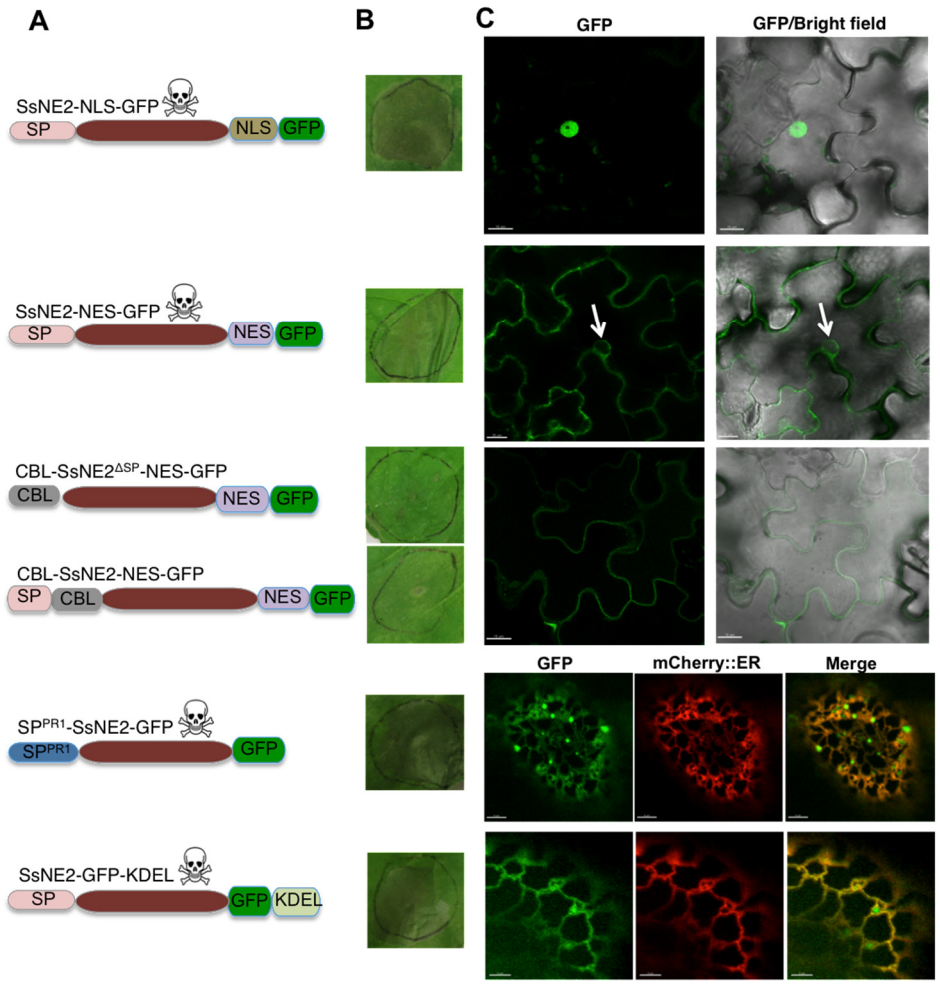

Fig. 4.6 Transient expression of SsNE2 with various targeting signals in *Nicotiana benthamiana.* (A) Schematic presentation of the designed constucts. (B) Analysis of cell death produced by each construct in *N. benthamiana* leaves. (C) Microscopic localization of SsNE2 tagged with various targeting signals. To confirm ER localization, GFP-fused candidate proteins were co-expressed with an mCherry::ER marker.

4.4.2.6. Expression of ER stress-related genes in *Nicotiana benthamiana* infiltrated with SsNE2

In Chapter 3, the necrotizing activity of SsNE2 was revealed to be independent of ER stress when it was transiently expressed in *N. benthamiana* using agro-infiltration system. To confirm that ER stress is not the main cause of cell death induction, the expression of ER stress-related genes encoding BLP4, PDI and bZIP60 was measured in *N. benthamiana* infiltrated with SsNE2 expressed in *E. coli.* This allowed teasing apart the ER stress responses induced by *A.*

tumefaciens vs. SsNE2. Infiltration of *N. benthamiana* leaves with ECS containing SsNE2 and ECSEV as a negative control induced the expression of ER stress-related genes to the level comparable or higher to the tunicamycin-infiltrated plants as a positive control (Fig. 4.7). Since negative control did not induce necrosis, ER stress can be ruled out as the mechanism of cell death induction by SsNE2.

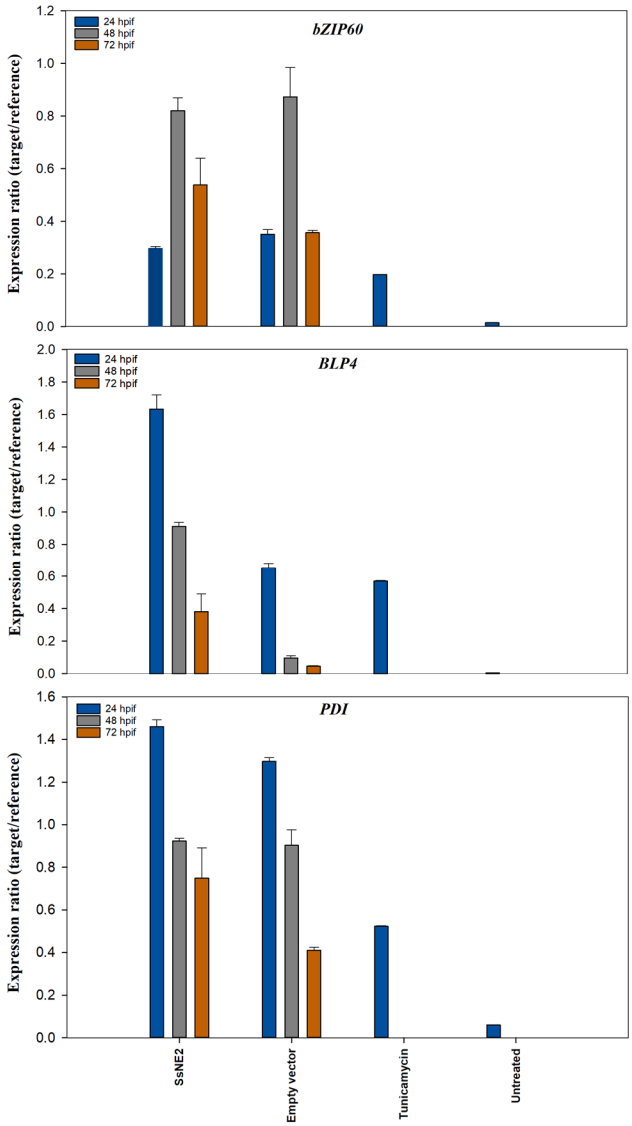

Fig. 4.7 Expression of ER stress-related genes (*bZIP60, BLP4* and *PDI*) as determined using ddPCR at 24, 48 and 72 hours post-infiltration (hpif) of *Nicotiana benthamiana* leaves with *Escherichia coli* culture supernatant containing SsNE2. Graphs show the relative expression ratio (target/*α-tubulin* reference gene) and are reported as means and standard errors of three biological replicates. Tunicamycin, a known inducer of ER stress pathway, was used as a positive control. *E. coli* culture supernatant from a strain containing the empty vector (empty vector) was used as a negative control. Untreated plants were used to assess the expression baseline for non-infiltrated plants.

4.4.2.7. BAK1 and SOBIR1 are associated with necrotizing activity of SsNE2

In Chapter 3, it was revealed that BAK1 and SOBIR1 were associated with necrotizing activity of SsNE2 when it was transiently expressed in *N. benthamiana* using the agro-infiltration system. To confirm the involvement of these two RLKs in the induction of cell death, the recombinant SsNE2 expressed in *E. coli* was infiltrated into *NbSOBIR1*- and *NbBAK1*-silenced plants. The incidence and severity of necrosis in both silenced plants was lower than the control plants (*GFP*-silenced or wild type plants) (Fig 4.8). This experiment confirmed the previous results and showed that the agro-infiltration is a reliable method to screen for necrotizing activity and for identifying requisite host genes using VIGS.

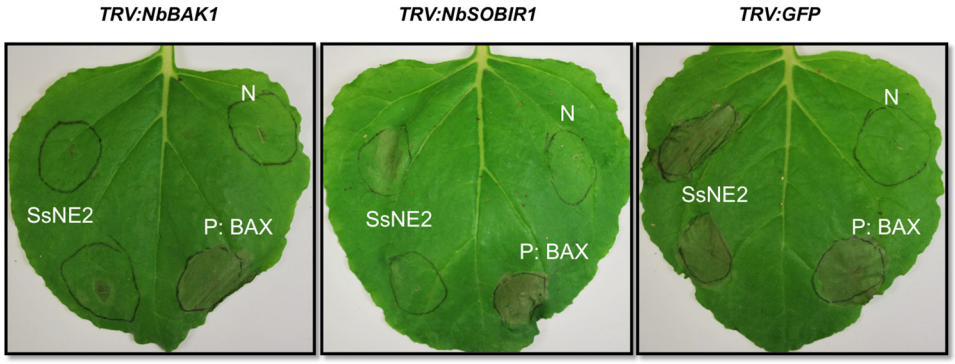

Fig. 4.8 The effect of *NbSOBIR1* and *NbBAK1* silencing on the necrotizing activity of SsNE2. *Nicotiana benthamiana* plants were subjected to VIGS using TRV-based vectors (*TRV:NbBAK1*, *TRV:NbSOBIR1* and *TRV:GFP*). *TRV:GFP* was used as a control. Leaves were infiltrated with recombinant SsNE2 expressed in *Escherichia coli* three weeks after TRV infiltration. Positive control (P:BAX, BAK1/SOBIR1-independent necrosis-inducing protein); negative control (N, *E. coli* culture supernatant expressing empty vector). The representatives of 20 replicates are shown.

4.4.2.8. Necrotizing activity of SsNE2 truncated peptides

To determine if a specific SsNE2 peptide sequence is recognized by plant receptors as PAMPs to induce cell death, five truncated peptides were generated (Fig. 4.9). When dissolved in distilled water and infiltrated in *N. benthamiana* leaves, none of these peptides were able to induce necrosis 7 days after infiltration indicating that only full-length SsNE2 can induce cell death in host plants.

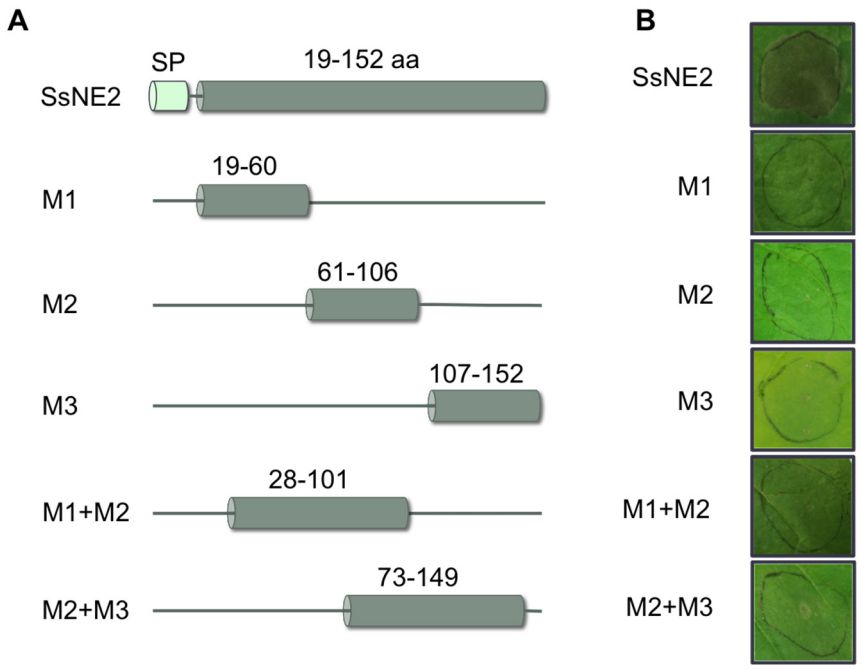

Fig. 4.9 Cell death-inducing activity of native SsNE2 and truncated peptides derived from SsNE2. (A) Schematic presentation of the designed peptides, namely M1, M2, M3, M1+M2, and M2+M3 compared to the native SsNE2 protein. (B) Analysis of necrosis produced by each truncated peptide in *Nicotiana benthamiana* leaves. (SP) signal peptide.

4.5. Discussion

In the current study, two necrosis-inducing effectors (SsNE1 and SsNE2) were subjected to further experimentation to investigate their function. Heterologous expression of SsNE1 in *E. coli* resulted in deposition in inclusion bodies, possibly due to incorrect disulfide bond formation occurring in the reducing environment within the bacterial cytoplasm. Expression of SsNE1 in *P. pastoris* improved solubility of protein; however, it did not induce necrosis when infiltrated into *N. benthamiana,* indicating that expression in yeast might have influenced protein folding or processing rendering the SsNE1 non-functional. The expression of active and highly soluble recombinant protein in heterologous systems has always been a challenge. Although the post-translational modifications in *P. pastoris* are typically its major advantage over the *E. coli* system, hyperglycosylation of proteins can be problematic (Gomes et al., 2016). Both systems used in this study were not efficient for the expression of SsNE1 outside its original context and application of other expression systems, like filamentous fungi or baculovirus/insect systems, could be tested for retrieving functional SsNE1 in future studies.

Among all six proteins expressed in the *E. coli* SHuffle strain, only SsNE2 generated necrosis symptoms *in planta*. The key advantage of using this strain is that it facilitates correct disulfide bond formation due to its more oxidizing cytoplasmic environment (Lobstein et al., 2012). Additional experiments are required to troubleshoot the expression of the other five necrosis-inducing effectors using other *E. coli* strains or other expression systems. Since functional recombinant protein was needed to pursue functional experiments, SsNE2 was selected for further study.

The collective evidence demonstrated that the four cysteine residues of SsNE2 might play a role in the necrotizing activity of this protein. Cysteine residues are important in disulfide bond formation and subsequently impact tertiary structure and stability of some proteins (Walker et al., 1996). Mutation of the cysteine residues at positions 38 and 45, which are within conserved motifs in SsNE2 and its orthologues, reduced the incidence and severity of necrosis less severely than the mutation in the other two cysteine residues at positions 64 and 86. The C^{64} and C^{86} residues and adjacent regions were, however, conserved between SsNE2 and the more phylogenetically distant FOXG_04016. C^{86} mutation showed the highest symptom reduction compared to others, indicating that this specific cysteine may have the highest impact on folding and stability of SsNE2. C^{64} was located in a region with high sequence identity among the proteins that shared structural homology with AltA-1 and PevD1 according to I-TASSER analysis. PevD1 plays a role in the induction of HR and targets cotton PR5-like protein to promote fungal infection (Zhang et al., 2019). Mutation in C^{64} caused a 50% reduction in necrosis incidence and severity, indicating the role of this in the folding, stability or activity of SsNE2. The cysteine mutations, either individually or simultaneously, did not completely abolish the necrotizing activity, indicating that despite their high degree of conservation within orthologous proteins, these residues are not absolutely required for necrotizing activity. However, they could still be important in the structural integrity and long-term stability of this protein to maximize the necrotizing activity of SsNE2 or in presenting an epitope to plant receptors. The partially impaired function of SsNE2 with mutated cysteine residues could also indicate that the cysteine residues might not form disulfide bonds. Binding to metal ions, such as $Fe^{2+/3+}$, Zn^{2+}, Cd^{2+}, and Cu^{+}, and redox activity are an additional property of cysteine residues, allowing interaction with ligands as is required for enzymatic catalysis (Giles et al., 2003). The replacement of cysteine residues in the human mu opioid receptor resulted in an impaired ligand

binding; however, it did not affect its targeting to the PM and only reduced the level of functionality (Zhang et al., 1999). The partially impaired function of SsNE2 mutated in cysteine residues could also be associated with reduced metal-binding activity that may impair interaction with cognate host target or receptor.

The results presented in Chapter 3 showed that transient expression of SsNE2 in the plant using agro-infiltration caused some degree of ER stress. As the *A. tumefaciens* itself caused stronger ER stress response than SsNE2, ER stress and/or induction of the UPR response are not likely to be the main cause of cell death induced by the transiently expressed SsNE2. To corroborate that secretion through ER in agro-infiltration system does not in itself induce ER stress response ending in cell death, the expression of ER stress genes was evaluated in *N. benthamiana* plants infiltrated with SsNE2 expressed in *E. coli*. Necrosis was observed with SsNE2, but not with the *E. coli* negative control confirming that ER stress is not linked to cell death.

VIGS of *BAK1* and *SOBIR1* resulted in reduced necrotizing activity with SsNE2 expressed in *E. coli*, indicating the dependency of this protein on the presence of BAK1 and SOBIR1. This is consistent with the previous results with the agro-infiltration system. The SsNE2 expressed in *E. coli* was used in the present study to rule out the possible effects of Agrobacterium and involvement of plant secretion pathway in the function of this effector, and confirmed the association of SsNE2 function with BAK1 and SOBIR1. This experiment also confirmed that the agro-infiltration is a reliable method for assessing necrotizing activity and for identification of host gene function using VIGS. Due to the technical simplicity of transient expression in *N. benthamiana*, it is recommended for studying the necrotizing activity of *S. sclerotiorum* effectors and possible host targets using the VIGS system.

SsNE1 and SsNE2 were localized to the ER/endomembrane system and nucleus, implying some secondary functions for these effectors. To assess if localization in the ER/endomembrane system and nucleus is also associated with necrotizing activity, SsNE1 and SsNE2 were fused to various subcellular targeting signals, and transiently expressed in *N. benthamiana* using agro-infiltration. Despite various subcellular localizations mediated by various targeting signals, cell death was only observed when the SP was included in the protein. For example, the constructs fused to NLS and NES induced cell death only in the presence of SP, suggesting that localization to the nucleus and cytoplasm were not necessary for the necrotizing activity of these effectors.

The NLS motif targets the proteins to the nucleus and NES targets them to the cytoplasm (Kalderon et al., 1984), although in this study the NES didn't completely translocate the proteins to the cytoplasm and only reduced the nuclear concentration of protein as was seen in NES-tagged Avr2 from *F. oxysporum* (Ma et al., 2013). Avr2 with its native SP localizes to the apoplast, while it localized to the cytoplasm and nucleus when lacking its SP. Using NLS-tagged Avr2, Ma et al. (2013) showed that nuclear localization of Avr2 is necessary for induction of R gene (I-2)-dependent cell death. Proteins with the KDEL motifs are retrieved from downstream compartments of the secretory pathway, mediated by receptors that recognize and bind to the KDEL motif, and return the protein to the ER (Stornaiuolo et al., 2003). Expression of secreted forms of SsNE1-GFP-KDEL and SsNE2-GFP-KDEL showed necrosis induction in the plant, suggesting that localization in ER might also be involved in necrotizing activity. However, according to a previous study, the rate of retrieval back to the ER conferred by KDEL is not absolute and low efficiency of retrieval from downstream compartments results in leakage of the protein from the ER (Stornaiuolo et al., 2003). Therefore, there is a possibility of leakage of some SsNE1-GFP-KDEL and SsNE2-GFP-KDEL to the apoplast. To rule out this possibility and clarify whether the ER was involved in necrotizing activity of these effectors, a CBL motif was incorporated into the chimaeric protein. The CBL motif is a PM targeting signal that uses a different transport system. Proteins with a CBL motif are initially targeted to the ER via N-myristoylation. *S*-acylation then causes the trafficking of the protein to the PM, independent of the Golgi organelle (Batistic et al., 2008). The CBL-SsNE1$^{\Delta SP}$-NES-GFP, CBL-SsNE2$^{\Delta SP}$-NES-GFP and CBL-SsNE2-NES-GFP constructs didn't induce cell death. These results not only demonstrated that trafficking via ER is not involved in cell death activity, but also indicated that prohibiting secretion of SsNE1 and SsNE2 into the extracellular space is the main reason for the lack of cell death induction in these constructs. Taken together, these findings provided more evidence that secretion to the extracellular space and physical interaction with some type of cell surface receptor(s) are required for necrotizing activity of these effectors.

Investigating the necrotizing activity of SsNE2 orthologues in four other fungal pathogens, including *B. cinerea*, *F. oxysporum*, *C. higginsianum* and *M. fructigena*, demonstrated that they have a similar function. As there were several well-conserved motifs among these orthologous proteins, I assessed if these conserved regions were involved in the necrotizing function of SsNE2. Testing various truncated peptides of SsNE2 *in planta* showed that none possessed

necrotizing activity and that the intact protein was necessary for function. These results indicated that despite the high degree of conserved peptide motifs within orthologues proteins, no smaller active epitopes were present that might be responsible for induction of necrosis, in contrast to that found with the *B. cinerea* BcXyl1 where 26-amino acid peptide was identified as the functional peptide to induce cell death and PTI responses in *N. benthamiana* (Yang et al., 2018b). The NLP proteins conserved 20-amino acid peptide is also not able to induce cell death in the host plant, but it is recognized by the host RLP23 leading to induction of PTI responses (Cabral et al., 2012; Böhm et al., 2014; Albert et al., 2015). Recent studies have characterized the ever increasing number of proteinaceus PAMPs that are recognized by plant PRRs and activate PTI (Zhang et al., 2014b; Franco-Orozco et al., 2017; Zhu et al., 2017). Further experiments are required to assess if SsNE2 and any of its truncated peptides act as a PAMP and activate PTI.

NLP proteins also share a conserved heptapeptide motif (GHRHDWE), which is different from nlp20, is essential for necrosis-inducing activity and the substitution of this heptapeptide completely abolished the necrosis symptom of *B. cinerea* Nep proteins (Cuesta Arenas et al., 2010). However, the infiltrated synthetic heptapeptide did not cause any necrosis symptoms by itself, suggesting that 3D structure of NLP proteins might be important in displaying this heptapeptide so that it may interact with target binding sites in the host plant (Schouten et al., 2008).

In conclusion, this study enabled the discovery of a novel necrosis-inducing effector in *S. sclerotiorum,* SsNE2, which might facilitate the colonization of host tissues during infection. The orthologues of this protein in other necrotrophs and hemibiotrophs induced necrosis, suggesting the conserved function of SsNE2 orthologues in different pathogen species. The necrotizing ability of SsNE2 was reduced in the absence of cysteine residues, supporting a role for them in necrotizing function. Moreover, this study provided further evidence that localization to the ER and nucleus is not involved in the cell death induction and secretion to the extracellular space and interaction with cell surface receptor(s) are required for SsNE2 necrotizing activity. This was supported by reduced necrotizing activity in plants when *BAK1*/*SOBIR1* were silenced.

CHAPTER 5. GENERAL DISCUSSION

Sclerotinia sclerotiorum is the causal agent of one of the most deleterious diseases of canola and has the ability to deploy a wide range of factors to establish and promote its infection. This pathogen is not only capable of sequential secretion of pathogenicity/virulence factors, but also escaping or suppressing host plant immunity and eventually using these reactions for its own benefit (Zhu et al., 2013; Seifbarghi et al., 2017). These likely allow this pathogen to be successful in attacking a wide range of host plants. During the last few decades, multiple studies have focused on the different mechanisms that enable *S. sclerotiorum* to infect a large number of host plants. This study focused on the identification and characterization of necrosis-inducing effectors, which are crucial for *S. sclerotiorum* infection and for development of its classical disease symptoms.

In this investigation, I first provided a global view of the genes that are sequentially expressed by *S. sclerotiorum* to facilitate infection of *B. napus*. My findings showed that the penetration process of *S. sclerotiorum* occurred from 1 to 12 hpi. This coincided with the differential expression of the genes involved in host penetration, such as *SsCuta*. For successful colonization, it also releases a cocktail of hydrolytic enzymes, detoxification compounds and effector proteins to contend with various host plant defense mechanisms and toxins.

The results suggested that there is a brief biotrophic stage at 12 to 24 hpi supported by the induction of the genes encoding LysM domain proteins or other chitin-binding proteins to protect the fungus in the apoplastic space from detection by the host plant immune system (Mentlak et al., 2012). Soon after penetration, most pathogens establish a biotrophic phase to evade host recognition in order to prolifrate and colonize the host (Oliveira-Garcia and Valent, 2015). The swich to the necrotrophic stage started from 24 hpi and was supported by the appearance of necrotic lesions and also the expression of genes encoding hydrolytic enzymes, enzymes involved in secondary metabolite synthesis or toxins to trigger host cell death. This was the first comprehensive study of how the *S. sclerotrium* genome is deployed during *B. napus* infection.

Recently Westrick et al. (2019) suggested that *S. sclerotiorum* is capable of adopting divergent virulence mechanisms on three different hosts, namely, *B. napus* (Seifbarghi et al., 2017), *P. vulgaris* (Oliveira et al., 2015), and *Glycine max* (Westrick et al., 2019), hence, the regulation of pathogenicity/virulence factors of this pathogen during the course of infection most

likely varies on different hosts. It was, thus, valuable to monitor the expression of candidate effectors during the infection of *B. napus* to capture host-specific virulence factors and candidate necrosis-inducing effectors. Such an adaptive mechanism also varied in lines of *G. max* with different levels of resistance since the pathogen produced melanin and hydrophobic surface proteins when infecting the more resistant lines, likely in an attempt to evade detection, suppress host innate immunity and/or defend against anti-fungal compounds (Westrick et al., 2019).

Using *in silico* approaches, I predicted 105 potential effectors encoded by the *S. sclerotiorum* genome; these were small, secreted, cysteine-rich proteins with no TM and GPI anchor. In a previous study, 78 candidate effectors from *S. sclerotiorum* were identified using different computational tools (Guyon et al., 2014). I examined all of the 105 candidate effectors for their expression profile in the *S. sclerotiorum-B. napus* pathosystem, and found 24 genes that were up-regulated during the course of infection; these were selected for an *in planta* screen using agro-infiltration. Of the 24 predicted effectors, six (SS1G_00849, SS1G_00872 and SS1G_08706, SS1G_09150, SS1G_09232 and SS1G_07027) induced necrosis in *N. benthamiana*, and only one of them (SS1G_09232) displayed a necrosis phenotype both in the presence and absence of the SP. The other five were able to induce cell death only in the presence of a SP.

I also determined the subcellular localization of these 24 effector candidates, with 11 localized to different compartments in the presence and absence of SP and the remainder having the same localization pattern with and without the SP. The main cellular targets of these effectors were either the ER and nucleus, or only the ER or the cytoplasm and nucleus.

Since five of six necrosis-inducing effectors were localized to the ER/endomembrane system in the presence of SP, this raised the possibility of ER stress response as a mechanism for necrosis. However, other proteins without necrotizing activity were localized to the ER, suggesting that localizing to the ER itself does not cause ER stress leading to induction of necrosis. To rule out the possibility of ER sress response associated with necrosis, the expression of *BLP4*, *bZIP60* and *PDI*, key indicators of ER stress, were determined. The results corroborated that ER stress is not the main mechanism of cell death induction for these effectors. This conclusion was supported by induction of ER stress indicator genes by SS1G_04519 that was localized in ER, but could not induce necrosis. This also suggested that while ER stress is not the primary trigger for cell death induction, it might be a consequence of the onset of cell death processes caused by these effectors.

The dependency of the five effectors (SS1G_00849, SS1G_00872 and SS1G_08706, SS1G_09150 and SS1G_07027) on a SP for secretion for necrotizing activity led to the hypothesis that these proteins might interact with receptor(s) in the apoplastic space. VIGS of *SOBIR1* and *BAK1* in *N. benthamiana*, which are co-receptors that act as downstream signaling pathways of the RLP complex (Monaghan & Zipfel, 2012; Liebrand *et al.*, 2013), supported the involvement of RLPs in recognition of these effectors. This is consistent with the identification of cell death inducing 1 (RcCDI1) effector of *Rhynchosporium commune*, which acts as PAMP and requires BAK1 and SOBIR1 for its cell death-inducing activity (Franco-Orozco et al., 2017). RcCDI1 also requires a SP for triggering cell death (Franco-Orozco et al., 2017).

Phytopathogens secrete proteinaceous effectors into the extracellular space between plant cells and these may either stay in this space or translocate into the cell (Oliveira-Garcia and Valent, 2015; Tan et al., 2015; Zhang et al., 2017). These facilitate infection and colonization of pathogens in the host plant; however, they can also be recognized by plant receptors either in apoplastic space or cytoplasm resulting in plant defense activation (Dodds and Rathjen, 2010). Necrotrophic pathogens hijack the plant defense mechanisms for their own benefit by secreting effectors that are recognized by immune receptors leading to cell death (Lorang et al., 2007; Hammond-Kosack and Rudd, 2008; Oliver and Solomon, 2010; Tan et al., 2015). Addressing the question as to whether the necrotizing effectors of *S. sclerotiorum* are capable of triggering typical PTI responses, such as ROS production, for induction of necrosis remains to be elucidated.

It is possible that *S. sclerotiorum* effectors could be recognized by multiple host immune receptors, therefore, multiple effector/receptor interactions that individually produce a degree of necrosis, could contribute additively to disease development, as seen in *Parastagonospora nodorum* ToxA, Tox1, and Tox3 effectors (Tan et al., 2015). In line with this, this study indicated that the five necrosis-inducing proteins are dependent on SP for their activity, are secreted first to the extracellular space and may be recognized by a cell surface receptor(s). These may then be translocated into the plant cell to access secondary targets, such as the ER and/or nucleus.

In this study, I further investigated SsNE2 (SS1G_00849), as recombinant SsNE2 expressed in *E. coli* possessed necrotizing activity. The expression of the key indicators of ER stress was assessed using recombinant SsNE2 to rule out that ER stress either direct or indirect caused by the agro-infiltration system in *N. bethamiana* contributes to necrosis. To test the involvement of

receptors, the VIGS silencing of *BAK1*/*SOBIR* was repeated using recombinant SsNE2. Both tests confirmed the previous results with the transient expression of SsNE2, supporting the notion that the recognition of SsNE2 by receptors is linked with the necrotizing activity of this effector. Transient expression of NLS-tagged SsNE2 in plants proved that localization to the nucleus was not required for the necrotizing activity. In addition, transient expression of CBL-tagged SsNE2 in plants suggested that trafficking via ER is not the main cause of the cell death activity, leaving recognition of SsNE2 by extracellular receptor as the only demonstrated requirement for necrotizing activity. Taken together, these results support the requirement of physical interaction between plant immune receptors and SsNE2 for induction of necrosis.

Investigating the necrotizing activity of SsNE2 orthologues, including those from *B. cinerea*, *C. higginsianum, M. fructigena* and *F. oxysporum,* proved that they had similar functions. Cysteine mutations, either individually or simultaneouslly, did not completely abolish necrotizing activity, indicating that despite their high degree of conservation within orthologues proteins, these residues do not determine the necrotizing activity of SsNE2, but quantitatively contribute to necrotizing activity of SsNE2 likely through contribution to the structural integrity and long-term stability of SsNE2. Testing various truncated peptides of SsNE2 showed that none of these well-conserved motifs were solely involved in necrotizing activity, suggesting that the necrotizing activity of SsNE2 is not due to recognition of a simple conserved motif, but requires intact protein for presentation of an epitope or recognition by PRRs.

In conclusion, the studies in this thesis contributed to the discovery of necrosis-inducing effectors of *S. sclerotiorum* that could be recognized by yet uncharacterized receptors in host plants, likely immune receptors acting as "susceptibility" genes in the *S. sclerotiorum*-host interaction. Identification of these receptors is critical for enhancing genetic resistance. The necrotizing effectors identified in this study are an important step for the identification of corresponding host receptors by providing the opportunity to evaluate the response of various host genotypes to individual necrotizing effectors. This will accelerate map-based cloning of the receptor genes and application of reverse genetic tools for proving the function of receptors in susceptibility. Identification of these receptor genes will contribute to developing new sources of resistance through mutagenesis, breeding or genetic modification. It also allows designing molecular markers to allow rapid selection for recessive resistant genes (null mutants in susceptibily genes) in early breeding cycles and pyramiding multiple resistance genes for

developing stem rot resistant varieties in canola. As such, the effectors identified in this study could be used for developing effector-assisted breeding tools to gradually remove susceptibility factors in a breeding program. Similar approaches have been used previously in the application of effector-guided breeding for identification of resistance genes to *P. infestans* (Vleeshouwers and Oliver, 2014) and *P. tritici-repentis* (Tran et al., 2017), supporting the possibility of applying the necrotizing effectors identified here as materials for screening in breeding; however, due to the quantitative nature of resistance to *S. sclerotiorum*, additional virulence factors, such as secondary metabolites, OA and CWDE must considered. It is also essential to study the necrotizing activity of these effectors on multiple hosts to decipher the association between these and the wide host range of the pathogen. This knowledge is critical for application of these effectors in effector-guided breeding.

REFERENCES

Albert I, Bohm H, Albert M, Feiler CE, Imkampe J, Wallmeroth N, Brancato C, Raaymakers TM, Oome S, Zhang H, et al (2015) An RLP23-SOBIR1-BAK1 complex mediates NLP-triggered immunity. Nat plants **1**: 15140.

Ambrose K V, Tian Z, Wang Y, Smith J, Zylstra G, Huang B, Belanger FC (2015) Functional characterization of salicylate hydroxylase from the fungal endophyte *Epichloë festucae*. Scientific Reports **5**: 10939.

Amselem J, Cuomo C a, van Kan J a L, Viaud M, Benito EP, Couloux A, Coutinho PM, de Vries RP, Dyer PS, Fillinger S, et al (2011) Genomic analysis of the necrotrophic fungal pathogens *Sclerotinia sclerotiorum* and *Botrytis cinerea*. PLoS Genet **7**: e1002230.

Annis S, Goodwin P (1997) Recent advances in the molecular genetics of plant cell wall-degrading enzymes produced by plant pathogenic fungi. Eur J Plant Pathol **103**: 1–14.

Antal Z, Rascle C, Cimerman A, Viaud M, Billon-Grand G, Choquer M, Bruel C (2012) The Homeobox BcHOX8 Gene in *Botrytis Cinerea* Regulates Vegetative Growth and Morphology. PLoS One **7**: 44–48.

Apel K, Hirt H (2004) Reactive oxygen species: metabolism, oxidative stress, and signal transduction. Annu Rev Plant Biol **55**: 373–399.

Baker CJ, Orlandi EW (1995) Active oxygen in plant pathogenesis. Annu Rev Phytopathol **33**: 299–321.

Barros J, Serk H, Granlund I, Pesquet E (2015) The cell biology of lignification in higher plants. Ann Bot . doi: 10.1093/aob/mcv046.

Bashi ZD, Hegedus DD, Buchwaldt L, Rimmer SR, Borhan MH (2010) Expression and regulation of *Sclerotinia sclerotiorum* necrosis and ethylene-inducing peptides (NEPs). Mol Plant Pathol **11**: 43–53.

Bashi ZD, Rimmer SR, Khachatourians GG, Hegedus DD (2012) Factors governing the regulation of *Sclerotinia sclerotiorum* cutinase A and polygalacturonase 1 during different stages of infection. Can J Microbiol **58**: 605–16.

Bashi ZD, Rimmer SR, Khachatourians GG, Hegedus DD (2013) *Brassica napus* polygalacturonase inhibitor proteins inhibit *Sclerotinia sclerotiorum* polygalacturonase enzymatic and necrotizing activities and delay symptoms in transgenic plants. Can J Microbiol **59**: 79–86.

Batistic O, Sorek N, Schultke S, Yalovsky S, Kudla J (2008) Dual fatty acyl modification determines the localization and plasma membrane targeting of CBL/CIPK Ca2+ signaling complexes in Arabidopsis. Plant Cell **20**: 1346–1362.

Bayram O, Braus GH (2012) Coordination of secondary metabolism and development in fungi: the velvet family of regulatory proteins. FEMS Microbiol Rev **36**: 1–24.

Beers EP, Woffenden BJ, Zhao C (2000) Plant proteolytic enzymes: possible roles during programmed cell death. Plant Mol Biol **44**: 399–415.

Blanco-Ulate B, Morales-Cruz A, Amrine KCH, Labavitch JM, Powell ALT, Cantu D (2014) Genome-wide transcriptional profiling of *Botrytis cinerea* genes targeting plant cell walls during infections of different hosts. Front Plant Sci **5**: 435.

Böhm H, Albert I, Oome S, Raaymakers TM, Van den Ackerveken G, Nürnberger T (2014) A conserved peptide pattern from a widespread microbial virulence factor triggers pattern-induced immunity in Arabidopsis. PLOS Pathog **10**: e1004491.

Boland GJ, Hall R (1994) Index of plant hosts of *Sclerotinia sclerotiorum*. Can J Plant Pathol **16**: 93–108.

Bolton MD, van Esse HP, Vossen JH, de Jonge R, Stergiopoulos I, Stulemeijer IJE, van den Berg GCM, Borras-Hidalgo O, Dekker HL, de Koster CG, et al (2008) The novel *Cladosporium fulvum* lysin motif effector Ecp6 is a virulence factor with orthologues in other fungal species. Mol Microbiol **69**: 119–136.

Bolton MD, Thomma BPHJ, Nelson BD (2006) *Sclerotinia sclerotiorum* (Lib.) de Bary: biology and molecular traits of a cosmopolitan pathogen. Mol Plant Pathol **7**: 1–16.

Bozkurt TO, Schornack S, Banfield MJ, Kamoun S (2012) Oomycetes, effectors, and all that jazz. Curr Opin Plant Biol **15**: 483–492.

Brito N, Espino JJ, Gonzalez C (2006) The endo-beta-1,4-xylanase xyn11A is required for virulence in *Botrytis cinerea*. Mol plant-microbe Interact **19**: 25–32.

Burch-Smith TM, Schiff M, Liu Y, Dinesh-Kumar SP (2006) Efficient virus-induced gene silencing in Arabidopsis. Plant Physiol **142**: 21–27.

Cabral A, Oome S, Sander N, Kufner I, Nurnberger T, Van den Ackerveken G (2012) Nontoxic Nep1-like proteins of the downy mildew pathogen *Hyaloperonospora arabidopsidis*: repression of necrosis-inducing activity by a surface-exposed region. Mol plant-microbe Interact **25**: 697–708.

Caillaud M-C, Piquerez SJM, Fabro G, Steinbrenner J, Ishaque N, Beynon J, Jones JDG (2012) Subcellular localization of the Hpa RxLR effector repertoire identifies a tonoplast-associated protein HaRxL17 that confers enhanced plant susceptibility. Plant J **69**: 252–265.

Calla B, Blahut-Beatty L, Koziol L, Zhang Y, Neece DJ, Carbajulca D, Garcia A, Simmonds DH, Clough SJ (2014) Genomic evaluation of oxalate-degrading transgenic soybean in response to *Sclerotinia sclerotiorum* infection. Mol Plant Pathol **15**: 563–575.

Carpita NC, Gibeaut DM (1993) Structural models of primary cell walls in flowering plants: consistency of molecular structure with the physical properties of the walls during growth. Plant J **3**: 1–30.

Carter C, Pan S, Zouhar J, Avila EL, Girke T, Raikhel N V (2004) The vegetative vacuole proteome of arabidopsis thaliana reveals predicted and unexpected proteins. Plant Cell **16**: 3285–3303.

Chaparro-Garcia A, Wilkinson RC, Gimenez-Ibanez S, Findlay K, Coffey MD, Zipfel C, Rathjen JP, Kamoun S, Schornack S (2011) The receptor-like kinase SERK3/BAK1 is required for basal resistance against the late blight pathogen *Phytophthora infestans* in *Nicotiana benthamiana*. PLoS One **6**: e16608.

Chen C, Dickman MB (2005) cAMP blocks MAPK activation and sclerotial development via Rap-1 in a PKA-independent manner in *Sclerotinia sclerotiorum*. Mol Microbiol **55**: 299–311.

Chen LQ, Hou BH, Lalonde S, Takanaga H, Hartung ML, Qu XQ, Guo WJ, Kim JG, Underwood W, Chaudhuri B, et al (2010) Sugar transporters for intercellular exchange and nutrition of pathogens. Nature **468**: 527–532.

Chen Y, Yu P, Luo J, Jiang Y (2003) Secreted protein prediction system combining CJ-SPHMM, TMHMM, and PSORT. Mamm Genome **14**: 859–865.

Choquer M, Fournier E, Kunz C, Levis C, Pradier J-M, Simon A, Viaud M (2007) *Botrytis cinerea* virulence factors: new insights into a necrotrophic and polyphageous pathogen. FEMS Microbiol Lett **277**: 1–10.

Collmer A, Keen NT (1986) The role of pectic enzymes in plant pathogenesis. Annu Rev Phytopathol **24**: 383–409.

Colmenares AJ, Aleu J, Durán-Patrón R, Collado IG, Hernández-Galán R (2002) The putative role of botrydial and related metabolites in the infection mechanism of *Botrytis*

cinerea. J Chem Ecol **28**: 997–1005.

Cook DE, Mesarich CH, Thomma BPHJ (2015) Understanding plant immunity as a surveillance system to detect invasion. Annu Rev Phytopathol **53**: 541–563.

Cotton P, Kasza Z, Bruel C, Rascle C, Fèvre M (2003) Ambient pH controls the expression of endopolygalacturonase genes in the necrotrophic fungus *Sclerotinia sclerotiorum*. FEMS Microbiol Lett **227**: 163–169.

De Cremer K, Mathys J, Vos C, Froenicke L, Michelmore RW, Cammue BPA, De Coninck B (2013) RNAseq-based transcriptome analysis of *Lactuca sativa* infected by the fungal necrotroph *Botrytis cinerea*. Plant Cell Environ **36**: 1992–2007.

Cresnar B, Petric S (2011) Cytochrome P450 enzymes in the fungal kingdom. Biochim Biophys Acta **1814**: 29–35.

Cuesta Arenas Y, Kalkman ERIC, Schouten A, Dieho M, Vredenbregt P, Uwumukiza B, Osés Ruiz M, van Kan JAL (2010) Functional analysis and mode of action of phytotoxic Nep1-like proteins of *Botrytis cinerea*. Physiol Mol Plant Pathol **74**: 376–386.

Cui H, Tsuda K, Parker JE (2015) Effector-triggered immunity: from pathogen perception to robust defense. Annu Rev Plant Biol **66**: 487–511.

Cunnac S, Lindeberg M, Collmer A (2009) *Pseudomonas syringae* type III secretion system effectors: repertoires in search of functions. Curr Opin Microbiol **12**: 53–60.

Dalio RJD, Herlihy J, Oliveira TS, McDowell JM, Machado M (2018) Effector biology in focus: a primer for computational prediction and functional characterization. Mol Plant Microbe Interact **31**: 22–33.

Dalmais B, Schumacher J, Moraga J, LE Pêcheur P, Tudzynski B, Collado IG, Viaud M (2011) The *Botrytis cinerea* phytotoxin botcinic acid requires two polyketide synthases for production and has a redundant role in virulence with botrydial. Mol Plant Pathol **12**: 564–579.

van Damme M, Bozkurt TO, Cakir C, Schornack S, Sklenar J, Jones AME, Kamoun S (2012) The Irish potato famine pathogen *Phytophthora infestans* translocates the CRN8 kinase into host plant cells. PLoS Pathog **8**: e1002875.

Davidson AL, Blahut-Beatty L, Itaya A, Zhang Y, Zheng S, Simmonds D (2016) Histopathology of *Sclerotinia sclerotiorum* infection and oxalic acid function in susceptible and resistant soybean. Plant Pathol. doi: 10.1111/ppa.12514.

Denton-Giles M, Derbyshire MC, Khentry Y, Buchwaldt L, Kamphuis LG (2018) Partial stem resistance in *Brassica napus* to highly aggressive and genetically diverse *Sclerotinia sclerotiorum* isolates from Australia. Can J Plant Pathol **40**: 551–561.

Derbyshire M, Denton-Giles M, Hegedus D, Seifbarghy S, Rollins J, van Kan J, Seidl MF, Faino L, Mbengue M, Navaud O, et al (2017) The complete genome sequence of the phytopathogenic fungus *Sclerotinia sclerotiorum* reveals insights into the genome architecture of broad host range pathogens. Genome Biol Evol **9**: 593–618.

Derbyshire MC, Denton-Giles M (2016) The control of sclerotinia stem rot on oilseed rape (*Brassica napus*): current practices and future opportunities. Plant Pathol **65**: 859–877.

DeZwaan TM, Carroll AM, Valent B, Sweigard JA (1999) *Magnaporthe grisea* pth11p is a novel plasma membrane protein that mediates appressorium differentiation in response to inductive substrate cues. Plant Cell **11**: 2013–2030.

Dickman MB, Park YK, Oltersdorf T, Li W, Clemente T, French R (2001) Abrogation of disease development in plants expressing animal antiapoptotic genes. PNAS 98 (12) 6957-6962.

Ding C, Vidanes GM, Maguire SL, Guida A, Synnott JM, Andes DR, Butler G (2011) Conserved and divergent roles of bcr1 and cfem proteins in *Candida parapsilosis* and *Candida albicans*. PLoS One **6**: e28151.

Ding X, Yu Q, Zhang B, Xu N, Jia C, Dong Y, Chen Y, Xing L, Li M (2014) The type II Ca2+/calmodulin-dependent protein kinases are involved in the regulation of cell wall integrity and oxidative stress response in *Candida albicans*. Biochem Biophys Res Commun **446**: 1073–1078.

Dodds PN, Lawrence GJ, Catanzariti A-M, Ayliffe MA, Ellis JG (2004) The *Melampsora lini* AvrL567 avirulence genes are expressed in haustoria and their products are recognized inside plant cells. Plant Cell **16**: 755–768.

Dodds PN, Rathjen JP (2010) Plant immunity: towards an integrated view of plant-pathogen interactions. Nat Rev Genet **11**: 539–548.

Dou D, Zhou J-M (2012) Phytopathogen effectors subverting host immunity: different foes, similar battleground. Cell Host Microbe **12**: 484–495.

Dowd CA, Buckley CM, Sheehan D (1997) Glutathione S-transferases from the white-rot fungus, *Phanerochaete chrysosporium*. Biochem J **324**: 243–248.

Duan Y, Ge C, Liu S, Wang J, Zhou M (2013) A two-component histidine kinase Shk1 controls stress response, sclerotial formation and fungicide resistance in *Sclerotinia sclerotiorum*. Mol Plant Pathol **14**: 708–718.

Earley KW, Haag JR, Pontes O, Opper K, Juehne T, Song K, Pikaard CS (2006) Gateway-compatible vectors for plant functional genomics and proteomics. Plant J **45**: 616–629.

Eisenhaber B, Bork P, Eisenhaber F (1998) Sequence properties of GPI-anchored proteins near the omega-site: constraints for the polypeptide binding site of the putative transamidase. Protein Eng **11** : 1155–1161.

Emanuelsson O, Brunak S, von Heijne G, Nielsen H (2007) Locating proteins in the cell using TargetP, SignalP and related tools. Nat Protoc **2**: 953–971.

Erental A, Harel A, Yarden O (2007) Type 2A phosphoprotein phosphatase is required for asexual development and pathogenesis of *Sclerotinia sclerotiorum*. Mol Plant-Microbe Interact **20**: 944–954.

Faber BW, van Gorcom RF, Duine JA (2001) Purification and characterization of benzoate-para-hydroxylase, a cytochrome P450 (CYP53A1), from *Aspergillus niger*. Arch Biochem Biophys **394**: 245–254.

Fang A, Han Y, Zhang N, Zhang M, Liu L, Li S, Lu F, Sun W (2016) Identification and characterization of plant cell death-inducing secreted proteins from *Ustilaginoidea virens*. Mol Plant Microbe Interact **29**: 405–416.

Favaron F, Sella L, D'Ovidio R (2004) Relationships among endo-polygalacturonase, oxalate, ph, and plant polygalacturonase-inhibiting protein (PGIP) in the interaction between *Sclerotinia sclerotiorum* and soybean. Mol Plant-Microbe Interact **17**: 1402–1409.

Figueroa M, A Manning V, Pandelova I, M Ciuffetti L (2015) Persistence of the host-selective toxin Ptr ToxB in the apoplast. Mol Plant Microbe Interact. doi: 10.1094/MPMI-05-15-0097-R.

Foreman J, Demidchik V, Bothwell JHF, Mylona P, Miedema H, Torres MA, Linstead P, Costa S, Brownlee C, Jones JDG, et al (2003) Reactive oxygen species produced by NADPH oxidase regulate plant cell growth. Nature **422**: 442–446.

Fraissinet-Tachet L, Fevre M (1996) Regulation by galacturonic acid of pectinolytic enzyme production by *Sclerotinia sclerotiorum*. Curr Microbiol **33**: 49–53.

Franco-Orozco B, Berepiki A, Ruiz O, Gamble L, Griffe LL, Wang S, Birch PRJ, Kanyuka

K, Avrova A (2017) A new proteinaceous pathogen-associated molecular pattern (PAMP) identified in Ascomycete fungi induces cell death in Solanaceae. New Phytol **214**: 1657–1672.

Frías M, Brito N, González C (2013) The *Botrytis cinerea* cerato-platanin BcSpl1 is a potent inducer of systemic acquired resistance (SAR) in tobacco and generates a wave of salicylic acid expanding from the site of application. Mol Plant Pathol **14**: 191–196.

Frías M, Gonzalez C, Brito N (2011) BcSpl1, a cerato-platanin family protein, contributes to *Botrytis cinerea* virulence and elicits the hypersensitive response in the host. New Phytol **192**: 483–495.

Frisch T, Motawia MS, Olsen CE, Agerbirk N, Moller BL, Bjarnholt N (2015) Diversified glucosinolate metabolism: biosynthesis of hydrogen cyanide and of the hydroxynitrile glucoside alliarinoside in relation to sinigrin metabolism in *Alliaria petiolata*. Front Plant Sci **6**: 926.

Garrido-Sanz D, Meier-Kolthoff JP, Goker M, Martin M, Rivilla R, Redondo-Nieto M (2016) Genomic and genetic diversity within the *Pseudomonas fluorescens* complex. PLoS One **11**: e0150183.

George HL, VanEtten HD (2001) Characterization of pisatin-inducible cytochrome P450s in fungal pathogens of pea that detoxify the pea phytoalexin pisatin. Fungal Genet Biol **33**: 37–48.

Germeier C., Hedke K., Tiedemann A V. (1994) The use of pH-indicators in diagnostic media for acid-producing plant pathogens. J Plant Dis Prot **101**: 498–507.

Gijzen M, Nurnberger T (2006) Nep1-like proteins from plant pathogens: recruitment and diversification of the NPP1 domain across taxa. Phytochemistry **67**: 1800–1807.

Gil-Durán C, Rojas-Aedo JF, Medina E, Vaca I, García-Rico RO, Villagrán S, Levicán G, Chávez R (2015) The pcz1 gene, which encodes a Zn(II)2Cys6 protein, is involved in the control of growth, conidiation, and conidial germination in the filamentous fungus *Penicillium roqueforti*. PLoS One **10**: e0120740.

Giles NM, Watts AB, Giles GI, Fry FH, Littlechild JA, Jacob C (2003) Metal and redox modulation of cysteine protein function. Chem Biol **10**: 677–693.

Gioti A, Simon A, Le Pecheur P, Giraud C, Pradier JM, Viaud M, Levis C (2006) Expression profiling of *Botrytis cinerea* genes identifies three patterns of up-regulation in

planta and an FKBP12 protein affecting pathogenicity. J Mol Biol **358**: 372–386.

Godoy G, Steadman JR, Dickman MB, Dam R (1990) Use of mutants to demonstrate the role of oxalic acid in pathogenicity of *Sclerotinia sclerotiorum* on *Phaseolus vulgaris*. Physiol Mol Plant Pathol **37**: 179–191.

Gomes Amitha Reena, Byregowda Sonnahallipura Munivenkatappa VB nahally, Muniveerappa BV murthy (2016) An overview of heterologous expression host systems for the production of recombinant proteins. Adv Anim Vet Sci **4**: 346–356.

Gonzalez-Fernandez R, Aloria K, Valero-Galvan J, Redondo I, Arizmendi JM, Jorrin-Novo J V (2014) Proteomic analysis of mycelium and secretome of different *Botrytis cinerea* wild-type strains. J Proteomics **97**: 195–221.

Greenberg JT, Yao N (2004) The role and regulation of programmed cell death in plant–pathogen interactions. Cell Microbiol **6**: 201–211.

de Guillen K, Ortiz-Vallejo D, Gracy J, Fournier E, Kroj T, Padilla A (2015) Structure analysis uncovers a highly diverse but structurally conserved effector family in phytopathogenic fungi. PLoS Pathog **11**: e1005228.

Guyon K, Balagué C, Roby D, Raffaele S (2014) Secretome analysis reveals effector candidates associated with broad host range necrotrophy in the fungal plant pathogen *Sclerotinia sclerotiorum*. BMC Genomics **15**: 336.

Hammond-Kosack KE, Rudd JJ (2008) Plant resistance signalling hijacked by a necrotrophic fungal pathogen. Plant Signal Behav **3**: 993–995.

Han Y, Joosten H-J, Niu W, Zhao Z, Mariano PS, McCalman M, van Kan J, Schaap PJ, Dunaway-Mariano D (2007) Oxaloacetate hydrolase, the C-C bond lyase of oxalate secreting fungi. J Biol Chem **282**: 9581–9590.

Han Y, Liu X, Benny U, Kistler HC, VanEtten HD (2001) Genes determining pathogenicity to pea are clustered on a supernumerary chromosome in the fungal plant pathogen *Nectria haematococca*. Plant J **25**: 305–314.

Harel A, Bercovich S, Yarden O (2006) Calcineurin is required for sclerotial development and pathogenicity of *Sclerotinia sclerotiorum* in an oxalic acid-independent manner. Mol Plant-Microbe Interact **19**: 682–693.

Harwood CS, Parales RE (1996) The beta-ketoadipate pathway and the biology of self-identity. Annu Rev Microbiol **50**: 553–590.

ten Have A, Breuil WO, Wubben JP, Visser J, van Kan JAL (2001) *Botrytis cinerea* endopolygalacturonase genes are differentially expressed in various plant tissues. Fungal Genet Biol **33**: 97–105.

ten Have A, Mulder W, Visser J, van Kan JAL (1998) The endopolygalacturonase gene bcpg1 is required for full virulence of *Botrytis cinerea*. Mol Plant-Microbe Interact **11**: 1009–1016.

ten Have A, Tenberge K, Benen JE, Tudzynski P, Visser J, van Kan JL (2002) The contribution of cell wall degrading enzymes to pathogenesis of fungal plant pathogens. *In* F Kempken, ed, Agric. Appl. SE - 17. Springer Berlin Heidelberg, pp 341–358.

Hayashi K, Schoonbeek H, De Waard MA (2002a) Expression of the ABC transporter BcatrD from *Botrytis cinerea* reduces sensitivity to sterol demethylation inhibitor fungicides. Pestic Biochem Physiol **73**: 110–121.

Hayashi K, Schoonbeek H-J, De Waard MA (2002b) Bcmfs1, a novel major facilitator superfamily transporter from *Botrytis cinerea*, provides tolerance towards the natural toxic compounds camptothecin and cercosporin and towards fungicides. Appl Environ Microbiol **68**: 4996–5004.

He P, Shan L, Lin N-C, Martin GB, Kemmerling B, Nurnberger T, Sheen J (2006) Specific bacterial suppressors of MAMP signaling upstream of MAPKKK in Arabidopsis innate immunity. Cell **125**: 563–575.

Heard S, Brown NA, Hammond-Kosack K (2015) An interspecies comparative analysis of the predicted secretomes of the necrotrophic plant pathogens *Sclerotinia sclerotiorum* and *Botrytis cinerea*. PLoS One **10**: e0130534.

Hegedus DD, Gerbrandt K, Coutu C (2016) The eukaryotic protein kinase superfamily of the necrotrophic fungal plant pathogen, *Sclerotinia sclerotiorum*. Mol Plant Pathol **17**: 634–647.

Hegedus DD, Rimmer SR (2005) *Sclerotinia sclerotiorum*: When "to be or not to be" a pathogen? Fed Eur Microbiol Soc Microbiol Lett **251**: 177–184.

von Heijne G (1998) Life and death of a signal peptide. Nature **396**: 111,113.

Horbach R, Navarro-Quesada AR, Knogge W, Deising HB (2011) When and how to kill a plant cell: infection strategies of plant pathogenic fungi. J Plant Physiol **168**: 51–62.

Horton P, Park K-J, Obayashi T, Fujita N, Harada H, Adams-Collier CJ, Nakai K (2007) WoLF PSORT: protein localization predictor. Nucleic Acids Res **35**: W585–7.

Houterman PM, Cornelissen BJC, Rep M (2008) Suppression of plant resistance gene-based

immunity by a fungal effector. PLoS Pathog **4**: e1000061–e1000061.

Howell HE (1975) Correlation of virulence with secretion in vitro of three wall-degrading enzymes in isolates of *Sclerotinia fructigena* obtained after mutagen treatment. J Gen Microbiol **90**: 32–40.

Hulvey J, Popko JTJ, Sang H, Berg A, Jung G (2012) Overexpression of ShCYP51B and ShatrD in *Sclerotinia homoeocarpa* isolates exhibiting practical field resistance to a demethylation inhibitor fungicide. Appl Environ Microbiol **78**: 6674–6682.

Iwata Y, Koizumi N (2005) Unfolded protein response followed by induction of cell death in cultured tobacco cells treated with tunicamycin. Planta **220**: 804–807.

Janusz G, Kucharzyk KH, Pawlik A, Staszczak M, Paszczynski AJ (2013) Fungal laccase, manganese peroxidase and lignin peroxidase: gene expression and regulation. Enzyme Microb Technol **52**: 1–12.

Jiang Y, Tripathy S, Govers F, Tyler B (2008) RXLR effector reservoir in two Phytophthora species is dominated by a single rapidly evolving superfamily with more than 700 members. Proc Natl Acad Sci U S A. doi: 10.1073/pnas.0709303105.

Johnson C, Kweon HK, Sheidy D, Shively CA, Mellacheruvu D, Nesvizhskii AI, Andrews PC, Kumar A (2014) The yeast Sks1p kinase signaling network regulates pseudohyphal growth and glucose response. PLoS Genet **10**: e1004183.

Jones DA, Bertazzoni S, Turo CJ, Syme RA, Hane JK (2018) Bioinformatic prediction of plant-pathogenicity effector proteins of fungi. Curr Opin Microbiol **46**: 43–49.

Jones JDG, Dangl JL (2006) The plant immune system. Nature **444**: 323.

de Jonge R, Peter van Esse H, Kombrink A, Shinya T, Desaki Y, Bours R, van der Krol S, Shibuya N, Joosten MHAJ, Thomma BPHJ (2010) Conserved fungal LysM effector Ecp6 prevents chitin-triggered immunity in plants. Science (80-) **329**: 953–955.

Joshi RK, Megha S, Rahman MH, Basu U, Kav NN V (2016) A global study of transcriptome dynamics in canola (*Brassica napus* L.) responsive to *Sclerotinia sclerotiorum* infection using RNA-Seq. Gene **590**: 57–67.

Jurick II WM, Rollins JA (2007) Deletion of the adenylate cyclase (sac1) gene affects multiple developmental pathways and pathogenicity in *Sclerotinia sclerotiorum*. Fungal Genet Biol **44**: 521–530.

Kabbage M, Williams B, Dickman MB (2013) Cell death control: the interplay of apoptosis

and autophagy in the pathogenicity of *Sclerotinia sclerotiorum*. PLoS Pathog **9**: e1003287.

Kabbage M, Yarden O, Dickman MB (2015) Pathogenic attributes of *Sclerotinia sclerotiorum*: switching from a biotrophic to necrotrophic lifestyle. Plant Sci **233**: 53–60.

Kalderon D, Roberts BL, Richardson WD, Smith AE (1984) A short amino acid sequence able to specify nuclear location. Cell **39**: 499–509.

Kamoun S (2006) A catalogue of the effector secretome of plant pathogenic oomycetes. Annu Rev Phytopathol **44**: 41–60.

Kanneganti T-D, Huitema E, Cakir C, Kamoun S (2006) Synergistic interactions of the plant cell death pathways induced by *Phytophthora infestans* Nepl-like protein PiNPP1.1 and INF1 elicitin. Mol Plant Microbe Interact **19**: 854–863.

Kars I, Krooshof GH, Wagemakers L, Joosten R, Benen JAE, van Kan JAL (2005) Necrotizing activity of five *Botrytis cinerea* endopolygalacturonases produced in *Pichia pastoris*. Plant J **43**: 213–225.

Kelkar HS, Skloss TW, Haw JF, Keller NP, Adams TH (1997) *Aspergillus nidulans* stcL encodes a putative cytochrome P-450 monooxygenase required for bisfuran desaturation during aflatoxin/sterigmatocystin biosynthesis. J Biol Chem **272** : 1589–1594.

Kennedy J, Auclair K, Kendrew SG, Park C, Vederas JC, Hutchinson CR (1999) Modulation of polyketide synthase activity by accessory proteins during lovastatin biosynthesis. Science (80-) **284**: 1368–1372.

Kettles GJ, Bayon C, Canning G, Rudd JJ, Kanyuka K (2017) Apoplastic recognition of multiple candidate effectors from the wheat pathogen *Zymoseptoria tritici* in the nonhost plant *Nicotiana benthamiana*. New Phytol **213**: 338–350.

Ben Khaled S, Postma J, Robatzek S (2015) A moving view: subcellular trafficking processes in pattern recognition receptor-triggered plant immunity. Annu Rev Phytopathol **53**: 379–402.

Khan M, Seto D, Subramaniam R, Desveaux D (2018) Oh, the places they'll go! A survey of phytopathogen effectors and their host targets. Plant J **93**: 651–663.

Kim H, Chen C, Kabbage M, Dickman MB (2011) Identification and characterization of *Sclerotinia sclerotiorum* NADPH oxidases. Appl Environ Microbiol **77**: 7721–7729.

Kim KS, Min J-Y, Dickman MB (2008) Oxalic acid is an elicitor of plant programmed cell death during *Sclerotinia sclerotiorum* disease development. Mol Plant-Microbe Interact **21**:

605–612.

Kim S, Park S-Y, Kim KS, Rho H-S, Chi M-H, Choi J, Park J, Kong S, Park J, Goh J, et al (2009) Homeobox transcription factors are required for conidiation and appressorium development in the rice blast fungus *Magnaporthe oryzae*. PLoS Genet **5**: e1000757.

Kleemann J, Rincon-Rivera LJ, Takahara H, Neumann U, van Themaat EVL, van der Does HC, Hacquard S, Stüber K, Will I, Schmalenbach W, et al (2012) Sequential delivery of host-induced virulence effectors by appressoria and intracellular hyphae of the phytopathogen *Colletotrichum higginsianum*. PLoS Pathog **8**: e1002643.

Kleman-Leyer KM, Siika-Aho M, Teeri TT, Kirk TK (1996) The cellulases endoglucanase I and cellobiohydrolase II of *Trichoderma reesei* act synergistically to solubilize native cotton cellulose but not to decrease its molecular size. Appl Environ Microbiol **62** : 2883–2887.

Korner CJ, Du X, Vollmer ME, Pajerowska-Mukhtar KM (2015) Endoplasmic reticulum stress signaling in plant immunity at the crossroad of life and death. Int J Mol Sci **16**: 26582–26598.

Lacomme C, Santa Cruz S (1999) Bax-induced cell death in tobacco is similar to the hypersensitive response. Proc Natl Acad Sci U S A **96**: 7956–7961.

Laurie JD, Ali S, Linning R, Mannhaupt G, Wong P, Guldener U, Munsterkotter M, Moore R, Kahmann R, Bakkeren G, et al (2012) Genome comparison of barley and maize smut fungi reveals targeted loss of RNA silencing components and species-specific presence of transposable elements. Plant Cell **24**: 1733–1745.

Lenarcic T, Albert I, Bohm H, Hodnik V, Pirc K, Zavec AB, Podobnik M, Pahovnik D, Zagar E, Pruitt R, et al (2017) Eudicot plant-specific sphingolipids determine host selectivity of microbial NLP cytolysins. Science **358**: 1431–1434.

Li M, Liang X, Rollins JA (2012) *Sclerotinia sclerotiorum* γ-glutamyl transpeptidase (Ss-Ggt1) is required for regulating glutathione accumulation and development of sclerotia and compound appressoria. Mol Plant-Microbe Interact **25**: 412–420.

Li M, Rollins JA (2009) The development-specific protein (Ssp1) from *Sclerotinia sclerotiorum* is encoded by a novel gene expressed exclusively in sclerotium tissues. Mycologia **101**: 34–43.

Li R, Rimmer R, Buchwaldt L, Sharpe AG, Séguin-Swartz G, Hegedus DD (2004) Interaction of *Sclerotinia sclerotiorum* with *Brassica napus*: cloning and characterization of

endo- and exo-polygalacturonases expressed during saprophytic and parasitic modes. Fungal Genet Biol **41**: 754–65.

Liang X, Liberti D, Li M, Kim Y-T, Hutchens A, Wilson R, Rollins JA (2015a) Oxaloacetate acetylhydrolase gene mutants of *Sclerotinia sclerotiorum* do not accumulate oxalic acid, but do produce limited lesions on host plants. Mol Plant Pathol **16**: 559–571.

Liang X, Moomaw EW, Rollins JA (2015b) Fungal oxalate decarboxylase activity contributes to *Sclerotinia sclerotiorum* early infection by affecting both compound appressoria development and function. Mol Plant Pathol **16**: 825–836.

Liang X, Rollins JA (2018) Mechanisms of broad host range necrotrophic pathogenesis in *Sclerotinia sclerotiorum*. Phytopathology **108**: 1128–1140.

Liang Y, Rahman MH, Strelkov SE, Kav NN V (2010) Developmentally induced changes in the sclerotial proteome of *Sclerotinia sclerotiorum*. Fungal Biol **114**: 619–627.

Liang Y, Yajima W, Davis MR, Kav NN V, Strelkov SE (2013) Disruption of a gene encoding a hypothetical secreted protein from *Sclerotinia sclerotiorum* reduces its virulence on canola (*Brassica napus*). Can J Plant Pathol **35**: 46–55.

Libault M, Wan J, Czechowski T, Udvardi M, Stacey G (2007) Identification of 118 Arabidopsis transcription factor and 30 ubiquitin-ligase genes responding to chitin, a plant-defense elicitor. Mol plant-microbe Interact **20**: 900–911.

Liebrand TWH, van den Berg GCM, Zhang Z, Smit P, Cordewener JHG, America AHP, Sklenar J, Jones AME, Tameling WIL, Robatzek S, et al (2013) Receptor-like kinase SOBIR1/EVR interacts with receptor-like proteins in plant immunity against fungal infection. Proc Natl Acad Sci U S A **110**: 10010–10015.

Liebrand TWH, van den Burg HA, Joosten MHAJ (2014) Two for all: receptor-associated kinases SOBIR1 and BAK1. Trends Plant Sci **19**: 123–132.

Liebrand TWH, Smit P, Abd-El-Haliem A, de Jonge R, Cordewener JHG, America AHP, Sklenar J, Jones AME, Robatzek S, Thomma BPHJ, et al (2012) Endoplasmic reticulum-quality control chaperones facilitate the biogenesis of Cf receptor-like proteins involved in pathogen resistance of tomato. Plant Physiol **159**: 1819–1833.

Lindeberg M, Cartinhour S, Myers CR, Schechter LM, Schneider DJ, Collmer A (2006) Closing the circle on the discovery of genes encoding Hrp regulon members and type III secretion system effectors in the genomes of three model *Pseudomonas syringae* strains.

Mol plant-microbe Interact **19**: 1151–1158.

Liu T, Song T, Zhang X, Yuan H, Su L, Li W, Xu J, Liu S, Chen L, Chen T, et al (2014) Unconventionally secreted effectors of two filamentous pathogens target plant salicylate biosynthesis. Nat Commun **5**: 4686.

Liu Y, Schiff M, Marathe R, Dinesh-Kumar SP (2002) Tobacco Rar1, EDS1 and NPR1/NIM1 like genes are required for N-mediated resistance to tobacco mosaic virus. Plant J **30**: 415–429.

Liu Z, Zhang Z, Faris JD, Oliver RP, Syme R, McDonald MC, McDonald BA, Solomon PS, Lu S, Shelver WL, et al (2012) The cysteine rich necrotrophic effector SnTox1 produced by *Stagonospora nodorum* triggers susceptibility of wheat lines harboring Snn1. PLoS Pathog **8**: e1002467.

Livak KJ, Schmittgen TD (2001) Analysis of relative gene expression data using real-time quantitative PCR and the 2(-Delta Delta C(T)) Method. Methods **25**: 402–408.

Lobstein J, Emrich CA, Jeans C, Faulkner M, Riggs P, Berkmen M (2012) SHuffle, a novel *Escherichia coli* protein expression strain capable of correctly folding disulfide bonded proteins in its cytoplasm. Microb Cell Fact **11**: 56.

Lorang JM, Carkaci-Salli N, Wolpert TJ (2004) Identification and characterization of victorin sensitivity in *Arabidopsis thaliana*. Mol Plant Microbe Interact **17**: 577–582.

Lorang JM, Sweat TA, Wolpert TJ (2007) Plant disease susceptibility conferred by a "resistance" gene. Proc Natl Acad Sci U S A **104**: 14861–14866.

Lumsden R (1979) Histology and physiology of pathogenesis in plant diseases caused by Sclerotinia species. Phytopathology. doi: 10.1094/Phyto-69-890.

Luo C-X, Schnabel G (2008) The cytochrome P450 lanosterol 14alpha-demethylase gene is a demethylation inhibitor fungicide resistance determinant in *Monilinia fructicola* field isolates from Georgia. Appl Environ Microbiol **74**: 359–366.

Lyu X, Shen C, Fu Y, Xie J, Jiang D, Li G, Cheng J (2016) A small secreted virulence-related protein is essential for the necrotrophic interactions of *Sclerotinia sclerotiorum* with its host plants. PLoS Pathog **12**: e1005435.

Lyu X, Shen C, Fu Y, Xie J, Jiang D, Li G, Cheng J (2015a) Comparative genomic and transcriptional analyses of the carbohydrate-active enzymes and secretomes of phytopathogenic fungi reveal their significant roles during infection and development.

Scientific Reports **5**: 15565.

Lyu X, Shen C, Fu Y, Xie J, Jiang D, Li G, Cheng J (2015b) The microbial opsin homolog sop1 is involved in *Sclerotinia sclerotiorum* development and environmental stress response. Front Microbiol **6**: 1504.

Ma L, Borhan MH (2015) The receptor-like kinase SOBIR1 interacts with *Brassica napus* LepR3 and is required for *Leptosphaeria maculans* AvrLm1-triggered immunity. Front Plant Sci **6**: 933.

Ma L, Cornelissen BJC, Takken FLW (2013) A nuclear localization for Avr2 from *Fusarium oxysporum* is required to activate the tomato resistance protein I-2. Front Plant Sci **4**: 94.

Ma L, Lukasik E, Gawehns F, Takken FW (2012) The use of agroinfiltration for transient expression of plant resistance and fungal effector proteins in *Nicotiana benthamiana* Leaves. *In* MD Bolton, BPHJ Thomma, eds, Plant Fungal Pathog. Humana Press, pp 61–74.

MacPherson S, Larochelle M, Turcotte B (2006) A fungal family of transcriptional regulators: the zinc cluster proteins. Microbiol Mol Biol Rev **70**: 583–604.

Magro P, Marciano P, di Lenna P (1988) Enzymatic oxalate decarboxylation in isolates of *Sclerotinia sclerotiorum*. FEMS Microbiol Lett **49**: 49–52.

Makizumi Y, Takeda S, Matsuzaki Y, Nakaune R, Hamamoto H, Akutsu K, Hibi T (2002) Cloning and selective toxicant-induced expression of BMR1 and BMR3, novel ABC transporter genes in *Botrytis cinerea*. J Gen Plant Pathol **68**: 338–341.

Malagnac F, Lalucque H, Lepere G, Silar P (2004) Two NADPH oxidase isoforms are required for sexual reproduction and ascospore germination in the filamentous fungus *Podospora anserina*. Fungal Genet Biol **41**: 982–997.

Malhotra JD, Kaufman RJ (2007) The endoplasmic reticulum and the unfolded protein response. Semin Cell Dev Biol **18**: 716–731.

Maxwell DP (1973) Oxalate formation in *Whetzelinia sclerotiorum* by oxaloacetate acetylhydrolase. Physiol Plant Pathol **3**: 279–288.

McLellan H, Boevink PC, Armstrong MR, Pritchard L, Gomez S, Morales J, Whisson SC, Beynon JL, Birch PRJ (2013) An RxLR effector from *Phytophthora infestans* prevents re-localisation of two plant NAC transcription factors from the endoplasmic reticulum to the nucleus. PLOS Pathog **9**: e1003670.

Melotto M, Underwood W, Koczan J, Nomura K, He SY (2006) Plant stomata function in

innate immunity against bacterial invasion. Cell **126**: 969–980.

Mentlak TA, Kombrink A, Shinya T, Ryder LS, Otomo I, Saitoh H, Terauchi R, Nishizawa Y, Shibuya N, Thomma BPHJ, et al (2012) Effector-mediated suppression of chitin-triggered immunity by *Magnaporthe oryzae* is necessary for rice blast disease. Plant Cell **24**: 322–335.

Mesarich CH, Griffiths SA, van der Burgt A, Okmen B, Beenen HG, Etalo DW, Joosten MHAJ, de Wit PJGM (2014) Transcriptome sequencing uncovers the Avr5 avirulence gene of the tomato leaf mold pathogen *Cladosporium fulvum*. Mol Plant Microbe Interact **27**: 846–857.

Mijatovic S (2008) Biochemical characterization of 2-nitropropane dioxygenase from hansenula MRAKII. Georgia State University.

Monaghan J, Zipfel C (2012) Plant pattern recognition receptor complexes at the plasma membrane. Curr Opin Plant Biol **15**: 349–357.

Movahedi S, Heale JB (1990) The roles of aspartic proteinase and endo-pectin lyase enzymes in the primary stages of infection and pathogenesis of various host tissues by different isolates of *Botrytis cinerea*. Physiol Mol Plant Pathol **36**: 303–324.

Mukhtar MS, McCormack ME, Argueso CT, Pajerowska-Mukhtar KM (2016) Pathogen tactics to manipulate plant cell death. Curr Biol **26**: R608–R619.

Myhre S, Tveit H, Mollestad T, Laegreid A (2006) Additional gene ontology structure for improved biological reasoning. Bioinformatics **22**: 2020–2027.

Nagaharu U (1935) Genome-analysis in Brassica with special reference to the experimental formation of *B. napus* and peculiarmode of fertilization. J japanese Bot **7**: 389–452.

Navarre DA, Wolpert TJ (1999) Victorin induction of an apoptotic/senescence–like response in oats. Plant Cell **11** : 237–249.

Nemri A, Saunders DGO, Anderson C, Upadhyaya NM, Win J, Lawrence GJ, Jones DA, Kamoun S, Ellis JG, Dodds PN (2014) The genome sequence and effector complement of the flax rust pathogen *Melampsora lini*. Front Plant Sci **5**: 98.

Nimchuk Z, Eulgem T, Holt BF 3rd, Dangl JL (2003) Recognition and response in the plant immune system. Annu Rev Genet **37**: 579–609.

Nishizawa M (2015) The regulators of yeast PHO system participate in the transcriptional regulation of G1 cyclin under alkaline stress conditions. Yeast **32**: 367–378.

Noda J, Brito N, González C (2010) The *Botrytis cinerea* xylanase Xyn11A contributes to virulence with its necrotizing activity, not with its catalytic activity. BMC Plant Biol **10**: 1–15.

Oide S, Moeder W, Krasnoff S, Gibson D, Haas H, Yoshioka K, Turgeon BG (2006) NPS6, encoding a nonribosomal peptide synthetase involved in siderophore-mediated iron metabolism, is a conserved virulence determinant of plant pathogenic ascomycetes. Plant Cell **18**: 2836–2853.

Oliveira MB, de Andrade R V, Grossi-de-Sa MF, Petrofeza S (2015) Analysis of genes that are differentially expressed during the *Sclerotinia sclerotiorum-Phaseolus vulgaris* interaction. Front Microbiol **6**: 1162.

Oliveira-Garcia E, Valent B (2015) How eukaryotic filamentous pathogens evade plant recognition. Curr Opin Microbiol **26**: 92–101.

Oliver RP, Friesen TL, Faris JD, Solomon PS (2012) *Stagonospora nodorum*: from pathology to genomics and host resistance. Annu Rev Phytopathol **50**: 23–43.

Oliver RP, Solomon PS (2010) New developments in pathogenicity and virulence of necrotrophs. Curr Opin Plant Biol **13**: 415–419.

Olivieri F, Eugenia Zanetti M, Oliva CR, Covarrubias AA, Casalongué CA (2002) Characterization of an extracellular serine protease of *Fusarium eumartii* and its action on pathogenesis related proteins. Eur J Plant Pathol **108**: 63–72.

Orshinsky AM, Hu J, Opiyo SO, Reddyvari-Channarayappa V, Mitchell TK, Boehm MJ (2012) RNA-Seq analysis of the *Sclerotinia homoeocarpa*-creeping bentgrass pathosystem. PLoS One **7**: e41150.

Pan Y, Xu Y, Li X, Yao C, Gao Z (2015) SsPemG1 encodes an elicitor-homologous protein and regulates pathogenicity in *Sclerotinia sclerotiorum*. Physiol Mol Plant Pathol **92**: 70–78.

Paoletti M, Clavé C (2007) The fungus-specific HET domain mediates programmed cell death in *Podospora anserina*. Eukaryot Cell **6** : 2001–2008.

Paoletti M, Saupe SJ (2009) Fungal incompatibility: Evolutionary origin in pathogen defense? BioEssays **31**: 1201–1210.

Park C-J, Peng Y, Chen X, Dardick C, Ruan D, Bart R, Canlas PE, Ronald PC (2008) Rice XB15, a protein phosphatase 2C, negatively regulates cell death and XA21-mediated innate immunity. PLOS Biol **6**: e231.

Parks LW, Casey WM (1995) Physiological implications of sterol biosynthesis in yeast. Annu Rev Microbiol **49**: 95–116.

Parlange F, Daverdin G, Fudal I, Kuhn M-L, Balesdent M-H, Blaise F, Grezes-Besset B, Rouxel T (2009) *Leptosphaeria maculans* avirulence gene AvrLm4-7 confers a dual recognition specificity by the Rlm4 and Rlm7 resistance genes of oilseed rape, and circumvents Rlm4-mediated recognition through a single amino acid change. Mol Microbiol **71**: 851–863.

Pedras MSC, Ahiahonu PWK (2004) Phytotoxin production and phytoalexin elicitation by the phytopathogenic fungus *Sclerotinia sclerotiorum*. J Chem Ecol **30**: 2163–2179.

Pedras MSC, Ahiahonu PWK, Hossain M (2004) Detoxification of the cruciferous phytoalexin brassinin in *Sclerotinia sclerotiorum* requires an inducible glucosyltransferase. Phytochemistry **65**: 2685–2694.

Pemberton CL, Salmond GPC (2004) The Nep1-like proteins—a growing family of microbial elicitors of plant necrosis. Mol Plant Pathol **5**: 353–359.

Pérez-Valle J, Rothe J, Primo C, Martínez Pastor M, Ariño J, Pascual-Ahuir A, Mulet JM, Serrano R, Yenush L (2010) Hal4 and Hal5 protein kinases are required for general control of carbon and nitrogen uptake and metabolism. Eukaryot Cell **9**: 1881–1890.

Perlin MH, Andrews J, Toh SS (2014) Essential letters in the fungal alphabet: ABC and MFS transporters and their roles in survival and pathogenicity. Adv Genet **85**: 201–253.

Petersen TN, Brunak S, von Heijne G, Nielsen H (2011) SignalP 4.0: discriminating signal peptides from transmembrane regions. Nat Methods **8**: 785–786.

Pitkin JW, Panaccionet DG, Walton JD (1996) A putative cyclic peptide efflux pump encoded by the TOXA gene of the plant-pathogenic fungus *Cochliobolus carbonurn*. Microbiology **142**: 1557–1565.

Podobnik B, Stojan J, Lah L, Krasevec N, Seliskar M, Rizner TL, Rozman D, Komel R (2008) CYP53A15 of *Cochliobolus lunatus*, a target for natural antifungal compounds. J Med Chem **51**: 3480–3486.

Postma J, Liebrand TWH, Bi G, Evrard A, Bye RR, Mbengue M, Joosten MHAJ, Robatzek S (2015) The Cf-4 receptor-like protein associates with the BAK1 receptor-like kinase to initiate receptor endocytosis and plant immunity. bioRxiv 19471.

Poussereau N, Creton S, Rascle C, Fevre M (2001a) Regulation of acp1 , encoding a non-

aspartyl acid protease expressed during pathogenesis of *Sclerotinia sclerotiorum*. Microbiology **147**: 717–726.

Poussereau N, Gente S, Rascle C, Billon-Grand G, Fevre M (2001b) aspS encoding an unusual aspartyl protease from *Sclerotinia sclerotiorum* is expressed during phytopathogenesis. FEMS Microbiol **194**: 27–32.

Prins TW, Wagemakers L, Schouten A, van Kan JAL (2000) Cloning and characterization of a glutathione S-transferase homologue from the plant pathogenic fungus *Botrytis cinerea*. Mol Plant Pathol **1**: 169–178.

Purdy LH (1979) *Sclerotinia sclerotiorum*: history, diseases and symptomatology, host range, geographic distribution, and impact. **69**: 875–880.

Qu X, Yu B, Liu J, Zhang X, Li G, Zhang D, Li L, Wang X, Wang L, Chen J, et al (2014) MADS-box transcription factor SsMADS is involved in regulating growth and virulence in *Sclerotinia sclerotiorum*. Int J Mol Sci **15**: 8049–8062.

Qutob D, Kamoun S, Gijzen M (2002) Expression of a *Phytophthora sojae* necrosis-inducing protein occurs during transition from biotrophy to necrotrophy. Plant J **32**: 361–373.

Raffaele S, Farrer RA, Cano LM, Studholme DJ, MacLean D, Thines M, Jiang RHY, Zody MC, Kunjeti SG, Donofrio NM, et al (2010) Genome evolution following host jumps in the Irish potato famine pathogen lineage. Science (80-) **330**: 1540–1543.

Raman H, Raman R, Nelson MN, Aslam MN, Rajasekaran R, Wratten N, Cowling WA, Kilian A, Sharpe AG, Schondelmaier J (2012) Diversity array technology markers: genetic diversity analyses and linkage map construction in rapeseed (*Brassica napus* L.). DNA Res An Int J Rapid Publ Reports Genes Genomes **19**: 51–65.

Rana D, van den Boogaart T, O'Neill CM, Hynes L, Bent E, Macpherson L, Park JY, Lim YP, Bancroft I (2004) Conservation of the microstructure of genome segments in *Brassica napus* and its diploid relatives. Plant J **40**: 725–733.

Ratcliff F, Martin-Hernandez AM, Baulcombe DC (2001) Technical Advance. Tobacco rattle virus as a vector for analysis of gene function by silencing. Plant J **25**: 237–245.

Reis H, Pfiff S, Hahn M (2005) Molecular and functional characterization of a secreted lipase from *Botrytis cinerea*. Mol Plant Pathol **6**: 257–267.

Rep M (2005) Small proteins of plant-pathogenic fungi secreted during host colonization. FEMS Microbiol Lett. doi: 10.1016/j.femsle.2005.09.014.

Rep M, van der Does HC, Meijer M, van Wijk R, Houterman PM, Dekker HL, de Koster CG, Cornelissen BJC (2004) A small, cysteine-rich protein secreted by *Fusarium oxysporum* during colonization of xylem vessels is required for I-3-mediated resistance in tomato. Mol Microbiol **53**: 1373–1383.

Riechers DE, Irzyk GP, Jones SS, Fuerst EP (1997) Partial characterization of glutathione S-transferases from wheat (*Triticum* spp.) and purification of a safener-induced glutathione S-transferase from *Triticum tauschii*. Plant Physiol **114**: 1461–1470.

Riou C, Freyssinet G, Fevre M (1992) Purification and characterization of extracellular pectinolytic enzymes produced by *Sclerotinia sclerotiorum*. Appl Environ Microbiol **58**: 578–583.

Riou C, Freyssinet G, Fevre M (1991) Production of cell wall-degrading enzymes by the phytopathogenic fungus *Sclerotinia sclerotiorum*. Appl Environ Microbiol **57**: 1478–1484.

Rivas S, Thomas CM (2005) Molecular interactions between tomato and the leaf mold pathogen *Cladosporium fulvum*. Annu Rev Phytopathol **43**: 395–436.

Robinson MD, Oshlack A (2010) A scaling normalization method for differential expression analysis of RNA-seq data. Genome Biol **11**: R25.

Rollins J a, Dickman MB (2001) pH signaling in *Sclerotinia sclerotiorum*: identification of a pacC/RIM1 homolog. Appl Environ Microbiol **67**: 75–81.

Rollins JA (2003) The *Sclerotinia sclerotiorum* pac1 gene is required for sclerotial development and virulence. Mol plant-microbe Interact **16**: 785–795.

Ron D, Walter P (2007) Signal integration in the endoplasmic reticulum unfolded protein response. Nat Rev Mol Cell Biol **8**: 519–529.

Ron M, Avni A (2004) The receptor for the fungal elicitor ethylene-inducing xylanase is a member of a resistance-like gene family in tomato. Plant Cell. doi: 10.1105/tpc.022475.

Rose JKC, Ham K-S, Darvill AG, Albersheim P (2002) Molecular cloning and characterization of glucanase inhibitor proteins: coevolution of a counterdefense mechanism by plant pathogens. Plant Cell **14**: 1329–1345.

Saijo Y, Loo EP-I, Yasuda S (2018) Pattern recognition receptors and signaling in plant-microbe interactions. Plant J **93**: 592–613.

Sakamoto T, Ishimaru M (2013) Peculiarities and applications of galactanolytic enzymes that act on type I and II arabinogalactans. Appl Microbiol Biotechnol **97**: 5201–5213.

Samolski I, de Luis A, Vizcaíno JA, Monte E, Suárez MB (2009) Gene expression analysis of the biocontrol fungus *Trichoderma harzianum* in the presence of tomato plants, chitin, or glucose using a high-density oligonucleotide microarray. BMC Microbiol **9**: 217.

Saunders DGO, Win J, Cano LM, Szabo LJ, Kamoun S, Raffaele S (2012) Using hierarchical clustering of secreted protein families to classify and rank candidate effectors of rust fungi. PLoS One **7**: e29847.

Schamber A, Leroch M, Diwo J, Mendgen K, Hahn M (2010) The role of mitogen-activated protein (MAP) kinase signalling components and the Ste12 transcription factor in germination and pathogenicity of *Botrytis cinerea*. Mol Plant Pathol **11**: 105–119.

Schoonbeek H, van Nistelrooy JGM, de Waard MA (2003) Functional analysis of ABC transporter genes from *Botrytis cinerea* identifies BcatrB as a transporter of eugenol. Eur J Plant Pathol **109**: 1003–1011.

Schoonbeek H, Del Sorbo G, De Waard MA (2001) The ABC transporter BcatrB affects the sensitivity of *Botrytis cinerea* to the phytoalexin resveratrol and the fungicide fenpiclonil. Mol plant-microbe Interact **14**: 562–571.

Schornack S, van Damme M, Bozkurt TO, Cano LM, Smoker M, Thines M, Gaulin E, Kamoun S, Huitema E (2010) Ancient class of translocated oomycete effectors targets the host nucleus. Proc Natl Acad Sci U S A **107**: 17421–17426.

Schouten A, Baarlen P van, Kan JAL van (2008) Phytotoxic Nep1-like proteins from the necrotrophic fungus *Botrytis cinerea* associate with membranes and the nucleus of plant cells. New Phytol **177**: 493–505.

Schrettl M, Bignell E, Kragl C, Joechl C, Rogers T, Arst HN, Haynes K, Haas H (2004) Siderophore biosynthesis but not reductive iron assimilation is essential for *Aspergillus fumigatus* virulence. J Exp Med **200**: 1213–1219.

Schumacher J, de Larrinoa IF, Tudzynski B (2008a) Calcineurin-responsive zinc finger transcription factor CRZ1 of *Botrytis cinerea* is required for growth, development, and full virulence on bean plants. Eukaryot Cell **7**: 584–601.

Schumacher J, Viaud M, Simon A, Tudzynski B (2008b) The Gα subunit BCG1, the phospholipase C (BcPLC1) and the calcineurin phosphatase co-ordinately regulate gene expression in the grey mould fungus *Botrytis cinerea*. Mol Microbiol **67**: 1027–1050.

Segmüller N, Kokkelink L, Giesbert S, Odinius D, van Kan J, Tudzynski P (2008) NADPH

oxidases are involved in differentiation and pathogenicity in *Botrytis cinerea*. Mol plant-microbe Interact **21**: 808–819.

Seifbarghi S, Borhan MH, Wei Y, Coutu C, Robinson SJ, Hegedus DD (2017) Changes in the *Sclerotinia sclerotiorum* transcriptome during infection of *Brassica napus*. BMC Genomics **18**: 266.

Selin C, de Kievit TR, Belmonte MF, Fernando WGD (2016) Elucidating the role of effectors in plant-fungal interactions: progress and challenges. Front Microbiol **7**: 600.

Sexton AC, Cozijnsen AJ, Keniry A, Jewell E, Love CG, Batley J, Edwards D, Howlett BJ (2006) Comparison of transcription of multiple genes at three developmental stages of the plant pathogen *Sclerotinia sclerotiorum*. FEMS Microbiol Lett **258**: 150–160.

Sexton AC, Howlett BJ (2000) Characterisation of a cyanide hydratase gene in the phytopathogenic fungus *Leptosphaeria maculans*. Mol Gen Genet **263**: 463–470.

Sexton AC, Minic Z, Cozijnsen AJ, Pedras MSC, Howlett BJ (2009) Cloning, purification and characterisation of brassinin glucosyltransferase, a phytoalexin-detoxifying enzyme from the plant pathogen *Sclerotinia sclerotiorum*. Fungal Genet Biol **46**: 201–9.

Siewers V, Viaud M, Jimenez-Teja D, Collado IG, Gronover CS, Pradier J-M, Tudzynski B, Tudzynski P (2005) Functional analysis of the cytochrome P450 monooxygenase gene bcbot1 of *Botrytis cinerea* indicates that botrydial is a strain-specific virulence factor. Mol plant-microbe Interact **18**: 602–612.

Simon A, Dalmais B, Morgant G, Viaud M (2013) Screening of a *Botrytis cinerea* one-hybrid library reveals a Cys2His2 transcription factor involved in the regulation of secondary metabolism gene clusters. Fungal Genet Biol **52**: 9–19.

Song K, Osborn TC (1992) Polyphyletic origins of *Brassica napus*: new evidence based on organelle and nuclear RFLP analyses. Genome **35**: 992–1001.

Del Sorbo G, Ruocco M, Schoonbeek H-J, Scala F, Pane C, Vinale F, De Waard MA (2008) Cloning and functional characterization of BcatrA, a gene encoding an ABC transporter of the plant pathogenic fungus *Botryotinia fuckeliana* (*Botrytis cinerea*). Mycol Res **112**: 737–746.

Sparkes IA, Runions J, Kearns A, Hawes C (2006) Rapid, transient expression of fluorescent fusion proteins in tobacco plants and generation of stably transformed plants. Nat Protoc **1**: 2019–2025.

Sperschneider J, Dodds PN, Gardiner DM, Manners JM, Singh KB, Taylor JM (2015a) Advances and challenges in computational prediction of effectors from plant pathogenic fungi. PLOS Pathog **11**: e1004806.

Sperschneider J, Williams AH, Hane JK, Singh KB, Taylor JM (2015b) Evaluation of secretion prediction highlights differing approaches needed for oomycete and fungal effectors. Front Plant Sci **6**: 1168.

Staats M, van Baarlen P, Schouten A, van Kan JAL, Bakker FT (2007) Positive selection in phytotoxic protein-encoding genes of Botrytis species. Fungal Genet Biol **44**: 52–63.

Stajich JE, Wilke SK, Ahren D, Au CH, Birren BW, Borodovsky M, Burns C, Canback B, Casselton LA, Cheng CK, et al (2010) Insights into evolution of multicellular fungi from the assembled chromosomes of the mushroom *Coprinopsis cinerea* (*Coprinus cinereus*). Proc Natl Acad Sci U S A **107**: 11889–11894.

Stefanato FL, Abou-Mansour E, Buchala A, Kretschmer M, Mosbach A, Hahn M, Bochet CG, Métraux J-P, Schoonbeek H (2009) The ABC transporter BcatrB from *Botrytis cinerea* exports camalexin and is a virulence factor on *Arabidopsis thaliana*. Plant J **58**: 499–510.

Stergiopoulos I, de Wit PJGM (2009) Fungal effector proteins. Annu Rev Phytopathol **47**: 233–263.

Stornaiuolo M, Lotti L V, Borgese N, Torrisi M-R, Mottola G, Martire G, Bonatti S (2003) KDEL and KKXX retrieval signals appended to the same reporter protein determine different trafficking between endoplasmic reticulum, intermediate compartment, and Golgi complex. Mol Biol Cell **14**: 889–902.

Stotz HU, Mitrousia GK, de Wit PJGM, Fitt BDL (2014) Effector-triggered defence against apoplastic fungal pathogens. Trends Plant Sci **19**: 491–500.

Sun Z, Yang D, Xie L, Sun L, Zhang S, Zhu Q, Li J, Wang X, Chen J (2013) Rice black-streaked dwarf virus P10 induces membranous structures at the ER and elicits the unfolded protein response in *Nicotiana benthamiana*. Virology **447**: 131–139.

Tan K-C, Phan HTT, Rybak K, John E, Chooi YH, Solomon PS, Oliver RP (2015) Functional redundancy of necrotrophic effectors-consequences for exploitation for breeding. Front Plant Sci **6**: 501.

Tanaka C and, Izumitsu K (2010) Two-component signaling system in filamentous fungi and

the mode of action of dicarboximide and phenylpyrrole fungicides. Fungic. pp 523–538.

Toruno TY, Stergiopoulos I, Coaker G (2016) Plant-pathogen effectors: cellular probes interfering with plant defenses in spatial and temporal manners. Annu Rev Phytopathol **54**: 419–441.

Tran VA, Reem A, Silva SI, Noureddine B, Dean S, Strelkov Stephen E. (2017) sensitivity of Canadian wheat genotypes to the necrotrophic effectors produced by *Pyrenophora tritici-repentis*. Can J plant Pathol **39 (2)**: 149–162.

Tripathy BC, Sherameti I, Oelmuller R (2010) Siroheme: an essential component for life on earth. Plant Signal Behav **5**: 14–20.

Tuori RP, Wolpert TJ, Ciuffetti LM (2000) Heterologous expression of functional Ptr ToxA. Mol Plant Microbe Interact **13**: 456–464.

VanEtten H, Temporini E, Wasmann C (2001) Phytoalexin (and phytoanticipin) tolerance as a virulence trait: why is it not required by all pathogens? Physiol Mol Plant Pathol **59**: 83–93.

Vardar F, Ünal M (2008) Proteolytic enzymes in plant programmed cell death. Türk Bilim Derlemeler Derg **1**: 65–78.

Vautard-Mey G, Cotton P, Fèvre M (1999) Expression and compartmentation of the glucose repressor CRE1 from the phytopathogenic fungus *Sclerotinia sclerotiorum*. Eur J Biochem **266**: 252–259.

Vitale, Raikhel (1999) What do proteins need to reach different vacuoles? Trends Plant Sci **4**: 149–155.

Vleeshouwers VGAA, Oliver RP (2014) Effectors as tools in disease resistance breeding against biotrophic, hemibiotrophic, and necrotrophic plant pathogens. Mol Plant-Microbe Interact **27**: 196–206.

Voigt C a., Schäfer W, Salomon S (2005) A secreted lipase of *Fusarium graminearum* is a virulence factor required for infection of cereals. Plant J **42**: 364–375.

Walker KW, Lyles MM, Gilbert HF (1996) Catalysis of oxidative protein folding by mutants of protein disulfide isomerase with a single active-site cysteine. Biochemistry **35**: 1972–1980.

Walton JD (2006) HC-toxin. Phytochemistry **67**: 1406–1413.

Wang X, Jiang N, Liu J, Liu W, Wang G-L (2014) The role of effectors and host immunity in plant-necrotrophic fungal interactions. Virulence **5**: 722–732.

Wei H, Scherer M, Singh A, Liese R, Fischer R (2001) *Aspergillus nidulans* alpha-1,3 glucanase (mutanase), mutA, is expressed during sexual development and mobilizes mutan. Fungal Genet Biol **34**: 217–227.

Westrick NM, Ranjan A, Jain S, Grau CR, Smith DL, Kabbage M (2019) Gene regulation of *Sclerotinia sclerotiorum* during infection of Glycine max: on the road to pathogenesis. BMC Genomics **20**: 157.

Willetts J. H, Wong A.,L. J (1980) The biology of *Sclerotinia sclerotiorum*, *S. trifoliorum*, and *S. minor* with emphasis on specific nomenclature. Bot Rev **46**: 101–165.

Williams B, Kabbage M, Kim H-J, Britt R, Dickman MB (2011) Tipping the balance: *Sclerotinia sclerotiorum* secreted oxalic acid suppresses host defenses by manipulating the host redox environment. PLoS Pathog **7**: e1002107.

Wolpert TJ, Dunkle LD, Ciuffetti LM (2002) Host-selective toxins and avirulence determinants: What's in a Name?. Annu Rev Phytopathol **40**: 251–285.

Xiao X, Xie J, Cheng J, Li G, Yi X, Jiang D, Fu Y (2014) Novel secretory protein Ss-Caf1 of the plant-pathogenic fungus *Sclerotinia sclerotiorum* is required for host penetration and normal sclerotial development. Mol Plant **27**: 40–55.

Xu H, Xu W, Xi H, Ma W, He Z, Ma M (2013) The ER luminal binding protein (BiP) alleviates Cd(2+)-induced programmed cell death through endoplasmic reticulum stress-cell death signaling pathway in tobacco cells. J Plant Physiol **170**: 1434–1441.

Xu L, Chen W (2013) Random T-DNA mutagenesis identifies a Cu/Zn superoxide dismutase gene as a virulence factor of *Sclerotinia sclerotiorum*. Mol Plant-Microbe Interact **26**: 431–441.

Xu L, Li G, Jiang D, Chen W (2018) *Sclerotinia sclerotiorum*: an evaluation of virulence theories. Annu Rev Phytopathol **56**: 311–338.

Xu L, Xiang M, White D, Chen W (2015) pH dependency of sclerotial development and pathogenicity revealed by using genetically defined oxalate-minus mutants of *Sclerotinia sclerotiorum*. Environ Microbiol **17**: 2896–2909.

Xue C, Park G, Choi W, Zheng L, Dean RA, Xu J-R (2002) Two novel fungal virulence genes specifically expressed in appressoria of the rice blast fungus. Plant Cell **14**: 2107–2119.

Yajima W, Kav NN V (2006) The proteome of the phytopathogenic fungus *Sclerotinia sclerotiorum*. Proteomics **6**: 5995–6007.

Yang B, Sugio A, White FF (2006) Os8N3 is a host disease-susceptibility gene for bacterial blight of rice. Proc Natl Acad Sci U S A **103**: 10503–10508.

Yang G, Tang L, Gong Y, Xie J, Fu Y, Jiang D, Li G, Collinge DB, Chen W, Cheng J (2018a) A cerato-platanin protein SsCP1 targets plant PR1 and contributes to virulence of *Sclerotinia sclerotiorum*. New Phytol **217**: 739–755.

Yang Y, Yang X, Dong Y, Qiu D (2018b) The *Botrytis cinerea* xylanase BcXyl1 modulates plant immunity. Front Microbiol **9**: 2535.

Yarden O, Veluchamy S, Dickman MB, Kabbage M (2014) *Sclerotinia sclerotiorum* catalase SCAT1 affects oxidative stress tolerance, regulates ergosterol levels and controls pathogenic development. Physiol Mol Plant Pathol **85**: 34–41.

Ye C-M, Chen S, Payton M, Dickman MB, Verchot J (2013) TGBp3 triggers the unfolded protein response and SKP1-dependent programmed cell death. Mol Plant Pathol **14**: 241–255.

Yeats TH, Rose JKC (2013) The formation and function of plant cuticles. Plant Physiol **163**: 5–20.

Yoshida Y (1993) Lanosterol 14α-Demethylase (Cytochrome P45014DM). *In* JB Schenkman, H Greim, eds, Cytochrome P450. Springer Berlin Heidelberg, Berlin, Heidelberg, pp 627–639.

Yu Y, Xiao J, Yang Y, Bi C, Qing L, Tan W (2015) Ss-Bi1 encodes a putative BAX inhibitor-1 protein that is required for full virulence of *Sclerotinia sclerotiorum*. Physiol Mol Plant Pathol **90**: 115–122.

Yu Y, Xiao J, Zhu W, Yang Y, Mei J, Bi C, Qian W, Qing L, Tan W (2016) Ss-Rhs1, a secretory Rhs repeat-containing protein, is required for the virulence of *Sclerotinia sclerotiorum*. Mol Plant Pathol. doi: 10.1111/mpp.12459.

Zhang H, Wu Q, Cao S, Zhao T, Chen L, Zhuang P, Zhou X, Gao Z (2014a) A novel protein elicitor (SsCut) from *Sclerotinia sclerotiorum* induces multiple defense responses in plants. Plant Mol Biol **86**: 495–511.

Zhang L, Kars I, Essenstam B, Liebrand TWH, Wagemakers L, Elberse J, Tagkalaki P, Tjoitang D, van den Ackerveken G, van Kan JAL (2014b) Fungal endopolygalacturonases are recognized as microbe-associated molecular patterns by the arabidopsis receptor-like protein responsiveness to Botrytis polygalacturonases1. Plant Physiol **164**: 352–364.

Zhang P, Johnson PS, Zollner C, Wang W, Wang Z, Montes AE, Seidleck BK, Blaschak CJ, Surratt CK (1999) Mutation of human mu opioid receptor extracellular "disulfide cysteine" residues alters ligand binding but does not prevent receptor targeting to the cell plasma membrane. Brain Res Mol Brain Res **72**: 195–204.

Zhang W, Fraiture M, Kolb D, Loffelhardt B, Desaki Y, Boutrot FFG, Tor M, Zipfel C, Gust AA, Brunner F (2013) Arabidopsis receptor-like protein30 and receptor-like kinase suppressor of BIR1-1/EVERSHED mediate innate immunity to necrotrophic fungi. Plant Cell **25**: 4227–4241.

Zhang X, Nguyen N, Breen S, Outram MA, Dodds PN, Kobe B, Solomon PS, Williams SJ (2017) Production of small cysteine-rich effector proteins in *Escherichia coli* for structural and functional studies. Mol Plant Pathol **18**: 141–151.

Zhang Y, Gao Y, Liang Y, Dong Y, Yang X, Qiu D (2019) Verticillium dahliae PevD1, an Alt a 1-like protein, targets cotton PR5-like protein and promotes fungal infection. J Exp Bot **70**: 613–626.

Zhao J, Buchwaldt L, Rimmer SR, Sharpe A, Mcgregor L, Bekkaoui D, Hegedus D (2009) Patterns of differential gene expression in *Brassica napus* cultivars infected with *Sclerotinia sclerotiorum*. Mol Plant Pathol **10**: 635–649.

Zhao X, Kim Y, Park G, Xu J-R (2005) A mitogen-activated protein kinase cascade regulating infection-related morphogenesis in *Magnaporthe grisea*. Plant Cell **17**: 1317–1329.

Zhao Z, Liu H, Wang C, Xu J-R (2013) Comparative analysis of fungal genomes reveals different plant cell wall degrading capacity in fungi. BMC Genomics **14**: 274.

Zhou R, Zhu T, Han L, Liu M, Xu M, Liu Y, Han D, Qiu D, Gong Q, Liu X (2017) The asparagine-rich protein NRP interacts with the Verticillium effector PevD1 and regulates the subcellular localization of cryptochrome 2. J Exp Bot **68**: 3427–3440.

Zhu W, Ronen M, Gur Y, Minz-Dub A, Masrati G, Ben-Tal N, Savidor A, Sharon I, Eizner E, Valerius O, et al (2017) BcXYG1, a secreted xyloglucanase from *Botrytis cinerea,* triggers both cell death and plant immune responses. Plant Physiol **175**: 438 LP – 456.

Zhu W, Wei W, Fu Y, Cheng J, Xie J, Li G, Yi X, Kang Z, Dickman MB, Jiang D (2013) A secretory protein of necrotrophic fungus *Sclerotinia sclerotiorum* that suppresses host resistance. PLoS One **8**: e53901.

Zhuang X, McPhee KE, Coram TE, Peever TL, Chilvers MI (2012) Rapid transcriptome

characterization and parsing of sequences in a non-model host-pathogen interaction; pea-*Sclerotinia sclerotiorum*. BMC Genomics **26**: 668.

Zimmermann S, Moelling K (1999) Phosphorylation and regulation of Raf by Akt (protein kinase B). Science (80) **286**: 1741–1744.

Zuccaro A, Lahrmann U, Güldener U, Langen G, Pfiffi S, Biedenkopf D, Wong P, Samans B, Grimm C, Basiewicz M, et al (2011) Endophytic life strategies decoded by genome and transcriptome analyses of the mutualistic root symbiont *Piriformospora indica*. PLoS Pathog **7**: e1002290.

APPENDICES

Appendix A. Supplementary tables

Table A.1 Oligonucleotides used for ddPCR to validate RNA-Seq analysis.

Gene ID	Primer Sequences 5'>3'	Probe Sequence 5'>3'
SS1G_07027	F: CAACTTGATCGACACACCTACT R: GGATAACCATCGAGTGCGAATA	FAM/AGCTCCTCAAGGTTTGAATGTATCATGCA
SS1G_07661	F: CTCGCGGAACAACTGAGATT R: GATAATCGACGCCGGTCATAG	FAM/AAGCCCTGCAATCTTCTCTCGGTT
SS1G_08104	F: CCAATCCAAGCTAGTGCAGTTAAT R: CCTTGGGCTCTGCAGGTA	FAM/AGCTGCAATCTTCATGGGTGATCCA
SS1G_08218	F: CGCTCCAACAACTTGGTTATG R: AGCCATCTCCTTTGAAGTGTAA	FAM/CTTGGTGCAGATGTTGGCTTGCTC
SS1G_10796	F: AGGATGGGCAAGACAACAA R: GCCAGTGTAACTCTCGGTATG	FAM/TGCGACTGAAATGGCTGGTGTAGA
SS1G_10167	F: GGAAGCGTTCTCGATGGTAA R: CTTCAAGGAGTGAGCGTAGAAG	FAM/ACGGTGGAAAGACCAAGCCAAAGT
SS1G_07355	F: AGAAGTGCTGGTGGACTTAAC R: GCGAGGTGTTGTTTCCTTTG	FAM/ACCGTTGGTTCTCCAACACCATCT
SS1G_14133	F: CGGAGCATCAACCTACAAGAC R: CTGGCTTTCCATCACCATCATA	FAM/CGGGAATGAGCAAGATGGTCAATGGA
SS1G_02486	F: ATCCGGGTGCCTTCTTTAC R: CAGTCTCATCTTCCATGCCATA	FAM/ATTTCGACAACAACGGCGTTTGGG
SS1G_05839	F: CACACAGGAATCGGTATTGGA R: CATCACCACCCACGGATTAG	FAM/CGCGCGCAATGTTTCAAAGTGGTT
SS1G_04652	F: ACCGTCGTCGAGCCATATAA R: TAGAGAGCCTCGTTGTCGATAC	HEX/TGGTCGAGAACTCTGACGAGACCT

R indicates reverse primer and F forward primer

Table A.2 Output summary generated by CLC Genomics Workbench of mapped Illumina reads against the *Sclerotinia sclerotiorum* 1980 reference transcriptome.

Replicate	Sample	High-quality paired-end reads	Single reads mapped to reference	%	Paired-end reads mapped to reference	%
Rep 1						
	S. sclerotiorum	2,816,990	2,068,369	73.42	1,807,130	64.15
	1h	2,056,400	1,225,180	59.58	1,082,390	52.64
	3h	900,572	518,607	57.59	455,912	50.62
	6h	1,284,272	709,409	55.24	633,452	49.32
	12h	747,264	445,373	59.60	398,704	53.36
	24h	1,474,458	892,355	60.52	802,708	54.44
	48h	1,937,564	1,156,895	59.71	1,026,910	53
	Total	11,217,520	7,016,188	60.81	6,207,206	53.93
Rep 2						
	S. sclerotiorum	708,336	520,981	73.55	443,386	62.6
	1h	834,200	441,343	52.91	396,692	47.55
	3h	868,250	526,234	60.61	474,374	54.64
	6h	2,004,794	1,216,407	60.67	1,073,478	53.55
	12h	1,900,228	1,123,755	59.14	994,114	52.32
	24h	1,250,450	663,567	53.07	569,734	45.56
	48h	1,750,276	1,134,031	64.79	996,268	56.92
	Total	9,316,534	5,626,318	60.68	4,948,046	53.31
Rep 3						
	S. sclerotiorum	3,059,020	2,189,731	71.58	1,936,758	63.31
	1h	3,667,108	2280561	62.19	2,034,016	55.47
	3h	2,294,968	1,451,796	63.26	1,289,402	56.18
	6h	1,673,268	1,010,817	60.41	883,100	52.78
	12h	1,918,732	1,186,506	61.84	1,046,994	54.57
	24h	3,835,786	2,267,534	59.12	1,984,244	51.73
	48h	3,227,198	1,867,826	57.88	1,659,720	51.43
	Total	19,676,080	12,254,771	62.33	10,834,234	55.07

Table A.3 Primers used for cloning of genes encoding candidate effectors.

Gene ID	Constructs to test the necrotizing activity	Constructs to test the subcellular localization	Primer Name[1]	Primer Sequences 5' >3'
SS1G_00872	Cons. #1 (primers F1-R1) Cons. #2 (primers F2-R1)	Cons. #3 (primers F1-R2) Cons. #4 (primers F2-R2)	F1-00872-SP	GGGGACAAGTTTGTACAAAAAAGCAGGCTTCATGAAGCCATTCGCTACTCTTGCAGCA
			R1-00872-SC[2]	GGGGACCACTTTGTACAAGAAAGCTGGGTCTCATAGGAACCAAGCAAGTGCAGCTCC
			F2-00872-NO-SP	GGGGACAAGTTTGTACAAAAAAGCAGGCTTCATGCAGGTTACCTATAACTCGACCACTGG
			R2-00872-NO-SC	GGGGACCACTTTGTACAAGAAAGCTGGGTCTAGGAACCAAGCAAGTGCAGCTCCC
SS1G_10096	Cons. #1 (primers F1-R1) Cons. #2 (primers F2-R1)	Cons. #3 (primers F1-R2) Cons. #4 (primers F2-R2)	F1-10096-SP	GGGGACAAGTTTGTACAAAAAAGCAGGCTTCATGCAATTCCCAACCATCGCC
			R1-10096-SC	GGGGACCACTTTGTACAAGAAAGCTGGGTCTTACAATCCACAAGCACTTGGGTCA
			F2-10096-NO-SP	GGGGACAAGTTTGTACAAAAAAGCAGGCTTCATGATCACCGTCTCCTACGACACCG
			R2-10096-NO-SC	GGGGACCACTTTGTACAAGAAAGCTGGGTCCAATCCACAAGCACTTGGGTCAAGT
SS1G_00849	Cons. #1 (primers F1-R1) Cons. #2 (primers F2-R1)	Cons. #3 (primers F1-R2) Cons. #4 (primers F2-R2)	F1-00849-SP	GGGGACAAGTTTGTACAAAAAAGCAGGCTTCATGCAATTCTCATCTGCTCTTATCTCTGC
			R1-00849-SC	GGGGACCACTTTGTACAAGAAAGCTGGGTCTTACCAGTCGTAGGTCAAGTCGAAAG
			F2-00849-NO-SP	GGGGACAAGTTTGTACAAAAAAGCAGGCTTCATGGCCACCATTGGACAACGTG
			R2-00849-NO-SC	GGGGACCACTTTGTACAAGAAAGCTGGGTCCCAGTCGTAGGTCAAGTCGAAAGCA
SS1G_09844	Cons. #1 (primers F1-R1) Cons. #2 (primers F2-R1)	Cons. #3 (primers F1-R2) Cons. #4 (primers F2-R2)	F1-09844-SP	GGGGACAAGTTTGTACAAAAAAGCAGGCTTCATGCTTTCCAAGACTATTATTTCTCTCCTC
			R1-09844-SC	GGGGACCACTTTGTACAAGAAAGCTGGGTCCTAACAATTATAATTCAAATAAACACCCCTAGC
			F2-09844-NO-SP	GGGGACAAGTTTGTACAAAAAAGCAGGCTTCATGTCTCCTGTACCAGATACCTTGAACG
			R2-09844-NO-SC	GGGGACCACTTTGTACAAGAAAGCTGGGTCACAATTATAATTCAAATAAACACCCCTAGCA
SS1G_13668	Cons. #1 (primers F1-R1) Cons. #2 (primers F2-R1)	Cons. #3 (primers F1-R2) Cons. #4 (primers F2-R2)	F1-13668-SP	GGGGACAAGTTTGTACAAAAAAGCAGGCTTCATGCAATTCTCCACACTCCTCACTCTCAT
			R1-13668-SC	GGGGACCACTTTGTACAAGAAAGCTGGGTCCTATGCAGAGCAAGAAACACTCCTGACTGT
			F2-13668-NO-SP	GGGGACAAGTTTGTACAAAAAAGCAGGCTTCATGCTTCCCCTCTCTCCACCCC
			R2-13668-NO-SC	GGGGACCACTTTGTACAAGAAAGCTGGGTCTGCAGAGCAAGAAACACTCCTGACTG
SS1G_13126	Cons. #1 (primers F1-R1) Cons. #2 (primers F2-R1)	Cons. #3 (primers F1-R2) Cons. #4 (primers F2-R2)	F1-13126-SP	GGGGACAAGTTTGTACAAAAAAGCAGGCTTCATGCTTCAACAAAGCCTCTTCACAATCTTC
			R1-13126-SC	GGGGACCACTTTGTACAAGAAAGCTGGGTCTCACATAATCTTTCCACTCTCCCCGG
			F2-13126-NO-SP	GGGGACAAGTTTGTACAAAAAAGCAGGCTTCATGTCTCCTCTCTACACTCATTCTTCAATATC
			R2-13126-NO-SC	GGGGACCACTTTGTACAAGAAAGCTGGGTCCATAATCTTTCCACTCTCCCCGGC
SS1G_11912	Cons. #1 (primers F1-R1) Cons. #2 (primers F2-R1)	Cons. #3 (primers F1-R2) Cons. #4 (primers F2-R2)	F1-11912-SP	GGGGACAAGTTTGTACAAAAAAGCAGGCTTCATGGTTGCCTTTGCCAAATCTC
			R1-11912-SC	GGGGACCACTTTGTACAAGAAAGCTGGGTCCTAGAAACTACTAGCCTTCACAAAGTTATT
			F2-11912-NO-SP	GGGGACAAGTTTGTACAAAAAAGCAGGCTTCATGATTCCCTTCCCATCAGAGC
			R2-11912-NO-SC	GGGGACCACTTTGTACAAGAAAGCTGGGTCGAAACTACTAGCCTTCACAAAGTTATTCTC
SS1G_07669	Cons. #1 (primers F1-R1) Cons. #2 (primers F2-R1)	Cons. #3 (primers F1-R2) Cons. #4 (primers F2-R2)	F1-07669-SP	GGGGACAAGTTTGTACAAAAAAGCAGGCTTCATGCAATTCACAACTTCCATCCTCG
			R1-07669-SC	GGGGACCACTTTGTACAAGAAAGCTGGGTCCTAAGCCGATCCCCCACCAGTAA
			F2-07669-NO-SP	GGGGACAAGTTTGTACAAAAAAGCAGGCTTCATGGGCACTGTCCACTTCGTCAA
			R2-07669-NO-SC	GGGGACCACTTTGTACAAGAAAGCTGGGTCAGCCGATCCCCCACCAGTAACA
SS1G_08706	Cons. #1 (primers F1-R1) Cons. #2 (primers F2-R1)	Cons. #3 (primers F1-R2) Cons. #4 (primers F2-R2)	F1-08706-SP	GGGGACAAGTTTGTACAAAAAAGCAGGCTTCATGAAGTTCACAATCACTTCTGTCGC
			R1-08706-SC	GGGGACCACTTTGTACAAGAAAGCTGGGTCCTATACAAAATACCAGGTGCCCTTGAC

			F2-08706-NO-SP	GGGGACAAGTTTGTACAAAAAAGCAGGCTTCATGGCTCCCGCTCCAGTATCTC
			R2-08706-NO-SC	GGGGACCACTTTGTACAAGAAAGCTGGGTCTACAAAATACCAGGTGCCCTTGAC
SS1G_04382	Cons. #1 (primers F1-R1) Cons. #2 (primers F2-R1)	Cons. #3 (primers F1-R2) Cons. #4 (primers F2-R2)	F1-04382-SP	GGGGACAAGTTTGTACAAAAAAGCAGGCTTCATGCATCTTTCCTATGCTTTGTCAGC
			R1-04382-SC	GGGGACCACTTTGTACAAGAAAGCTGGGTCCTATGCCTCAAAGCCGATTTCTCTC
			F2-04382-NO-SP	GGGGACAAGTTTGTACAAAAAAGCAGGCTTCATGTCTCTTACAATCAACAATTGGTGCTC
			R2-04382-NO-SC	GGGGACCACTTTGTACAAGAAAGCTGGGTCTGCCTCAAAGCCGATTTCTCTC
SS1G_09232	Cons. #1 (primers F1-R1) Cons. #2 (primers F2-R1)	Cons. #3 (primers F1-R2) Cons. #4 (primers F2-R2)	F1-09232-SP	GGGGACAAGTTTGTACAAAAAAGCAGGCTTCATGCGTACCTCATTCATCGCC
			R1-09232-SC	GGGGACCACTTTGTACAAGAAAGCTGGGTCTTACTCATAATTTTGAACCTTCTCCTCTAC
			F2-09232-NO-SP	GGGGACAAGTTTGTACAAAAAAGCAGGCTTCATGCAATACACAAATCAATCCGC
			R2-09232-NO-SC	GGGGACCACTTTGTACAAGAAAGCTGGGTCCTCATAATTTTGAACCTTCTCCTCTACAA
SS1G_01235	Cons. #1 (primers F1-R1) Cons. #2 (primers F2-R1)	Cons. #3 (primers F1-R2) Cons. #4 (primers F2-R2)	F1-01235-SP	GGGGACAAGTTTGTACAAAAAAGCAGGCTTCATGTTCAAAAATCTCCCACTCCTCC
			R1-01235-SC	GGGGACCACTTTGTACAAGAAAGCTGGGTCTCACAGAGCCTTCCACTTCAGACTAA
			F2-01235-NO-SP	GGGGACAAGTTTGTACAAAAAAGCAGGCTTCATGTCCCCAACTCCTGAACCTCTAA
			R2-01235-NO-SC	GGGGACCACTTTGTACAAGAAAGCTGGGTCCAGAGCCTTCCACTTCAGACTAAAAGA
SS1G_09420	Cons. #1 (primers F1-R1) Cons. #2 (primers F2-R1)	Cons. #3 (primers F1-R2) Cons. #4 (primers F2-R2)	F1-09420-SP	GGGGACAAGTTTGTACAAAAAAGCAGGCTTCATGTTGTATCAAATTTATATTCCCGTCTTG
			R1-09420-SC	GGGGACCACTTTGTACAAGAAAGCTGGGTCTCAACCCACCGAAGCAGTAATACC
			F2-09420-NO-SP	GGGGACAAGTTTGTACAAAAAAGCAGGCTTCATGTATTGGATACAATTTTACTCCGAGCC
			R2-09420-NO-SC	GGGGACCACTTTGTACAAGAAAGCTGGGTCACCCACCGAAGCAGTAATACCTCTCT
SS1G_02904	Cons. #1 (primers F1-R1) Cons. #2 (primers F2-R1)	Cons. #3 (primers F1-R2) Cons. #4 (primers F2-R2)	F1-02904-SP	GGGGACAAGTTTGTACAAAAAAGCAGGCTTCATGTCGAAATTCTTCAGTTCCGTGC
			R1-02904-SC	GGGGACCACTTTGTACAAGAAAGCTGGGTCTTAACCGTTGCTAGGAAGAGTATTGCAA
			F2-02904-NO-SP	GGGGACAAGTTTGTACAAAAAAGCAGGCTTCATGGCTCCAGCAAGCGCC
			R2-02904-NO-SC	GGGGACCACTTTGTACAAGAAAGCTGGGTCACCGTTGCTAGGAAGAGTATTGCAATT
SS1G_00263	Cons. #1 (primers F1-R1) Cons. #2 (primers F2-R1)	Cons. #3 (primers F1-R2) Cons. #4 (primers F2-R2)	F1-00263-SP	GGGGACAAGTTTGTACAAAAAAGCAGGCTTCATGCATTTCTCCATGATTGCTTCTATCC
			R1-00263-SC	GGGGACCACTTTGTACAAGAAAGCTGGGTCCTAAGCCTGGCAAGCATAATCGGTG
			F2-00263-NO-SP	GGGGACAAGTTTGTACAAAAAAGCAGGCTTCATGGCTCCAACTGCCGCTCC
			R2-00263-NO-SC	GGGGACCACTTTGTACAAGAAAGCTGGGTCAGCCTGGCAAGCATAATCGGTGT
SS1G_13696	Cons. #1 (primers F1-R1) Cons. #2 (primers F2-R1)	Cons. #3 (primers F1-R2) Cons. #4 (primers F2-R2)	F1-13696-SP	GGGGACAAGTTTGTACAAAAAAGCAGGCTTCATGCACATCTCGAGCTCCCTCCT
			R1-13696-SC	GGGGACCACTTTGTACAAGAAAGCTGGGTCCTACAACTCACTCCTACACACATCCCCC
			F2-13696-NO-SP	GGGGACAAGTTTGTACAAAAAAGCAGGCTTCATGGATTTCCACTACGGACTCGTAGATT
			R2-13696-NO-SC	GGGGACCACTTTGTACAAGAAAGCTGGGTCCAACTCACTCCTACACACATCCCCC
SS1G_10534	Cons. #1 (primers F1-R1) Cons. #2 (primers F2-R1)	Cons. #3 (primers F1-R2) Cons. #4 (primers F2-R2)	F1-10534-SP	GGGGACAAGTTTGTACAAAAAAGCAGGCTTCATGCAACATTCTCTCGATCTCTCTCATTAT
			R1-10534-SC	GGGGACCACTTTGTACAAGAAAGCTGGGTCTCAGAACCACTTCCCTCTTCCGC
			F2-10534-NO-SP	GGGGACAAGTTTGTACAAAAAAGCAGGCTTCATGGTTAGAGGTCCCTCCTTCCGA
			R2-10534-NO-SC	GGGGACCACTTTGTACAAGAAAGCTGGGTCGAACCACTTCCCTCTTCCGCTCTC
SS1G_09248	Cons. #1 (primers F1-R1) Cons. #2 (primers F2-R1)	Cons. #3 (primers F1-R2) Cons. #4 (primers F2-R2)	F1-09248-SP	GGGGACAAGTTTGTACAAAAAAGCAGGCTTCATGCAATTCACAACCGCAACACTC
			R1-09248-SC	GGGGACCACTTTGTACAAGAAAGCTGGGTCTTAAGCAGAAGCAGCAGTGCAAAGA
			F2-09248-NO-SP	GGGGACAAGTTTGTACAAAAAAGCAGGCTTCATGTCTCCCCTCCAACCACGTC

			R2-09248-NO-SC	GGGGACCACTTTGTACAAGAAAGCTGGGTCAGCAGAAGCAGCAGTGCAAAGAAC
SS1G_01867	Cons. #1 (primers F1-R1) Cons. #2 (primers F2-R1)	Cons. #3 (primers F1-R2) Cons. #4 (primers F2-R2)	F1-01867-SP	GGGGACAAGTTTGTACAAAAAAGCAGGCTTCATGTCAAAACTACTCTTCTCCTTCCTCCTC
			R1-01867-SC	GGGGACCACTTTGTACAAGAAAGCTGGGTCTCAAATCAACCCCTTCCTCGCC
			F2-01867-NO-SP	GGGGACAAGTTTGTACAAAAAAGCAGGCTTCATGCAATTCCAATTCTTCGAACAAATG
			R2-01867-NO-SC	GGGGACCACTTTGTACAAGAAAGCTGGGTCAATCAACCCCTTCCTCGCCAAC
SS1G_04519	Cons. #1 (primers F1-R1) Cons. #2 (primers F2-R1)	Cons. #3 (primers F1-R2) Cons. #4 (primers F2-R2)	F1-04519-SP	GGGGACAAGTTTGTACAAAAAAGCAGGCTTCATGCAGCTCCCGCAAATTCTTTC
			R1-04519-SC	GGGGACCACTTTGTACAAGAAAGCTGGGTCCTAAATGATCTGATAAGCCAAAAGCGG
			F2-04519-NO-SP	GGGGACAAGTTTGTACAAAAAAGCAGGCTTCATGTCCCCCCTCCTGCAAACC
			R2-04519-NO-SC	GGGGACCACTTTGTACAAGAAAGCTGGGTCAATGATCTGATAAGCCAAAAGCGGA
SS1G_09150	Cons. #1 (primers F1-R1) Cons. #2 (primers F2-R1)	Cons. #3 (primers F1-R2) Cons. #4 (primers F2-R2)	F1-09150-SP	GGGGACAAGTTTGTACAAAAAAGCAGGCTTCATGGTGTCTTTCAAGAAAATCTTTTTTGC
			R1-09150-SC	GGGGACCACTTTGTACAAGAAAGCTGGGTCCTACTGAGACTGCTTGCAAACTCTCTCAC
			F2-09150-NO-SP	GGGGACAAGTTTGTACAAAAAAGCAGGCTTCATGCAATCCCCAGCTAGTACGCTG
			R2-09150-NO-SC	GGGGACCACTTTGTACAAGAAAGCTGGGTCCTGAGACTGCTTGCAAACTCTCTCACC
SS1G_05939	Cons. #1 (primers F1-R1) Cons. #2 (primers F2-R1)	Cons. #3 (primers F1-R2) Cons. #4 (primers F2-R2)	F1-05939-SP	GGGGACAAGTTTGTACAAAAAAGCAGGCTTCATGAAGTTTATGTATCTCGGACTTCTCCTC
			R1-05939-SC	GGGGACCACTTTGTACAAGAAAGCTGGGTCTTAACATTCATTCCAGTACCAGTTATCGC
			F2-05939-NO-SP	GGGGACAAGTTTGTACAAAAAAGCAGGCTTCATGGACAATGCCTACAGATGCAAGA
			R2-05939-NO-SC	GGGGACCACTTTGTACAAGAAAGCTGGGTCACATTCATTCCAGTACCAGTTATCGCC
SS1G_00744	Cons. #1 (primers F1-R1) Cons. #2 (primers F2-R1)	Cons. #3 (primers F1-R2) Cons. #4 (primers F2-R2)	F1-00744-SP	GGGGACAAGTTTGTACAAAAAAGCAGGCTTCATGAAGATTCCTTTTGCACTTGCTATCCTA
			R1-00744-SC	GGGGACCACTTTGTACAAGAAAGCTGGGTCTTAATAGTTCGACCCCGTCATAACCG
			F2-00744-NO-SP	GGGGACAAGTTTGTACAAAAAAGCAGGCTTCATGAAAACCGTGCTTGATGTCGAAC
			R2-00744-NO-SC	GGGGACCACTTTGTACAAGAAAGCTGGGTCATAGTTCGACCCCGTCATAACCGC
SS1G_07027	Cons. #1 (primers F1-R1) Cons. #2 (primers F2-R1)	Cons. #3 (primers F1-R2) Cons. #4 (primers F2-R2)	F1-07027-SP	GGGGACAAGTTTGTACAAAAAAGCAGGCTTCATGTATTTTTCAAAACTTCTCCTCTTTTCCG
			R1-07027-SC	GGGGACCACTTTGTACAAGAAAGCTGGGTCTCAACAGAACTCGCACTTCTCGCTG
			F2-07027-NO-SP	GGGGACAAGTTTGTACAAAAAAGCAGGCTTCATGCAACAATTCATGGTTCCTGCC
			R2-07027-NO-SC	GGGGACCACTTTGTACAAGAAAGCTGGGTCACAGAACTCGCACTTCTCGCTG

[1]**Description**

Primers F1 and R1 were used to clone into pEarlyGate100 vector to test the necrotizing activity of each protein with signal peptide (SP)
Primers F2 and R1 were used to clone into pEarlyGate100 vector to test the necrotizing activity of each protein without SP
Primers F1 and R2 were used to clone into pEarlyGate103 vector to test the subcellular localization of each protein with SP
Primers F2 and R2 were used to clone into pEarlyGate103 vector to test the subcellular localization of each protein without SP

[2]**SC** indicates stop codon

Table A.4 Oligonucleotides used for ddPCR to evaluate expression of host plant ER stress-related genes.

Gene Name	Primer Sequences 5' >3'	Probe Sequence 5' >3'
bZIP60	F: CTCCTGTTCAGTCCGATCATTC R: TCTCCTTGTCTTTGTCGTCATC	FAM/TTCCAAGGTTTCAAGTGGCTCCGA
PDI	F: AACAGTGAAGGAGGGACTAATG R: GTCTCATCCAGCACAATTTCATC	FAM/CCGTCAAGCGTTGTGGTGCTATCT
BLP4	F: AGCAGACAACAGTGACAATCC R: GCTGGAGCTATTCCGGTTAAAT	FAM/TGAGACTGCGTTCACCTTCAAAGACC
α-tubulin	F: CCTCCTATGCTCCTGTCATTTC R: ATGGCGAGGATCACACTTAAC	HEX/AGTTGCAGAGATCACCAACAGTGCT

F indicates forward primer and R reverse primer

Table A.5 Primers used for cloning of genes encoding necrosis-inducing proteins for expression in *Escherichia coli.*

Gene ID	Primer Sequences 5'>3'
SS1G_07027	F: TGCTCTAGAAATAATTTTGTTTAACTTTAAGAAGGAGATATACCATGCAACAATTC ATGGTTCCTGCC R: CCGCTCGAGCACAGAACTCGCACTTCTCGCTGG
SS1G_00849	F: TGCTCTAGAAATAATTTTGTTTAACTTTAAGAAGGAGATATACCATGGCCACCATT GGACAACGTG R: CCGCTCGAGCCCAGTCGTAGGTCAAGTCGAAAGCAGT
SS1G_00872	F: TGCTCTAGAAATAATTTTGTTTAACTTTAAGAAGGAGATATACCATGCAGGTTACC TATAACTCGACCACTG R: CCGCTCGAGCTAGGAACCAAGCAAGTGCAGCTCC
SS1G_08706	F: TGCTCTAGAAATAATTTTGTTTAACTTTAAGAAGGAGATATACCATGGCTCCCGCTC CAGTATCTCC R: CCGCTCGAGCTACAAAATACCAGGTGCCCTTGACG
SS1G_09150	F: TGCTCTAGAAATAATTTTGTTTAACTTTAAGAAGGAGATATACCATGCAATCCCCA GCTAGTACGCTG R: CCCAAGCTTGCTGAGACTGCTTGCAAACTCTCTCACC
SS1G_09232	F: TGCTCTAGAAATAATTTTGTTTAACTTTAAGAAGGAGATATACCATGCAATACACA AATCAATCCGCCC R: CCGCTCGAGCCTCATAATTTTGAACCTTCTCCTCTACAAAGACC

R indicates reverse primer and F forward primer

Table A.6 Synthetic DNA sequences of *SsNE1* and *SsNE2* tagged with various targeting signals.

Construct name	DNA sequence
SsNE1$^{\Delta SP}$-NLS	GGGG**ACAAGTTTGTACAAAAAAGCAGGCTTC**ATGCAACAATTCATGGTTCCTGCCCCA TGGTATGTCCAAAAAATCAGCATTGGAAACATCAGACACGGCACCGGCGGCTTCTGGT CATTCAACTTGATCGACACACCTACTCCAGCTCCTCAAGGTTTGAATGTATCATGCAG TTATACCTCTCAAACTACTTATATATTCGCACTCGATGGTTATCCAGTTGATGCACCA TGCAGTGGTGATCCCAATGTGACTTTCAGTCTATACCCTGATGGCGATCATTTTACCT TCAATATCACGCATTTGTATGGAAATTGCGGAACTGCGGATAGCCCAGCCCCTTGCAA CGACAATGGAACATGGCAATTCAGTTGGGATGACGTTAGGGGACAAGAGCAAGATGTC CAAAATAACTTTGGACAATCTGGAAGCTTCTATAGAGAAGGCATTTCCATGTATCCAA ATCGGGCGATACCCAGCGAGAAGTGCGAGTTCTGTCCTAAGAAGAAGAGAAAGGTT*GA **CCCAGCTTTCTTGTACAAAGTGGT**CCCC
SsNE1$^{\Delta SP}$-NES	GGGG**ACAAGTTTGTACAAAAAAGCAGGCTTC**ATGCAACAATTCATGGTTCCTGCCCCA TGGTATGTCCAAAAAATCAGCATTGGAAACATCAGACACGGCACCGGCGGCTTCTGGT CATTCAACTTGATCGACACACCTACTCCAGCTCCTCAAGGTTTGAATGTATCATGCAG TTATACCTCTCAAACTACTTATATATTCGCACTCGATGGTTATCCAGTTGATGCACCA TGCAGTGGTGATCCCAATGTGACTTTCAGTCTATACCCTGATGGCGATCATTTTACCT TCAATATCACGCATTTGTATGGAAATTGCGGAACTGCGGATAGCCCAGCCCCTTGCAA CGACAATGGAACATGGCAATTCAGTTGGGATGACGTTAGGGGACAAGAGCAAGATGTC CAAAATAACTTTGGACAATCTGGAAGCTTCTATAGAGAAGGCATTTCCATGTATCCAA ATCGGGCGATACCCAGCGAGAAGTGCGAGTTCTGTAACGAGCTTGCTCTTAAGTTGGC TGGACTTGATATT**GACCCAGCTTTCTTGTACAAAGTGGT**CCCC
CBL-SsNE1$^{\Delta SP}$-NES	GGGG**ACAAGTTTGTACAAAAAAGCAGGCTTC**ATGGGCTGCTTCCACTCAAAGGCAGCA AAAGAATTTCAACAATTCATGGTTCCTGCCCCATGGTATGTCCAAAAAATCAGCATTG GAAACATCAGACACGGCACCGGCGGCTTCTGGTCATTCAACTTGATCGACACACCTAC TCCAGCTCCTCAAGGTTTGAATGTATCATGCAGTTATACCTCTCAAACTACTTATATA TTCGCACTCGATGGTTATCCAGTTGATGCACCATGCAGTGGTGATCCCAATGTGACTT TCAGTCTATACCCTGATGGCGATCATTTTACCTTCAATATCACGCATTTGTATGGAAA TTGCGGAACTGCGGATAGCCCAGCCCCTTGCAACGACAATGGAACATGGCAATTCAGT TGGGATGACGTTAGGGGACAAGAGCAAGATGTCCAAAATAACTTTGGACAATCTGGAA GCTTCTATAGAGAAGGCATTTCCATGTATCCAAATCGGGCGATACCCAGCGAGAAGTG CGAGTTCTGTAACGAGCTTGCTCTTAAGTTGGCTGGACTTGATATT**GACCCAGCTTTC TTGTACAAAGTGGT**CCCC
SsNE1-GFP-KDEL	GGGG**ACAAGTTTGTACAAAAAAGCAGGCTTC**ATGTATTTTTCAAAACTTCTCCTCTTT TCCGCTGGAGCCATAACTACAGGCCTCGCTCAACAATTCATGGTTCCTGCCCCATGGT ATGTCCAAAAAATCAGCATTGGAAACATCAGACACGGCACCGGCGGCTTCTGGTCATT CAACTTGATCGACACACCTACTCCAGCTCCTCAAGGTTTGAATGTATCATGCAGTTAT ACCTCTCAAACTACTTATATATTCGCACTCGATGGTTATCCAGTTGATGCACCATGCA GTGGTGATCCCAATGTGACTTTCAGTCTATACCCTGATGGCGATCATTTTACCTTCAA TATCACGCATTTGTATGGAAATTGCGGAACTGCGGATAGCCCAGCCCCTTGCAACGAC AATGGAACATGGCAATTCAGTTGGGATGACGTTAGGGGACAAGAGCAAGATGTCCAAA ATAACTTTGGACAATCTGGAAGCTTCTATAGAGAAGGCATTTCCATGTATCCAAATCG GGCGATACCCAGCGAGAAGTGCGAGTTCTGTAGTAAAGGAGAAGAACTTTTCACTGGA GTTGTCCCAATTCTTGTTGAATTAGATGGTGATGTTAATGGGCACAAATTTTCTGTCA GTGGAGAGGGTGAAGGTGATGCAACATACGGAAAACTTACCCTTAAATTTATTTGCAC TACTGGAAAACTACCTGTTCCGTGGCCAACACTTGTCACTACTTTCTCTTATGGTGTT CAATGCTTTTCAAGATACCCAGATCATATGAAGCGGCACGACTTCTTCAAGAGCGCCA TGCCTGAGGGATACGTGCAGGAGAGGACCATCTTCTTCAAGGACGACGGGAACTACAA GACACGTGCTGAAGTCAAGTTTGAGGGAGACACCCTCGTCAACAGGATCGAGCTTAAG GGAATCGATTTCAAGGAGGACGGAAACATCCTCGGCCACAAGTTGGAATACAACTACA ACTCCCACAACGTATACATCATGGCCGACAAGCAAAAGAACGGCATCAAAGCCAACTT CAAGACCCGCCACAACATCGAAGACGGCGGCGTGCAACTCGCTGATCATTATCAACAA AATACTCCAATTGGCGATGGCCCTGTCCTTTTACCAGACAACCATTACCTGTCCACAC AATCTGCCCTTTCGAAAGATCCCAACGAAAAGAGAGACCACATGGTCCTTCTTGAGTT TGTAACAGCTGCTGGGATTACACATGGCATGGATGAACTATACAAAAAAGATGAGTTG

	TGA**GACCCAGCTTTCTTGTACAAAGTGGT**CCCC
SP^{PR1}-SsNE1$^{\Delta SP}$	GGGG**ACAAGTTTGTACAAAAAAGCAGGCTTC**ATGGGATTTGTTCTCTTTTCACAATTG CCTTCATTTCTTCTTGTCTCTACACTTCTCTTATTCCTAGTAATATCCCACTCTTGCC GTGCCCAACAATTCATGGTTCCTGCCCCATGGTATGTCCAAAAAATCAGCATTGGAAA CATCAGACACGGCACCGGCGGCTTCTGGTCATTCAACTTGATCGACACACCTACTCCA GCTCCTCAAGGTTTGAATGTATCATGCAGTTATACCTCTCAAACTACTTATATATTCG CACTCGATGGTTATCCAGTTGATGCACCATGCAGTGGTGATCCCAATGTGACTTTCAG TCTATACCCTGATGGCGATCATTTTACCTTCAATATCACGCATTTGTATGGAAATTGC GGAACTGCGGATAGCCCAGCCCCTTGCAACGACAATGGAACATGGCAATTCAGTTGGG ATGACGTTAGGGGACAAGAGCAAGATGTCCAAAATAACTTTGGACAATCTGGAAGCTT CTATAGAGAAGGCATTTCCATGTATCCAAATCGGGCGATACCCAGCGAGAAGTGCGAG TTCTGT**GACCCAGCTTTCTTGTACAAAGTGGT**CCCC
SsNE2-NLS	GGGG**ACAAGTTTGTACAAAAAAGCAGGCTTC**ATGCAATTCTCATCTGCTCTTATCTCT GCCATCACCGTTGCTCTTGCTTCGGCTGCCACCATTGGACAACGTGACGAGGCCGTCT TCAAGGTCTCTGACTTCAGCGCAGGCTGTATCCAACACAGCACCCAGTGCCTCTACCA CTTCACTCTCATCCAACCCGGTACCATGGAGACCGTCGGTGTTGAATGTTCCGCCCTC GTTAGCGCCTACACCAATGGCTCCCTCCCCAACATCGGCAAATGGCAAGGCAAATGCA AGGATTCTTCCCGCACTTTCTGGGTTGTCCGTCAAAACGAGGGTCTTAAGCTCTGGGC TTCTCAACCAGTTACTCCAGCTAGCAACCAAACCGCATCCCACCTCCTCCCAGGCACT GACTTTGAAATGATCAAATACTCTATCGGTAGCGTTGACAGCTACACTGGACCAACTG CTTTCGACTTGACCTACGACTGGCCTAAGAAGAAGAGAAAGGTT**GACCCAGCTTTCTT GTACAAAGTGGT**CCCC
SsNE2-NES	GGGG**ACAAGTTTGTACAAAAAAGCAGGCTTC**ATGCAATTCTCATCTGCTCTTATCTCT GCCATCACCGTTGCTCTTGCTTCGGCTGCCACCATTGGACAACGTGACGAGGCCGTCT TCAAGGTCTCTGACTTCAGCGCAGGCTGTATCCAACACAGCACCCAGTGCCTCTACCA CTTCACTCTCATCCAACCCGGTACCATGGAGACCGTCGGTGTTGAATGTTCCGCCCTC GTTAGCGCCTACACCAATGGCTCCCTCCCCAACATCGGCAAATGGCAAGGCAAATGCA AGGATTCTTCCCGCACTTTCTGGGTTGTCCGTCAAAACGAGGGTCTTAAGCTCTGGGC TTCTCAACCAGTTACTCCAGCTAGCAACCAAACCGCATCCCACCTCCTCCCAGGCACT GACTTTGAAATGATCAAATACTCTATCGGTAGCGTTGACAGCTACACTGGACCAACTG CTTTCGACTTGACCTACGACTGGAACGAGCTTGCTCTTAAGTTGGCTGGACTTGATAT T**GACCCAGCTTTCTTGTACAAAGTGGT**CCCC
CBL-SsNE2$^{\Delta SP}$-NES	GGGG**ACAAGTTTGTACAAAAAAGCAGGCTTC**ATGGGCTGCTTCCACTCAAAGGCAGCA AAAGAATTTGCCACCATTGGACAACGTGACGAGGCCGTCTTCAAGGTCTCTGACTTCA GCGCAGGCTGTATCCAACACAGCACCCAGTGCCTCTACCACTTCACTCTCATCCAACC CGGTACCATGGAGACCGTCGGTGTTGAATGTTCCGCCCTCGTTAGCGCCTACACCAAT GGCTCCCTCCCCAACATCGGCAAATGGCAAGGCAAATGCAAGGATTCTTCCCGCACTT TCTGGGTTGTCCGTCAAAACGAGGGTCTTAAGCTCTGGGCTTCTCAACCAGTTACTCC AGCTAGCAACCAAACCGCATCCCACCTCCTCCCAGGCACTGACTTTGAAATGATCAAA TACTCTATCGGTAGCGTTGACAGCTACACTGGACCAACTGCTTTCGACTTGACCTACG ACTGGAACGAGCTTGCTCTTAAGTTGGCTGGACTTGATATT**GACCCAGCTTTCTTGTA CAAAGTGGT**CCCC
CBL-SsNE2-NES	GGGG**ACAAGTTTGTACAAAAAAGCAGGCTTC**ATGCAATTCTCATCTGCTCTTATCTCT GCCATCACCGTTGCTCTTGCTTCGGCTGGCTGCTTCCACTCAAAGGCAGCAAAAGAAT TTGCCACCATTGGACAACGTGACGAGGCCGTCTTCAAGGTCTCTGACTTCAGCGCAGG CTGTATCCAACACAGCACCCAGTGCCTCTACCACTTCACTCTCATCCAACCCGGTACC ATGGAGACCGTCGGTGTTGAATGTTCCGCCCTCGTTAGCGCCTACACCAATGGCTCCC TCCCCAACATCGGCAAATGGCAAGGCAAATGCAAGGATTCTTCCCGCACTTTCTGGGT TGTCCGTCAAAACGAGGGTCTTAAGCTCTGGGCTTCTCAACCAGTTACTCCAGCTAGC AACCAAACCGCATCCCACCTCCTCCCAGGCACTGACTTTGAAATGATCAAATACTCTA TCGGTAGCGTTGACAGCTACACTGGACCAACTGCTTTCGACTTGACCTACGACTGGAA CGAGCTTGCTCTTAAGTTGGCTGGACTTGATATT**GACCCAGCTTTCTTGTACAAAGTG GT**CCCC
SsNE2-GFP-KDEL	GGGG**ACAAGTTTGTACAAAAAAGCAGGCTTC**ATGCAATTCTCATCTGCTCTTATCTCT GCCATCACCGTTGCTCTTGCTTCGGCTGCCACCATTGGACAACGTGACGAGGCCGTCT TCAAGGTCTCTGACTTCAGCGCAGGCTGTATCCAACACAGCACCCAGTGCCTCTACCA

	CTTCACTCTCATCCAACCCGGTACCATGGAGACCGTCGGTGTTGAATGTTCCGCCCTC GTTAGCGCCTACACCAATGGCTCCCTCCCCAACATCGGCAAATGGCAAGGCAAATGCA AGGATTCTTCCCGCACTTTCTGGGTTGTCCGTCAAAACGAGGGTCTTAAGCTCTGGGC TTCTCAACCAGTTACTCCAGCTAGCAACCAAACCGCATCCCACCTCCTCCCAGGCACT GACTTTGAAATGATCAAATACTCTATCGGTAGCGTTGACAGCTACACTGGACCAACTG CTTTCGACTTGACCTACGACTGGAGTAAAGGAGAAGAACTTTTCACTGGAGTTGTCCC AATTCTTGTTGAATTAGATGGTGATGTTAATGGGCACAAATTTTCTGTCAGTGGAGAG GGTGAAGGTGATGCAACATACGGAAAACTTACCCTTAAATTTATTTGCACTACTGGAA AACTACCTGTTCCGTGGCCAACACTTGTCACTACTTTCTCTTATGGTGTTCAATGCTT TTCAAGATACCCAGATCATATGAAGCGGCACGACTTCTTCAAGAGCGCCATGCCTGAG GGATACGTGCAGGAGAGGACCATCTTCTTCAAGGACGACGGGAACTACAAGACACGTG CTGAAGTCAAGTTTGAGGGAGACACCCTCGTCAACAGGATCGAGCTTAAGGGAATCGA TTTCAAGGAGGACGGAAACATCCTCGGCCACAAGTTGGAATACAACTACAACTCCCAC AACGTATACATCATGGCCGACAAGCAAAAGAACGGCATCAAAGCCAACTTCAAGACCC GCCACAACATCGAAGACGGCGGCGTGCAACTCGCTGATCATTATCAACAAAATACTCC AATTGGCGATGGCCCTGTCCTTTTACCAGACAACCATTACCTGTCCACACAATCTGCC CTTTCGAAAGATCCCAACGAAAAGAGAGACCACATGGTCCTTCTTGAGTTTGTAACAG CTGCTGGGATTACACATGGCATGGATGAACTATACAAAAAAGATGAGTTGTGA**GACCC** **AGCTTTCTTGTACAAAGTGGT**CCCC
SP^{PR1}-SsNE2$^{\Delta SP}$	GGGG**ACAAGTTTGTACAAAAAAGCAGGCTTC**ATGGGATTTGTTCTCTTTTCACAATTG CCTTCATTTCTTCTTGTCTCTACACTTCTCTTATTCCTAGTAATATCCCACTCTTGCC GTGCCGCCACCATTGGACAACGTGACGAGGCCGTCTTCAAGGTCTCTGACTTCAGCGC AGGCTGTATCCAACACAGCACCCAGTGCCTCTACCACTTCACTCTCATCCAACCCGGT ACCATGGAGACCGTCGGTGTTGAATGTTCCGCCCTCGTTAGCGCCTACACCAATGGCT CCCTCCCCAACATCGGCAAATGGCAAGGCAAATGCAAGGATTCTTCCCGCACTTTCTG GGTTGTCCGTCAAAACGAGGGTCTTAAGCTCTGGGCTTCTCAACCAGTTACTCCAGCT AGCAACCAAACCGCATCCCACCTCCTCCCAGGCACTGACTTTGAAATGATCAAATACT CTATCGGTAGCGTTGACAGCTACACTGGACCAACTGCTTTCGACTTGACCTACGACTG G**GACCCAGCTTTCTTGTACAAAGTGGT**CCCC

AttB site sequences are denoted in bold font.

* Various targeting signals in each construct are marked in grey.

Table A.7 Amino acid sequences of peptides derived from SsNE2.

Peptide name	Peptide sequence
M1	ATIGQRDEAVFKVSDFSAGCIQHSTQCLYHFTLIQPGTMETV
M2	GVECSALVSAYTNGSLPNIGKWQGKCKDSSRTFWVVRQNEGLKLWA
M3	SQPVTPASNQTASHLLPGTDFEMIKYSIGSVDSYTGPTAFDLTYD
M1+M2	VFKVSDFSAGCIQHSTQCLYHFTLIQPGTMETVGVECSALVSAYTNGSLPNIGKWQGKC KDSSRTFWVVRQNEG
M2+M3	NGSLPNIGKWQGKCKDSSRTFWVVRQNEGLKLWASQPVTPASNQTASHLLPGTDFEMIK YSIGSVDSYTGPTAFDL